UNIVERSITY OF OXFORD

Investigating primary and secondary B cell responses in cattle after immunisation with existing and novel vaccines

Clare F. J. Grant

A thesis submitted in partial fulfillment for the degree of Doctor of Philosophy

Trinity 2013

Declaration of Authorship

I, CLARE FRANCES JANE GRANT, declare that this thesis titled, 'Investigating primary and secondary B cell responses in cattle after immunisation with existing and novel vaccines' and the work presented in it is my own. I confirm that:

- I have read and understood the Universitys disciplinary regulations concerning conduct in examinations and, in particular, the regulations on plagiarism.
- I have read and understood the Education Committees information and guidance on academic good practice and plagiarism.
- The thesis is entirely my own work unless indicated otherwise.
- It has not been submitted, either partially or in full, for another Honour School or qualification of this University, or at any other institution.
- I have clearly indicated the presence of all material that I have quoted from other sources, including any diagrams, charts, tables or graphs.
- I have clearly indicated the presence of all paraphrased material with appropriate references.
- I have acknowledged appropriately any assistance that I have received in addition to that provided by my supervisors.
- I have not copied from the work of any other candidate.
- I have not used the services of any agency providing specimen, model or ghost-written work in the preparation of this thesis.
- I agree to retain an electronic copy of this work until the publication of my final examination result, except where submission in hand-written format is permitted.
- I agree to make any such electronic copy available to the examiners should it be necessary to confirm my word count or to check for plagiarism.

Signed: _____

Date: 10th October 2013 _____

"When you feel like giving up, remember why you held on for so long in the first place."

Anon

INVESTIGATING PRIMARY AND SECONDARY B CELL RESPONSES IN CATTLE AFTER IMMUNISATION WITH EXISTING AND NOVEL VACCINES.

Clare F. J. Grant, St. Cross College, DPhil. in Paediatrics, Trinity 2013.

ABSTRACT

Antibodies play a pivotal role in protecting against viral infection, maintenance of this protective response is provided by plasma and memory B cells. Foot and mouth disease virus (FMDV) is a highly contagious pathogen and studies in cattle have shown that protection from the virus is antibody-mediated. However, FMDV vaccines are unable to achieve long durations of immunity. Therefore, understanding the FMDV-specific B cell responses in cattle is essential to inform future vaccine design.

Antigen-specific ELIspot assays were used to determine the kinetics of the bovine B cell response to T-dependent and -independent antigens. An ELIspot assay was developed to allow enumeration of FMDV-specific plasma and memory B cells following vaccination and live-virus challenge. In addition, a novel surgical technique was also developed to allow enumeration of antigen-specific B cells when exiting a regional lymph node, following vaccination. The bovine immunoglobulin repertoire was investigated at the peak of the B cell responses using deep sequencing.

T-dependent B cell responses in cattle were characterised by a small burst of antigen-specific plasma cells occurring after the primary vaccination, which was coupled with an increase in antigen-specific IgG titres. In keeping with the central dogma of immunological priming, the plasma cell burst post booster vaccination was larger and more rapid. Antigen-specific memory B cells were detectable for over 6 months. In contrast, immunisation with a T-independent antigen resulted in no detectable plasma or memory B cells. Vaccination with inactivated FMDV, novel FMDV antigens and live-virus challenge induced in a burst of FMDV-specific plasma cells but low numbers of memory B cells. Deep sequencing of immunoglobulin transcripts at the peak of the antigen-specific plasma cell response post vaccination, detected increases in bovine IgG transcripts in both blood and efferent lymph following booster vaccination, indicating that they are likely to be FMDV-specific. Deep sequencing has also revealed that cattle exhibit a broad range of heavy chain CDR3 lengths and highly similar light-chain transcripts that are shared between animals. Overall, this data suggests that the kinetics of the bovine plasma and memory B cell response to antigen is similar to that demonstrated in humans and mice. However, the bovine antibody V region structure is different and is likely to interact with its cognate antigen differently.

Acknowledgements

There are many people that have supported and encouraged me over the past four years.

To all of you, I'm extremely grateful for all of the support you've given me.

Firstly, I would like to thank my supervisors Bryan Charleston, Eric Lefevre and Andrew Pollard for their support, kind words of encouragement and discussions. I would also like to thank John Hammond who, despite being incredibly busy, managed to find the time to help me with the bovine Ig transcript analysis work. Also, Merial Animal Health, in particular Catherine Charreyre, for its funding, delicious French cuisine and discussions throughout my DPhil.

I would also like to acknowledge my laboratory colleagues: Veronica Carr for keeping me sane whilst in the lab, Karen Billington for her patience whilst I remembered how to 'do molecular', Helen Prentice for her kind words and her excellent care and dedication to the efferent lymphatic cannulation animals, and finally Claudine Porta for allowing me to use her FMDV capsids in my studies. The animal attendants at The Pirbright Institute also deserve a mention, this type of work would not be possible without their hard work and dedication to keeping the animals in such good condition.

To my fellow PhD students at the Pirbright Institute, there's always comfort in knowing that others are going through the same experiences as you. In particular, I'd like to acknowledge Nicholas Sanderson for his help and patience whilst I stumbled through using the Linux platform.

I would also like to give a special acknowledgement to my former colleagues in the Molecular Pathology Department at The University of Southampton NHS Trust, in particular Philip Evans and Sue Harris; without your encouragement to take this step I wouldn't be on the path I am today.

Finally, I would like to thank my friends and family for keeping the stress at bay with laughter, kind words and wine! In particular my partner Owen, who has had to cope with all of the ups and downs over the past four years, without his support I really don't think I'd be where I am today. My Mum, for all the last minute 'horse duties' that have been called upon over the years and for telling me to keep going when I said I couldn't. I would like to mention That Scallywag Prince, possibly the only equine in the world that is educated in dressage, FMDV and B cell biology in cattle!

Thanks for the patience everybody, I know it has not been an easy journey at times.

Contents

Declaration of Authorship i

Abstract iii

Acknowledgements iv

List of Figures x

List of Tables xii

Abbreviations xiii

1 Introduction 1
- 1.1 The adaptive immune response . . . 1
  - 1.1.1 Lymphocyte development . . . 2
- 1.2 Immunoglobulin structure and function . . . 5
  - 1.2.1 The B cell receptor . . . 6
  - 1.2.2 Immunoglobulin function . . . 6
    - 1.2.2.1 IgM . . . 7
    - 1.2.2.2 IgG . . . 8
    - 1.2.2.3 IgA . . . 8
    - 1.2.2.4 IgE . . . 9
    - 1.2.2.5 IgD . . . 9
  - 1.2.3 Bovine immunoglobulin isotypes . . . 9
  - 1.2.4 Serological response to viral infection . . . 9
- 1.3 Organisation of the lymphoid system . . . 10
  - 1.3.1 The lymph node . . . 11
    - 1.3.1.1 Lymphocyte trafficking . . . 12
    - 1.3.1.2 Antigen delivery . . . 13
  - 1.3.2 B cell activation . . . 15
    - 1.3.2.1 $CD4^+$ T Follicular Helper cells . . . 16
    - 1.3.2.2 The Germinal Centre . . . 17
    - 1.3.2.3 Class switch recombination . . . 19
    - 1.3.2.4 B cell fate . . . 21

1.3.2.5 GC-independent memory B cells . . . 23
1.3.3 Maintenance of long-term serological protection . . . 24
1.3.3.1 BAFF and APRIL signalling . . . 26
1.4 B cell subsets . . . 27
1.4.1 Follicular B cells . . . 27
1.4.2 Marginal zone B cells . . . 27
1.4.3 B-1 B cells . . . 28
1.5 T-dependent and T-independent antigens . . . 29
1.6 Foot-and-mouth disease virus . . . 30
1.6.1 Viral structure . . . 32
1.6.2 FMDV serotypes . . . 32
1.6.3 FMDV pathogenesis . . . 34
1.6.4 FMDV immunogenicity . . . 35
1.6.5 Experimental vaccines against FMDV . . . 36
1.6.5.1 Ad5-FMD Vaccine . . . 36
1.6.5.2 Double marker cDNA-derived killed FMDV platform . . . 37
1.6.5.3 FMDV peptide vaccines . . . 37
1.6.5.4 Alternative Virus-like particles (VLP) Platform . . . 38
1.7 Understanding the B cell response in cattle . . . 38
1.8 Thesis aims and objectives . . . 39

2 Understanding the bovine T-dependent and T-independent B cell response 40
2.1 Chapter objectives . . . 40
2.2 Introduction . . . 40
2.3 Material and methods . . . 41
2.3.1 Calves and immunisation protocols . . . 41
2.3.2 Bovine peripheral blood mononuclear cell (PBMC) isolation . . . 42
2.3.3 Memory B cell culture . . . 42
2.3.4 Plasma and memory B cell quantification by ELIspot . . . 43
2.3.5 Enzyme-linked immunoabsorbent assays (ELISA) . . . 43
2.3.6 Statistical analysis . . . 44
2.4 Results . . . 44
2.4.1 Antibody titre kinetics following primary and booster immunisations with a TD versus TI-2 antigen. . . . 44
2.4.2 Plasma cell and memory B cell kinetics following primary and booster immunisations with a TD versus TI-2 antigen. . . . 46
2.4.3 Immunisation with TTC induces an increase in TTC-specific plasma and memory B cells. . . . 47
2.4.4 Immunisation with TTC induces an increase in TTC-specific IgG titres in calves. . . . 51
2.5 Discussion . . . 51

3 Defining the bovine B cell response to foot-and-mouth disease virus 55
3.1 Chapter objectives . . . 55
3.2 Introduction . . . 55
3.2.1 FMDV vaccine potency testing . . . 57
3.3 Materials and methods . . . 58

3.3.1 Calves and immunisation protocol . . . 58
3.3.2 FMDV O1-Manisa and O-SKR-specific ELIspot . . . 58
3.3.3 FMDV O1-Manisa and O-SRK-specific virus neutralisation test, liquid phase blocking ELISA (LPBE) and FMDV non-structural protein (NSP) ELISA . . . 59
3.3.3.1 Virus neutralisation assay . . . 59
3.3.3.2 Liquid phase blocking ELISA (LPBE) . . . 60
3.3.3.3 Non-structural protein ELISA . . . 61
3.3.3.4 Statistical analysis . . . 61
3.3.4 PBMC proliferation by thymidine incorporation . . . 61
3.4 Results . . . 62
3.4.1 O1-Manisa-specific ELIspot development . . . 62
3.4.2 Clinical outcome following vaccination and live virus challenge . . . 63
3.4.3 Kinetics of the antigen-specific B cell response following O-serotype vaccination and live-virus challenge . . . 65
3.4.4 Kinetics of the serological response following FMDV O-serotype vaccination and live virus challenge . . . 68
3.4.4.1 Liquid phase blocking (LPB) ELISA . . . 68
3.4.4.2 Virus neutralisation assay . . . 71
3.4.4.3 Non-structural protein ELISA (NSP) . . . 73
3.4.5 Correlation between serological response and plasma cell number . . . 74
3.4.6 PBMC proliferative response following O-serotype FMDV vaccination and live virus challenge . . . 76
3.5 Discussion . . . 76

4 Efferent lymphatic cannulation: a novel model to explore antigen-specific bovine B cell response to FMDV 83
4.1 Chapter objectives . . . 83
4.2 Introduction . . . 83
4.2.1 Efferent lymphatic cannulation . . . 87
4.3 Materials and methods . . . 89
4.3.1 Calves and experimental protocol for TNP-CGG and FMDV O1-Manisa immunisations . . . 89
4.3.2 Calves and experimental protocol for FMDV O1-Manisa capsid antigen immunisations . . . 89
4.3.3 Efferent lymphatic cannulation technique . . . 90
4.3.4 Bovine mononuclear cell isolation . . . 91
4.3.4.1 Mononuclear cell isolation from efferent lymph . . . 91
4.3.5 FMDV O1-Manisa and TNP-CGG-specific ELIspot assays . . . 92
4.3.6 FMDV O1-Manisa-specific IgG ELISA . . . 92
4.3.7 Fluorescent antibody staining of cells for analysis of surface antigens by flow cytometry . . . 93
4.4 Results . . . 94
4.4.1 Kinetics of mononuclear cell subsets in efferent lymph post booster immunisation . . . 97
4.4.2 Antigen-specific plasma cell kinetics following primary and booster immunisation with TNP-CGG and inactivated FMDV O1-Manisa in peripheral blood and efferent lymph . . . 97

4.4.3 Antibody titre kinetics following primary and booster immunisation with TNP-CGG and inactivated FMDV O1-Manisa in peripheral blood . . . 99
4.4.4 Antigen-specific plasma cell kinetics following primary and booster immunisation with FMDV O1-Manisa capsids in peripheral blood and efferent lymph . . . 99
4.4.5 Antigen-specific memory B cell kinetics following primary and booster immunisation with FMDV O1-Manisa capsids in peripheral blood . . . 102
4.4.6 Antibody titre kinetics following following primary and booster immunisation with FMDV O1-Manisa capsid antigens . . . 104
4.5 Discussion . . . 105

5 Using next generation sequencing to explore the bovine B cell response to FMDV vaccination in peripheral blood and efferent lymph. 110
5.1 Chapter objectives . . . 110
5.2 Introduction . . . 110
5.3 Materials and methods . . . 113
5.3.1 Calves and immunisation protocol . . . 113
5.3.2 Selection of samples for sequencing . . . 115
5.3.3 Bovine PBMC isolation . . . 115
5.3.4 Total RNA extraction from bovine mononuclear cells . . . 115
5.3.5 Bovine immunoglobulin heavy and light chain constant region primer design . . . 116
5.3.6 Bovine immunoglobulin heavy and light chain primer validation . . . 117
5.3.7 Bovine immunoglobulin heavy and light chain 5′-RACE strategy . . . 120
5.3.8 PCR product visualisation and quantification . . . 124
5.3.9 454-sequencing . . . 125
5.3.10 Immunoglobulin sequence analysis . . . 125
5.3.11 Ig sequence abundance calculation . . . 128
5.3.12 Identifying highly similar Ig transcripts at multiple time points . . . 128
5.3.13 Complementarity determining region identification . . . 128
5.3.14 Immunoglobulin structure modelling . . . 129
5.4 Results . . . 129
5.4.1 Bovine IgG heavy chain . . . 132
5.4.1.1 The abundance pattern of IgG V region transcripts increases post-vaccination . . . 132
5.4.1.2 Bovine immunoglobulin heavy V regions show variation in length . . . 136
5.4.1.3 Variation of the amino acid residues occurs within the predicted CDR regions of the bovine heavy and light chain V-regions . . . 137
5.4.1.4 Variation in bovine IgG heavy chain CDR3 length is not affected by repeated immunisations . . . 138
5.4.1.5 Bovine IgG individual transcript abundances alter following booster immunisation. . . . 140
5.4.2 Bovine Ig light chain . . . 141

5.4.2.1 Cattle exhibit low levels of immunoglobulin light-chain κ expression . . . 141
5.4.2.2 Bovine immunoglobulin light chain V region shows little variation in length . . . 141
5.4.2.3 Bovine immunoglobulin light chain V regions show amino acid variation within predicted CDRs . . . 144
5.4.2.4 The relative abundance of Igλ transcripts is similar between peripheral blood and efferent lymph . . . 144
5.4.2.5 Predominance of one light-chain V-region at peak of plasma cell response . . . 145
5.4.3 Predicted structures of bovine immunoglobulin heavy and light chain V regions . . . 147
5.4.3.1 Highly dominant Igλ transcripts are similar between animals . . . 147
5.4.3.2 The predicted Igλ structure is very similar between animals 149
5.4.3.3 The predicted structure of bovine IgG heavy chain V-region suggests that the elongated CDR3 region is involved in antigen-binding . . . 150
5.5 Discussion . . . 154

6 Conclusions and further work 163
6.1 Conclusions . . . 163
6.1.1 The kinetics of the B cell response to antigen in cattle is similar to that in mice and humans . . . 163
6.1.2 Foot-and-mouth disease virus does not induce memory B cells . . . 165
6.1.3 Bovine immunoglobulins are structurally different to human and mouse . . . 169
6.2 Further work . . . 170
6.2.1 Improved FMDV vaccines . . . 170
6.2.2 Resolving the crystal structure of bovine antibodies . . . 172
6.2.3 Broadly neutralising cross reactive antibodies in cattle . . . 172

A List of Publications 175

B Bioinformatic scripts and procedures 176
B.1 Python script to rank the bovine Ig trancript FASTA files . . . 176
B.2 Python script to strip Gap4 related nomenclature from the sequence name 177
B.3 Pentaho pipeline to extract IgG reads from MIRA assembly .caf files . . . 178
B.4 SQL server procedures . . . 178
B.5 Pentho pipeline to extract Paratome identified CDRs from .txt files . . . 183

C Bovine immunoglobulin variable gene segment sequences 184

Bibliography 185

List of Figures

1.1 B cell development . . . 3
1.2 Immunoglobulin molecule structure . . . 5
1.3 Lymph node structure . . . 12
1.4 Germinal centre reaction . . . 16
1.5 CSR signalling pathways . . . 20
1.6 B cell differentiation . . . 22
1.7 FMDV clinical symptoms in cattle . . . 31
1.8 FMDV genomic structure . . . 33
1.9 FMDV capsid structure . . . 33
1.10 FMDV global distribution . . . 34

2.1 TNP- and CGG- specific immunoglobulin titres following primary and booster immunisation . . . 45
2.2 TNP- and CGG- specific antibody secreting cells following primary and booster immunisation . . . 48
2.3 Kinetic of TNP-, CGG- and TTC-specific plasma and memory B cells post TTC immunisation . . . 50
2.4 TNP- and CGG- specific antibody secreting cells following primary and booster immunisation . . . 52

3.1 FMDV O1-Manisa specific ELIspot validation . . . 64
3.2 Kinetic of FMDV O-serotype specific plasma cells . . . 67
3.3 Kinetic of FMDV O-serotype specific blocking antibodies post-vaccination and live-virus challenge . . . 70
3.4 Kinetic of FMDV O-serotype specific virus neutralising antibodies post-vaccination and live-virus challenge . . . 72
3.5 Kinetic of the non-structural protein (NSP) specific antibody titres . . . 73
3.6 Statistical analysis of the B cell response to O-serotype FMDV vaccination and live-virus challenge . . . 74
3.7 PBMC proliferative responses following FMDV O-serotype vaccination and live virus challenge . . . 75

4.1 Bovine lymphatic system . . . 84
4.2 Efferent Lymphatic Cannulation model . . . 88
4.3 Kinetic of mononuclear cell counts in efferent lymph post-booster immunisation with TNP-CGG and FMDV O1-Manisa inactivated vaccine antigen . . . 96
4.4 Kinetic of mononuclear cell counts in efferent lymph post-booster immunisation with FMDV O1-Manisa capsid antigens . . . 96

4.5 Kinetic of mononuclear cell subsets in efferent lymph post-booster immunisation . . . 98
4.6 Kinetic of TNP-, CGG- and FMDV O1-Manisa specific plasma cells . . . 100
4.7 Kinetic of TNP-, CGG- and FMDV O1-Manisa specific plasma cells . . . 101
4.8 Kinetic of FMDV O1-Manisa specific plasma cells . . . 103
4.9 Kinetic of FMDV O1-Manisa specific memory B cell response . . . 104
4.10 Kinetic of FMDV O1-Manisa specific IgG titres . . . 105

5.1 Schematic diagram of immunoglobulin recombination events . . . 111
5.2 Cannulation experimental protocol . . . 114
5.3 Bovine IgG constant region domain 1 sequence alignment . . . 117
5.4 Bovine Igλ constant region domain 1 sequence alignment . . . 118
5.5 Bovine Igκ constant region domain 1 sequence alignment . . . 118
5.6 IgG, Igλ and Igκ GSP evaluation . . . 120
5.7 Bovine immunoglobulin 5′ RACE strategy . . . 123
5.8 Schematic of the 454-sequencing process . . . 126
5.9 Relative abundance of the top 200 bovine IgG transcripts at D0, D7 and D24/5 post primary immunisation . . . 133
5.10 Area under the curve values of the top 200 bovine IgG transcripts at D0, D7 and D24/5 post primary immunisation . . . 134
5.11 Total amino acid length of bovine IgG heavy chain V regions . . . 136
5.12 Amino acid variation of the bovine IgG heavy chain V region . . . 138
5.13 Length of the CDR3 region at D0, D7 and D24/5 post primary immunisation 139
5.14 Bovine IgG transcript abundance pre- and post-booster immunisation . . . 142
5.15 Total amino acid length of bovine Igλ V regions . . . 143
5.16 Amino acid variation of the bovine Igλ V regions . . . 144
5.17 Relative abundance of the top 200 bovine Igλ transcripts . . . 146
5.18 Sequence alignment of the top 3 most abundant Igλ transcripts . . . 148
5.19 Sequence identity matrix of the top 3 most abundant Igλ transcripts . . . 148
5.20 Phylogenetic tree of the top 3 most abundant Igλ sequences from FMDC16, FMDC17 and FMDC18 . . . 149
5.21 Predicted structure of bovine Igλ V region . . . 151
5.22 Amino acid composition of the bovine IgG CDR3 region . . . 153
5.23 Predicted structure of bovine IgG V regions . . . 155
5.24 Predicted structure of the combined bovine IgG and Igλ V regions . . . 156

B.1 Pipeline used to extract read sequences from .caf files . . . 178
B.2 Pipeline used to extract CDR sequences and length from .txt file . . . 183

C.1 Sequence alignment of the functional bovine IGHV gene segments . . . 184

List of Tables

1.1 Structure and function of human immunoglobulin isotypes 7
1.2 Cytokines involved in class switch recombination 21

2.1 Total number of IgG TNP-specific antibody secreting cells in PBMC population 47
2.2 Total number of IgG antigen-specific antibody secreting cells in PBMC population following immunisation with Tetanus toxoid C (TTC) 49

3.1 Clinical outcome post FMDV O-SKR live-virus challenge 65
3.2 Total number of IgG FMDV O-serotype antibody secreting cells in PBMC population 68

4.1 Volume of efferent lymph obtain from each animal 95

5.1 Details of samples and MID tags used for bovine IgG and Igλ 454-sequencing 116
5.2 PCR cycling parameters for amplification of bovine immunoglobulin transcripts 119
5.3 Bovine IgG and Igλ constant region MID tagged primer sequences 122
5.4 5′-RACE PCR reaction set up 124
5.5 Total number of IgG and Igλ reads and consensus transcripts 131
5.6 Distribution of IgG transcripts at D0, D7 and D24/5 post primary immunisation in peripheral blood and efferent lymph 132
5.7 Bovine IgG V region predicted CDR lengths 137
5.8 Number and length of super long CDR3 regions found in bovine IgG heavy chain transcripts 139
5.9 Bovine Igλ predicted CDR lengths 143
5.10 Relative abundance of the top 10 Igλ transcripts at peak of antigen-specific plasma cell burst following booster immunisation (D24/5). 147
5.11 Bovine Igλ sequences selected for modelling 150

Abbreviations

AEC	3-**a**mino-9-**e**thyl**c**arbazole
AECM	**A**mino**e**thyl**c**arboxy**m**ethyl
AID	**A**ctivation-*i*nduced **d**eaminase
APC	**A**ntigen **P**resenting **C**ell
AUC	**A**rea **u**nder the **c**urve
APRIL	**A** **Pr**oliferation-**i**nducing **L**igand
ASC	**A**ntibody **S**ecreting **C**ell
BAFF	**B** cell **A**ctivating **F**actor of the TNF **F**amily
BALT	**B**ronchial **A**ssociated **L**ymphoid **T**issue
BCR	**B** **c**ell **r**eceptor
BEI	**B**inary **E**thylene**i**mine
BHK	**B**aby **h**amster **k**idney
BLIMP	**B** **l**ymphocyte-**i**nduced **m**aturation **p**rotein
BRV	**B**ovine **r**hinitis **v**irus
C4bp	**C4** **b**inding **p**rotein
C region	**C**onstant region
CD	**C**luster **D**ifferentiation
CDR	**C**omplimentarity **D**etermining **R**egion
$\mathbf{C}_H$	**C**onstant region **h**eavy chain
CGG	**C**hicken **G**amma **G**lobulin
CH1	Heavy chain constant region domain 1
CL1	Light chain constant region domain 1 (CL1)
$\mathbf{C}_L$	**C**onstant region **l**ight chain
CPE	**C**yto**p**athic **e**ffect
c.p.m.	**C**ounts **p**er **m**inute

CSR	**C**lass **s**witch **r**ecombination
D	**D**ay
DC	**D**endritic **C**ell
DNA	**D**eoxyribo**n**ucleic **a**cid
dNTP	**d**eoxyribo**n**ucleotide **t**ri**p**hosphate
dPBS	**D**ulbecco's **P**hosphate-**B**uffered **S**aline
eIF4F	**E**ukaryotic **i**nitiation **f**actor 4F
ELISA	**E**nzyme **L**inked **I**mmunosorbant **A**ssay
ELMC	**E**fferent **l**ymph **m**ononuclear **c**ell
emPCR	**Em**ulsion **p**olymerase **c**hain **r**eaction
FCS	**F**oetal **c**alf **s**erum
FDC	**F**ollicular **D**endritic **C**ell
FITC	**F**luorescein **i**so**t**hio**c**yanate
FMD	**F**oot and **M**outh **D**isease
FMDV	**F**oot and **M**outh **D**isease **V**irus
FR	**F**ramework **r**egion
FRC	**F**ibroblastic **R**eticular **C**ell
FSC	**F**orward **Sc**atter
GAG	**G**lyco**a**mino**g**lycan
GALT	**G**ut **A**ssociated **L**ymphoid **T**issue
GC	**G**erminal **C**enter
GSP	**G**ene **s**pecific **p**rimer
HEV	**H**igh **e**ndothelial **v**enules
HIV	**H**uman **i**mmunodeficiency **v**irus
HRP	**H**orse**r**adish **p**eroxidase
IC	**I**mmune **c**omplex
ICAM-1	**I**ntra**c**ellular **A**dhesion **M**olecule-1
ICOS	**I**nducible T-cell **cos**timulator
ICOSL	**I**nducible T-cell **cos**timulator **l**igand
IFA	**I**ncomplete **F**reund's **a**djuvant
Ig	**I**mmuno**g**lobulin
IgH	**I**mmuno**g**lobulin **h**eavy-chain
IgL	**I**mmuno**g**lobulin **l**ight-chain

IL	**I**nter**L**eukin
IGLL1	**I**mmuno**g**lobulin **l**ambda-**l**ike polypeptide **1**
IPP	**I**leal **P**eyer's **p**atch
IRES	**I**nternal **R**ibosome **E**ntry **S**ite
IS	**I**mmune **s**ynapse
ITAM	**I**mmunoreceptor **t**yrosine-based **a**ctivation **m**otif
ITIM	**I**mmunoreceptor **t**yrosine-based **i**nhibitory **m**otif
KDE	**K**appa **D**eleting **E**lement
LCMV	**L**ymphocytic **c**horio**m**eningitis **v**irus
LFA-1	**L**ymphocyte **F**unction **A**ssociated **A**ntigen-1
LMW	**L**ow **m**olecular **w**eight
LN	**L**ymph **n**ode
LPB	**L**iquid **P**hase **B**locking
Lpro	**L**eader **pro**tein
MAC	**M**embrane **a**ttack **c**omplex
MAC-1	**MAC**rophage receptor**-1**
MALT	**M**ucosal **A**ssociated **L**ymphoid **T**issue
MHC-II	**M**ajor **H**istocompatibility **C**omplex class **II**
MID	**M**olecular **id**entifier
MZ	**M**arginal **z**one
NCBI	**N**ational **C**enter for **B**iotechnology **I**nformation
NGS	**N**ext **g**eneration **s**equencing
NSP	**N**on **S**tructural **P**rotein
O1M	FMDV **O1**-**M**anisa
OD	**O**ptical **Density**
OIE	**O**ffice **I**nternational des **E**pizooties
O-SKR	FMDV **O**-**S**outh **K**o**r**ean
PAMP	**P**athogen **a**ssociated **m**olecular **p**attern
PBMC	**P**eripheral **B**lood **M**ononuclear **C**ell
PBS	**P**hosphate-**B**uffered **S**aline
pb	**p**ost **b**ooster
pc	**P**ost-**c**hallenge
PCR	**P**olymerase **C**hain **R**eaction

PD50	**P**rotective **d**ose **50**
PDB	**P**rotein **D**ata **B**ank
PEG	**P**oly**e**thylene **g**lycol
pi	**P**rimary-**i**mmunisation
PNAd	**P**eripherl lymph **N**ode **Ad**ressin
pv	**P**ost-**v**accination
RACE	**R**apid **a**mplificatoin of **c**DNA **e**nds
RAG	**R**ecombination **a**ctivating **g**ene
RGD	Arginine (**R**) - Glycine (**G**) - Aspartic acid (**D**)
RNA	**R**ibo**n**ucleic **a**cid
RPMI	**R**oswell **P**ark **M**emorial **I**nstitute
RSS	**R**ecombination **s**ignal **s**equence
S1P	**S**phingosine-**1**-**p**hosphate
SAP	**S**LAM-**a**ssociated **p**rotein
SCS	**S**ubs**c**apsular **S**inus
SHM	**S**omatic **H**yper**m**utation
sIg	**s**urface **I**mmuno**g**lobulin
SLAM	**S**ignaling **L**ymphocytic **A**ctivation **M**olecule
SSC	**S**ide **Sc**atter
TACI	**T**ransmembrane **a**ctivator and **c**alcium modulator and cyclophilin ligand **i**nteractor
Taq	***T**hermus **aq**uaticus*
TCAG	**T**hymine, **C**ytosine, **A**denosine and **G**uanine
TCR	**T** **c**ell **r**eceptor
TD	**T**-**D**ependent or **T**hymus **D**ependent
TdT	**T**erminal **d**eoxynucleotidyl **t**ransferase
$\mathbf{T}_{FH}$	**T** **F**ollicular **H**elper cell
TI	**T**-**i**ndependent
TI-1	**T**-**I**ndependent antigen type-**1**
TI-2	**T**-**I**ndependent antigen type-**2**
TLR	**T**oll-**l**ike **r**eceptor
TMB	3,3',5,5'-**T**etra**m**ethyl**b**enzidine
TNF	**T**umour **N**ecrosis **F**actor
TNP	2,4,6-**T**ri**n**itro**p**henol

TTC	**T**etanus **t**oxoid **C**
UTR	**Un**translated **r**egion
VCAM-1	**V**ascular **c**ell **a**dhesion **m**olecule **1**
VDJ	**V**ariable, **D**iversity and **J**oining
VNT	**V**irus **N**eutralisation **T**est
V-region	**V**ariable region

For Owen...

Chapter 1

Introduction

1.1 The adaptive immune response

The immunological response can be subdivided into two parts: the innate and adaptive immune responses. The innate provides a rapid and broad response to immunological challenge, the adaptive is characterised by an antigen-specific response and, under certain circumstances, the development of immunological memory. B cells form part of the adaptive immune response, each cell expresses and produces an individual immunoglobulin (Ig) specificity, resulting in a huge population of different antibody specificities circulating within an individual. Upon binding to their cognate antigen, antibodies facilitate either direct or indirect elimination of a pathogen during the immune response.

Long-term protection is achieved by a sustained level of circulating protective antibodies, produced by long-lived plasma cells and memory B cells. A successful vaccine aims to induce protective antibody titres that are sustained for a prolonged period of time, and thus protection against future antigenic challenge. However, not all vaccines are able to induce a long duration of immunity, and require regular booster immunisations to maintain protective antibody levels.

Memory B cells are a population of B cells that have previously responded to an antigen and remain within the individual for prolonged periods of time in a resting state but can be reactivated at a much lower threshold as compared to their naïve counterparts. Long-lived plasma cells, as their name would suggest, are long lived and reside within an individual for prolonged periods after antigenic stimulation, continuously secreting antibodies into the circulation. A population of short-live plasma cells are also produced during the B cell response to antigen, providing a rapid source of antibody-mediated protection whilst the long-lived plasma and memory B cells are developed.

Upon antigenic challenge, a specialised micro environment, known as the germinal centre (GC), is induced within the highly structured secondary lymphoid organs. The specialised, cellular rich GC region leads to the induction of both long lived plasma cells and memory B cells from naïve B cells that are generated in the bone marrow. The GC serves not only to produce long-lived plasma cells and memory B cells but also to 'fine tune' the B cell response, by introducing point mutations in the highly variable antigen-binding region of the B cell receptor. Through this process, fine tuning of the B cell receptor greatly improves the affinity of the antibody, thus improving the ability of the antibody to bind to its cognate antigen. This process is not achieved by B cells alone, T cells and follicular dendritic cells also cooperate in the B cell response to antigen to induce the formation of B cell memory.

B cells are also able to produce antibodies in the absence of GC formation. This response, known as the T-independent response is classically characterised by a lack of memory induction. The foot and mouth disease virus vaccine is unable to achieve a long duration of immunity in cattle, thus improving our knowledge of the B cell response to antigen, in cattle, will inform future vaccine design, particularly in vaccines that are unable to induce a long duration of immunity.

1.1.1 Lymphocyte development

Lymphocytes, B and T cells, express highly diverse membrane-bound antigen-specific receptors, which allow them to respond to a broad array of antigenic challenges. Both lymphoid lineages are derived from haemopoietic stem cells that are found, in humans, primarily in the bone marrow [1].

Lymphoid progenitors that are destined to become T cells migrate from the bone marrow to the thymus early in their differentiation where they continue to develop through thymic-education to become naïve T cells.

In contrast, B cell progenitors continue to develop within the bone marrow until a functional antigen receptor is expressed and the resulting naïve B cell exits the bone marrow (Figure 1.1) [3]. Both lineages of naïve lymphocytes (B and T cell) then re-circulate between the blood and the secondary lymphoid organs, increasing the probability of encountering their cognate antigen.

Membrane-bound antigen specific B cell receptors (BCR) are encoded by germline gene segments that recombine during B cell development to produce a functional BCR. Developing B cells will not progress beyond the pre-B cell stage without expression of a functioning BCR. The variable region (V region) of the BCR heavy chain is encoded

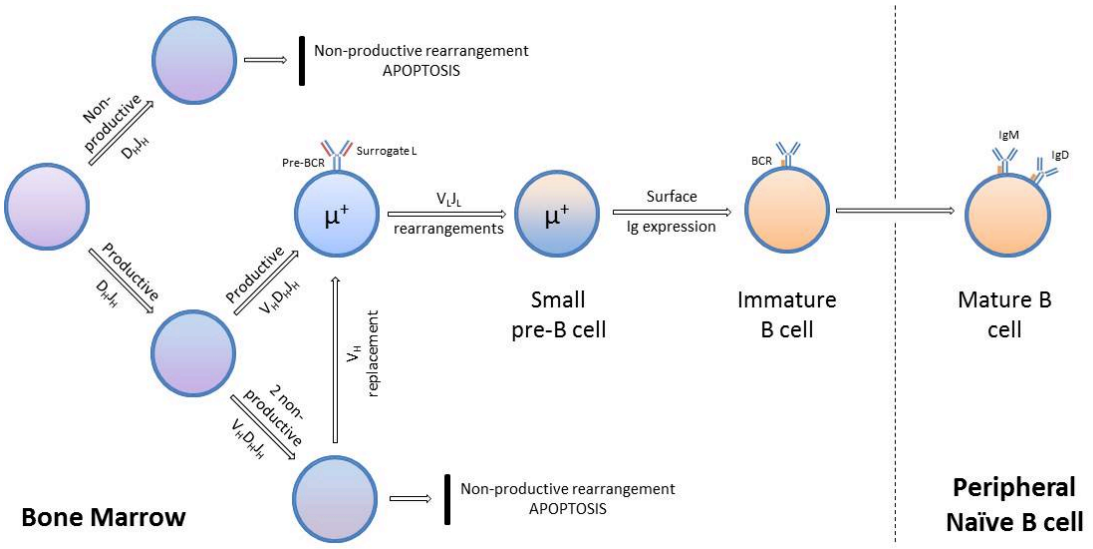


FIGURE 1.1: Schematic showing B cell development from haemopoietic stem cell in the bone marrow through to naïve B cell in peripheral circulation. During development the progenitor B cell undergoes a number of rounds of gene recombination to produce an in-frame antigen receptor. The first round of gene recombination is D_H to J_H followed by the addition of V_H. If rearrangement is functional the Ig heavy (IgH, μ) chain is expressed on the cell surface with a surrogate light chain to form the pre-B cell receptor (preBCR). Expression of the preBCR signals Ig light (IgL) chain gene recombination (κ or λ). If a functional V_L-J_L gene recombination is produced then it is expressed on the cell surface along with the IgH. This leads to the expression of a functional B cell receptor (BCR). If the cell is unable to produce a functional V_H-D_H-J_H or V_L-J_L gene recombination on both chromosomes (i.e. 2 attempts) the cell may be able to salvage itself by attempting recombination with gene segments that have not been used previously. However, if this is not successful the cell undergoes apoptosis. Adapted from [2].

by three gene segments; the variable (V_H), diversity (D_H) and joining (J_H) gene segments. Whereas, the light chain is encoded by only two gene segments; V_L and J_L. Recombination of these germline gene segments is facilitated by DNA (Deoxyribonucleic acid) repair enzymes (e.g. DNA-dependent protein kinases and Ku70/80) and also lymphoid-specific proteins, which are encoded by the recombination-activating genes (RAG), known as RAG-1 and -2. The RAG-1 and -2 recognise the recombination signal sequence (RSS) elements found adjacent to the V(D)J gene segments in the germline [4]. During the intrachormosomal V(D)J gene segment recombination, the DNA between the gene segments of interest is looped out to align the gene segments. DNA double stranded breaks are then introduced by RAG-1 and -2 and KU70/80 binds the broken double stranded DNA ends [5, 6]. DNA repair enzymes, such as DNA-dependent protein kinase then repair the broken DNA strands, resulting in two gene segments being aligned adjacently [4].

There is a step-wise process of gene-segment recombination during B cell receptor development to ensure only in-frame, functional BCRs are produced (Figure 1.1). Briefly,

during pro-B cell development the D_H to J_H gene segments will recombine first, before the V_H recombines with the in-frame DJ_H. Once an in-frame,functional VDJ_H recombination is produced the B cell is then able to express μH chains. The μH chain then associates, temporarily, with a surrogate light chain to form the pre-B cell receptor. The surrogate light chain is composed of a two polypeptides, the V_{preB} and the immunoglobulin lambda-like polypeptide 1 (IGLL1), that are homologous to the light chain V and C regions, respectively [7, 8]. The newly formed pre-B cell receptor is then expressed on the pre-B cell surface [8]. Expression of the pre-B cell receptor blocks RAG1 and -2 expression, preventing further VDJ_H recombinations occurring, in a process known as allelic exclusion [2]. After 4 to 6 rounds of cell division RAG-1 and -2 expression is restarted and the light chain V_L and J_L gene segments undergo recombination. Upon successful production of an in-frame, functional VJ_L the light chain V region is then transcribed with either a Lκ or Lλ constant region. The genomic organisation of the light chain loci usually means that the Igκ is rearranged first. If this is unsucessful a kappa deleting element that serves to control the expression of the non-functional Igκ VJ rearrangement, eliminating the kappa locus before the Igλ locus can undergo rearrangement, thus providing a mechanism of allelic exclusion [9]. After successful production of a functional light chain, conventional IgM of one specificity is then expressed on the surface of the immature B cell. B cells that have expressed IgM on their surface utilise alternative splicing to co-transcribe both IgM and IgD, leading to an IgM^+ IgD^+ phenotype. Both IgM and IgD share the same V region, and are both involved in antigen-binding and signalling. It is hypothesised that IgD plays a role in fine tuning the B cell response by balancing the IgM signalling, thereby defining the reactivity repertoire of the B cells. The newly matured B cells then exit the bone marrow and circulate in the periphery [2, 10].

In cattle, the continuous B cell development occurs in both the bone marrow and the gut-associated lymphoid tissue (GALT), ileal Peyer's patch (IPP). Pre-B cells, that are intracellular IgM^+, can be detected in the bovine bone marrow from late gestation to juvenile age, but not in the adult animal [11]. Thus, the pre-immune BCR repertoire, in cattle, is fixed at an early age and relies upon post-recombination modifications to further diversify the B cell repertoire.

BCR diversity generated during the V(D)J gene segment recombination is termed recombinational diversity. The recombined V region is then combined with a constant region (C region) to complete the antigen receptor [3, 12]. Antigen receptor diversity is further increased by the addition of non-template (N) and palindromic (P) nucleotides between the V(D)J gene segments via a process known as junctional diversity [4, 13]. Immunoglobulin diversity generation, particularly in cattle, is discussed further in Chapter 5.

1.2 Immunoglobulin structure and function

Antibodies or immunoglobulins (Ig) are produced by activated antigen-specific B cells that have undergone terminal differentiation to become plasma cells. They are secreted proteins that are composed of two chains, the heavy and light chain, which are bound by a disulphide bond (Figure 1.2). Each immunoglobulin light and heavy chain has a variable region (V region) and a constant region (C region). The heavy chain has 3 or 4 constant region domains (dependent upon the immunoglobulin isotype, termed C_H1 - 4), whereas the light chain has only one domain, termed C_L (Figure 1.2).

In humans and mice there are 2 different light chain C regions, κ and λ, and 5 isotypes of heavy chain C region, μ, γ, α, ϵ and δ (Figure 1.2). The variable region of both the heavy and light chains, combine to confer the antigen-binding specificity of the antibody, whereas the constant region of the heavy chain provides the biological functions of the molecule (e.g. complement fixation and Fc receptor binding, Figure 1.2).

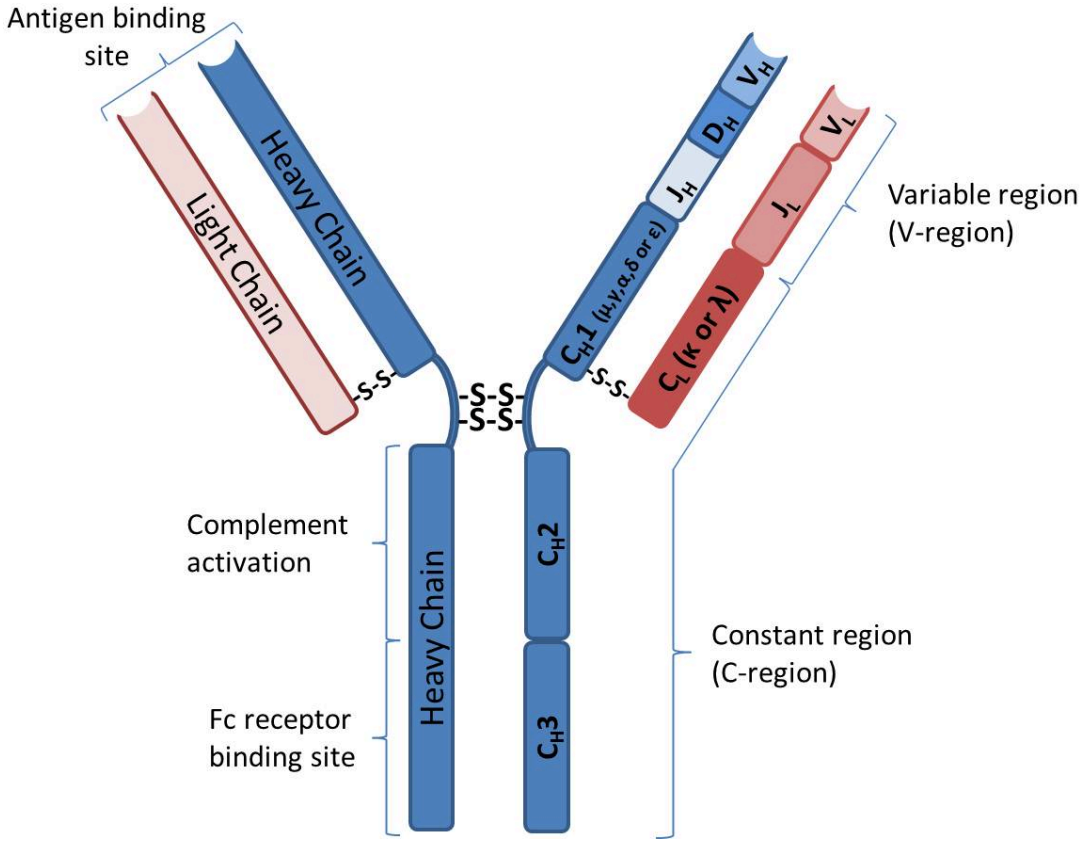


FIGURE 1.2: Schematic representation of an immunoglobulin molecule.

1.2.1 The B cell receptor

The BCR is a functional immunoglobulin molecule that is membrane-bound and complexed with a transmembrane heterodimer CD79a and b (formerly known as Igα/ Igβ), to form the BCR complex.

B cell stimulation is achieved by binding the BCR with its cognate antigen leading to cross linking of the BCR complex. This recruits tyrosine-kinases to the immunoreceptor tyrosine-based activation motifs (ITAMs) found on the cytoplasmic tails of the CD79a and b heterodimer, which in turn leads to activation of downstream signalling pathways [14]. The downstream signalling pathways that are activated by BCR signalling lead to a number changes, such as BCR internalisation, cytoskeletal changes and activation of transcription factors (e.g. NFκB) [15]. However, B cell activation is also dependent upon signalling through other accessory receptors that act to regulate the magnitude of the B cell response [2]. Both CD19 and CD40 are expressed on the surface of the B cell and serve to regulate the activation threshold of the BCR complex (CD19) and B cell fate e.g. class switching and germinal centre formation (CD40) [15].

1.2.2 Immunoglobulin function

Antibodies play an important role in protecting against infection by eliminating pathogens via neutralisation (binding leads to making the pathogen biologically inactive) or by opsonisation (coating the antigen) marking it for clearance. Different isotypes of immunoglobulin have evolved to provide a number of different specialised effector functions, some of which are required to control viral infection (see section 1.2.4). Amongst the various isotypes; IgG and IgM are the most abundant in the sera. Upon binding to antigen a complex of antigen and immunoglobulin is formed, termed the immune complex (IC). Immune complexes can be formed from high-affinity antibodies produced by plasma cells that have been stimulated by a specific antigen or from naturally occurring antibodies that are polyreactive and able to bind multiple epitopes that are often shared between pathogens [16]. The complement protein C1q binds to the C_H2 domain of the Fc domain of the immunoglobulin molecule (Figure 1.2) [17]. The binding of C1q to the immune complex leads to the activation of the classical complement pathway and formation of the membrane attack complex (MAC), which punches a hole in the pathogen surface [17].

The Fc domain on the immunoglobulin molecule binds to Fc receptors, which are expressed on a number of different immune cells (Figure 1.2). There are four different types of Fc receptor that bind the different isotypes of immunoglobulin, each with differing affinities for the immunoglobulin subclasses (Table 1.1). There are both activating

and inhibitory Fc receptors that exert their biological effects via the immunoreceptor tyrosine-based activation (ITAM) or inhibitory motifs (ITIM), respectively [18]. The ITIM bearing Fc receptor, FcγRII (CD32), binds the Fc portion of all IgG subclasses with a low binding affinity [18]. Thus, the activation of Fc receptors, by binding ICs, and the co expression of both activating and inhibitory Fc receptors on the effector cell serve to regulate the activation threshold of the cell [19].

TABLE 1.1: Structure and function of human immunoglobulin isotypes

	Serum (%)	**Structure**	**Complement fixation**	**Opsonisation**	**Cross-placenta**	**Other functions**	**FcR**
IgG	75	Monomer	+	+++	+	Secondary response: Neutralises toxins and viruses	FcγR
IgG1	67% IgG		Yes	Yes	+		I, II, III
IgG2	22% IgG		Yes	Yes	+		II
IgG3	7% IgG		Yes	Yes	+		I, II, III
IgG4	4% IgG		No	No	+		I, II
IgM	10	Pentamer	+++	+	–	Primary response	
IgA	15	Monomer/ Dimer	–	–	–	Mucosal response	FcαR (CD89)
IgA1			–	–	–		
IgA2			–	–	–		
IgD	<0.5	Monomer	–	–	–	Homeostasis	FcδR
IgE	<0.01	Monomer	–	–	–	Allergy	FcεRI, II

Physical and physiological characteristics of the different immunoglobulin isotyes in humans. Adapted from [20].

1.2.2.1 IgM

IgM is the primary antibody produced during an acute antigenic challenge, because it can be produced without the need for class switch recombination (CSR, discussed in 1.3.2.3, Table 1.1). Since IgM is produced during the early phase of the immune response the variable region has undergone very little somatic hypermutation (SHM), so tends to be more polyreactive, allowing IgM^+ B cells to respond quickly to a broader array of antigens[20].

Human IgM monomers form a pentameric mushroom-like structure by binding the polypeptide J-chain, which forms disulphide bonds between the J-chain and the Fc region of the IgM monomer [21]. This pentameric structure makes IgM very efficient at complement fixation and particle agglutination. The pentamer has a total of 10 possible antigen binding sites,which despite each site having a low individual antigen-binding affinity, give the IgM pentamer a high overall avidity due to the total number

of antigen-binding sites. Due to its large pentameric structure, IgM is predominantly found in the blood and to a lesser extent the lymph and tissues. The serum half-life of IgM is approximately 2 days, thus large numbers of antibody secreting cells (ASCs) are required to maintain high titres of IgM antibodies [22].

1.2.2.2 IgG

IgG is the most predominant isotype of immunoglobulin found in serum. In humans there are 4 subclasses (IgG1 - 4) which differ in their C_H domain structure and function (Table 1.1). IgG is able to enter the extravascular compartment allowing further dissemination of this antibody isotype. IgG1, 2 and 3 are able to fix complement, but their CH2 domains have a differing affinity for the complement protein C1q (IgG3 > IgG1 > IgG2, Table 1.1). During acute antigenic challenge there is often a skewing of IgG subclasses induced. For example, the proinflammotory cytokine, produced by $CD4^+T_h1$ cells, IFN-γ induces production of IgG2a and IgG3 whereas IL-4, produced by $CD4^+$ T_h2 cells, induces IgG1 production [23, 24]. The type of antigen leads to differential IgG secretion, with protein antigens usually inducing IgG1 and 3, whereas polysaccharides induce IgG2 and 4 [20].

IgG has a longer serum half-life, approximately 7 days, thus isotype switching the antibody heavy chain from IgM to IgG requires fewer ASCs to maintain a protective antibody titre and is a more efficient use of resources [25].

1.2.2.3 IgA

IgA is predominantly found in mucosal secretions, providing protection against toxin, bacterial and viral entry [20]. IgA is present at the mucosal surface as a dimer which, like IgM, is formed via disulphide bond formation between the J-chain and the IgA monomer [20]. The IgA dimer is transported to the mucosa surface by the polymeric immunoglobulin (poly-Ig) receptor, which is expressed on epithelial cells lining the mucosal surface [20]. IgA is internalised, via binding to the poly-Ig receptor and is transcytosed [20]. The extracellular domain of the receptor is then cleaved (and becomes known as the secretory component) to allow the IgA dimer to enter the mucosal secretions [20].

There are two different subclasses of IgA, IgA1 and IgA2, which differ in the length of their hinge region (Table 1.1). IgA1 has an elongated hinge region which makes it more susceptible to cleavage by bacterial proteases [20]. IgA2 is the predominant IgA subclass in mucosal secretions and IgA1 in sera [20].

1.2.2.4 IgE

In humans IgE is found in serum at very low levels. However, it is a highly potent immunoglobulin that, upon binding FcϵRI, leads to rapid degranulation of mast cells, basophils and eosinophils (Table 1.1) [20]. IgE binds to its receptor with a very high affinity and IgE expression leads to upregulation of FCϵRI on granulocytes. Thus the high affinity binding and receptor upregulation makes IgE a very potent effector molecule. IgE is secreted in response to parasitic helminth infections and also causes hypersensitive reactions (allergies) in individuals.

1.2.2.5 IgD

IgD is usually found as a membrane-bound immunoglobulin on B cells that exit the bone marrow and is often co-expressed with IgM. IgD can replace IgM during BCR signalling, in association with the CD79a and b heterodimer [20]. Despite extensive research the function of IgD remains poorly understood, although it has been proposed that IgD plays a role in regulating B cell fate at specific developmental stages [26]. Circulating IgD is found at very low levels in the serum, although its function has not been attributed to any major effector mechanisms. The hinge region of IgD is very sensitive to proteolysis, thus the soluble form to the antibody has a very short half-life [20].

1.2.3 Bovine immunoglobulin isotypes

Cattle also express IgM, IgG, IgA, and IgE isotype antibodies. They have 2 subclasses of IgG: IgG1 and IgG2. In normal conditions bovine sera contains undetectable levels of IgE, very low levels of IgA ($<100\mu$g/ml), IgM (3mg per ml), and IgG1 and IgG2 (10mg per ml) [27]. The amount of IgG2 usually exceeds IgG1 as it is the predominant isotype found in bovine sera [27]. IgG1 is also found in very high concentrations (exceeding 100mg per ml) in colostrum, providing antibody mediated protection to newborn calves [27, 28]. IgM and IgA are also found in colostrum but at much lower concentrations [28]. IgA is also found in the mucosal secretions of cattle [28].

1.2.4 Serological response to viral infection

Antibodies play a vital role in providing an individual with the ability to primarily control a viral infection and then offer protection against re-challenge, provided a sufficient titre of antibody is maintained. During the course of a viral infection a broad array of antibodies are generated directed against numerous viral antigens. Viral control and

protection is achieved via a number of mechanisms including neutralisation, opsonisation and complement fixation [25].

Neutralising antibodies have a direct anti-viral activity by binding, with a high affinity, to exposed structures on the viral capsid [29]. Thus interfering with cellular entry by either directly binding cellular entry receptors, steric hindrance or causing conformational changes in the viral capsid [30, 31]. However, neutralising antibodies only represent a small proportion of all antibodies generated following vaccination or during a viral infection. The majority are directed against internal viral antigens (e.g. non structural proteins), which will offer little protection during viral infection [25]. However, some non-neutralising antibodies are directed against structural viral proteins and are able to fix complement during a viral infection and may offer some protection despite their inability to neutralise the virus [25].

1.3 Organisation of the lymphoid system

The lymphoid system is organised into primary and secondary sites, each with a specific role in lymphocyte development. In adult mammals the primary lymphoid tissues are the bone marrow and the thymus, where lymphocyte development and maturation occurs.

The secondary lymphoid tissues are the spleen, lymph nodes, bronchial-, mucosal- and gut-associated lymphoid tissue (BALT, MALT and GALT, respectively) which includes the ileal Peyer's patches (IPP). The secondary lymphoid tissues are the sites where the adaptive immune responses are initiated [32]. Mature lymphocytes recirculate between the blood and the secondary lymphoid organs; an immune response may be initiated in that secondary lymphoid organ if the lymphocyte's cognate antigen is present.

Tissue-derived interstitial fluids or lymph, which may contain antigens, immune complexes and antigen presenting cells (APC) drains into the regional lymph nodes via the lymphatic system, allowing the immunogenic status of a particular site to be sampled. This provides an efficient mechanism for naïve lymphocytes to contact their cognate antigen [32]. The naïve lymphocytes must contact their cognate antigen in the context of an APC, either on a dendritic cell (DC), in the context of MHC II, for T cells or as intact antigen on a follicular dendritic cell (FDC) or a DC for B cells [33].

Follicular dendritic cells are non-motile cells that are found in the germinal centre, and are derived from stromal cells [33]. They have extensive processes, known as dendrites, that extend throughout the B cell follicle creating an extensive antigen retaining reticula, allowing contact with many motile B cells [34]. The FDCs account for approximately 1% of the germinal centre cells [35]. FDCs present intact, immune-complexed antigen,

bound to the dendrite surfaces via complement receptors (CD21 and CD35) and Fc receptors (FcγRIIB), to naïve B cells [36, 37]. The immune complexed antigen can be held on the surface of the FDC for prolonged periods of time, from months to years [33]. However, antigen presentation is not the only role performed by FDCs in the B cell response to antigen. FDCs also provide survival signals (proliferative and anti-apoptotic signals) to B cells within the germinal centre [33].

1.3.1 The lymph node

The immune system is a diffuse cellular system, with cells migrating throughout the body. Coordinating this system requires communication via both chemical signalling and cell-cell contact. The secondary lymphoid organs contain highly specialised micro environments which serve to coordinate the antigen and lymphocyte interaction.

The lymph node is a highly organised structure that consists of two histologically distinct concentric regions: the cortex and the medulla (Figure 1.3). The cortex is further subdivided into the paracortex (T cell region) and the follicles (B cell region). During antigenic challenge the follicles will also contain germinal centres (GC) [38]. Two-photon microscopy has revealed that under normal conditions, B and T cells crawl randomly, and rapidly, within their distinct regions of the lymph node along a network of stormal cells [39]. The distinct B and T cell niches within the lymph node are maintained by the expression of different cytokine receptors on the B and T cells, this serves to control contact between the lymphocytes during the highly regulated immune response [40].

A naïve lymphocyte will spend 8 to 24 hours within a lymph node. If it does not contact its cognate antigen within that period it will return to the circulation, via the efferent lymphatic vessels, and re-enter another lymph node within 30 minutes [39, 41].

Lymph enters the lymph node via the afferent lymphatic vessel into the subcapsular sinus (SCS) and then drains from the lymph node via the efferent lymphatic vessel (Figure 1.3). A 3-dimensional network of channels, known as the conduit network, projects from the SCS into the paracortex, allowing distribution of antigens, cytokines and chemokines throughout the lymph node (Figure 1.3) [38]. The conduit network is composed of collagen fibres surrounded by extracellular proteins and is produced by fibroblastic reticular cells (FRCs) [32]. Resident and tissue-derived DCs settle around the conduit network and probe the passing lymph for antigen as it drains through the lymph node [32, 42]. The FRC cells express perlecan, which has three long glycoaminoglycan (GAG) chains that act as a 'display board' for locally produced cytokines and chemokines [32].

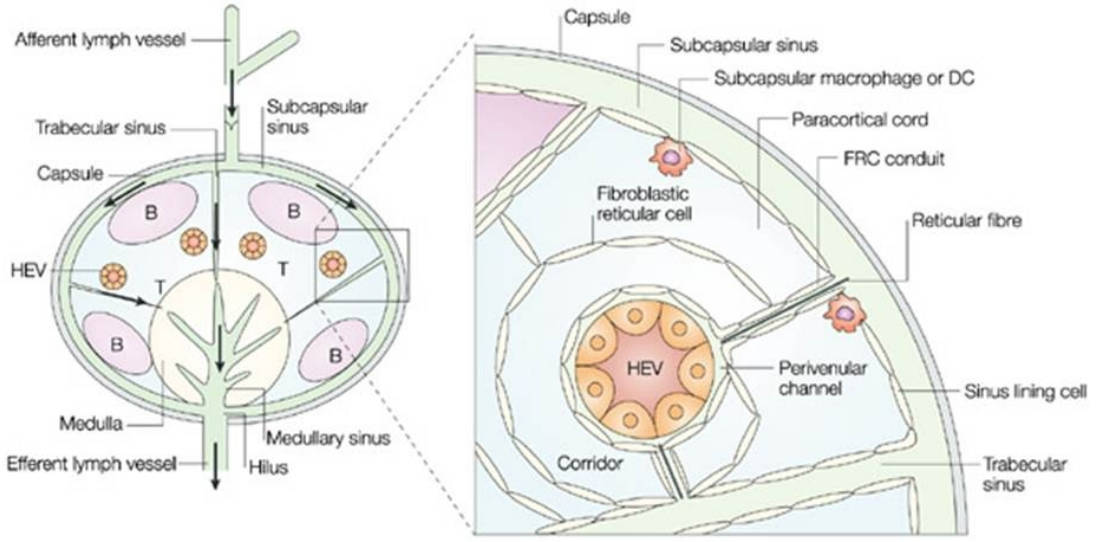


FIGURE 1.3: Schematic representation of the lymph node structure. The arrows indicate the lymph flow through the lymph node. The paracortex is indicated by the blue region and the follicles are shown in purple. The image on the right shows a more detailed view of the conduit network and the high endothelial venule (HEV). Adapted from [38].

1.3.1.1 Lymphocyte trafficking

Using in-situ fluorescent microscopy, it has been shown that B and T lymphocytes are constantly moving within and through the lymph node at a rate of 6- and 11μm/min^{-1}, respectively, thus increasing the rate of interaction with a potential cognate antigen [43]. However, this rate is likely to increase during antigenic challenge as blood flow through a draining lymph node increases by approximately 50% during an inflammatory response [32].

Lymphocytes enter the lymph node via the lymph and the high endothelial venules (HEVs, Figure 1.3). The lymphocytes express selectin molecules (e.g. L-selectin) which selectively bind the peripheral lymph node adressin (PNAd) molecule expressed on the HEV surface, slowing lymphocyte migration making them roll along the HEV wall [44]. The lymphocyte then adheres to the HEV surface via the integrin, lymphocyte function associated antigen-1 (LFA-1) binding to the intercellular adhesion molecule-1 (ICAM-1) which is expressed on HEV endothelial cells [32]. Lymphocytes then undergo extravasation into the lymph node [32]. During an inflammatory response local interleukin-6 (IL-6) production increases, which in turn increases ICAM-1 expression on the HEVs, thereby increasing lymphocyte migration into a local draining lymph node [32].

Naïve lymphocytes migrate to their respective regions of the lymph node, via FRC and FDC expressed ICAM-1 and Vascular cell adhesion molecule 1 (VCAM-1) binding,

following a chemokine gradient [39, 45]. Naïve B cells track along the conduit network to the B cell follicle following a CXCL13 chemokine gradient, which is secreted by the FDCs, bound to the surface of the conduit network and the FDCs by surface glycosaminoglycans (Figure 1.3) [46]. CXCL13 is recognised by the chemokine receptor CXCR5, which is expressed on B cells [46].

Within the lymph node antigen-primed DCs preferentially settle around the HEV, acting as a screening mechanism for incoming naïve lymphocytes before they migrate to either the paracortex or the follicles [47].

Lymphocytes exit the lymph node by migrating across the endothelial barrier of the efferent sinus, from the medullary chord, which leads to the efferent lymphatic vessel (Figure 1.3). Migration through the secondary lymphoid organ is regulated by the sphingosine 1-phosphate ($S1P_1$) receptors, which bind the ligand S1P. Both lymphocytes and lymphatic endothelial cells express $S1P_1$ receptors [48]. S1P is found in high levels in both the blood and lymph, but at low levels in the lymph node, thus there is a S1P gradient between the secondary lymphoid tissue and the periphery [49]. Under normal conditions, the highly motile lymphocytes are brought to the efferent sinuses through their random migration paths [39]. However during antigenic challenge the S1P gradient between the lymph node and the periphery is disrupted, via local up regulation of S1P in the lymph node, which is mediated by tumour necrosis factor (TNF) [49]. This leads to a retention of lymphocytes in the lymph node [49]. Antigen-specific lymphoctyes also down regulate $S1P_1$ receptor expression, which in turn leads to an accumulation of antigen-specific lymphocytes in the lymph node [50].

1.3.1.2 Antigen delivery

There are three routes of delivering antigen to the B cell within the secondary lymph node.

Low molecular weight (LMW) antigen (<70kDa), is delivered to the margin of the B cell follicle via the conduit network [51]. These soluble antigens then diffuse into the B cell follicle, within 1 minute, and rapidly spread by passive diffusion throughout the follicle [39]. Within 10 minutes of antigen entry the antigen-specific B cells have engaged with and taken up their cognate antigen [39]. The antigen is then processed and presented on the B cell surface in the context of major histocompatibility complex class II (MHC II) within 4 hours [39].

Lymph-borne particulate and large IC antigens are unable to enter the B cell follicle by diffusion. Instead, the subcapsular boundary acts as a sieve, restricting entry to larger

antigen [39]. Live cell imaging studies have shown that the SCS macrophages, that line the subcapsular boundary, are able capture IC antigens [52]. The SCS macrophages capture the antigen, via the complement receptor macrophage receptor-1 (MAC-1), handing the IC complexes to passing B cells as they migrate into the B cell follicle [52, 53]. The SCS macrohpages do not phagocytose the captured antigen, instead, it is moved from the subcapsular luminal side of the cell to the follicle side, where it is presented on long process for the migrating B cells to pick up [39]. It has been demonstrated that SCS macrophages are able to retain and present antigen to naïve B cells for up to 72 hours post initial antigen exposure [54]. Naïve B cells transfer the SCS macrophage presented IC antigen into the B cell follicle, in a non antigen-specific manner, via a binding of the complement receptors CR1 and 2 [52]. These non-antigen specific B cells carry their cargo on a long uropod at their trailing edge, trailing their cargo behind them [52]. Antigen-specific B cells are also able to acquire antigen from B cells that are carrying IC antigen into the follicle [52].

Once inside the follicle B cells transfer the IC antigen to the FDCs via binding of the FcγRIIb on the FDC surface [39]. The FDCs are then able to rapidly internalise the IC antigen into a non-degradative compartment [55]. The antigen is then recirculated, periodically, to the FDC surface and displayed to cognate B cells [55]. This combined mechanism of antigen retention, relocation and preservation ensures that the antigen load persists within the follicle for late arriving B cells to encounter [52].

If the B cell that collects the antigen from the SCS macrophage is antigen-specific it will pause for a longer period at the macrophage and engage its BCR, allowing more antigen to be collected [52]. This in turn triggers migration of the activated B cell toward the T cell region [52].

Recently homed B cells are also able to capture antigen outside of the B cell follicle. As mentioned previously, DCs are continuously probing the conduit network for incoming antigen. This antigen is then taken up by the DC and processed and presented to $CD4^+$ T cells in the context of MHC II; whole antigen is also presented on the surface of DCs for B cells to encounter [39]. Immediately after entering the lymph node, via the HEV, the B cells survey the DCs, scanning them for cognate antigen [45]. If the cognate antigen is present, the B cells will stall and uptake the antigen from the DC. These B cells will remain outside of the B cell follicle and receive $CD4^+$ T cell help from the surrounding T cells [45]. Upon antigen encounter on a DC, the B cells remain in contact with the DC by upregulating the chemokine receptor CCR7 [45]. The newly engaged B cell also upregulates CD86, which acts as a costimulatory molecule for CD28 which is expressed on $CD4^+$ T cells [45].

1.3.2 B cell activation

B cells are activated via engagement of the BCR by cognate antigen, either on its own or as an IC on the surface of an FDC (Figure 1.4, phase I). Prior to BCR engagement, B cells randomly migrate within the follicle at 6 - 7μm/min [43]. In order to engage with the antigen, the B cell migration is arrested by LFA-1 expression on the B cells, which is promoted by CXCL13 expression by the FDC [56]. Upon BCR engagement, the BCR complexes undergo a rapid actin-dependent membrane spreading response, which increases the number of BCR-antigen interactions [57]. The BCR microclusters then enter a contraction phase that also recruits cytosolic signalling and constimulatory molecules (CD19) to become a microsignalosome [58]. The clustered microsignalosomes form the central part of the immune synapse (IS), which is surrounded by an outer ring of adhesion molecules [58]. The outer ring of adhesion molecules reduces the activation threshold of the BCR, particularly for low-affinity cognate antigens [59]. After IS formation the presented antigen is then freed from the APC, via localised protease release into the IS [60]. The BCR is then endocytosed and the captured antigen is then degraded and processed to form MHC-II-antigen complexes, which are then transported to the surface of the B cell [61]. The BCR captured antigen is processed in compartments with a low pH [62]. The expression of HLA-DO in B cells leads to the preferential presentation of peptides obtained via BCR capture to $CD4^+$ T cells [62]. The affinity of the BCR for the antigen is proportional to the capacity of the B cell to present antigen to $CD4^+$ T cells [63]. BCR engagement also induces CD86 expression, which is required for $CD4^+$ T cell activation [64].

The activated B cell then migrates towards the T cell boundary, along a CCL19/21 gradient, where the MHC-II-antigen complexes are then presented to $CD4^+$ T cells (Figure 1.4, phase II) [65, 66]. B cells polarise the MHC-II-antigen complexes on their surface and form a second IS with the $CD4^+$ T cell. Bidirectional signalling occurs in this second IS, providing TCR stimulation from the B cell and activation signals from the T cell to the B cell [67]. The activation signals received from the $CD4^+$ T cell include cytokine stimulation and CD40 to CD40L interaction between the B and T cell. The CD40-derived signals leads to the increase in antigen presentation by the B cell, stabilisation of CD86 expression and also induction of CD80 (an important T cell priming molecule), leading to activation of both cells.

Upon the formation of the B and T cell partnership at the follicle edge, forming within 30 hours after antigenic challenge, the partnership forms a stable, motile pairing that remains in contact for more than 45 minutes [68]. The pairing are highly motile, with the B cell dragging its T cell partner around the follicle edge [68]. During this interaction, the $CD4^+$ T cells are able to secrete cytokines in a polarised manner, allowing local

secretion of IL-2 and IFN-γ into the IS, whilst secreting pro-inflammatory, IL-4 and TNF, cytokines into the surrounding tissues [39, 69]. This movement of the B and T cell partnership, allows the distribution of pro-inflammatory cytokines whilst the B cell receives adequate T cell help. The motile B and T cell partnership may also serve to bring T cell help into the follicle, by dragging T cells into the follicle [39].

After the CD4$^+$ T cell interaction the activated B cells migrate to the extra-follicular region, where they secrete low-affinity antibodies as short-lived plasma cells for a short period of time providing a rapid serological response against their cognate antigen (Figure 1.4) [70, 71, 72]. At the same time another group of BCR activated B cells, which have a high level of CXCR5 expression, migrate to the intra follicular zone where they continue to proliferate and form the germinal centre (GC, as discussed in 1.3.2.2) [73].

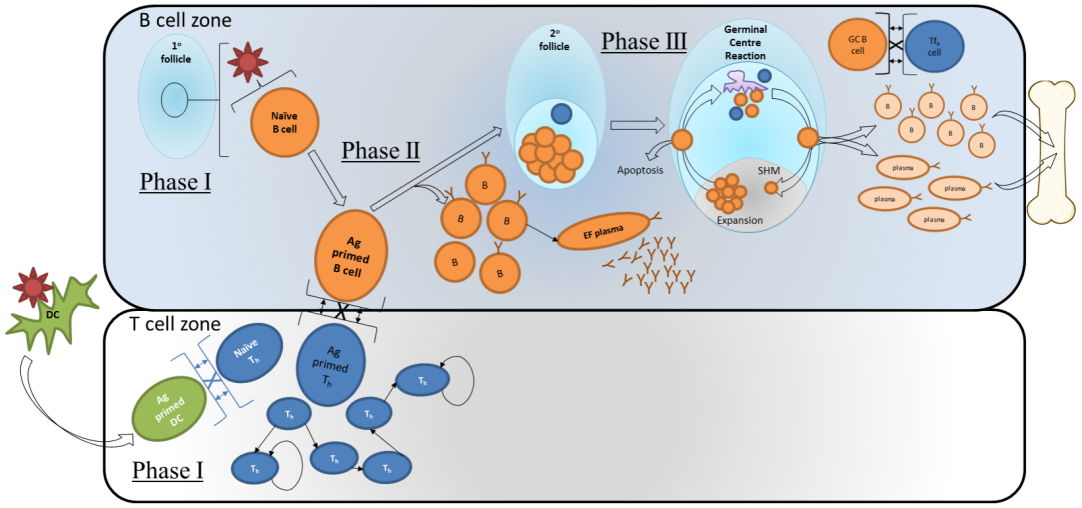


FIGURE 1.4: Schematic representation of the germinal centre reaction in response to a TD antigen. From left to right, phase I shows the naïve B cell interacting with an antigen primed FDC, this occurs in primary B cell follicle located within the B cell zone of the secondary lymphoid organ. Simultaneously an antigen-primed DC is also interacting with a naïve CD4$^+$ T cell, resulting in T cell activation and proliferation. Phase II shows the interaction between the antigen-primed activated B and T cells, resulting in proliferation of the antigen-primed B cells and differentiation into short-lived plasma cells secreting low affinity antibodies. A proportion of the antigen-primed B cells form a secondary follicle and a germinal centre. Phase III shows the germinal centre reaction with B cells circulating from the dark zone to the light zone resulting in interactions between the FDC, germinal centre B cell and germinal centre CD4$^+$ T cell, resulting in either apoptosis of the cell or differentiation into memory B cells or long-lived plasma cells. Adapted from [74].

1.3.2.1 CD4$^+$ T Follicular Helper cells

Follicular helper T (T_{FH}) cells are polarised CD4$^+$ T cells that are specialised to provide help to B cells. They participate in many aspects of the B cell response to antigen,

including early B cell proliferation, extra-follicular B cell response, GC development and maintenance, affinity maturation and the development of both long lived plasma and memory B cells [75]. T_{FH} differentiation begins during antigen priming by DCs, which up regulates, the transcription factor, Bcl-6 and the chemokine receptor CXCR5. The up-regulation of Bcl-6 leads to the up regulation of CD40L on the cell surface [76]. The $CD4^+$ T_{FH} cell then migrates to the B-T cell border of the follicle. Antigen is then presented to the $CD4^+$ T cell, in the context of MHC-II, by an antigen-specific B cell, which also expresses an inducible co-stimulator ligand (ICOSL) [77]. The B cell is stimulated by the CD40L expression on $CD4^+$ T cells. Engagement of ICOSL with an inducible co-stimulator (ICOS), which is expressed on the surface of $CD4^+$ T cell, leads to further expression of Bcl-6 [77]. The inhibitory PD-1 receptor is also up regulated by B cell stimulation of $CD4^+$ T cells [77]. Once polarised the $CD4^+$ T_{FH} cells are able to secrete IL-21, an important B cell survival factor and migrate into the germinal centre, where they initiate the GC reaction. The induction of T_{FH} cells occurs rapidly, with detectable T_{FH} cells from 48 hours after acute Lymphocytic choriomeningitis virus (LCMV) infection [77].

1.3.2.2 The Germinal Centre

The B cell follicle is a specialised micro environment that serves to support the cellular interactions required to promote a high-affinity antibody response to antigen. Within the GC micro environment the stimulated B cells undergo a process of affinity maturation [78] which serves to improve BCR affinity for its cognate antigen by approximately 1 to 2 orders of magnitude [79]. Unlike their higher-affinity counterparts the extra-follicular plasma cells are unable to undergo affinity maturation but are able to undergo class-switch recombination enabling them to secrete antibodies with different heavy chain subclasses [74]. The B cells that are destined to become GC B cells down regulate the expression of the chemokine receptor EBI2, which allows migration of the stimulated B cells into the centre of the B cell follicle, initiating the GC reaction [80]. GC B cells also adopt an elongated dendritic morphology whilst in the GC [39].

The classical representation of a GC is of spatially separated zones; the dark zone for B cell proliferation and SHM and the light zone for affinity selection. In the dark zone the B cells, known as centroblasts, down regulate their BCR expression, express the cell cycle protein Ki-67 and undergo rounds of proliferation (Figure 1.4) [81]. The centroblast V region undergoes random point mutations which serves to increase immunoglobulin V region diversity, thereby changing the affinity of the BCR for its cognate antigen; this process is known as SHM. The accumulation of these random point mutations is in the order of 10^{-3} to 10^{-4} mutations per base per cell division [82]. In humans it has

been shown that there are two mechanisms involved in SHM; one targets mutational hotspots to areas within the V region that contains a purine\G\pyrimidine\A amino acid motif [83]. The other mechanism utilised during SHM leads to the incorporation of error-prone DNA synthesis, which leads to mismatched nucleotides between the original and template DNA strands [84].

Once SHM is completed the centroblasts re-enter the cell cycle, the BCR is re-expressed and they become known as centrocytes. The B cells circulate between the dark and light zones of the GC and only emerge from the light zone if their BCR is of a suitable affinity for the cognate antigen. The antigen is presented on the surface of the FDCs and survival signals are provided by the $CD4^+$ T_{FH} cells present in the GC [85]. However, recent studies have shown that GC B cells do not need to migrate between the light and dark zone to be selected [86].

Affinity maturation is a directional selection process, which is driven by the ability of B cells to access antigen on the FDC [87]. B cells with a high affinity BCR are able to out-compete B cells with a lower affinity BCR for antigen and therefore provide $CD4^+T_{FH}$ cells with survival signals. Both proliferation and survival signals are generated by the $CD4^+T_{FH}$ cells and FDCs during the affinity maturation process, including FDC expressed CD23 interacting with B cell expressed CD21 and also production of the proliferation inducing cytokine IL-2 [88, 89, 90]. GC B cells will die within hours without $CD4^+T_{FH}$ cell help, highlighting the importance of $CD4^+T_{FH}$ cell survival signals in the maintenance of the GC microenvironment [76]. $CD4^+T_{FH}$ cells produce IL-4, an important survival factor for GC B cells [91]. IL-4 production, by $CD4^+T_{FH}$ cells is dependent upon the ligation of the signalling lymphocytic activating molecule (SLAM)-associated protein (SAP). SLAM is a homophyllic receptor, that binds SAP, and is highly expressed on GC B cells located within the light zone [92]. Thus the interaction between the $CD4^+T_{FH}$ cell and the GC B cell, allows the GC B cells to induce IL-4 from the $CD4^+T_{FH}$ cell [91]. The interaction timing between the GC B cell and the $CD4^+T_{FH}$ cells is much shorter than the previously described interaction at the B cell follicle border during the primary induction of the B cell response [39]. IL-21 is also another important cytokine produced by $CD4^+T_{FH}$ cells and is required to sustain the GC reaction [93]. Indeed, programmed death receptor 1 (PD-1) signalling, via ligation of the PD-1L/2L expressed on the GC B cell, promotes IL-21 expression by the $CD4^+T_{FH}$ cells [94].

Higher affinity B cells are able to uptake more antigen from the FDC surface and are therefore able to present more MHC-II-peptide complexes on their surface, which in turn leads to selection through survival signals from GC T_{FH} cells [92, 95]. It has recently been demonstrated that affinity maturation is also regulated by the presence and affinity

of antigen-specific antibodies produced by GC plasma cells [87]. By blocking access to antigen presented on the FDC, unless a higher affinity BCR is present, antibodies produced by GC plasma cells serve to drive the development of high-affinity B cells by competing against centrocytes for antigen presented on the FDC [87].

1.3.2.3 Class switch recombination

The isotype of the antibody secreted by a plasma cell is highly regulated and dependent upon the type of antigen encountered and the signalling pathways activated [5]. Class switch recombination enables the Cμ heavy chain constant region to be to switched to another Ig C_H region, leading to a switch of isotype expression from IgM to IgG, IgA or IgE [96]. The process requires 2 stimuli, the first stimuli can be T-dependent or T-independent and leads to the induction of the enzyme activation-induced cytidine deaminase (AID) and other CSR related transcription factors, which are required to implement CSR [97]. The second stimuli is provided by cytokines (IL-4, IL-5, IFNγ and TGFβ) and targets which Ig heavy chain constant region is to be recombined (Figure 1.5, Table 1.2).

Pathogen pattern recognition receptors bind conserved epitopes on a broad array of pathogens. On the basis of differential binding by these receptors the immune system is able to adapt the type of $CD4^+$ T cell response, inducing different cytokine secretion from T cells (Table 1.2). T_h1 cells generate cytokines, such as interferon (IFN)-γ, interleukin (IL)-1β, and tumor necrosis factor (TNF)-α, which support cell-mediated immunity [98]. Conversely, T_h2 cells produce IL-4, IL-5 and IL-10, and also down-regulate the T_h1-cell response [99]. T_h17 cells produce IL-17 [100]. This allows the immune response to be tailored towards different pathogenic threats, for example a intracellular viral and bacterial infection is likely to induce a T_h1 response, whereas a fungal infection will induce a T_h17 response and a helminth infection a T_h2 response [99], although the cytokine milieu produced during infection is not always clear cut [101]. The Th1/Th2/Th17 $CD4^+$ T cell polarisation has also been recently identified in cattle [102]. The cytokines induced by the polarisation of the $CD4^+$ T cell response are able to initiate CSR in the GC B cell, thereby tailoring the antibody response to the pathogen (Table 1.2).

The IgC_H locus is highly ordered with repetitive regions of DNA, known as S regions, that flank the 5′ end of each C_H gene [5, 103]. The type of CSR (i.e. stimulating cytokine) signal determines which S region is targeted for transcription [104]. The process of CSR involves an intrachromosomal rearrangement that occurs between 2 S regions, leading to an excised loop of DNA that contains upstream C_H genes [96]. The

Cμ gene is located at the proximal end of the V_H cluster, thus during CSR the required C_H gene is inserted adjacent to the previously recombined V region (as described in 1.1.1). The enzyme AID is crucial during both CSR and SHM, its expression is B cell lineage specific and is highly expressed in B cells that are undergoing CSR [97, 105]. During both V region or C_H1 S region transcription, the DNA helix is opened to reveal single stranded DNA. This region is deaminated by AID to create mismatched DNA base pairs. Differential repair of the lesion created by AID then leads to either SHM or CSR, depending upon whether the S region is absent or present, respectively [105].

T-dependent CSR occurs within the GC and is induced by engagement of CD40, expressed on the GC B cell surface, with CD40L (CD154) expressed on the $CD4^+$ T_{FH} cell surface (Figure 1.5) [106]. CD40 engagement coupled with IL-4 signalling induces the expression of high levels of IgG1 and IgE isotype antibodies [107]. Whereas the same CD40 signalling coupled with IL-5 or TGFβ leads to IgA isotype expression [107]. IFNγ signalling during a TD response induces IgG2a isotype antibodies [107] (Table 1.2).

Class switch recombination can occur independently of $CD4^+$ T cell stimulation, allowing rapid production of class-switched antibodies before T cell help becomes available [97]. Synergistic signalling between the BCR and the Toll-like receptors (TLR1, 2, 4, 7 or 9), which recognise a number of conserved pathogen associated molecular patterns on pathogens, can induce CSR to IgG3 [97, 108]. This dual BCR-TLR signalling can also induce other immunoglobulin isotypes in the presence of IL-4, IFNγ and TGFβ (Table 1.2) [108]. Signalling via transmembrane activator and calcium modulator and cyclophilin ligand interactor (TACI), the B cell activating factor of the TNF family (BAFF) and a proliferation-inducing ligand (APRIL) receptors (see section 1.3.3.1), can also induce CSR to IgA in synergy with BCR signalling [108]. CSR can also be induced by syngistic signalling from both TACI (via BAFF) and TLR7 and 9 [108]. Therefore the combination of T-independent (TI) and -dependent (TD) mechanisms of inducing CSR allows a rapid response to TD antigens whilst the GC reaction can develop, but equally provide a means of protection against TI antigens.

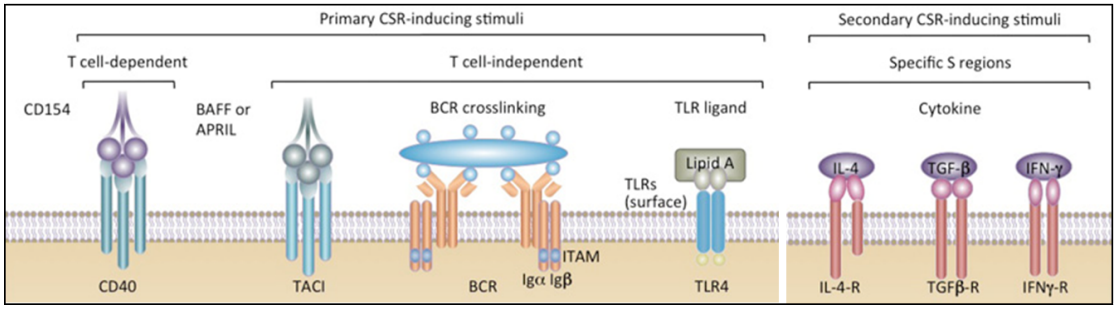


FIGURE 1.5: Schematic representation of the T-dependent and T-independent signalling pathways involved in CSR. Adapted from [97].

TABLE 1.2: Cytokines involved in class switch recombination

$CD4^+$ T cells	Stimulating Cytokine	Immunoglobulin isotype					
		IgG1	IgG2a	IgG2b	IgG3	IgA	IgE
T_h1	IFNγ	−	+	−	−	−	−
T_h2	IL-4	+	−	−	−	−	+
	IL-5					+	$^+/_-$
T_h17	IL-17		+		+		
T_{reg}	TGFβ			−	−	+	

+ = induces secretion, − = inhibits secretion, $^+/_-$ = Augments secretion.

Immunoglobulin isotypes induced or inhibited by cytokine stimulation produced from $CD4^+$ T cell subsets. Adapted from [17].

Thus B cells that have undergone SHM and CSR have tailored both the antigen-binding ability (V region) and the effector mechanism (C region) of their antibody to best control that particular antigen.

1.3.2.4 B cell fate

The molecular mechanism for determining B cell fate (long-lived plasma or memory B cell) is not clearly understood. Several possible mechanisms of how B cell fate is determined have been proposed.

It has been proposed that it may be governed by BCR affinity [109]. High affinity receptor B cells are initially pushed towards plasma cell differentiation and then pushed towards the memory B cell compartment once secreted high affinity antibody levels have reached a concentration that leads to simultaneous interactions of the FcγRII receptor and the BCR on the centrocyte surface (Figure 1.6) [109].

The CD40 signalling on the B cell along with cytokine stimulation (provided by $CD4^+$ T_{FH} cells) has also been shown to drive B cell differentiation. Stimulation by IL-4 along with a prolonged ligation of CD40, expressed on GC B cells, by CD40L, expressed on $CD4^+T_{FH}$ cells, leads to memory B cell differentiation [89, 95]. Whereas, a shorter period of ligation of CD40 and IL-10 stimulation leads to plasma cell differentiation [89, 95]. IL-21, secreted by $CD4^+T_{FH}$ cells, has also been implicated in the differentiation towards long-lived plasma cells [94].

Another proposed explanation of how GC B cell fate is determined could be a temporal switch between long-lived plasma cell or memory B cell differentiation. Early failure of the GC reaction leads to a considerably reduced number of long-lived plasma cells but

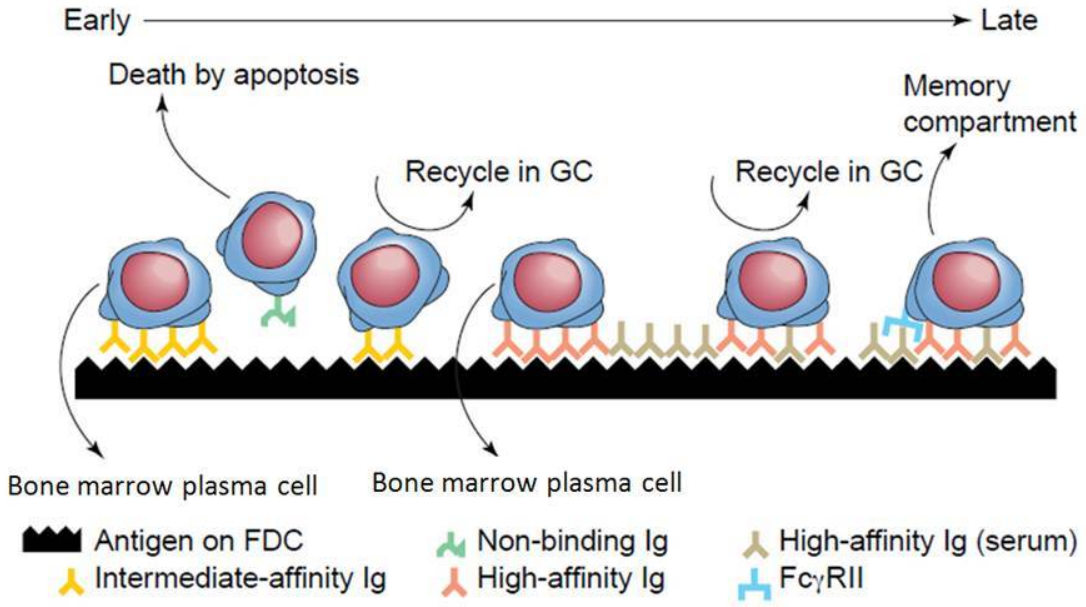


FIGURE 1.6: Model representing plasma cell and memory B cell differentiation, in the germinal centre over the duration of an immunological response, based upon their BCR affinity. Taken from [109].

with little impact upon the number of memory B cells. It has also been shown that memory B cells tend to express BCRs with a lower affinity for their cognate antigen, compared to their long-lived plasma cell counter parts [110]. The V regions of memory B cells also tend to be less mutated, suggesting that very little SHM has occurred [111]. Taken together this would suggest that memory B cells are differentiated early during the GC reaction, with long-lived plasma cells undergoing differentiation later in the reaction [112]. However, the conditions that promote this temporal switch are yet to be elucidated.

It is of note that the number of memory B cells generated after immunisation declines over time, with a large decrease (by approximately two thirds) in the number of memory B cells over a relatively short period (8 weeks) following the peak of the memory B cell response, suggesting that not all memory B cells generated during a response are destined to become long-lived memory B cells [113].

Typically memory B cells are referred to as being $CD27^+$, although there are a subset of memory B cells that are negative for this marker [114]. Since not all memory B cells are destined to become long lived memory B cells, perhaps the $CD27^+$ subset of memory B cells are expressing a marker of activation, rather than one of longevity [115].

The drive towards plasma cell differentiation switches the expression of the membrane-bound form of the immunoglobulin molecule to a secreted form, coupled with an large

increase in antibody production per cell [16]. Indeed, plasma cells can express and secrete antibody within 30 minutes of stimulation, secreting between 0.5 - 1 x 10^8 antibody molecules per hour [116, 117]. Thus a relatively small population of plasma cells (0.1 - 0.6 % of nucleated cells in the bone marrow) are able to maintain a pool of circulating antibody [118]. However, antibody half-life is relatively short (0.5 - 8 days, depending upon antibody isotype). To maintain protective antibody levels requires continuous secretion of antibody by plasma cells. Therefore, the plasma cell pool must have a mechanism of persistence or maintenance [16, 119].

1.3.2.5 GC-independent memory B cells

The generation of long-lived plasma cells appears to be exclusively via the formation of the GC reaction. Memory B cells, on the other hand can also be generated in a GC-independent manner. There are a number of memory B cells subsets that differ in their cell surface marker expression, dependence on survival factors, V region mutation status and BCR isotype expression [112]. This suggests heterogeneity within the memory B cell compartment, which is likely to be generated via a number of mechanisms.

A recall antibody response can be generated against antigens that do not elicit T cell help (T-independent (TI) antigens, see later section 1.5). Transfer of B cells from immunised mice into a host that lacked antigen-specific antibodies resulted in the induction of a recall antigen-specific antibody response upon primary immunisation in the new host [120]. It has also been shown that in Bcl-6 negative mice, which lack the ability to form GCs, memory B cells were able to be generated. However they exhibited non-mutated V regions [112]. Thus in the absence of GCs, the B cell memory compartment can be produced [112]. However, the number of memory B cells produced is low, the BCR is generally of a lower affinity and there are fewer isotype switched cells in this in the absence of GC formation [112]. These GC-independent memory B cells are also not long-lived with a half-life that is the same as a naïve B cells [113, 121]. It has been shown that under strong antigenic-stimulation transient GCs are able to form in the presence of TI antigens, although it is not clear if these GCs are fully functional [122]. However, they may serve to induce memory B cells against TI antigens.

GC-independently formed B cells tend to be of an IgM isotype, with fewer IgG isotype cells [112]. It has been proposed that IgM^+ memory B cells preferentially regenerate GCs upon re-stimulation, whereas IgG^+ memory B cells will differentiate into plasma cells [112]. The functional role of these memory B cell subsets is yet to be fully elucidated, but clearly both subsets are likely to act in concert with the long-lived plasma cells to provide long-term humoral protection.

1.3.3 Maintenance of long-term serological protection

Following immunisation or infection, protective antibody titres can be detected in an individual for many years [16]. Immunological memory provides an individual with a means of responding to an antigenic re-challenge promptly and with a greater affinity to the antigen. As described in 1.3.2.2, long-lived plasma and memory B cells are generated by the GC reaction during the primary antigenic challenge. Thus a successful vaccine strives to achieve a life-long protective antibody response, quantified by the presence of circulating antigen-specific antibodies and memory B cells that can respond should the individual be re-challenged. For example, smallpox vaccine stimulates the generation of detectable antigen-specific circulating antibodies and memory B cells for more than 50 years in the absence of any further antigenic stimulation [123]. However, a question remains as to how serological and cellular memory can be maintained throughout an individual's lifetime, and whether there is the need for a persistent antigen source to provide a means of continuous re-stimulation.

Memory B cells provide a rapid high affinity serological response to re-challenge and are detectable in peripheral circulation for a prolonged period after the primary challenge [124]. They can either be class-switched (i.e. express IgG, IgA or IgE) or non-switched (i.e. express IgM). Non-switched memory B cells are described as being recirculating memory B cells and show a scattered splenic distribution [125]. Whereas IgG^+ memory B cells have been shown to localise to regions next to vestigial germinal centres [125]. These class-switched memory B cells are able to present antigen to $CD4^+$ T cells and also require $CD4^+$ T cells stimulation for their reactivation [125]. Upon reactivation they are able to rapidly repopulate the GC micro environment and produce high-affinity plasma cells [125], thus providing an interim protective mechanism before the naïve B cell population has matured.

Upon antigen-specific activation, a proportion of the stimulated memory B cells differentiate into plasma cells which are detectable in the periphery 3-4 days post boost immunisation [124]. It has also been demonstrated that memory B cells can also be activated in the absence of $CD4^+$ T cells during viral infection [126]. This is thought to be via BAFF and APRIL signalling and via the complement regulatory protein C4 binding protein (C4bp) which is able to mimic CD40L and activate memory B cells in a TI manner [127].

It has long been noted that the bone marrow is the primary site of persistent antibody production [128]. After formation in the GC, plasma cells migrate to the bone marrow where they undergo terminal differentiation and secrete large amounts of antibody [16]. These long-lived, non-proliferating, antigen-specific plasma cells secrete antibody from

specific niches in the bone marrow, and can continue to secrete antibody in the absence of antigen [129, 130]. Survival signals are provided by the bone marrow stromal cells, promoting survival and preventing the plasma cells from undergoing apoptosis [131]. The number of plasma cells found within the bone marrow remains constant (approximately 0.5%) throughout an individuals lifetime [132]. This constant plasma cell frequency suggests that newly formed plasma cells must compete with the previously establish plasma cell pool to gain entry into the specific bone marrow niches [133]. In mice, it has been demonstrated that long-lived plasma cell have a half life of approximately 40 days, thus the plasma cell pool in the bone marrow must be continuously replenished in order to maintain protective antibody titres [134]. Unlike naïve B cells that have an absolute requirement for BCR signalling for activation, memory B cells can be activated via polyclonal stimuli derived from microbial infection (e.g. CpG motifs binding the toll-like receptor 4) or bystander activated $CD4^+$ T cells [134]. Bernasconi *et al.* has shown the re-emergence of a previously established antigen-specific plasma cell response after immunisation with a third-party antigen, suggesting that bystander stimulation of the memory B cell pool could provide a mechanism of replenishing the long-lived plasma cell pool and the resulting antibody production [134]. However, the re-emergence of a previously established plasma cell response could also be the long-lived plasma cells being out-competed for the bone marrow niche by the newly generated plasma cells that have resulted from the third party immunisation [133].

Crotty *et al.* demonstrated that memory B cells generated after smallpox vaccination are initially expanded in number (representing approximately 1.5 % of the total IgG^+ memory B cell population) followed by a decline (half-life of < 1 year) and then a plateau (representing approximately 0.1 % of the total IgG^+ memory B cell population) that is maintained for more than 50 years [123]. The biphasic kinetic of the memory B cell response to antigen could be attributed to the migration of memory B cells out of circulation, cellular competition or retention of stimulating antigen on FDCs that is then lost after the initial memory B cell expansion, causing the decline in numbers [123]. The segregation of IgG^+ memory B cells to regions adjacent to vestigial GCs may explain the decline in the number of circulating antigen-specific IgG^+ memory B cells [123]. This niche supports these memory B cells in their quiescent state until they encounter their cognate antigen and can rapidly repopulate the nearby GC micro environment and expand into a affinity-matured high-affinity plasma cell pool [125].

Follicular dendritic cells play a key role in presenting intact antigen during the germinal centre reaction, they have also been implicated in maintaining the memory B cell pool by retaining multiple antigens on their surface for prolonged periods of time [135]. Indeed, FMDV is detectable on the FDC network within the light-zone of the germinal centre for up to 38 days after infection [136]. FDCs are also able to obtain immune-complexed

antigen from non-cognate B cells and 'store' it within a non-degradative compartment. The antigen is then recycled to the surface, periodically, to stimulate antigen-specific B cells [55]. This mechanism of antigen presentation and recycling by FDCs shows how the memory B cell pool can be maintained for a long period of time without any further exogenous antigen (infection or vaccination) being administered. The proximity of the class-switched memory B cell compartment to vestigial GCs may allow the interaction of FDCs with the memory B cells, thereby stimulating plasma cell differentiation and maintenance of the long-lived plasma cell pool.

It is likely that the maintenance of long-term serological protection is achieved in both an antigen-dependent manner, via a persisting antigen pool, and in an antigen-independent manner, via bystander stimulation. Thus providing three mechanisms that ultimately result in the maintenance of a protective antibody pool.

1.3.3.1 BAFF and APRIL signalling

Both BAFF and APRIL play an important role in the regulation of the B cell response and have been shown to provide B cell survival signals during the maturation process, plasma cell differentiation and GC maintenance [137, 138]. They have also been implicated in the T-independent antigen response [139]. They are both members of the tumour necrosis factor (TNF) family and are expressed as membrane-bound cytokines, which then undergo proteolytic cleavage to produce their soluble form [137]. BAFF and APRIL bind the transmembrane receptors B cell maturation antigen (BCMA) and transmembrane activator and TACI, although not with the same affinity [137]. BAFF also binds a third receptor, the BAFF receptor (BAFFR) [137]. The BAFF and APRIL receptors, TACI and BCMA, show differential expression patterns on a number of B cell subsets [140]. It has been shown that BCMA signalling can induce antigen presentation in activated B cells [141]. Dual BCR and TACI, or TACI and Toll-like receptor (TLR), signalling on B cells can also induce CSR [97].

BAFF and APRIL are produced by FDCs and monocytes, respectively [142, 143]. It has been demonstrated that IFNα, IFNγ, lipopolysaccharide (LPS) and CD40L signalling are able to induce BAFF and APRIL expression in both monocytes and FDCs [144]. Both BAFF and APRIL are also produced by bone marrow stromal cells, sustaining long-lived plasma cells within the bone marrow niche [145]. Thus, BAFF and APRIL play an important role in the regulation of the B cell response to both T-dependent and T-independent antigens.

1.4 B cell subsets

Within an individual there are many different antibody specificities, derived from an array of B cells, circulating at any one time. Mature B cells can be divided into 3 subsets: follicular or conventional B cells (B-2 cells), marginal zone (MZ) B cells, and B-1 cells, each subset differing in its ability to respond to antigen and tissue distribution [145].

1.4.1 Follicular B cells

Follicular B cells express antigen-specific BCRs that are, in general, monoreactive [146]. Naïve follicular B cells that exited the developmental niche of the bone marrow are able to recirculate between the blood and secondary lymphoid organs. They are able respond to both TI and TD antigens within the B cell follicles of the secondary lymphoid organs forming extra-follicular plasma cells, long-lived plasma cells and memory B cells [145].

1.4.2 Marginal zone B cells

Marginal zone (MZ) B cells express an 'innate-like' BCR that is polyreactive and can respond to an array of epitopes [146]. In mice, they are non-circulating B cells that reside in the marginal zone of the spleen, which acts as an interface between the circulation and the lymphoid tissue [147]. This interface allows the interaction between circulating blood-borne antigens and MZ B cells due to the low flow rate of the blood passing through the splenic marginal zone [148]. In humans, MZ B cells have also been identified in the inner wall of the SCS of the lymph node, the epithelium of the tonsular crypts and the subepithelium of the MALT. The cellular composition of these regions are similar to the splenic marginal zone [149]. There is also evidence, in humans at least, that MZ B cells are able to recirculate in the periphery [150, 151]. Bovine MZ B cells are yet to be defined, however immunohistochemical staining of wax embedded spleen samples has shown that approximately 90% of the nucleated cells in the splenic marginal zone are positive for the B cell marker BLA.36 [152]. Pega *et al.* have also shown the presence of antigen-specific antibody secreting cells in cattle spleen tissue, following live-virus challenge with foot-and-mouth disease virus (FMDV) [153]. Thus suggesting the presence of marginal zone B cells in cattle. However the phenotype and whether these spleen-resident antibody secreting cells are able to circulate is yet to be confirmed.

Marginal zone B cells are able to respond to intact antigen presented by macrophages, DC or neutrophils, which induces plasmablast differentiation and large amounts of low

affinity IgM, rapidly [147]. This rapid induction of IgM secretion provides a protective mechanism to bridge the time lag until the induction of high-affinity Igs are produced by follicular B cells [147]. Like follicluar B cells, MZ B cells are able to undergo class-switch recombinaton, to secrete IgG and IgA, and there is also evidence of SHM in the BCR, although the mechanism of SHM is unclear [149]. MZ B cells are also able to differentiate into short-live plasma cells via toll-like receptor signalling, in the absence of BCR signalling [154].

Marginal zone B cells are also able to participate in antigen uptake and presentation, via high expression of CD21 (antigen uptake of immune complexed antigen) and presentation due to high expression levels of MHC-II [145, 155]. This gives them the ability to activate naïve $CD4^+$ T cells in the secondary lymphoid organs, thus eluding to a role in the initiation of the TD response to antigen [155].

1.4.3 B-1 B cells

B1 B cells express antibodies that are of a low affinity but are able to bind multiple antigens that are often shared between a number of pathogens [16]. These naturally occurring, 'innate-like' antibodies are usually IgM, IgA or IgG3 isotype and provide early protection against pathogen infection without the requirement of GC formation [16]. B-1 B cells are continuously activated by bacterial antigen, mitogens and autoantigens but are short-lived, thus are constantly replaced by newly differentiated B-1 plasma cells [16]. There is also evidence to suggest that these B cells are able to form a TI protective IgM^+ memory B cell response following *Borrelia hermsii* infection in mice [156].

B-1 B cells can be further subdivided by their CD5 expression, B-1a ($CD5^+$) and B-2a ($CD5^-$), both are found in the pleural and peritoneal cavities [157]. These cells are highly sensitive to lipopolysaccharide (LPS) stimulation, thus providing rapid protection against bacterial infection [158]. B-1 B cells are also able to secrete IgA, providing protection against mucosal pathogens [159].

Induction, via antigen and TLR stimulation, of antibody secretion from both MZ and B1 B cells is much more rapid than from follicular B cells, thus providing a rapid mechanism of generating antibody during pathogenic challenge [147]. Both of these B cell subtypes also express B-lymphocyte-induced maturation protein 1 (BLIMP), which is required for the formation and terminal differentiation of plasma cells, thus these cells are primed to rapidly differentiate into plasma cells and secrete antibody [160].

1.5 T-dependent and T-independent antigens

Depending upon the size and structure of the antigen, the type of immunological response generated to that antigen can be classified as requiring T cell help, termed thymus-dependent antigens (TD) or the absence of T cell help, termed thymus-independent antigens (TI) [161]. Both types of antigen are able to initiate a serological response. However, it has long been noted that in order to generate a long-term high-affinity antibody response to antigen, $CD4^+$ T cell help is required [162]. The TD response was described using thymectomised mice; the TD response to sheep red blood cells was absent in these mice showing the requirement of thymic T cells to stimulate the B cell response [163]. The hallmark of the TD response is the generation of high-affinity long-lived memory B cells, which formed during the germinal centre (GC) reaction, the formation of which is reliant upon the presence $CD4^+$ T cells.

Immune complexed antigen presented on the surface of FDCs, via FcR binding, are spaced 200 - 500$\mathring{A}$ apart on the FDC dendrites. The complement proteins, C3 and C4bp, co-localise on the FDC surface [164]. The complement protein C4bp is able to provide an accessory signal, akin to the CD40-CD40L signalling provided by $CD4^+$ T cells, in the absence of T cell signalling [164]. Thus FDCs are able to activate B cells in the absence of T cell signalling. Indeed, depletion of $CD4^+$ T cells, in mice, has shown that TD antigens can initiate a T-I response, via FDC presentation and signalling through complement proteins, leading to a rapid induction of antigen-specific IgM [165]. FDCs are able to activate B cells in a TI manner, providing a mechanism of early induction of protective IgM prior to the GC reaction and production of high-affinity antibodies to antigen.

There are two types of TI antigen; type I (TI-1) and type II (TI-2). These types differ on whether they are a polyclonal B cell stimulant (TI-1) or not (TI-2). Recent literature, also suggests a third TI antigen (TI-3), which require bone-marrow derived innate helper cell signalling to initiate a humoral response [158].

Type II TI antigens possess highly organised structures, with antigenic epitopes that are spaced between 95 - 675$\mathring{A}$ apart [165]. This epitope spacing is optimal for simultaneously engaging and cross-linking BCRs, leading to naïve B cell activation and rapid IgM induction in the absence of $CD4^+$ T cell help [165, 166, 167].

A secondary signal is required to stimulate the B cell and this is achieved either via toll-like receptor signalling or via complement activation and CD21 binding [161, 167, 168]. TI-2 antigens are able to elicit a very good extra-follicular plasma cell response but any GC formation has been shown to be non-productive with no memory B cell formation [122, 168, 169]. As discussed in section 1.3.2.3, synergistic signalling between the BCR

and TLRs is able to induce CSR, thus providing extra-follicular plasma cells with a mechanism of producing isotype switched antibodies against TI-2 antigens [170].

Whilst the B cells are activated and produce extra-follicular plasma cells in response to TI-2 antigens, the development of long-term memory B cells to these antigens is limited, particularly in young children [169] and neonatal mice [168]. This makes TI-2 antigens problematic vaccine candidates as it can be difficult to achieve long term B cell memory against these antigens. However, it has been previously demonstrated that TI-2, in particular polysaccharides, can be altered, via conjugation of a TD protein carrier, to produce a TD immunological response resulting in the induction of a more sustained memory response to the TI-2 antigen [171, 172]. Indeed, Avci *et al.* have demonstrated that conjugation of the group B streptococcal type III polysaccharide with a protein carrier (either Ovalbumin or tetanus toxoid) induces an enhanced polysaccharide-specific IgG response following booster vaccination [173]. The boosted polysaccharide-specific IgG was dependent upon the presence of $CD4^+$ T cells and not the protein carrier, thus demonstrating that $CD4^+$ T cells are able to recognise carbohydrate epitopes [173]. The authors have also shown that the carbohydrate are processed in the endosomal pathway and presented in the context of MHC-II, along with carrier protein derived peptide, on the surface of an APC [173]. Thus Avci *et al.* have proposed that conjugation of polysaccharides to a protein carrier results in carbohydrate-specific B cells recognising epitopes on the polysaccharide, which leads to BCR cross-linking and antigen uptake [173]. The antigen is then processed in the endosomal pathway and carbohydrate and carrier protein peptides are presented on the surface of the B cell in the context of MHC-II to a carbohydrate-specific $CD4^+$ T cell [173]. This in turn leads to stimulation of the $CD4^+$ T cell which induces cytokine secretion and B cell activation [173], resulting in a TD B cell response to a polysaccharide.

1.6 Foot-and-mouth disease virus

Foot-and-mouth disease (FMD) is a highly contagious viral infection that affects both domesticated and wild cloven-hoofed animals. The disease pathology leads to vesicles and skin erosions of the cutaneous mucosal surfaces and hairless skin areas, resulting in decreased animal productivity and increased mortality risk in young stock (Figure 1.7) [174]. The virus is able to spread rapidly and can be difficult to control due to the presence of both wild and domestic virus reservoirs [175]. Cattle that have recovered from FMDV infection often develop into carriers of FMDV, with replicating virus being isolated from the oropharynx of cattle up to 2.5 years post-infection [176].



FIGURE 1.7: Images of FMDV lesions in cattle taken during an FMD outbreak in Kenya, 1996. Top panel, left to right:FMDV lesions in the hoof cleft , lesions on the tongue. Bottom panel: Lesions on the gum, lesions on the udder. Taken from [177].

Control of FMDV is mediated via a number of zoo-sanitary measures; including import control, early FMD detection and culling when clinical signs are detected and FMD seropositivity is confirmed [175]. If an FMD outbreak occurs, the source of the outbreak is traced, animal movement is restricted and the aforementioned control measures are implemented [175]. FMDV-free status offers countries major economic incentives and trade opportunities, however large scale investment is required to achieve this freedom, and is beyond the means of most countries [175].

The current FMDV vaccine is manufactured as a whole virus preparation that is produced in large-scale suspension or monolayer cultures of baby hamster kidney cells (BHK-21) [178]. The filtered FMDV antigens are then inactivated using the aziridine, binary ethyleneimine (BEI) and mixed with an adjuvant [178]. The inactivated FMDV antigens are concentrated using polyethylene glycol (PEG) precipitation and ultrafiltration [179]. Even after concentration FMDV vaccines contain 1000-fold more cellular proteins than virus particles [179]. Clearly, this method of vaccine production has a number of disadvantages, the most notable being the requirement of high level bio-secure

containment during production [175]. Vaccine safety must also be proven after each batch of vaccine is produced to ensure that vaccine is free from infectious virus [179]. A final inocuity test is performed *in vitro* on a representative sample of the vaccine batch after the full inactivation period to ensure that there is less than 1 infectious virus unit per 10,000 litres of bulk antigen [180]. Vaccine potency must also be assessed, usually using cattle. The protective dose (PD_{50} value) is calculated from the number of animals protected from FMDV infection during live-virus challenge 21 days after vaccination with the inactivated FMDV vaccine batch (Further discussed in 3.2.1) [180].

The current vaccine has several limitations. It has a limited shelf life and must be kept at 4^oC until it is administered [175], and it also provides limited long-term immunity, with repeated booster vaccines required every 4 to 12 months to maintain a protective neutralising antibody titre [179]. This presents a number of logistical and economic barriers in countries that are striving for FMDV-free status [179].

1.6.1 Viral structure

Foot and mouth disease virus is a member of the *Picornaviridae* family of viruses and forms part of the *Aphthovirus* genus. There are three other members of the *Aphthovirus* genus, bovine rhinitis virus (BRV) A and B and equine rhinitis virus (ERV). FMDV can be distinguished from other members of the *Picornaviridae* family by pH sensitivity, as the FMDV capsid is acid labile [175]. The FMDV viral capsid is a non-enveloped icosohedral structure that is approximately 30nm in diameter and the wall is $33\mathring{A}$ [175]. The genome is a single stranded positive sense RNA genome of approximately 8.5 kilobases in length. The genome is translated into a single open reading frame viral polyprotein, which is then cleaved by viral encoded proteinases to produce the mature viral proteins [181]. There are four structural proteins that form the FMDV capsid: VP1, VP2, VP3 and VP4, which are encoded by 1D, 1B, 1C and 1A viral genes, respectively (Figure 1.8) [181]. The structural proteins, VP1 - 4, combine during the capsid assembly process to form a protomer, 60 of which assemble to form the capsid structure (Figure 1.9) [182, 183].

1.6.2 FMDV serotypes

There are seven FMDV serotypes that have been described: A, O, C, Asia 1 and Southern Africa Territories (SAT) 1 - 3. There is a high degree of antigenic variability between each of the serotypes [179].

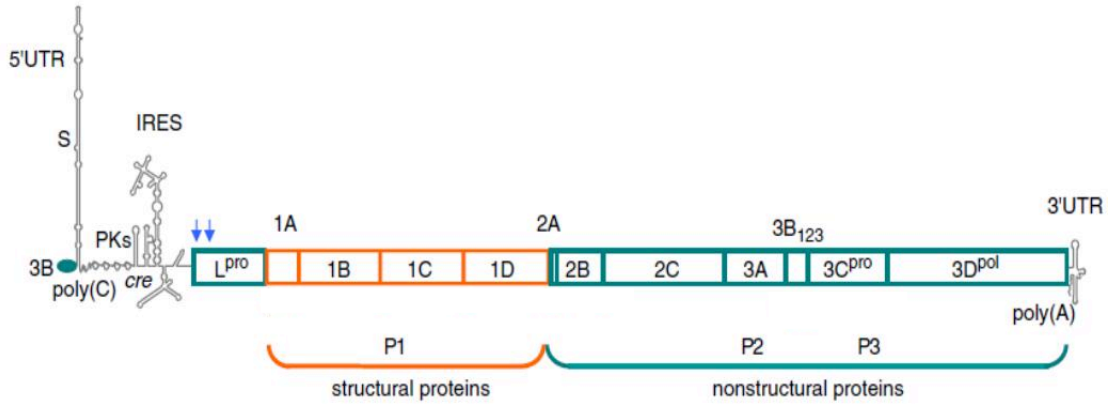


FIGURE 1.8: Shows the genomic structure of the FMDV single stranded RNA genome. The structural viral proteins are shown in orange and the non-structural proteins are in green. The 5' untranslated region (UTR) also shows the internal ribosome entry site (IRES) which is utilised in the cap-independent transcription mechanism. Taken from [184].

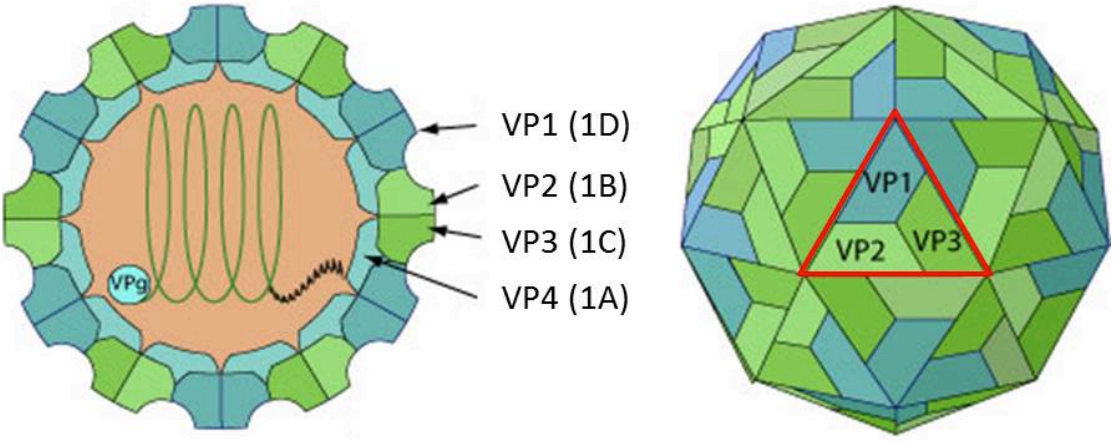


FIGURE 1.9: The structural organisation of the FMDV capsid, a cross-sectional view (left) and an external view (right). Each protomer (highlighted in red on the right) consists of 4 structural proteins, VP 1-4, with the corresponding viral gene shown in brackets. Each capsid is composed of 60 protomer units. Adapted from [184].

Worldwide there are three endemic regions of FMD: Asia, Africa and South America, within these regions there are 7 regional virus pools, each with regional strains and more than one FMDV serotype (Figure 1.10) [175]. Each FMDV serotype shows between 30-50% nucleotide variation within their VP1 sequence and within strains the sequence can differ by up to 15% [185].

The FMDV serotypes are clinically indistinguishable, however, each strain has its own antigenic and epidemiological characteristics [187]. This makes vaccine development and planning difficult as vaccine derived immunity is often strain specific, with little intra-strain immunity [188].

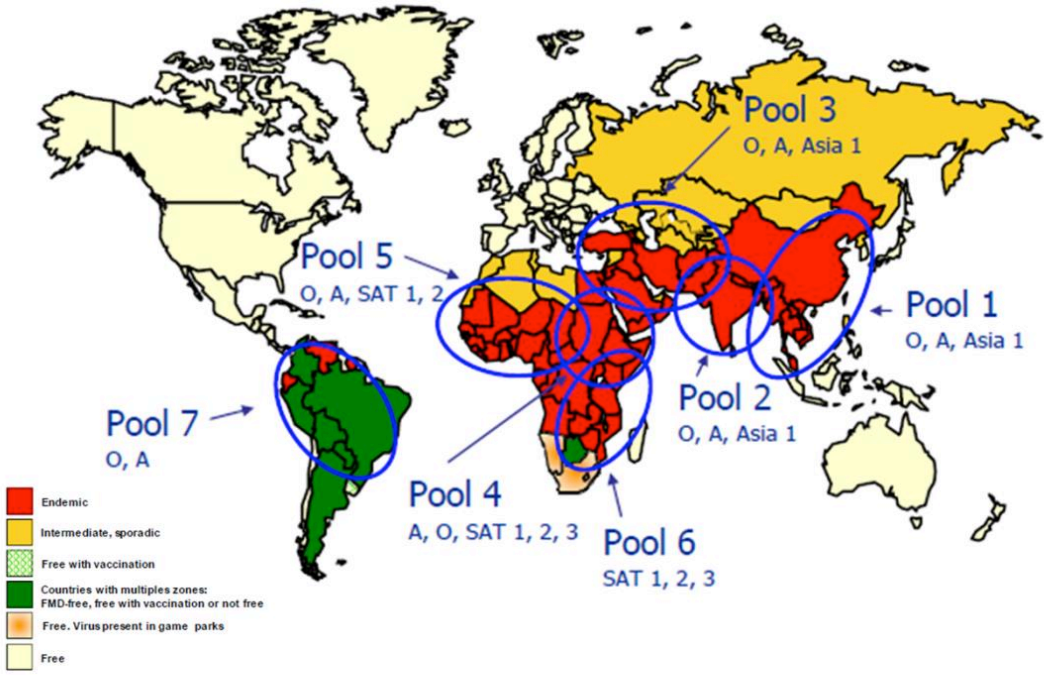


FIGURE 1.10: Schematic showing the global distribution of FMDV and also the 7 defined virus pools with the detailed list of FMDV serotypes circulating within each pool. Taken from [186].

1.6.3 FMDV pathogenesis

Viruses are obligate intracellular pathogens that are reliant upon their host for propagation and survival. FMDV utilises integrins, which are heterodimeric glycoproteins, to gain access to the host epithelial cells. *In vitro* studies have shown that FMDV is able to bind four different integrins: $\alpha V\beta 1$, $\alpha V\beta 3$, $\alpha V\beta 6$, and $\alpha V\beta 8$. However, FMDV has the highest affinity for $\alpha V\beta 3$ and $\alpha V\beta 6$, which are expressed on epithelium, both before and during FMDV infection, with a proportionally higher expression of $\alpha V\beta 6$ [189]. This may indicate that $\alpha V\beta 6$ is likely to be the receptor during primary infection. Whereas, $\alpha V\beta 3$ has a higher expression in blood vessels thus suggesting a role during viral spread and secondary infection [189]. The viral capsid binds the integrin via a highly conserved RGD (Arginine (R) - Glycine (G) - Aspartic acid (D)) motif of the βG-βH loop that protrudes from within the VP1 protein [175, 190].

Once bound to its integrin receptor, FMDV is internalised via receptor-mediated endocytosis into the endosome [191]. The low pH within the endosome leads to capsid

dissociation and viral genome release [191]. It has also been suggested that the structural protein, VP4 also plays a roles in the release of viral genome, although the exact mechanism is yet to be elucidated [175]. Once within the cytosol the viral genome is translated via a cap-independent mechanism, which is due to the presence of an internal ribosome entry site (IRES) located in the 5' untranslated region (UTR) of the genome (Figure 1.8) [192]. During cap-dependent translation the eukaryotic initiation factor 4F (eIF4F) complex recruits the ribosomal 40s subunit to the mRNA prior to translation [193]. However, in a FMDV infected cell the non-structural viral protein, leader protein (Lpro), encodes a proteinase that is able to cleave the eIF, thus disrupting and hijacking the host's protein synthesis mechanism to produce more viral progeny [192].

1.6.4 FMDV immunogenicity

There are several different confirmations of the FMDV structural proteins: the whole virus particle (146S), empty virus particles (75S) and a pentameric cluster formed of VP1, 2 and 3 (12S) [179]. The immunogenicity of each of these virion structures differs, with 146S being the most immunogenic and 12S the least [194]. There is also a hierarchy in the ability of 146S particles from different serotypes in inducing a potent immune response, with A and C being more potent than O serotype FMDV; more O-serotype specific antibodies are required to protect against challenge [179].

The FMDV capsid is an inherently unstable structure which is sensitive to both heat and pH. The pH sensitivity of FMDV differs between serotypes; with C serotype viruses being more acid labile than A and O, particle integrity and infectivity were decreased at pH 7.5 (serotypes A and O) and 7.0 (serotype C) [179]. Thermal stability also differs between serotypes with A and Asia-1 being the most stable and SAT 1-3 the least. The O and C serotypes have intermediate thermal stability, although virus inactivation is likely to reduce the thermal stability of all serotypes. There is a correlation between the thermal stability of the FMDV virion and its immunogenicity, with 146S virus particles being more thermo-stable and immunogenic as compared to 75S and 12S, which are very thermo-stable [194, 195]. Thus, stability of the 146S structure is essential for promoting good vaccine efficacy and the poor thermal stability exhibited by the FMDV capsid may account for the lack long-term immunity derived from FMDV vaccination [179].

Passive immunity studies in cattle have shown that protection from FMDV infection is mediated by antibody [196]. These studies were performed in cattle and demonstrated that calves born to dams that had been regularly vaccinated against FMDV serotypes A, O and C had protective levels of FMDV-specific antibodies that were maternally

derived, i.e. obtained via the colostrum, as the levels of maternal antibodies declined in the calves, the FMDV neutralising antibody titres also declined [196].

Adoptive transfer studies in mice have shown that post-FMDV vaccination the protective antibody response is generated via a T-independent mechanism [197]. Indeed, depletion of $CD4^+$ T cells in cattle has shown that the neutralising antibodies generated against FMDV are T-independent, but the response to FMDV non-structural proteins is T-dependent [198]. Thus, it can be concluded that FMDV is a largely T-independent antigen. However, Carr *et al.* have recently shown that stimulating the $CD4^+$ T cell response during FMDV vaccination is important for generating an optimum protective antibody titre in cattle [199].

1.6.5 Experimental vaccines against FMDV

The use of the current commercially available, chemically inactivated FMDV vaccines presents a number of barriers, including the requirement for stringent biosecurity measures during production. The structural proteins of the FMDV capsid are the main antigens that are responsible for inducing a protective immune response, thus recombinant DNA (rDNA) technologies have been utilised to produce FMDV vaccines that may offer improvements in efficacy, safety, and disease control and eradication.

1.6.5.1 Ad5-FMD Vaccine

It has recently been shown that naturally occurring FMDV capsids that lack nucleic acid (empty capsids) are as immunogenic as the current commercially available inactivated vaccines and are able to induce protective immunity [200, 201, 202]. This knowledge has been utilised to produce a replication deficient adenovirus vector (Ad5) that contains all relevant portions of the FMDV genome required for empty capsid synthesis and assembly. The Ad5-FMD vaccine also lacks the FMDV non-structural proteins which allow differentiation of infected from vaccinated animals (DIVA). Production of this vaccine does not require high-containment facilities for production as the process does not involve live virus. Studies in cattle have shown that immunisation with a single dose of Ad5-FMD vaccine demonstrated full protection against FMDV challenge [203]. The Ad5-FMD subtype A24 Cruzerio vaccine has recently been licensed for use in cattle by the United States Department of Agriculture Centre for Veterinary Biologics (USDA CVB). To date, this vaccine has been tested in over 300 cattle and demonstrated greater than 95% protection against FMDV disease generalisation and viremia as early as 7 days post vaccination.

1.6.5.2 Double marker cDNA-derived killed FMDV platform

This vaccine platform (FMD-LL3B3D) utilises a genetically engineered attenuated FMDV backbone, that has been altered by the deletion of the Leader protein (Lpro) and the addition of a conserved B cell immunodominant epitope. This allows the serological differentiation of vaccinated from infected animals, via the use of competitive ELISA techniques [204]. The system has been further modified by adding restriction endonulcease sites that allow the rapid replacement of FMDV capsid coding sequences, which allows emerging field strains to be incorporated into the vaccine platform [204]. This vaccine platform is still in the early stages of development but early protection studies have shown that vaccination with chemically inactivated FMD-LL3B3D virus and protected 100

1.6.5.3 FMDV peptide vaccines

The use of FMDV capsid based peptide vaccines has had some considerable success in small animal model (mice and guinea pigs). Immunisation of these animal models has induced FMDV VNT titres and protection against FMDV challenge. However, these results have not been reproduced in cattle

The GH-loop, of the VP1 FMDV capsid protein, has been used as a synthetic peptide vaccine candidate. Taboga *et al.* tested 4 different FMDV serotype C GH-loop peptides in 138 cattle, using different vaccine doses and vaccination regime but was only able to induce 40% protection against live-virus challenge [205]. Attempts to try and improve the GH-loop peptide vaccine were made, incorporation of promiciuos T_H sites into the GH-loop was able to induce a high level of protection in pigs [206]. However, this success did not transfer to cattle with the vaccine failing to protect against live-virus challenge 21 days after vaccination [207]. Attempts have been made to improve the immunogenicity of FMDV peptide vaccine by adding the cholera toxin to the vaccine, studies in mice have shown that the vaccine is able to induce neutralising antibodies [208]. However, this vaccine has not been trialed in pigs or cattle.

The most recent development in the peptide vaccine field is dendrimeric peptides, which contain one copy of an FMDV T-cell epitope branching into four copies of a B-cell epitope [209]. Cubillos *et al.* have shown that pigs immunised with the dendrimeric peptide are protected against live-virus challenge, and were also protected from FMDV transmission to contact animals [209]. However, this dendrimeric vaccine has not been tested in cattle. Thus significant further research is required to produce a sucessful FMDV peptide vaccine in cattle.

1.6.5.4 Alternative Virus-like particles (VLP) Platform

Virus-like particles (VLPs) are structurally indistiguishable from their parental virus [210]. However, VLPs present a major advantage over inactivated FMDV vaccines in that they are non-replicating and non-pathogenic. They are similar in size and conformation to intact virions and are formed by the self-assembly of capsid proteins in an expression system. There are a number of expression systems that have been used for the expression of VLPs including mamalian cell lines with vaccinia virus expression vector, plants cell lines with a baculovirus expression vector, yeast and bacterial cells. However, the optimum production of viable VLPs has been from the mammalian cell line with a vaccinia virus expression vector and plant cell lines with a baculovirus expression vector (C. Porta, Personal communication). Mammalian cell lines are able to produce assembled VLPs that are of a high quality, however the yield is lower than that of the baculovirus/plant cell line expression system (C. Porta, Personal communication). Thus, VLPs produced on the baculovirus/plant cell line are most likely to be commercially viable. Indeed, it has recently been demonstrated that VLPs produced using this expression system, have been able to induce protective immunity in cattle [211].

1.7 Understanding the B cell response in cattle

Antibodies play a pivotal role in protecting cattle against FMDV infection and most of our current knowledge of the B cell response to antigen has been obtained through studies in humans or mice. The hallmark of an effective vaccine is long duration of humoral immunity (e.g. small pox) [123]. Induction and maintenance of the B cell memory response, both antibody titres and memory B cells, is clearly complex with many mechanisms acting to ensure long-durations of immunity.

To date, the majority of studies into the bovine B cell response have been largely limited to monitoring antigen-specific antibody titres and the ability of antibody to neutralise virus. The shortfall in detailed studies on the B cell response in cattle is largely due to a lack of bovine-specific reagents. The detailed descriptions of B cell biology that have been presented in this introduction have been largely derived from studies in humans and mice. Thus, improving our understanding of the bovine plasma and memory B cell response to antigen, in particular FMDV, will help to drive informed vaccine design.

1.8 Thesis aims and objectives

This thesis looks to improve the currently knowledge on the antigen-specific bovine B cell to FMDV. Data suggests that FMDV is a largely T-independent antigen. Thus the kinetics of the bovine B cell response to a TD and TI-2 antigen must first be defined before applying this knowledge to a FMDV vaccination and challenge model. The B cell response to novel FMDV antigens in both the peripheral blood and also the lymph compartment will also be defined. Finally, next generation sequencing will be used to explore the bovine B cell receptor repertoire in response to vaccination with novel FMDV antigens. The thesis aims will be achieved by the following objectives:

1. Define the important immunological parameters that characterise T-independent and T-dependent immune responses in cattle.
2. Determine if bystander stimulation is a possible mechanism of maintaining a long-duration of immunity.
3. Development of FMDV specific ELIspot assay.
4. Define the FMDV-specific B cell response after vaccination with conventional inactivated FMDV vaccines.
5. Define the FMDV-specific B cell response after live-FMDV challenge.
6. Define the FMDV-specific B cell response after vaccination with novel FMDV vaccine antigens in peripheral blood and efferent lymph.
7. Investigate the bovine immunoglobulin repertoire following primary and booster vaccination.
8. Identify potentially FMDV-specific immunoglobulin transcripts.

Chapter 2

Understanding the bovine T-dependent and T-independent B cell response

2.1 Chapter objectives

1. Define the important immunological parameters that characterise T-independent and T-dependent immune responses in cattle.
2. Determine if bystander stimulation is a possible mechanism of maintaining a long-duration of immunity.

2.2 Introduction

It has been shown that the structure of a viral capsid impacts upon the type of immunological response generated during viral infection. Viruses with capsids that have random or mobile antigenic sites tend to generate a T-dependent immune response. Whereas capsids that have a more repetitive/non-random structure, with antigenic epitopes spaced 510nm apart, will preferentially generate a T-independent immunological response [25]. Viral infection models in mice have shown that acute cytopathic viruses frequently induce T-cell independent antibody responses [212]. FMDV is a non-glycosylated icosahedral capsid formed from 60 copies each of the structural polypeptides VP1 to VP4 [213], thus the capsid structure is highly organised, and is likely to have repeating epitopes.

Studies in calves born to dams that have been regularly vaccinated against FMDV have shown that the calves are protected from FMDV infection due to the presence of

protective FMDV-specific antibodies in the colostrum [196]. However, adoptive transfer studies, in mice, have shown that post-vaccination the protective antibody response was generated via a T-independent mechanism [197]. Indeed, depletion of $CD4^+$ T cells in cattle has shown that the neutralising antibodies generated against FMDV are T-independent, whilst the response to FMDV non-structural proteins were generated via a T-dependent mechanism [198]. Thus, it can be concluded that FMDV is a largely T-independent antigen. The duration of immunity is limited following FMDV vaccination, with regular repeated booster vaccines being required every 4 to 12 months to maintain a protective neutralising antibody titre [179]. Thus understanding the bovine B cell response to antigen, in particular, FMDV will allow improved vaccine design.

However, before the B cell response to FMDV can be explored the kinetics and profile of the bovine antigen-specific plasma and memory B cell response to a model TD and TI-2 antigen must be defined. To assess this in cattle the kinetics of the antigen-specific plasma and memory B cells were defined by immunising cattle with either a well defined TD antigen (the hapten 2,4,6-trinitrophenyl, TNP, conjugated to chicken gamma globulin, TNP-CGG) or a TI-2 antigen (TNP conjugated to aminoethylcarboxymethyl-FICOLL, TNP-AECM-FICOLL). A subsequent immunisation with a third party TD antigen was given to determine if there was an effect upon the recall B cell response previously established to either the TD or TI-2 antigen.

2.3 Material and methods

2.3.1 Calves and immunisation protocols

Ten male 8-month-old conventionally reared Holstein-Friesian calves (*Bos Taurus*, Pirbright Institute, Compton, UK) were split into two randomly selected groups of five. In the first group, each calf was subcutaneously immunised with 3 mg of the hapten 2,4,6-trinitrophenyl (TNP) conjugated to the TD antigen chicken gamma globulin (TNP-CGG, Biosearch technologies, Novato, CA, USA) in QuilA adjuvant (Superfos Speciality Chemical a/s, Vedbaek, Denmark). In the second group, each calf was subcutaneously immunised with 3 mg of TNP conjugated to the TI-2 antigen aminoethylcarboxymethyl-FICOLL (TNP-AECM-FICOLL, Biosearch technologies, Novato, CA, USA) in QuilA adjuvant (Superfos Speciality Chemical a/s). All calves were boost-immunised 29-days later with the same immunising antigens, as described above (TNP-CGG in the TD group and TNP-AECM-FICOLL in the TI-2 group). At day 134 post-primary immunisation (pi) all calves, from both groups, were subcutaneously immunised with 3 mg of

tetanus toxin fragment C (TTC, PXTherapeutics, Grenoble, France) in incomplete Freunds adjuvant (IFA, Difco Laboratories, Detroit, MI, USA). Subsequently, all animals were boosted with TTC and IFA at day 197 pi. A group of control animals was given a primary and booster immunisation of adjuvant alone (including IFA). These animals showed no detectable antigen-specific plasma, memory B cells or IgG titres throughout the study. Heparinised peripheral blood and serum samples were taken from all animals at various time points following the immunisations. All experiments were approved by the Pirbright Institute's ethical review process and were in accordance with national guidelines on animal use.

2.3.2 Bovine peripheral blood mononuclear cell (PBMC) isolation

Bovine PBMCs were isolated from the heparinised peripheral blood samples using density gradient centrifugation. The blood samples were diluted 1:2 using Dulbeccos phosphate buffered saline (dPBS, Invitrogen), layered over Histopaque 1.083 g/mL (Sigma-Aldrich) and centrifuged for 30 min at 1200g. The mononuclear cell layer was recovered after centrifugation and remaining red cells were lysed using ammonium chloride lysis buffer (155 mM NH_4Cl, 10 mM $KHCO_3$, 0.1 mM EDTA, pH7.2). After two further washing steps using dPBS, the PBMCs were enumerated using a Neubauer haemocytometer (Hawksley, Lancing, UK). A fraction of the enumerated fresh PBMCs were diluted to the required concentration and stored at 4^oC until required for the detection of plasma cells.

2.3.3 Memory B cell culture

An ELIspot medium was used in all experiments aimed at quantifying plasma and memory B cells and consisted of RPMI 1640 with L-Glutamine and 25 mM Hepes (Invitrogen, Paisley, UK) supplemented with penicillin (100 units/mL), streptomycin (100 μg/mL), 1 x non-essential amino acids (Sigma-Aldrich, Gillingham, UK), 1 mM sodium pyruvate and 15% heat-inactivated horse serum (Sigma-Aldrich). At the indicated time-points, some PBMCs were cultured as described below to induce the terminal differentiation of memory B cells into antibody secreting cells (ASC) prior to their detection by ELIspot assay. Briefly, $2x10^7$ bovine PBMCs were cultured for 6 days in 20 mL of ELIspot media (final PBMC concentration: $1x10^6$/mL) supplemented with 5 μg/mL pokeweed mitogen (PWM, Sigma-Aldrich), 10 μg/mL anti-bovine CD40 mAb (ILA158, kindly donated by ILRI, Kenya), 20 ng/mL recombinant human IL-2 (AMS Biotechnology Ltd, Abingdon, UK) and 7.3 units/mL bovine IL-10 (kindly donated by Dr G Entrican, Moredun Research Institute, Midlothian, UK). At the end of the culture period, the 6 day-cultured

PBMC were recovered, washed twice in ELIspot media, enumerated and stored on ice until being used for the detection of induced ASC by ELIspot assay.

2.3.4 Plasma and memory B cell quantification by ELIspot

MultiScreenHA plates (Millipore, Watford, UK) were coated with either 0.25 μg/mL TNP-Ovalbumin (TNP-Ova), $^1/_{1000}$ Chicken serum (containing CGG, Sigma-Aldrich) or 10 μg/mL TTC (PXTherapeutics) in 0.1 M carbonate buffer (pH 9.6) for 2 h at 37^{o}C. Plates were then washed 5 times in PBS and then blocked using 4% dried milk (Marvel, Premier Foods, St Albans, UK) in PBS. Following blocking, the plates were washed 5 times in PBS and stored at 4^{o}C until required.

Fresh or 6 day-cultured PBMCs were suspended at 5x10^6 cells/mL and 1:2 serial dilutions were performed in ELIspot medium down to 1.5x10^5 cells/mL. 100 μL/well of each suspension (in duplicate) was then incubated on the coated plates overnight at 37^{o}C in a 5% CO_2 incubator. Subsequently, the PBMCs were washed from the plates 5 times using PBS containing 0.05% Tween20 (Sigma-Aldrich). 100 μL per well of a $^1/_{1000}$ dilution of sheep anti-bovine IgG conjugated to horseradish peroxidase (AbD Serotec, Kidlington, UK) was then added to the plates for 3 h at room temperature. Following the incubation step, the plates were again washed 5 times using PBS containing 0.05% Tween20. Detection was performed by the addition of 100 μL/well of 3-amino-9-ethylcarbonate substrate (AEC, Merck, Darmstadt, Germany) and subsequent incubation at room temperature for 1 h. The reaction was stopped by washing the plates with tap water and allowing them to dry overnight at room temperature.

Enumeration of the red coloured spots on the dried ELIspot plates was performed using the automated AID ELIspot reader (Autoimmun Diagnostika GmbH, Strasbourg, Germany). Each individual 'spot' was used as an indicator for an ASC. The ELIspot results were manually validated for false positives and expressed as ASC number per 10^6 PBMCs for plasma cells and induced-ASC number per 10^6 cultured PBMCs for memory B cells (mean of duplicates). During the ELIspot data analysis any well with less than 2 spots was considered to be negative and were treated as having zero ASCs detected (minimum sensitivity: 4 ASCs per 1x10^6 PBMCs). There was very little variance (<17%) shown between the duplicate observations within each animal.

2.3.5 Enzyme-linked immunoabsorbent assays (ELISA)

96-well plastic plates (BD biosciences, Oxford, UK) were coated for 1 h at room temperature with 100 μL/well of either 20 μg/mL TNP-OVA (Biosearch Technologies) or

10 μg/mL TTC (PXTherapeutics) in carbonate buffer. Following incubation the plates were washed 5 times in PBS containing 1% Tween20 (Sigma-Aldrich). The plates were then blocked for 1 h using 100 μL/well of PBS containing 1% Tween20 and 4% dried milk (blocking buffer), followed by a washing step, as described above. Serum samples (in duplicate) were serially diluted 1:3 in blocking buffer starting at $^1/_{50}$ dilution, and 100 μL per well of each diluted serum was added before incubating the plate for 1 h at room temperature. For determination of the plate background optical density (OD) values, some wells were incubated with blocking buffer alone. Following the incubation, the plates were washed and incubated for 1 h at room temperature after addition of 100 μL/well of $^1/_{100,000}$ dilution of sheep anti-bovine IgG conjugated to horseradish peroxidase (AbD Serotec). Following washing, the plates were incubated for 10 min with 3,3,5,5-tetra-methyl benzidine (TMB, Sigma-Aldrich) substrate at room temperature. The reaction was stopped by the addition of 50 μL of 1.2 M H $_2SO_4$. The OD values at 450 nm and 690 nm were determined, for each well using a Biotek ELx808 absorbance plate reader (Biotek, Winooski, VT, USA). The antigen-specific antibody titres were calculated as follows: the $\log_{10}$ values of sample dilutions were plotted against the $\log_{10}$ values of sample OD and a regression analysis was performed on the linear part of the curve allowing the endpoint titre to be calculated using an OD of twice the background. Results were expressed as the mean of duplicate determinations.

2.3.6 Statistical analysis

Data for the number of antigen-specific IgG ASCs (for plasma and memory B cells) were log (n+1) transformed, then analysed using mixed linear models including time (as a factor) and vaccine (TNP-CGG or TNP-AECM-Ficoll), and an interaction between them as fixed effects and between animals as a random effect. Model selection proceeded by stepwise deletion of non-significant ($P > 0.05$) terms as judged by likelihood ratio tests. Data were considered significant if the calculated P values were < 0.05.

2.4 Results

2.4.1 Antibody titre kinetics following primary and booster immunisations with a TD versus TI-2 antigen.

The TNP-specific IgG titres in the TD (TNP-CGG) and the TI-2 (TNP-AECM-FICOLL) groups began to increase from day 6-8 post-primary TNP immunisation (pi) and peaked at approximately day 10pi for the TD group (8,905 $\pm$ 1,417, n=5) and approximately

day 22pi for the TI-2 group (1,664 ± 314, n=5, Figure 2.1). Subsequently, the TNP-specific IgG titres in both groups also showed an increase starting from day 4 post-TNP boost that peaked at day 12 post-TNP boost (TD group: 162,103 ± 33,339; TI-2 group: 11,226 ± 3,573, day 41pi, n=5, Figure 2.1). At most time-points, the TI-2 group TNP-specific IgG titres were over five times lower than the TD group titres (Figure 2.1). The TD group TNP-specific IgM titres showed an increase from day 6pi, peaked at day 8pi (24,635 ± 7,854, n=5) and remained elevated until day 16pi (34,838 ± 18,730, n=5, Figure 2.1). Following boost immunisation, the IgM titres in the TD group peaked at day 6 to 8 post-TNP boost (46,637 ± 17,044, day 37pi, n=5) before declining gradually (Figure 2.1). The TI-2 group also showed an increase in TNP-specific IgM titres, peaking 6 to 8 days after both the primary (2120 ± 867, day 8pi, n=5) and boost (4694 ± 578, day 37pi, n=5) TNP immunisations (Figure 2.1).

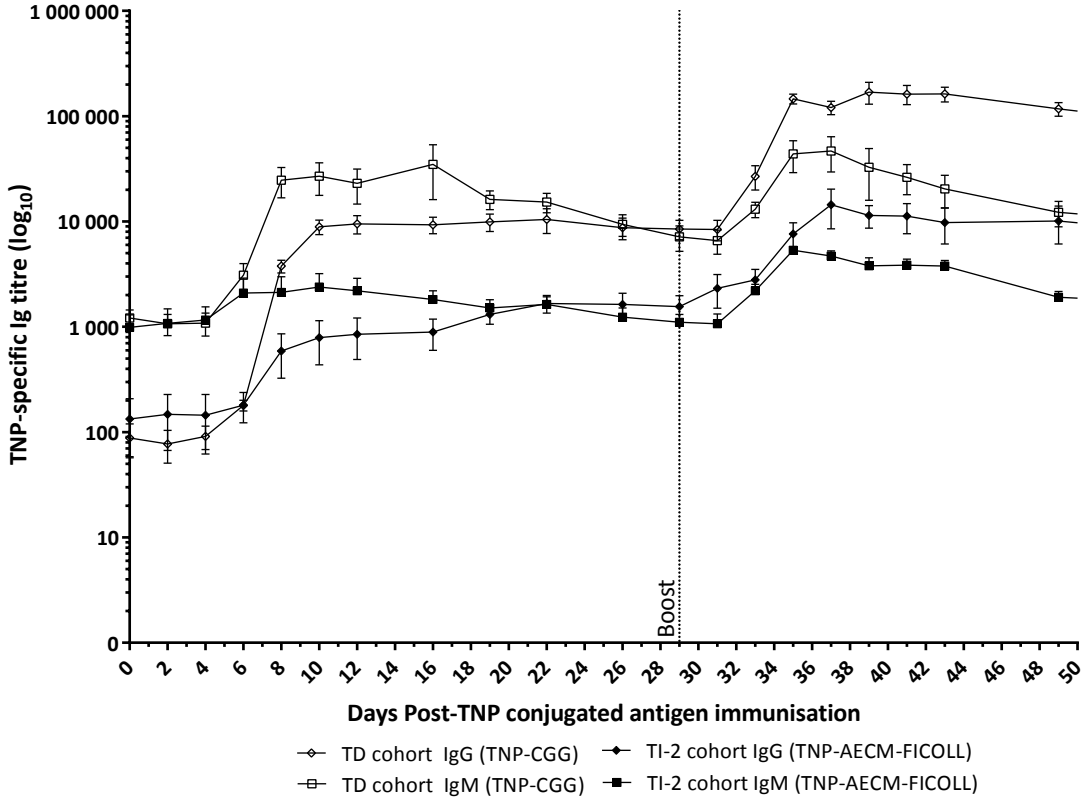


FIGURE 2.1: Kinetics of TNP-specific Ig titres following primary and boost immunisations with TNP-conjugated antigens. Five calves were subcutaneously immunised with 3mg TNP-CGG or TNP-AECM-FICOLL in QuilA then boosted 29 days later with the same immunising antigens. The dotted vertical line indicates when the booster TNP-CGG/TNP-AECM-FICOLL immunisations were given (day 29pi). Blood samples were taken at various time-points following these injections and TNP-specific IgG (diamond symbols) and IgM (square symbols) titres were determined by ELISA in calves from the T-D group (open symbols) or T-I group (filled symbols). Results are expressed as the mean of determinations from individual calves in each group ± SEM, n=5.

2.4.2 Plasma cell and memory B cell kinetics following primary and booster immunisations with a TD versus TI-2 antigen.

In the TD group, a small number of TNP-specific plasma cells were detectable at day 6-7 post primary immunisation (3 ± 1 TNP-specific ASC per 10^6 PBMC, day 7pi, n=5, Table 2.1). A burst of TNP-specific plasma cells was observed at days 3-5 post-TNP boost (280 ± 149 TNP-specific ASC per 10^6 PBMC, day 33pi, n=5, Figure 2.2, Table 2.1). Although no TNP-specific memory B cells were detected in the TD group following the primary immunisation (Table 2.1), TNP-specific memory B cells were detected from day 3 post-TNP boost, peaking at day 6-7 post-TNP boost (2,307 ± 1,187 TNP-specific induced ASC per 10^6 cultured PBMCs, day 36pi, n=5, Figure 2.2, Table 2.1) and were still detectable at day 34 post-TNP boost (17 ± 4 TNP-specific induced ASC per 10^6 cultured PBMCs, day 63pi, n=5, Table 2.1). At day 34 post-TNP boost, the memory B cell response was assessed to CGG using chicken serum as a positive control within the assay. CGG-specific memory B cells were only detected in the TD group and were approximately 5-6 fold more numerous than TNP-specific memory B cells (130 ± 40 CGG-specific induced ASC per 10^6 cultured PBMCs, day 63pi, n=5, data not shown). In the TI-2 group, TNP- or CGG-specific plasma or memory B cells were not detected at any time-point following either the primary or booster TNP immunisation (Table 2.1).

TABLE 2.1: Total number of IgG TNP-specific antibody secreting cells in PBMC population

Days post immunisation (pi)	Days post boost (pb)	TD group ($n = 5$)		TI-2 group ($n = 5$)	
		Plasma	Memory	Plasma	Memory
0		0	0	0	0
1		0	NP	0	NP
2		0	NP	0	NP
3		0	NP	0	NP
4		0	NP	0	NP
5		0	NP	0	NP
6		1 ± 0.8	NP	0	NP
7		3 ± 1	0	0	0
14		0	0	0	0
21		0	0	0	0
29	0	0	0	0	0
32	3	149 ± 30	9 ± 2	0	0
33	4	280 ± 149	114 ± 27	0	0
34	5	43 ± 25	408 ± 94	0	0
35	6	7 ± 4	1802 ± 954	0	0
36	7	1 ± 0.8	2307 ± 1187	0	0
37	8	1 ± 0.8	180 ± 61	0	0
41	12	1 ± 0.8	NP	0	NP
43	14	0	440 ± 243	0	0
49	20	0	NP	0	NP
63	34	NP	17 ± 4	NP	0

Results are expressed as the grouped mean of duplicate determinations from each animal ± SEM. NP = Not performed.

2.4.3 Immunisation with TTC induces an increase in TTC-specific plasma and memory B cells.

Each of the calves from both the TD and TI-2 groups were immunised with a third party antigen, TTC, at day 134pi and were re-immunised with TTC at day 197pi.

A burst of TTC-specific IgG plasma cells was detected between day 7 to 14 post-primary TTC immunisation in all animals (45 ± 25 TTC-specific ASC per 10^6 PBMCs, day 148pi, n=10, Figure 2.3A, Table 2.2). Following boost-immunisation with TTC at day 197pi, TTC-specific plasma cells were detected from day 3 post-TTC boost and peaked at day

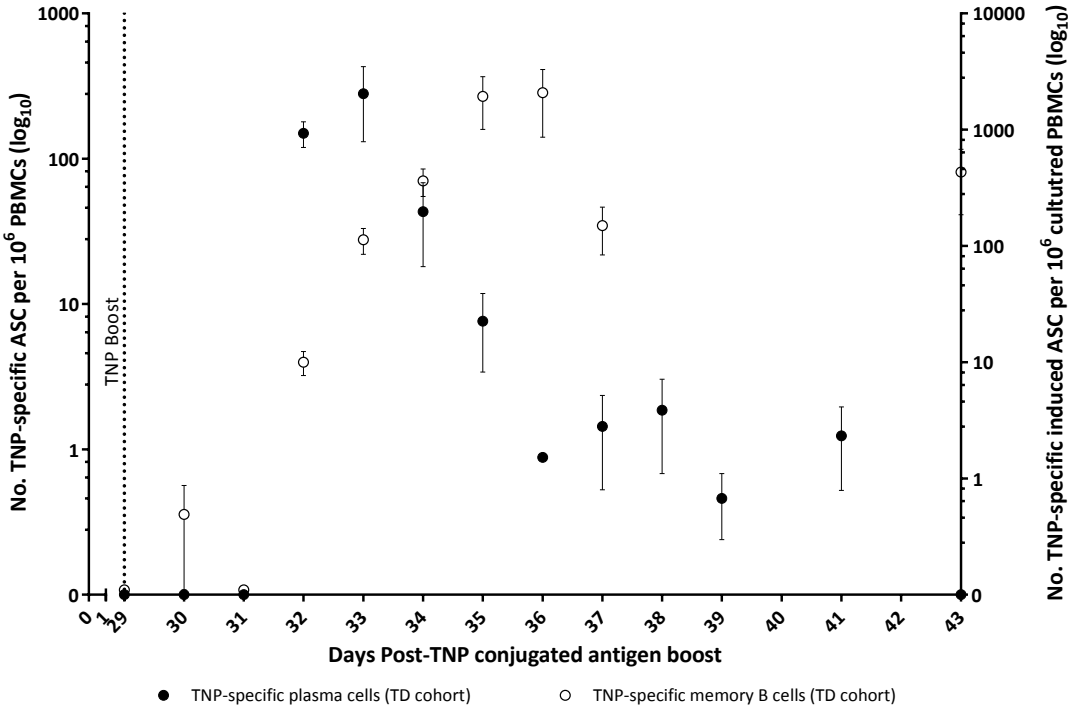


FIGURE 2.2: TNP-specific plasma and memory B cell detection post-boost immunisation with TNP-CGG (TD group). Five calves were subcutaneously immunised with 3mg TNP-CGG in QuilA then boosted 29 days later with the same immunising antigen. The dotted vertical line indicates when the booster TNP-CGG immunisation was given (day 29pi). Blood samples were taken at various time-points following the immunisations. TNP-specific IgG, plasma cell (filled circles, left-axis) and memory B cell (open circles, right-axis) numbers were determined by B cell ELIspot. Results were expressed as ASC per 10^6 PBMC for plasma cells and induced ASC per 10^6 cultured PBMC for memory B cells (mean of determinations from individual calves in each group ± SEM, n=5).

4 to 5 post-TTC boost (740 ± 179 TTC-specific ASC per 10^6 PBMCs, day 202pi, n=10, Figure 2.3A, p<0.001, Table 2.2). A small burst of IgG TNP- (2 out of 5 calves) and CGG-(5 out of 5 calves) specific plasma cells was also observed in the TD group at days 3 to 14 post-TTC primary immunisation (2 out of 5 calves showed 6 and 4 TNP-specific ASC per 10^6 PBMCs, day 141pi, n=2 and 11 ± 6 CGG-specific ASC per 10^6 PBMCs, day 141pi, n=5). Another small burst of CGG-specific plasma cells was observed in 3 out of 5 calves at days 3 to 5 post-TTC boost (3 out of 5 calves showed 4, 5 and 11 CGG-specific ASC per 10^6 PBMCs, day 201pi, n=3, p<0.05) in the animals that had previously been immunised with the TD antigen, TNP-CGG (Figure 2.3A, Table 2.2).

TABLE 2.2: Total number of IgG antigen-specific antibody secreting cells in PBMC population following immunisation with Tetanus toxoid C (TTC)

Days post immunisation (pi)	Days post TTC immunisation	Days post TTC boost	All animals (n = 10)		TD group (n = 5)			
			TTC		TNP		CGG	
			Plasma	Memory	Plasma	Memory	Plasma	Memory
134	0		0	0	0	3±2	0	125±46
137	3		0	NP	0	NP	1±1	NP
138	4		0	NP	0	NP	3±1	NP
139	5		0	NP	1±1	NP	4±1	NP
140	6		0	NP	1±1	NP	3±2	NP
141	7		4±2	0	2±1	6±5	11±6	122±34
148	14		45±25	NP	1±1	NP	2±1	NP
156	22		0	1±1	0	1±0	0	19±8
162	28			13±11	0	2±1	1±1	22±5
197	63	0	0	23±7	0	0	5±4	29±12
200	66	3	34±13	NP	0	NP	4±2	NP
201	67	4	662±240	NP	0	NP	3±1*	NP
202	68	5	740±179 *	NP	0	NP	0	NP
203	69	6	NP	1301±391	NP	3±3	NP	115±38
204	70	7	139±61	4111±700	0	8±5	1±1	117±56
205	71	8	NP	3995±1965	NP	7±6	NP	200±129
211	77	14	120±157	1163±376	0	4±2	0	173±60
218	84	21	1±1	482±156	0	1±1	0	141±55

Results are expressed as the grouped mean of duplicate determinations from each animal ± SEM. NP = Not performed.* = $p<0.05$.

All of the animals demonstrated a steady increase in the number of TTC-specific memory B cells from day 28 post-TTC primary immunisation (13 ± 8 TTC-specific induced ASC per 10^6 cultured PBMCs, day 162pi, n=10, Figure 2.3B). The number of TTC-specific memory B cells increased significantly following the boost immunisation with TTC, peaking at days 6 to 8 post-TTC boost (4,111 ± 495 TTC-specific induced ASC per 10^6 cultured PBMCs, day 205pi, n=10) and then gradually declining (Figure 2.3B). TTC-specific memory B cells were still detectable in all animals at day 21 post-TTC boost (482 ± 110 TTC-specific induced ASC per 10^6 PBMCs, day 218pi, n=10). There was also an increase in the number of TNP- and CGG-specific memory B cells in calves previously immunised with the TD antigen at day 6-8 post-TTC boost (8 ± 5 TNP-specific induced ASC per 10^6 cultured PBMCs and 200 ± 129 CGG-specific induced ASC per 10^6 cultured PBMCs, day 205pi, n= 5, Figure 2.3B).

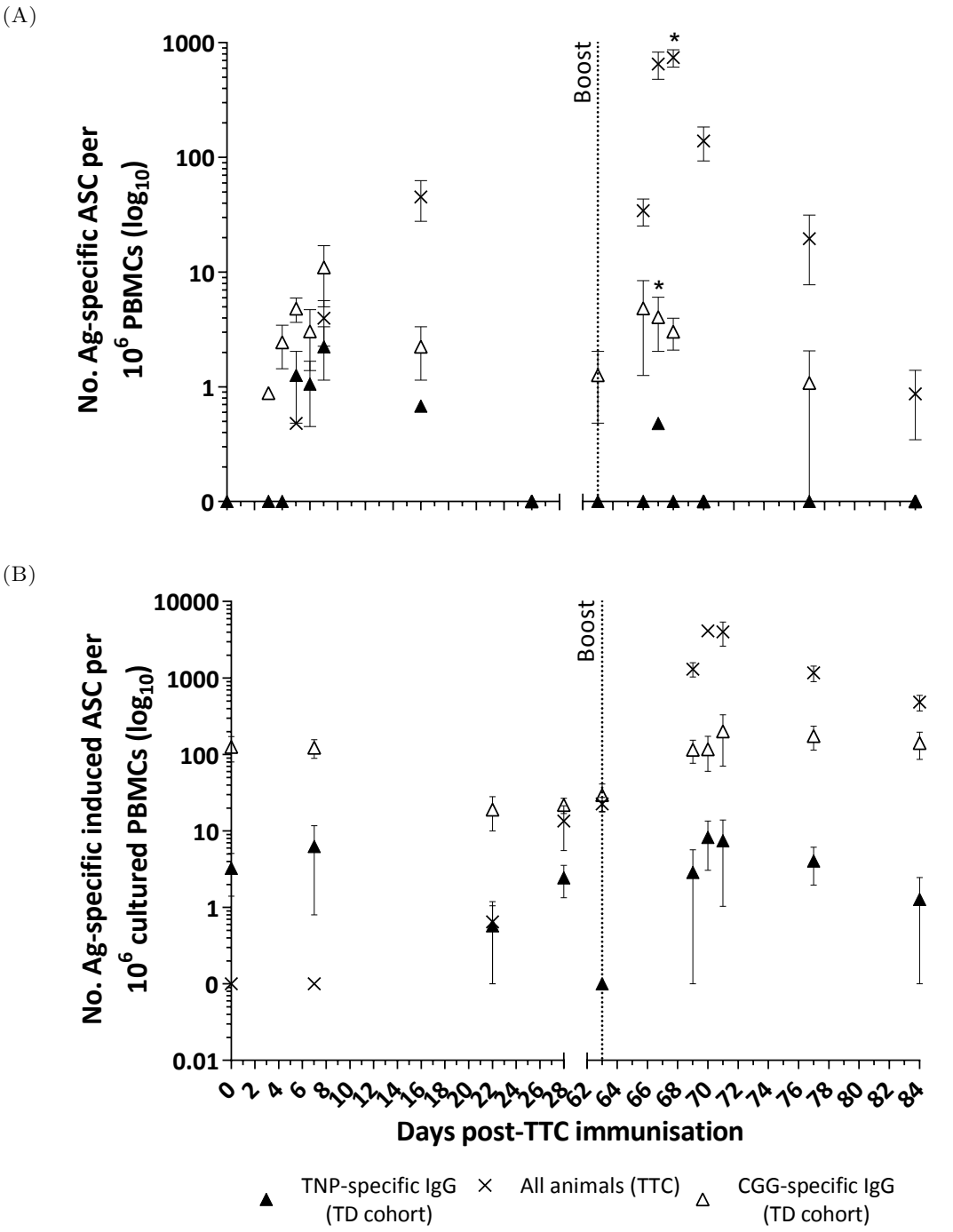


FIGURE 2.3: Kinetic of the TNP-CGG and TTC-specific (A) plasma cell and (B) memory B cell response post-TTC primary and booster (indicated by vertical dotted line) immunisation. (TNP: triangles, n=5; CGG: open triangles, n=5 and TTC: crosses, n=10). Data shown are mean of duplicate determinations for each group ± SEM. * = $p < 0.05$.

2.4.4 Immunisation with TTC induces an increase in TTC-specific IgG titres in calves.

All animals demonstrated an increase in TTC-specific IgG titres from day 14 post-TTC primary immunisation (17,074 5,889, day 148pi, n=10) and day 7 post-TTC boost (1,004,210 ± 594,085, day 204pi, n=10, Figure 2.4). Using a linear regression model, a positive correlation was demonstrated between the number of TTC-specific plasma cells post primary TTC immunisation (day 147pi) and the end-point TTC-specific IgG titre (day 218pi, $R^2 = 0.914$).

There was a small, although not statistically significant, increase in TNP-specific IgG titres at day 3 post-TTC primary immunisation in the TD group (22,794 ± 7,762, day 137pi, n=5) as compared to day 0 post-TTC primary immunisation (12,868 ± 2,913, day 134pi, n=5, Figure 2.4). There was also a small increase in TNP-specific IgG titres at day 3 post-TTC boost in the TD group (6,186 ± 2,675, day 200pi, n=5) as compared to day 0 post-TTC boost (5,327 ± 1,962, day 197pi, n=5). In the TI-2 group; TNP-specific IgG titres were not increased following either the TTC primary or boost immunisation (Figure 2.4). There was no significant increase in TNP-specific IgM titres, in either the T-D or TI-2 groups, following primary or booster immunisation with TTC (Data not shown).

2.5 Discussion

This is the first time the magnitude and the kinetics of the TD and TI-2 antigen specific B cell response has been described in cattle. Briefly, the response to the TD antigen was characterised by an expansion of TNP-specific plasma cells peaking at day 7 post-TNP primary immunisation, which was associated with a subsequent increase in the titre of TNP-specific IgG antibodies. Following booster immunisation, a larger TNP-specific plasma cell burst was detected at day 3 to 5 post-TNP boost, and was similarly associated with a larger increase in TNP-specific IgG titres. The timing and magnitude of the TD antigen-specific plasma cell bursts is in agreement with the findings of a previously published study, in which calves were immunised with another TD model antigen, ovalbumin [124]. Moreover, a plasma cell burst has also been previously detected (with identical kinetics: 6 to 7 days post-primary immunisation) in humans following their immunisation with a number of different antigens, such as inactivated influenza virus, respiratory syncytial virus, serogroup C meningococcal polysaccharides and tetanus toxoid [134, 171, 214, 215]. The timing and magnitude of the secondary plasma cell burst

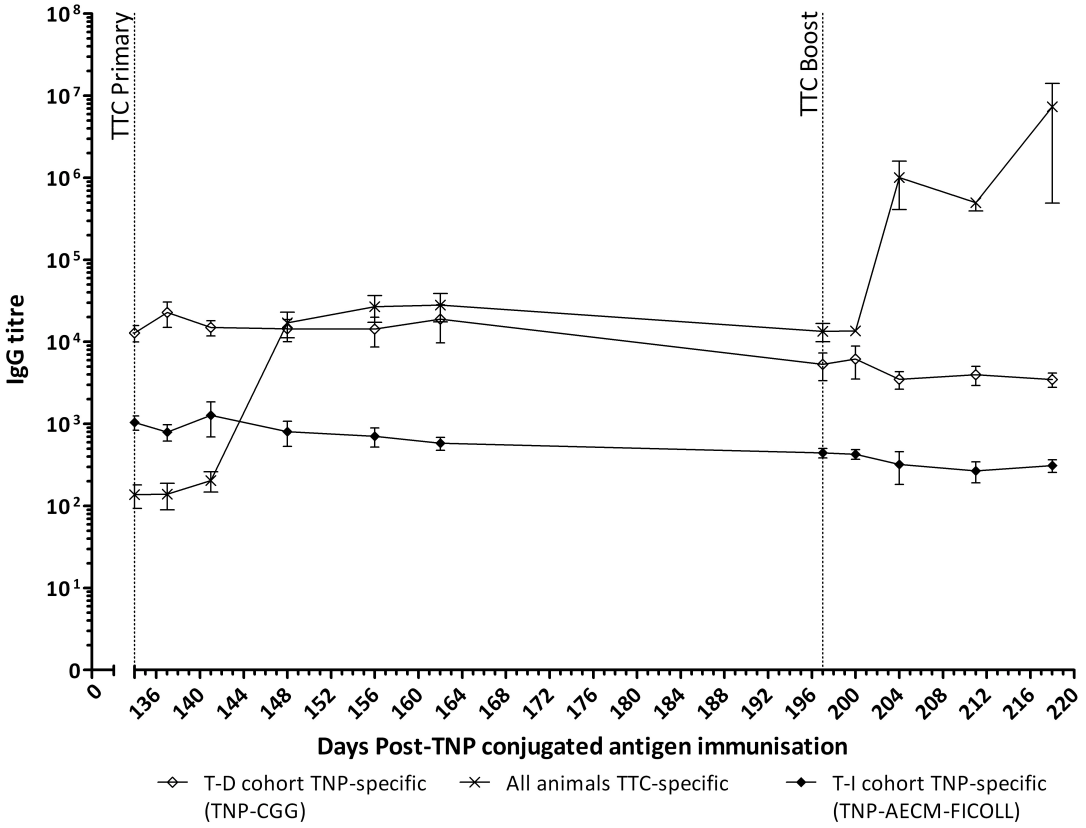


FIGURE 2.4: TNP-specific IgG titres in calves from the TD group (open diamonds) or TI-2 group (filled diamonds) and TTC-specific IgG titres in all calves (cross symbols) were determined by ELISA. The dotted vertical lines indicate when the primary and booster TTC immunisations were administered (days 134 and 197 pi, respectively). Results are expressed as the mean of determinations from individual calves in each group for the TNP-specific responses ($n = 5$) and the mean of determinations from all calves for the TTC responses($n = 10$).

and increased IgG response, i.e. a rapid and larger secondary response, is in keeping with the central dogma of immunological priming by a TD antigen [171, 216].

There was an increase in the number of TNP-specific memory B cells from day 3 post-TNP-CGG boost that peaked at day 6 to 7 post-TNP boost. TNP-specific and CGG-specific memory B cells were still detectable in the blood of calves from the TD group at day 34 post-TNP boost. The timing and magnitude of this TD antigen specific response, following booster immunisation, is in keeping with other previously published data [124]. Although no TNP-specific memory B cells were detected in the TD group following the primary immunisation. Previous studies in both humans and cattle have shown low numbers of antigen-specific memory B cells following primary immunisation with a TD antigen [124, 171]. The rapid induction of TNP-specific plasma cells from day 3 post-TNP boost and the associated increase in TNP-specific IgG antibody titres observed in the TD group suggests that a number of TNP-specific memory B cells were

indeed generated after primary immunisation, but the quantities in blood were below the detection levels of our ELIspot assay.

T-independent antigens are unable to prime individuals for a secondary immune response [171]. In this study the TI-2 group showed no detectable TNP-specific plasma or memory B cells, after either the primary or booster immunisation with TNP-AECM-FICOLL. Despite the lack of detectable antigen-specific plasma or memory B cells in the blood, there was a small increase in TNP-specific IgG titres in this group following primary and booster immunisations. It is likely that this increase in antibody titres results from the in situ generation of short-lived plasma cells, as previously described [74]. These findings are in keeping with Fink *et al.* who suggest that the absence of antigen-specific T cell help resulted in non-productive germinal centres that had a limited life-span [122]. Kelly *et al.* have also shown that following primary immunisation with a TI-2 antigen, serogroup C meningococcal capsular polysaccharide, very low/undetectable numbers of antigen-specific memory B cells were generated [171]. The results from the present study shows that in cattle the kinetics and magnitude of the TI-2 antigen-specific plasma and memory B cell response is similar to that of the human and mouse. However, it is of note that the ELIspot assay is only able to detect antibody secreting cells that are present in the peripheral blood, thus it is unable to assess responses to antigen that occur in local lymphoid tissues (e.g. BALT or GALT) or extra follicular plasma cells that remain within the lymphoid tissue.

Immunisation with the third party antigen (TTC) in this study resulted in similar TTC-specific plasma and memory B cell kinetics that have been previously described for other TD antigens [124, 171, 214, 215]. Briefly, a burst of TTC-specific plasma cells was detected from day 7 to 14 post-TTC primary immunisation and from day 3 to 5 post-TTC boost in all animals. The TTC-specific plasma cell bursts in the TD group was also associated with a small increase in the number of TNP- and CGG-specific plasma cells post-TTC primary immunisation and/or boost. These results are consistent with those previously published by Bernasconi *et al.*, which demonstrated a bystander polyclonal differentiation of memory B cells into plasma cells specific for various recall antigens (Toxoplasma gondii and measles virus) following the immunisation of humans with an unrelated TD antigen (tetanus toxoid) [134].

There was a steady increase in the number of TTC-specific memory B cells post-TTC primary immunisation followed by at least a 14 fold increase in the number of these cells post-TTC boost. The TD group also showed an increase in the number of TNP- and CGG-specific memory B cells only post-TTC boost (at day 6-8 post-TTC boost). Based on the timing of emergence of the TNP- and CGG memory B cells, it is unlikely that these memory B cells were generated from newly activated naïve B cells, but instead

suggests that pre-existing TNP- and CGG-specific memory B cells were subjected to one (or more) round(s) of antigen-independent (bystander) proliferation within the T-cell regions of the draining lymph node. This bystander stimulation of TD antigen-specific plasma and memory B cells may provide a mechanism for maintaining long term TD antigen-specific antibody titres.

In conclusion, the present study showed that bystander stimulation of an established TD B cell memory response may occur in cattle, providing a possible mechanism of maintaining protective antibody titres for long periods of time. Our findings also provided a better characterisation of the key differences between TD and TI-2 immune responses in cattle. This knowledge will be particularly useful in elucidating the B cell response to the largely TI-2 antigen, FMDV [198]. Indeed as mentioned previously, most natural pathogens contain both TI-2 and TD antigens, but viruses such as FMDV tend to preferentially generate a TI-2 immunological response [198]. Therefore, applying the knowledge gained from this study to a detailed assessment of the B cell response against FMDV in cattle could provide important data to underpin a better evaluation of novel candidate vaccines that induce a robust and sustained TD rather than a TI-2 response.

Chapter 3

Defining the bovine B cell response to foot-and-mouth disease virus

3.1 Chapter objectives

1. Development of FMDV specific ELIspot assay.
2. Define the FMDV-specific B cell response after vaccination with conventional inactivated FMDV vaccines.
3. Define the FMDV-specific B cell response after live-FMDV challenge.

3.2 Introduction

FMDV is a highly contagious virus infecting cloven-hoofed animals, leading to vesicle formation on the mouth and hooves followed by skin erosions of the cutaneous mucosa. The virus has a significant global socio-economic impact, and the maintenance of FMDV-free status is critical for the free trade of animals and animal products [174]. One of the main methods of FMDV disease control and eradication is through vaccination with inactivated FMDV virus [174]. However, the current FMDV vaccine only promotes short-term humoral immunity with regular repeat vaccinations being required to maintain protective antibody titres [179, 198].

Protection from FMDV infection is mediated by antibody. Studies from the 1920's in Germany have shown that transfer of pre-immune serum to susceptible calves immediately before challenge with FMDV conveys substantial protection [217]. Passive immunity studies have also been performed in cattle, showing that calves born to dams that had been regularly vaccinated against FMDV serotypes A, O and C had protective levels of FMDV-specific antibodies that were maternally derived, i.e. obtained via passive transfer. The FMDV neutralising antibody titres began to decrease by 2 months of age, coinciding with the decline in maternal antibody levels [196].

Adoptive transfer studies, using B cells from pre-immunised mice that were transferred into irradiated recipients, have shown that post FMDV vaccination, the protective antibody response is generated via a T-independent mechanism [197]. Indeed, depletion of $CD4^+$ T cells in cattle has shown that the neutralising antibodies generated against FMDV are T-independent, but the response to FMDV non-structural proteins is T-dependent [198]. Thus, it can be concluded that FMDV is a largely T-independent antigen. However, Carr *et al.* have recently shown that stimulating the $CD4^+$ T cell response during FMDV vaccination is important for generating an optimum protective antibody titre in cattle [199].

Vaccination with one FMDV serotype does not confer protection against another serotype [179]. This lack of cross-protection has been demonstrated when using bi-, tri- and tetravalent FMDV vaccines, which do not prevent FMDV outbreaks due to the antigenic variation of FMDV serotypes [179]. This lack of serotype cross-protection also extends to some strains, with some strains differing sufficiently to require a strain-specific vaccine to be developed [179]. *In vitro* cross protection assays can be used to determine the degree of cross-reactivity between FMDV strains and whether one FMDV vaccine is likely to give protection against another strain. This can be a useful technique when it is difficult to generate a satisfactory FMDV vaccine from a field isolate.

One example of a field isolate that has been difficult to quantify after FMDV antigen growth and concentration is the O-serotype South Korean virus (O-SKR). The virion particles form large aggregates during the concentration process, thus making it difficult to quantify the antigen for vaccine production (Merial Animal Health, personal communication). Due to the difficulties in O-SKR vaccine production it was proposed that a closely related vaccine strain may provide intra-strain protection against O-SKR challenge, therefore negating the requirement to produce O-SKR vaccine. The related strain chosen as a potentially cross-protective vaccine candidate was O1-Manisa as it already had proven vaccine efficacy.

3.2.1 FMDV vaccine potency testing

As previously mentioned, the potency of FMDV vaccines is usually tested in cattle using guidelines outlined in the European Pharmacopoeia [180]. The monograph states that a potency test must consist of three groups of cattle that are at least 6 months of age, with at least five cattle in each group [180]. Each group must be given decreasing vaccine volume, starting from a full dose, which must be administered via the prescribed route (i.e. intramuscularly) [180]. Twenty one days after vaccination the vaccinated animals and a control group, consisting of at least 2 non-vaccinated animals, are given a live-virus challenge intradermolingually with an appropriate virus strain (i.e. a strain that is similar or the same as the vaccine strain) [180]. The challenge virus must be cattle adapted and fully virulent [180]. All of the live-virus challenged animals are observed for 8 days and any vaccinated animal showing lesions at a site other than the tongue are deemed to be unprotected from the live-virus challenge strain.[180] The control animals must show lesions in at least three feet otherwise the potency test is marked as a failure [180].

Two potency tests were performed in parallel to determine if an inactivated FMDV O1-Manisa vaccine would offer heterologous protection against FMDV O-SKR live-virus challenge and also to determine the potency of the inactivated FMDV O-SKR vaccine with homologous live-virus challenge. The vaccination groups (6 groups of 5 animals per group) were given either a full-dose, half-dose or quarter dose of either inactivated FMDV O1-Manisa or O-SKR. At day 21 post-vaccination all calves (30 vaccinated animals plus 3 non-vaccinated control animals) were challenged with live-FMDV O-SKR virus, in accordance with Office International des Epizooties (OIE) FMDV vaccine potency testing guidelines [180].

Antigen-specific ELIspots have been previously used to detect bovine antibody secreting cells following immunisation with a number of different antigens [124, 218]. Thus by developing a FMDV O1-Manisa and O-SKR-specific ELIspot assay the FMDV O1-Manisa and O-SKR-specific plasma and memory B cell response could be monitored in cattle. The previously described vaccine potency study afforded a unique opportunity to determine the kinetics of the FMDV O1-Manisa and O-SKR-specific B cell responses in two cohorts of vaccinated animals, that each received the full-dose vaccine (FMDV O1-Manisa and O-SKR) following vaccination and live-virus challenge, using the newly developed FMDV-specific ELIspot.

3.3 Materials and methods

3.3.1 Calves and immunisation protocol

Thirteen 6-month-old conventionally reared Holstein-Friesian male calves (*Bos Taurus*, Pirbright Institute) were split into two groups of five and a control group of 3 animals. Each calf in the first cohort (group 1) was immunised intramuscularly with a full dose of inactivated FMDV O1-Manisa vaccine (Merial Animal Health, Lyon, France). Each calf in the second cohort (group 4) was immunised intramuscularly with a full dose of inactivated FMDV-OSK vaccine (Merial Animal Health). The non-vaccinated controls (group 7) were not vaccinated.

All calves (groups 1, 4 and 7) were challenged with live-FMDV-OSK virus at day 21 post-vaccination (day 0 post-challenge), in accordance with OIE FMDV vaccine potency testing guidelines [180]. The animals were challenged, with 0.2mL containing $10^{5.7}$ ID50 of live FMDV-OSK intradermolingually into two different sites on the upper surface of the tongue (0.1mL per site) [180]. All animals were observed and the general health status, hoof sensitivity and presence of tongue and hoof lesions were recorded for 8 days post-live virus challenge. The presence of lesions on the hoof was deemed to be spread of the virus from the site of primary challenge (tongue), and thus was deemed as a lack of protection in that animal.

Heparinised peripheral blood and serum samples were taken from all animals at various time points following both immunisation and live-virus challenge. All experiments were approved by the Pirbright Institutes ethical review process and were in accordance with national guidelines on animal use.

3.3.2 FMDV O1-Manisa and O-SKR-specific ELIspot

MultiScreenHA plates (Millipore, Watford, UK) were coated with 100μl/well of a $^{1}/_{5000}$ dilution of rabbit anti-FMDV O1 UKG polyclonal antibody (Pirbright Institute) in 0.1M carbonate buffer (pH 9.6) for 2 hours at 37^{o}C. Plates were then washed 5 times in PBS and then blocked using 4% dried milk (Marvel) in PBS. Following blocking, the plates were washed 5 times in PBS. Inactivated FMDV antigens (FMDV O1-Manisa or O-SKR, Merial Animal Health) were then added to the plate (100μl/well of 1μg/mL diluted antigen in PBS). The plates were then washed and stored at 4^{o}C until required.

Fresh or 6 day-stimulated PBMCs were suspended at 5 x 10^6 cells/mL and 1:2 serial dilutions were performed in ELIspot medium down to 1.5 x 10^5 cells/mL. 100μL/well of each suspension (in duplicate) was then incubated on the coated plates overnight

at 37^{o}C in a 5% CO_2 incubator. Subsequently, the PBMCs were washed from the plates 5 times using PBS containing 0.05% Tween20 (Sigma-Aldrich). One hundred μl per well of a $^1/_{1000}$ dilution of sheep anti-bovine IgG conjugated to horse radish peroxidase (HRP, AbD Serotec) was then added to the plates for 3 hours at room temperature. Following the incubation step, the plates were again washed 5 times using PBS containing 0.05% Tween20. Detection was performed by the addition of 100μL/well of AEC and subsequent incubation at room temperature for 1 hour. The reaction was then stopped by washing the plates with tap water and allowing them to dry overnight at room temperature. During the live-virus challenge phase of the study, after washing in tap water the ELIspot plates were submerged in 4% paraformaldehyde (PFA, Sigma-Aldrich) for 1 hour, prior to air drying overnight.

3.3.3 FMDV O1-Manisa and O-SRK-specific virus neutralisation test, liquid phase blocking ELISA (LPBE) and FMDV non-structural protein (NSP) ELISA

Pre- and post-vaccination sera were prepared from blood samples taken at D0, D7, D13, daily from D21 to D29, D32 and D35 post vaccination from all animals in groups 1 (FMDV O1-Manisa vaccinates), 4 (FMDV O-SKR vaccinates) and 7 (non-vaccinate controls). The sera were stored at $^-$20^{o}C until the time course of sera collection was complete. All of the serological assessments (VNT, LPB and NSP ELISA) of the sera were performed by the FMDV World Reference Laboratory (Pirbright Institute).

3.3.3.1 Virus neutralisation assay

The virus neutralisation assay quantitatively asses the strain-specific anti-FMDV antibodies that are able to neutralise live-virus in tissue culture (virus neutralisation titre, VNT). The assay was performed using the same stock virus as the vaccine antigens (FMDV O1-Manisa and FMDV O-SKR, provided by Merial Animal Health). The neutralizing activities of the sera were determined using the VNT assay method described in the OIE Manual of Diagnostic Tests and Vaccines for Terrestrial Animals [219]. The sera from all of the animals were tested in duplicate, using serial 2-fold dilutions and the end point titres were calculated according to the method of Reed and Muench [220]. Titres of FMDV-specific antibodies were expressed as the final dilution of serum present in the serum/virus mixture that gives $\geq$50% neutralization of virus growth as determined by the presence of cytopathic effect (CPE) on cell growth. The control sera from the non-vaccinated animals were included in each assay. A serum sample with a VNT of $\geq$ $^1/_{45}$ was considered to be positive. The positive cut off value for the VNT assay was

determined using sera obtained from 137 vaccinated and 8 non-vaccinated, British cattle [221]. Sera was taken from the animals at day 21 post-vaccination prior to live FMD-virus challenge [221]. At day 21 post-vaccination the animals were challenged with live FMD virus intradermolingually and the generalisation of lesions was observed. Cattle the exhibited lesions in one or more of the feet were deemed to be clinically unprotected [221]. The VNT assay was performed using homologous FMD virus and the antibody titres were correlated with clinical outcome. The animals that were completely protected from FMD virus generalisation had antibody titres that were $\geq {}^{1}/_{32}$ [221]. Thus the positive cut off value for VNT titres was determined to be $\geq {}^{1}/_{45}$.

3.3.3.2 Liquid phase blocking ELISA (LPBE)

The liquid phase blocking ELISA (LPBE) assay was used to detect the presence of FMDV-specific antibodies in the test sera. Using the methodology described by Hamblin *et al.* the assay is based upon specific blocking of the FMDV antigen (O1-Manisa or O-SKR) in liquid phase by antibodies in the test serum [222]. Briefly, rabbit antisera specific for FMDV O-serotype is passively adsorbed on to polystyrene microwells. A five-fold dilution of each test serum is mixed with either FMDV O1-Manisa or O-SKR inactivated virus; any antigen-specific antibodies present in the test serum will bind the FMDV antigen, resulting in the formation of immune complexes. Duplicates of the test serum/antigen mixture are then transferred to an ELISA plate coated with rabbit anti-FMDV trapping antibodies. Any free FMDV antigen that is not bound in an immune complex will be immobilised by the rabbit anti-FMDV trapping antibody. Any trapped FMDV antigen is then detected by the addition of a guinea pig anti-FMDV detecting antibodies, which is visualised by an anti-guinea pig Ig conjugated to HRP. A substrate/chromogen solution is then added to the ELISA and the resulting colour development is observed using a photometer. The LPB end-point titre is then calculated by comparing the OD of the test serum with the positive free antigen controls. Any serum with a LPB titre of greater than or equal to ${}^{1}/_{40}$ is considered to be positive and that animal is deemed to be protected against FMDV infection. The positive cut off value for the LPBE was determined using sera obtained from more than 300 non-FMDV vaccinated, uninfected British cattle [223]. The LPBE assay was performed against all seven FMDV serotypes (O1, A, C, ASIA-1, SAT-1, -2 and- 3, only titres of less than 1 in 40 was observed in this sero-negative population [223].

3.3.3.3 Non-structural protein ELISA

The FMDV non-structural protein ELISA detects FMDV-specific antibodies that are directed against the non-structural 3ABC protein of the FMDV virion, which is not present in FMDV vaccine preparations. The ELISA utilises a purified expressed recombinant 3ABC FMDV protein, that is homologous in all FMDV serotypes [224]. The assay is performed using a $^{1}/_{20}$ dilution of the test serum, along with a serial dilution of a known serum for a standard curve. The NSP titre is calculated by comparing the OD of the test serum with the standard curve. A serum sample with a NSP titre of greater than or equal to $^{1}/_{45}$ was considered to be positive [224].

3.3.3.4 Statistical analysis

The normality of the data sets was tested using the D'Agostino-Pearson omnibus test [225], using GraphPad Prism software (Version 6.00 for Windows, GraphPad Software, La Jolla, CA, USA). Data analysed using this method with a P-value of >0.05 was considered to be of a normal distribution. These data points were then subsequently treated using parametric analyses downstream. Any data points that a P-value of $<$ 0.05 were not considered to be sampled from a normal distribution and were treated using non-parametric analysis downstream.

To test the statistical significance of the FMDV-specific LPBE, VNT and NSP titres following vaccination a one-way ANOVA was performed, followed by either Holm-Sidak's (parametric) or Dunn's (non-parametric data points) multiple comparison tests (non-parametric) using GraphPad Prism (GraphPad Software). Any time-points that had a p-value of <0.05 were considered to be significantly different to the day of vaccination (D0pv).

3.3.4 PBMC proliferation by thymidine incorporation

Antigen-specific proliferation of PBMCs was assessed in a 6 day assay measuring [methyl-3H] thymidine incorporation. Enumerated PBMCs were resuspended in RPMI 1640 medium (Invitrogen) supplemented with 5% (v/v) heat inactivated foetal calf serum (FCS, TCS Cellworks, Buckingham, UK), 1 mM sodium pyruvate (Sigma-Aldrich), 1 x non-essential amino acids (Sigma-Aldrich), 50 μM 2-mercapto-ethanol (Sigma-Aldrich), and 500 μl Gentamicin (10 μg/mL, Sigma-Aldrich). The resuspended PBMCs were then distributed in 96-well, round-bottom, microtitre plates at 2 x 10^5 cells/well. FMDV-specific vaccine antigens (FMDV O1-Manisa and O-SKR, provided by Merial) were prepared from the same FMDV strains as the vaccination regime. The vaccine antigens

were prepared in a range of serial dilutions (1, 0.1, 0.01 and 0.001 μg/mL). BHK-21 cell lysate (cellular control) was also set up with the same concentration range. Pokeweed mitogen (PWM, positive control, Sigma-Aldrich, 2.5 μg/mL final concentration) or medium alone (negative control) were used in the *in vitro* assays. The antigen concentrations refer to the total amount of protein of the preparation, rather than the specific FMDV-related protein component. Each antigen was set up in triplicate. The cultures were incubated in a humidified atmosphere for 6 days at 37^{o}C with 5% CO_2. For the last $16 - 18$ hours of the assay, the cultures were pulsed with 1 μCi per well of [methyl-3H] thymidine (GE Healthcare Life Sciences) and the labelled cells were then harvested on to glass fibre filter mats using a semi-automated cell harvester. Incorporation of the radio-label was determined by liquid scintillation counting. Results were expressed as mean counts per minute (c.p.m.) values of the triplicate cultures.

3.4 Results

3.4.1 O1-Manisa-specific ELIspot development

The ELIspot methodology has been successfully used to detect bovine antigen-specific antibody secreting cells following immunisation with a number of different antigens [124, 218]. However, when starting this study there was no published methodology for a FMDV O-serotype specific ELIspot. Thus, before starting a FMDV O-serotype immunisation and challenge study, a FMDV O1-Manisa and O-SKR-specific ELIspot first had to be developed. An in-house FMDV O1-Manisa-specific ELISA protocol and the previously described ELIspot methodology (Section 2.3.4) were used as the starting point for the development of the FMDV O-serotype-specific ELIspot methodology.

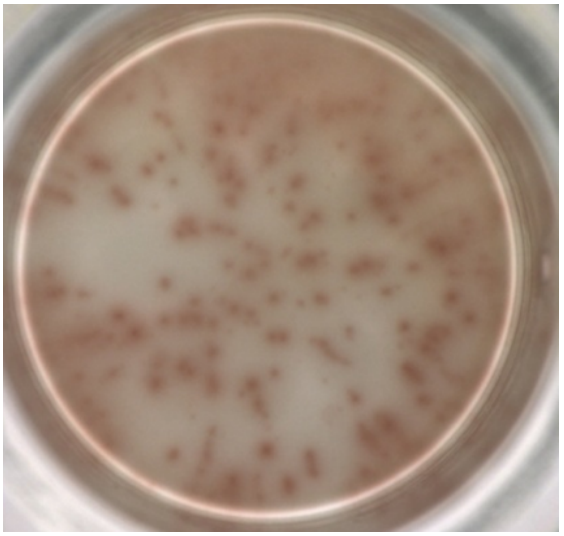
There are currently no bovine antigen-specific antibody secreting cell-lines available. Thus, to test the newly devised FMDV O1-Manisa ELIspot, a FMDV O1-Manisa-specific mouse hybridoma (IB11, Pirbright Institute) was used. The polyclonal rabbit O1-UKG coating antibody (Pirbright Institute), concentration of the coating antigen (inactivated FMDV O1-Manisa vaccine antigen, Merial Animal Health), and the HRP-conjugated detection antibody were all tested at different concentrations using a checker board titration with the IB11 hybridoma as the source of secreted antibody. However, despite improving the clarity of the ELIspot by altering the previously mentioned variables, the ELIspot still had an unusual pattern to the 'spots', which looked more like the mouse hybridomas were 'crawling' across the ELIspot wells, rather than secreting antibody in one location (Figure 3.1A). The antigen that was being used for the ELIspots had undergone several rounds of freeze thawing. So, to improve the quality of the ELIspot

'spots', freshly defrosted antigen was used, which resulted in improved the 'spot' quality (Figure 3.1B). There were still some 'trailing spots' even when using freshly defrosted antigen on the ELIspot plates; this is likely to be inherent in the nature of the IB11 hybridoma used to test the ELIspot plate coating conditions, as this phenomenon was not seen when using bovine PBMCs in the assay (Figure 3.1C).

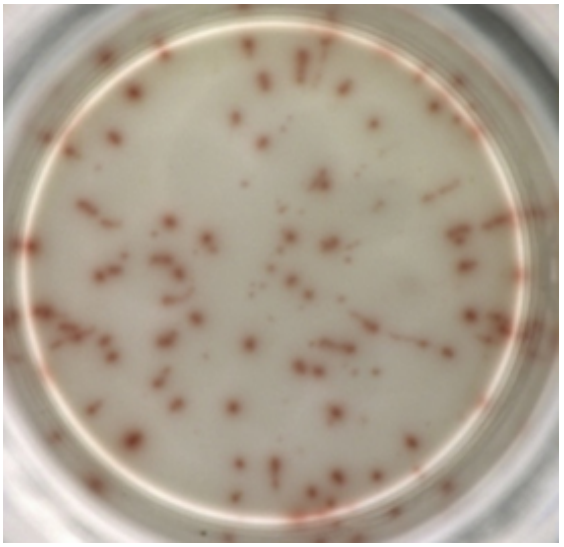
3.4.2 Clinical outcome following vaccination and live virus challenge

Following vaccination, the vaccinated animals (Groups 1 and 4) and the non-vaccinate controls (Group 7) were challenged with live FMDV O-SKR virus at day 21 post immunisation (D0 post-challenge). The clinical outcomes of the animals that received the intradermolingual live-virus challenge is shown in Table 3.1. Both groups of animals that received either the inactivated FMDV O1-Manisa (Group 1) or FMDV O-SKR (Group 4) vaccine were 100% protected against live-virus challenge with FMDV O-SKR virus, with no spread of FMDV lesions to the hooves (Table 3.1). The non-vaccinate controls were not protected from live-virus challenge and all three animals showed lesions on all four of their hooves, demonstrating dissemination of the FMDV virus and a lack of protection (Table 3.1).

(A)



(B)



(C)

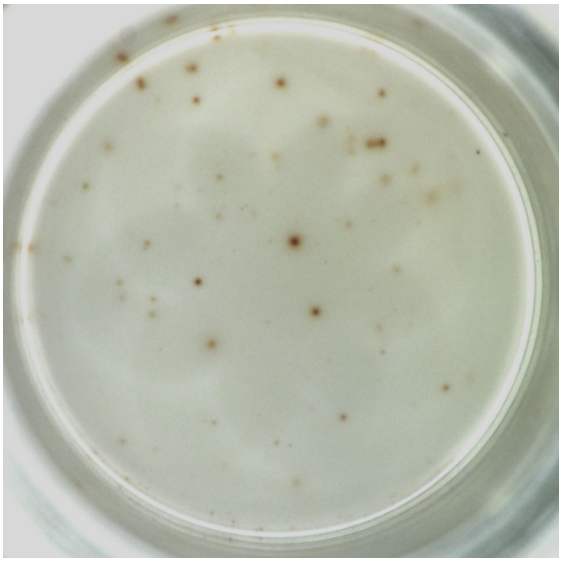


FIGURE 3.1: Development of the FMDV O1-Manisa specific ELIspot assay using the murine IB11 hybridoma: (A) using multiple freeze-thawed FMDV O1-Manisa vaccine antigen, (B) using single freeze-thawed vaccine antigen and (C) using bovine PBMCs and single freeze-thawed FMDV O1-Manisa vaccine antigen.

TABLE 3.1: Clinical outcome post FMDV O-SKR live-virus challenge

FMDV Vaccine	Animal Number	Vaccine Dose	Observation of lesions						Protection Status	% Protection
			Primary lesions		Secondary lesions					
			T	OSM	RF	LF	RH	LH		
O1-Manisa	FMD182	Full	+	−	−	−	−	−	Protected	100
	FMD183		+	+	−	−	−	−	Protected	
	FMD184		+	+	−	−	−	−	Protected	
	FMD185		+	−	−	−	−	−	Protected	
	FMD186		+	−	−	−	−	−	Protected	
O-SKR	FMD197	Full	−	−	−	−	−	−	Protected	100
	FMD198		−	−	−	−	−	−	Protected	
	FMD199		+	−	−	−	−	−	Protected	
	FMD200		+	−	−	−	−	−	Protected	
	FMD201		−	−	−	−	−	−	Protected	
NVC	FMD212	N/A	+	+	+	+	+	+	Unprotected	0
	FMD213		+	+	+	+	+	+	Unprotected	
	FMD214		+	+	+	+	+	+	Unprotected	

NVC = Non-vaccinated controls, T = Tongue, OSM = Oral/snout/mouth, RF= Right fore, LF = Left fore, RH = Right hind, LH = Left hind, + = presence of lesion, − = absence of lesion

Clinical observations of the cattle post-FMDV O-SKR live-virus challenge. Animals were observed for 8 days post challenge and the presence and location of lesions were noted for each animal.

3.4.3 Kinetics of the antigen-specific B cell response following O-serotype vaccination and live-virus challenge

The kinetics of the antigen-specific IgG plasma and memory B cell response was monitored by ELIspot in all thirteen animals following immunisation, with either inactivated FMDV O1-Manisa (Group 1) or FMDV O-SKR (Group 4) or no vaccination (Group 7). Post-vaccination (pv) a burst of plasma cells that were specific to both FMDV O1-Manisa (O1M) and O-SKR (OSKR) was observed at D7pv in both vaccination cohorts (Group 1: O1M: 34 ± 29, OSKR: 27 ± 23; Group 4: O1M: 10 ± 4, OSKR: 16 ± 11 -specific ASCs per 10^6 PBMCs, Figures 3.2A and B, respectively and Table 3.2). There were no detectable antigen-specific plasma cells in the non-vaccinated control animals (Group 7) at the same time-point (Figure 3.2C and Table 3.2). By D13pv there were

no antigen-specific plasma cells detectable in any of the animals (Figure 3.2 and Table 3.2).

At day 21pv (day 0 post-challenge (D0pc)) all of the animals received an intradermolingual live FMDV O-SKR virus challenge. In the group that received the inactivated FMDV O1-Manisa vaccine (group 1), a burst of both FMDV O1-Manisa and O-SKR specific plasma cells was observed between days 4 and 7pc, peaking at D7pc (D24-28pv, Group 1: O1M: 47 ±37, OSKR: 52 ±38 -specific ASCs per 1066 PBMCs, Figure 3.2A and Table 3.2). By D14pc there were no antigen-specific plasma cells detectable in peripheral blood (Figure 3.2A and Table 3.2).

Following live-virus challenge, only FMDV O-SKR-specific plasma cells were detected in the group that received the inactivated FMDV O-SKR vaccine (Group 4) and the non-vaccinated controls (Group 7). The group that was vaccinated with inactivated FMDV O1-Manisa (Group 1) had both FMDV O1-Manisa and O-SKR-specific plasma cell detectable by ELIspot. Both the inactivated FMDV O-SKR vaccinate group (Group 4) and the FMDV O1-Manisa vaccinates (Group 1) showed a similar plasma cell burst kinetic, with a burst of FMDV O-SKR-specific plasma cells at day 3 to 7pc, again peaking at D7pc (D25 to 28pv, Group 4: OSKR: 39 ±22 -specific ASCs per 1066 PBMCs, Figure 3.2B and Table 3.2). The non-vaccinate group also showed a burst of FMDV O-SKR specific plasma cells at D7pc (Group 7: OSKR: 7 ±3 -specific ASCs per 10^6 PBMCs, Figure 3.2B and Table 3.2). By D14pc there were no antigen-specific plasma cells detectable in peripheral blood (Figure 3.2C and Table 3.2). Again, by D14pc there were no antigen-specific plasma cells detectable in either the inactivated FMDV O-SKR vaccinates (Group 4) or the non-vaccinate controls (Group 7, Figure 3.2B and C, respectively and Table 3.2).

Statistical analysis of any correlations between the magnitude of the plasma cell burst and the antibody titres is discussed in Section 3.4.5.

The presence of antigen-specific memory B cells was also monitored in all animals following both vaccination and FMDV O-SKR live-virus. However, no FMDV O1-Manisa or O-SKR-specific memory B cells were detected at any time-point following either vaccination or live-virus challenge (Data not shown).

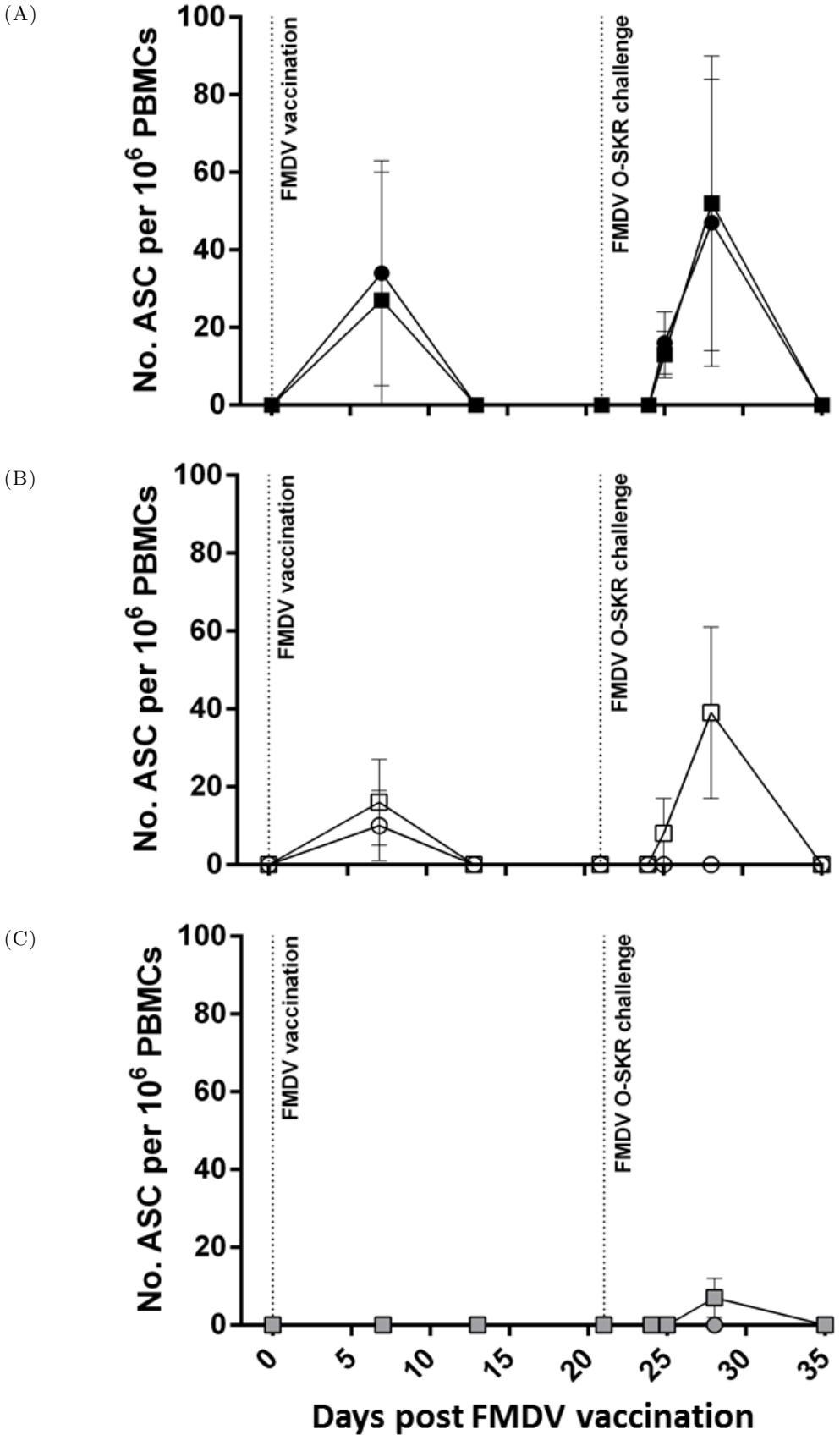


FIGURE 3.2: Kinetic of the O-serotype (O1-Manisa: circles, O-SKR: squares) FMDV-specific plasma cell response post vaccination and intradermolingual live FMDV O-SKR virus challenge (indicated by vertical dotted line). (A) O1-Manisa vaccinated animals (Group 1, black symbols, $n = 5$), (B) O-SKR vaccinated cohort (Group 4, open symbols, $n = 5$) and (C) non-vaccinate controls (Group 7, grey symbols, $n = 3$). Results are expressed as the grouped mean of duplicate determinations from each calf ± S.D.

TABLE 3.2: Total number of IgG FMDV O-serotype antibody secreting cells in PBMC population

Days post-vaccination (Days post-challenge)	Total number of FMDV O-serotype-specific ASCs per 10^6 PBMC					
	Group 1 (n=5)		Group 4 (n=5)		Group 7 (n=3)	
	O1M	O-SKR	O1M	O-SKR	O1M	O-SKR
0	0	0	0	0	0	0
7	34 ±29	27 ±23	10 ±4	16 ±11	0	0
13	0	0	0	0	0	0
21 (0pc)	0	0	0	0	0	0
24 (3pc)	0	0	0	0	0	0
25 (4pc)	16 ±8	13 ±6	0	8 ±4	0	0
28 (7pc)	47 ±37	52 ±38	0	39 ±22	0	7 ±3
35 (14pc)	0	0	0	0	0	0

O1M: FMDV O1-Manisa, OSKR: FMDV O-SKR

Results are expressed as the grouped mean of duplicate determinations from each animal ± S.D.

3.4.4 Kinetics of the serological response following FMDV O-serotype vaccination and live virus challenge

The serological response to FMDV O1-Manisa and O-SKR was also monitored in serum following vaccination and FMDV O-SKR live virus challenge using liquid phase blocking ELISA, virus neutralisation test and FMDV non-structural protein ELISA. Isotype specific (IgG or IgM) anti-FMDV ELISAs were not performed on sera obtained during this study.

3.4.4.1 Liquid phase blocking (LPB) ELISA

The liquid phase blocking (LPB) ELISA was used to quantitatively assess the titre of antibodies present in the serum that are capable of binding to either the FMDV O1-Manisa or O-SKR virus. If an animal had a LPB titre of greater then $^1/_{40}$ (expressed as a titre of 40) then that animal was deemed to be protected against challenge from that virus.

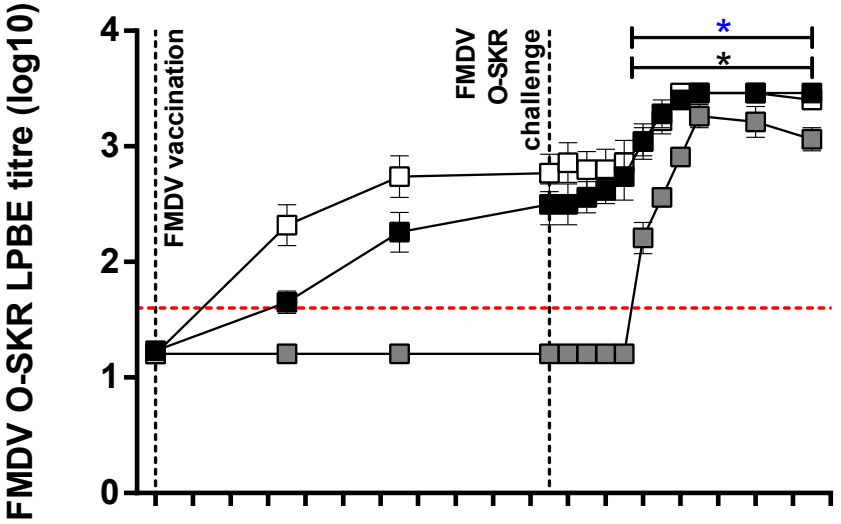
The animals that were immunised with the inactivated FMDV O-SKR vaccine (Group 4) developed a protective titre of FMDV O-SKR-specific blocking antibodies from D7pv (Group 4: 262.4 ±144.6 FMDV O-SKR LPB titre), which further increased at D13pv

(Group 4: 760.2 ±632.2 FMDV O-SKR LPB titre, Figure 3.3A). Following FMDV O-SKR live-virus challenge at D21pv (D0pc) there was a large increase in O-SKR LPB titre from D4pc (D25pv, Group 4: 1086 ±1115.8 FMDV O-SKR LPB titre), peaking at D7pc (D28pv, Group 4: 2896 FMDV O-SKR LPB titre, Figure 3.3A). This group also developed blocking antibodies that were specific for FMDV O1-Manisa, the kinetics of the antibody titres were similar to those described for FMDV O-SKR-specific blocking antibodies (Figure 3.3B). Although, the induction of a protective blocking antibody titre of FMDV O1-Manisa specific antibodies did not occur until D13pv (Group 4: 186.6 ±127.5 FMDV O1-Manisa LPB titre, Figure 3.3B). The FMDV O1-Manisa blocking titres did not increase until D6pc (D27pv, Group 4: 464 ±240.9 FMDV O1-Manisa LPB titre, Figure 3.3B), peaking at D8pc (D29pv, Group 4: 1375.6 ±971.3 FMDV O1-Manisa LPB titre) and remaining elevated until D14pc (D35pv, Group 4: 1448 ±886.7 FMDV O1-Manisa LPB titre, Figure 3.3B).

The animals that were vaccinated with inactivated FMDV O1-Manisa (Group 1) also developed protective titres of blocking antibodies that were specific for FMDV O-SKR and O1-Manisa (Figures 3.3A and B, respectively). The kinetics of blocking antibody response, against both FMDV O1-Manisa and O-SKR, was similar in this group (Group 1) to that seen in the inactivated FMDV O-SKR (Group 4) animals. Although, the induction of a protective blocking antibody titre against both FMDV O1-Manisa and O-SKR, was delayed in this group of animals, occurring at D13pv, as compared to D7pv in Group 4 (Group 1: O1M: 434.4 ±, OSKR: 255.6 ±266.2 LPB titre, Figures 3.3A and B, respectively). Following FMDV O-SKR live-virus challenge the FMDV O1-Manisa vaccinated group of animals showed an increase in FMDV O-SKR blocking antibody titre from D4pc (D25pv, Group 1: 796 ±634.8 FMDV O-SKR LPB titre, Figure 3.3A), reaching the assay maximum titre at D8pc (D29pv, Group 1: 2896 FMDV O1-Manisa LPB titre, Figure 3.3A). This group also showed an increase in FMDV O1-Manisa blocking antibody titre from D6pc (D27pv, Group 1: 941.2 ±485.7 FMDV O1-Manisa LPB titre, Figure 3.3B), peaking at D8pc (D29pv, Group 1: 2352 ±828.2 FMDV O1-Manisa LPB titre, Figure 3.3B) and remaining elevated until D14pc (D35pv, Group 1: 2316.8 ± 793.1 FMDV O1-Manisa LPB titre, Figure 3.3B).

The non vaccinate control group (Group 7) did not develop a protective titre of blocking antibodies specific for either FMDV O-SKR or O1-Manisa until D5pc (D26pv, Group 7: OSKR: 175.7 ±83.1, O1M: 150.7 ±52.5 LPB titre, Figures 3.3A and B, respectively). The blocking antibody titres specific for both FMDV O-SKR and FMDV O1-Manisa continued to increase until the end of the study (D14pc, D35pv), although the FMDV O-SKR-specific blocking antibody titres reached a higher titre than the FMDV O1-Manisa titre at D14pc (Group 7: OSKR: 1206.7 ± 418 versus O1M: 844.7 ± LPB titre, Figures 3.3A and B, respectively).

(A)



(B)

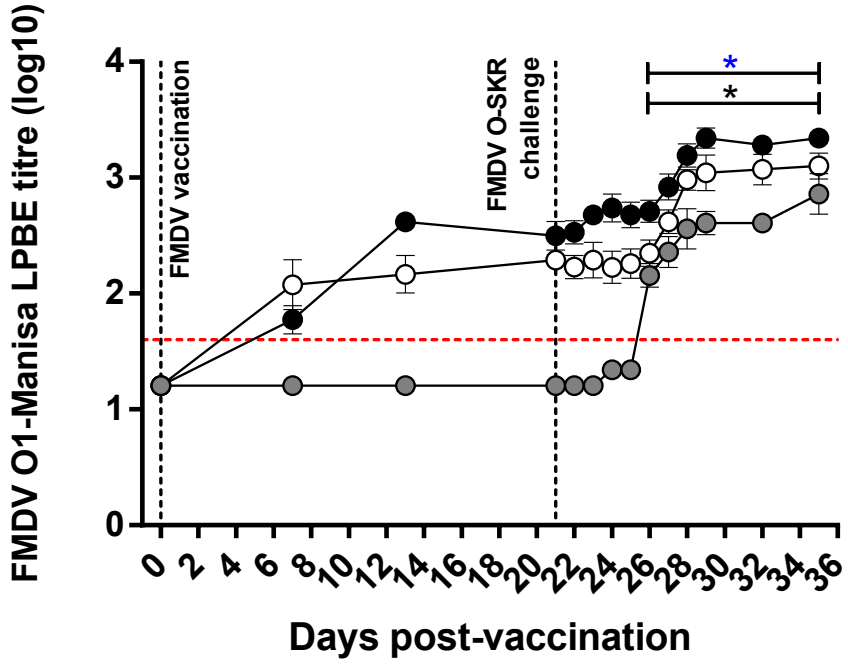


FIGURE 3.3: Kinetic of the (A) FMDV O-SKR specific and (B) FMDV O1-Manisa specific liquid phase blocking antibody titres post vaccination and FMDV O-SKR live virus challenge in the FMDV O1-Manisa vaccinated cohort (Black symbols), the FMDV O-SKR vaccinated cohort (Open symbols) and the non-vaccinate controls (Grey symbols). Results are expressed as the log10 transformed grouped mean of duplicate determinations from each calf ± S.D. Statistically significant time-points ($p<0.05$) indicated by * symbol (FMDV O1-Manisa vaccinated cohort = *, FMDV O-SKR vaccinated cohort = *).

3.4.4.2 Virus neutralisation assay

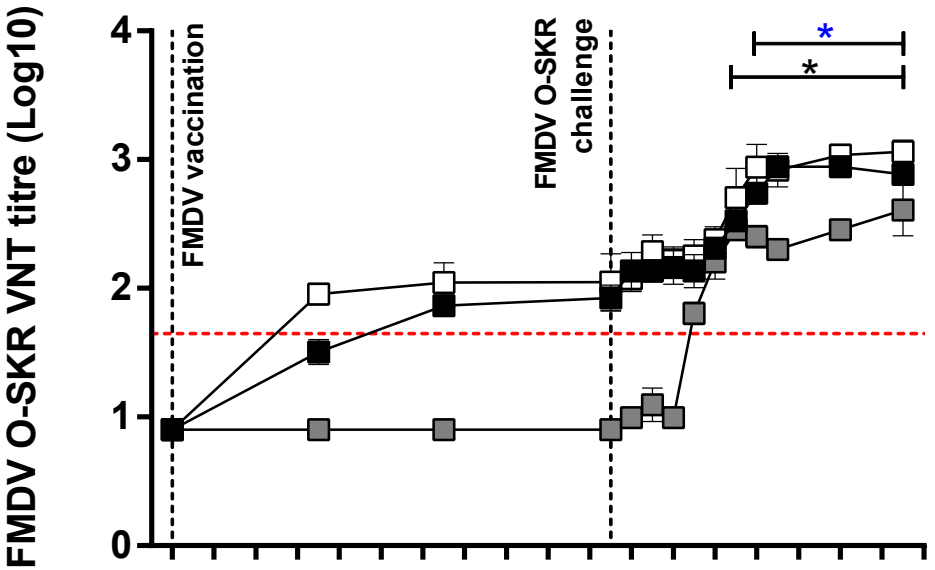
The virus neutralisation assay was used to quantitatively assess the titre of antibodies present in the serum that were capable of neutralising either FMDV O1-Manisa or O-SKR (virus neutralisation titre, VNT). If an animal had a VNT of greater then $^{1}/_{45}$ (expressed as a titre of 45) then that animal was deemed to be protected against challenge from that virus.

The animals that received the FMDV O1-Manisa vaccine (Group 1) achieved a protective FMDV O-SKR VNT by D13pv (Group 1: 78.2 ± 32.11 FMDV O-SKR VNT, Figure 3.4A). This group (FMDV O1-Manisa vaccinates) also had a protective VNT specific for FMDV O1-Manisa by D13pv (Group 1: 56.4 ±10.4 FMDV O1-Manisa VNT, Figure 3.4B). Following FMDV O-SKR live-virus challenge there was a boost in both the FMDV O-SKR and O1-Manisa VNTs from D6 to D7pc (D28pv, Group 1: O-SKR: 551.2 ±87.7, O1M: 321.2 ±141.7 VNT, Figure 3.4A and B, respectively). By D14pc (D35pv) the FMDV O-SKR and O1-Manisa VNTs had further increased to 795.2 ±223.7 and 771 ±454.5, respectively (Figure 3.4A and B).

The group that received the inactivated FMDV O-SKR vaccine (Group 4) also achieved a protective FMDV O-SKR specific VNT, but 7 days earlier than Group 1, by D7pv, (Group 4: 96.2 ±34.4, Figure 3.4A). The FMDV O-SKR VNT increased further at D6pc (D27pv, Group 4: 705.8 ±391.9 FMDV O-SKR VNT, Figure 3.4A). The end-point (D14pc, D35pv) FMDV O-SKR specific VNT achieved by group 4 was 1232.8 ±402.9 (Figure 3.4A). This group also developed a protective titre of FMDV O1-Manisa-specific virus neutralising antibodies but not until after live-virus challenge by D5pc (D26pv, Group 4: 174.2 ±117.4 FMDV O1-Manisa VNT, Figure 3.4B). The end-point (D14pc, D35pv) FMDV O1-Manisa VNT achieved by this group was 782.6 ±450.5 (Figure 3.4B).

The non-vaccinate group (Group 7) did not develop a protective VNT for either FMDV O-SKR or O1-Manisa until after FMDV O-SKR live-virus challenge (Figure 3.4A and B, respectively). The FMDV O-SKR VNT did not reach a protective titre until D5pc (D26pv, Group 7: 174.7 ±22.6, Figure 3.4A). The end-point (D14pc, D35pv) FMDV O-SKR VNT achieved by group 7 was 512 ±443.4 (Figure 3.4A). However, a protective FMDV O1-Manisa VNT was not achieved by this group until D11pc (D32pv, Group 7: 115.3 ± 21.9 FMDV O1-Manisa VNT, Figure 3.4B). The FMDV O1-Manisa VNT achieved by this group by D14pc (D35pv) was 203.7 ±113.1 (Figure 3.4B).

(A)



(B)

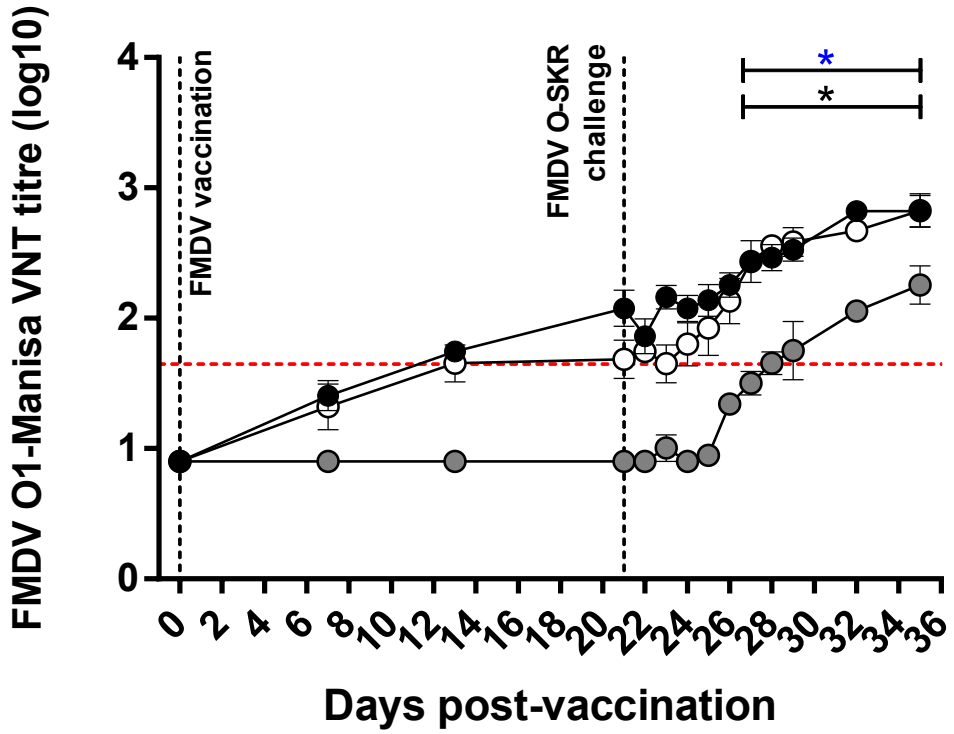


FIGURE 3.4: Kinetic of the O-serotype (A) FMDV O-SKR specific and (B) FMDV O1-Manisa specific virus neutralisation titre (VNT) post vaccination and FMDV O-SKR live virus challenge in the FMDV O1-Manisa vaccinated cohort (Black symbols), the FMDV O-SKR vaccinated cohort (Open symbols) and the non-vaccinate controls (Grey symbols). Results are expressed as the log10 transformed grouped mean of duplicate determinations from each calf ± S.D. Statistically significant time-points ($p<0.05$) indicated by * symbol (FMDV O1-Manisa vaccinated cohort = *, FMDV O-SKR vaccinated cohort = *).

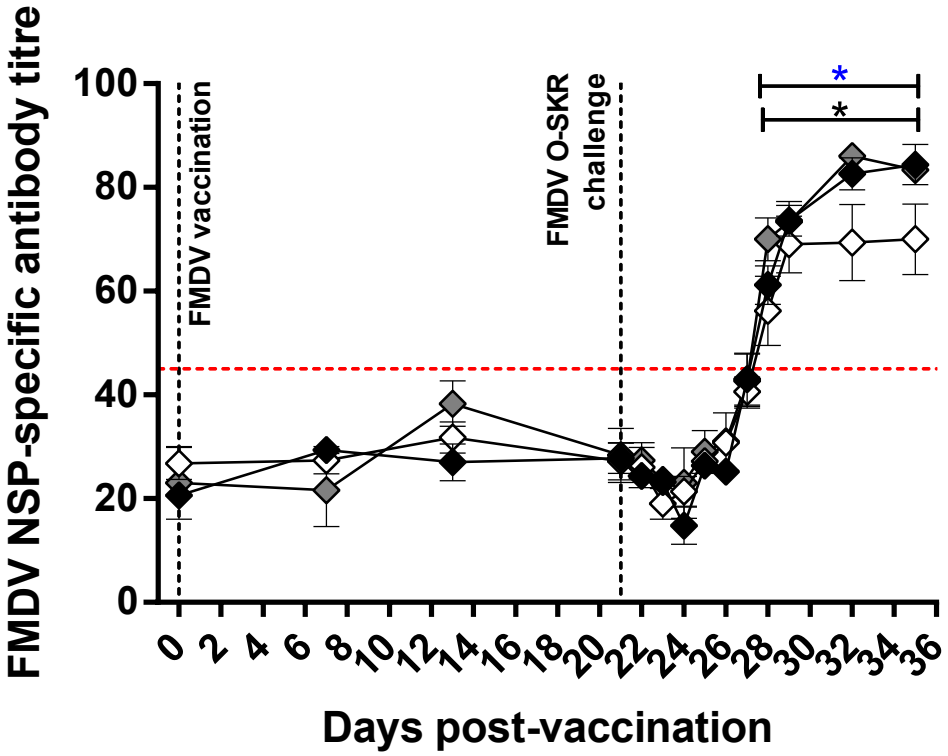


FIGURE 3.5: Kinetic of the FMDV non-structural protein (NSP) specific antibody titres following vaccination and FMDV O-SKR live virus challenge in the FMDV O1-Manisa vaccinated cohort (Group 1, black diamonds), the FMDV O-SKR vaccinated cohort (Group 4, open diamonds) and the non-vaccinate controls (Group 7, grey diamonds).Statistically significant time-points ($p<0.05$) indicated by * symbol (FMDV O1-Manisa vaccinated cohort = *, FMDV O-SKR vaccinated cohort = *).

3.4.4.3 Non-structural protein ELISA (NSP)

The FMDV non-structural protein (NSP) ELISA quantitatively assesses the presence of antibodies that are specific for FMDV NSPs. The assay is specific for all FMDV serotypes and an animal is deemed to be seropositive, if the NSP titre exceeds $^{1}/_{45}$. All three groups of animals did not become seropositive for NSP-specific antibodies until D7pc (D28pv, Group 1: 61.2 ±8.3, Group 4: 56.2 ±14.8, Group 7: 70 ±7.2 NSP titre, Figure 3.5). The NSP-specific antibody titres continued to rise in all animals until plateauing at D11pc (D32pv, Group 1: 82.6 ±6.9, Group 4: 69.4 ±16.4, Group 7: 86 ±3 NSP titre, Figure 3.5) and remained elevated until the end of the study (D14pc, D35pv, Group 1: 84.4 ±8.6, Group 4: 70 ± 15.1, Group 7: 83.3 ±4 NSP titre, Figure 3.5).

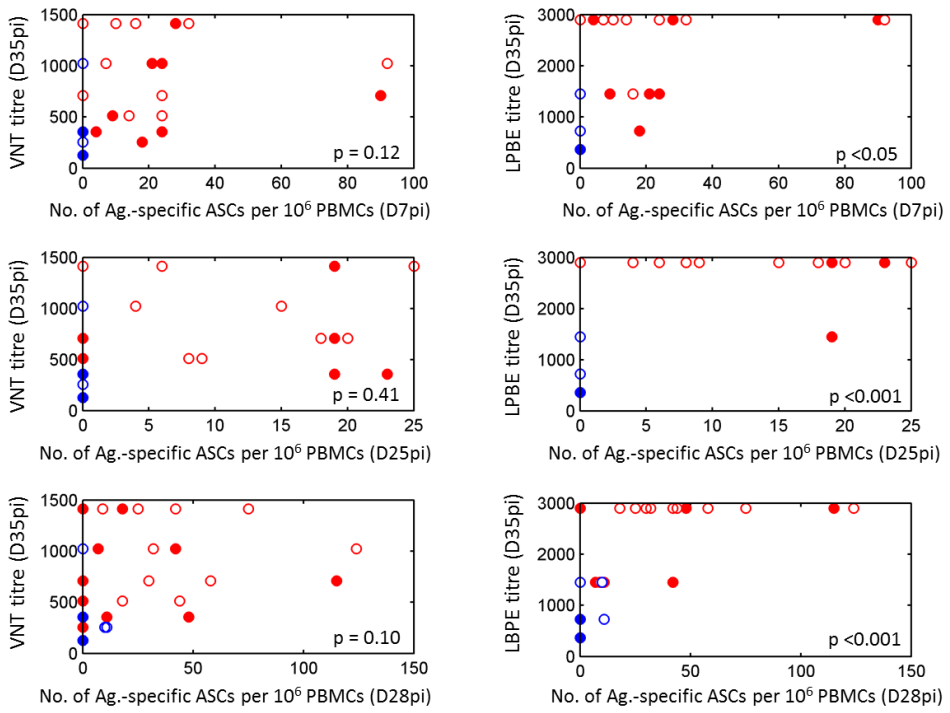


FIGURE 3.6: Statistical analysis of the B cell response to O-serotype FMDV vaccination and live-virus challenge. Plasma cell burst size at D7 (top panel), D24 (D3pc, middle panel) and D28 (d7pc, bottom panel) vs. the end-point (D35, D14pc) virus neutralisation titre (VNT, left) and liquid phase blocking ELISA titre (LPBE, right). Vaccinated animals (Groups 1 and 4, red symbols), Non-vaccinate controls (NVC, Group 7, blue symbols), FMDV O1-Manisa specific data (filled symbols) and FMDV O-SKR specific data (open symbols).

3.4.5 Correlation between serological response and plasma cell number

In order to try to establish a correlation between the antibody titres and the peak number of plasma cells generated following both vaccination and live-virus challenge, a Spearman's rank correlation coefficient (rho) was computed between the size of the plasma cell burst at the peak of the burst post-vaccination (Day 7pv, D7pv) and post live-virus challenge (D25pv and D28pv) versus both the end-point LPB and VNTs (D35pv).

Following vaccination there was no correlation between the number of plasma cells at the peak of the primary burst (D7pv) and the VNT (D35pv, Figure 3.6). However, there was a weak correlation between the D7pv plasma cell burst and the LPB titre at D35pv ($p < 0.05$, Figure 3.6). After live-virus challenge there was also no significant correlation between the post-challenge peak of plasma cell burst (D25pv and D28pv) and the end-point VNTs (D35pv, Figure 3.6). However, there was a significant correlation between the plasma cell number at both D25pv ($P < 0.001$) and D28pv ($P < 0.001$) with the LPB end-point titre (D35pv, Figure 3.6).

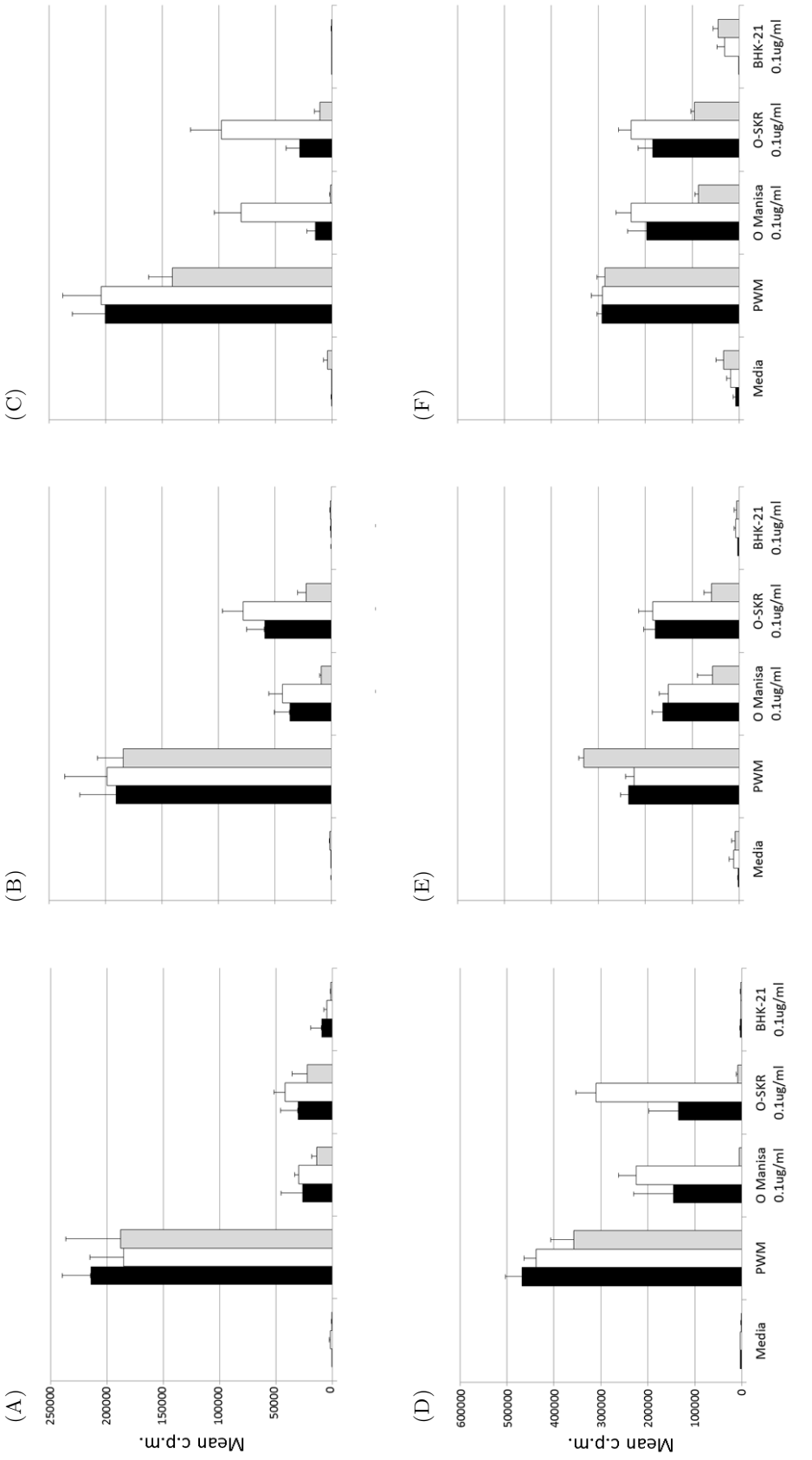


FIGURE 3.7: Proliferation response by thymidine incorporation in response to *in vitro* stimulation to FMDV O1-Manisa and O-SKR (0.1μg/mL) vaccine antigens, pokeweed mitogen (PWM, positive control), media and BHK-21 cell lysate (0.1μg/mL, negative controls) in group 1 (FMDV O1-Manisa vaccinates, black bars, $n = 5$), 4 (FMDV O-SKR vaccinates, white bars, $n = 5$) and 7 (non-vaccinate controls, grey bars, $n = 3$) at (A) D0pv, (B) D7pv and (C) D13pv and (D) D0pc (D21pv), (E) D7pc (D28pv) and (F) D14pc (D35pv). Data represented is the grouped mean of the individual animal mean derived from triplicate determinations ± SEM

3.4.6 PBMC proliferative response following O-serotype FMDV vaccination and live virus challenge

Following vaccination a PBMC proliferative response to both FMDV O1-Manisa and O-SKR was observed in both of the inactivated FMDV O1-Manisa and O-SKR vaccinated groups (Groups 1 and 4, respectively) from D7pv (Figure 3.7B). The animals in Group 4 (FMDV O-SKR vaccinates) demonstrated a greater proliferative response against both the FMDV O1-Manisa and O-SKR antigens, as compared to the O1-Manisa vaccinated group (Group 1) from D7pv onwards (D13pv, Group 4: O1M: 80,262 ±23,801, OSKR: 97,619.6 ±27,395.9 versus Group 1: O1M: 14,867.4 ±7320.9, OSKR: 28,679.6 ±26,588.3, Figure 3.7). This proliferative response remained elevated at all later time-points (Figure 3.7). The non-vaccinate control animals (Group 7) did not demonstrate a PBMC proliferative response to either FMDV O-SKR or O1-Manisa antigens until D7pc (D28pv, Group 7: O1M: 57,197.3 ±32,267.3, OSKR: 59,340 ±15,281.7, Figure 3.7E). However, the proliferative response to both FMDV O1-Manisa and O-SKR antigens was lower at D7pc (D28pv) in the non-vaccinate controls (Group 7) as compared to the inactivated FMDV O1-Manisa and O-SKR vaccinated groups (Groups 1 and 4, respectively, Group 7: O1M: 57,197.3 ±32,267.3, OSKR: 59,340 ±15,281.7 versus Group 1: O1M: 197,051.4 ±41,248.3, OSKR: 184,355.6 ±31,213 and Group 4: O1M: 229,917 ±32,677.8, OSKR: 229,901.4 ±27,352.6, Figure 3.7E).

3.5 Discussion

This is the first study to assess the kinetics and magnitude of the FMDV-specific B cell response following vaccination and live-virus challenge, using a FMDV-specific IgG ELIspot assay. The plasma and memory B cell response against FMDV O1-Manisa and O-SKR was assessed following both vaccination and FMDV O-SKR live-virus challenge. This allowed the B cell response to be assessed following homologous (FMDV O-SKR vaccinates) and heterologous (FMDV O1-Manisa vaccinates) live-virus challenge. Following live-virus challenge both of the vaccinated groups of animals were clinically protected. The non-vaccinated control group was not protected against live-virus challenge, and developed with FMDV lesions on all hooves.

Following primary immunisation with either inactivated FMDV O-SKR or O1-Manisa, there was an expansion of both FMDV O1-Manisa and O-SKR-specific plasma cells, which peaked at day 7pv. The burst of antigen-specific plasma cell numbers, in both of the vaccinated groups, was coupled with an increase in both the liquid-phase blocking and virus neutralising antibody titres. The timing of the antigen-specific plasma cell

burst following primary immunisation is in keeping with previously published data on cattle [124, 218] and humans [134, 171, 214, 226]. Indeed, Lefevre *et al.* demonstrated that following primary immunisation with ovalbumin a burst of antigen-specific plasma cells at day 7 [124]. In humans, both Halliley *et al.* and Wrammert *et al.* showed a burst of influenza-specific plasma cells occurring days 7 post immunisation with seasonal influenza vaccines [214, 226]. Bernasconi et al. also demonstrated that immunising humans with tetanus toxin vaccine resulted in a burst of antigen-specific plasma cells at day 6 to 8 post vaccination [134]. Finally, Kelly *et al.* demonstrated that immunisation with meningococcal serogroup C polysaccharide that is either conjugated to a carrier protein or non-conjugated results in an antigen-specific plasma cell burst from day 6 to 7 post vaccination, although the conjugated vaccine resulted in a burst with a larger magnitude [171].

The detection of plasma cells that were specific for both FMDV O1-Manisa and O-SKR, following FMDV O1-Manisa vaccination, indicates that the FMDV O1-Manisa vaccine is able to induce cross reactive plasma cells. This finding was confirmed by the presence of both liquid phase blocking and virus neutralising antibodies specific from both FMDV O1-Manisa and O-SKR. Similarly, the FMDV O-SKR vaccinated group had bursts of both FMDV O-SKR and O1-Manisa specific plasma cells, again indicating that the inactivated FMDV O-SKR vaccine was able to induce cross reactive plasma cells. This was again confirmed by the presence of liquid phase blocking and virus neutralising antibodies specific for both FMDV O-SKR and O1-Manisa.

The vaccinated and non-vaccinated control animals were challenged with live-virus 21 days after primary immunisation. The virus challenge resulted in a larger antigen-specific plasma cell burst which peaked 7 days after live-virus challenge. This was coupled with an increase in both the liquid-phase blocking antibody and virus neutralising antibody titres, in all of the animals. The timing of the IgG plasma cell burst is in keeping with data recently published by Pega *et al.* who demonstrated, post live-virus infection, an increase in IgG FMDV-specific antibody secreting cells in lymphoid tissues from day 4 to day 6 post-infection [153].

The group of FMDV O1-Manisa vaccinated animals developed a burst of plasma cells, that were specific for both FMDV O1-Manisa and O-SKR. The magnitude of the plasma cell burst was similar between the two FMDV vaccine antigens but was larger than the plasma cell burst shown post-immunisation. The plasma cell burst post challenge was coupled with an increase in both the liquid phase blocking and virus neutralising antibodies, which were specific for both FMDV O1-Manisa and O-SKR. The group that had been previously immunised with inactivated FMDV O-SKR also demonstrated an

increased plasma cell burst following live-virus challenge, which was only FMDV O-SKR-specific. Despite the induction of FMDV O1-Manisa specific plasma cells post primary immunisation, no FMDV O1-Manisa specific plasma cells were detected in this group of animals post-FMDV O-SKR live virus challenge. This data shows that the homologous live-virus challenge had resulted in driving the plasma cell response towards a FMDV O-SKR specific response, resulting in the loss of the previously developed FMDV O1-Manisa plasma cell response. The affinity of the BCR for its cognate antigen is an important factor in driving the B cell response. Indeed, studies in transgenic mice have shown that altering the affinity of the BCR-antigen interaction can affect the B cell fate [227]. Thus, it is likely that the B cells that were specific for FMDV O-SKR in the O-SKR vaccinated group were of a higher affinity for the challenge virus (FMDV O-SKR) which resulted in those B cells out-competing any FMDV O1-Manisa specific B cells post live-virus challenge.

However, despite the lack of detectable FMDV O1-Manisa specific plasma cells in the FMDV O-SKR vaccinated group there was an increase in both the liquid phase blocking and virus neutralising antibodies specific for FMDV O1-Manisa. This would indicate that there was a compartment of antibody secreting cells that were not detectable in the peripheral blood. Pega *et al.* have recently shown that following FMDV live-virus challenge there is a rapid induction of FMDV-specific antibody secreting cells in tissues where the FMDV virus undergoes proliferation (i.e. the tracheobronchial lymph nodes). The magnitude of the IgG FMDV-specific antibody secreting cell response in the local lymphoid tissues, detected by Pega *et al.*, was much greater than that shown in the peripheral blood of the animals in this study [153]. Thus, the data from this study adds weight to the finding's of Pega *et al.* that the majority of the FMDV-specific response is largely confined to the local lymphoid tissues post-challenge [153]. Indeed, it has been previously described by McHeyzer-Williams, that short-lived extra-follicular plasma cells remain in-situ and secrete antibody into the circulation after antigenic challenge [74]. Although kinetic of the isotype-specific (IgM, IgG1 and IgG2) anti-FMDV antibody response was not determined in this study. It has recently been shown by Pega *et al.* that the anti-FMDV antibody response is predominated by IgM isotype antibodies in cattle that have been infected with FMDV following aerosol exposure and represented a large proportion of the neutralising capability of the cattle sera at days 5 and 6 post infection [153]. The increase in anti-FMDV IgM isotype antibodies in the cattle sera coincided with the reduction in FMDV viral RNA from the peripheral blood [153]. This data suggests that the early induction of the IgM anti-FMDV response following FMDV infection is crucial to control FMDV infection and is likely to be the result of short-lived extrafollicular plasma cells in the local lymphoid tissues. The previously vaccinated animals demonstrated an increase in antigen-specific plasma cell number

from day 4 post live-virus challenge, whereas the non-vaccinated control animals showed a delayed and smaller FMDV O-SKR-specific plasma cell burst at day 7 post-infection. The timing of the plasma cell burst in the non-vaccinate control animals would be consistent with a naïve B cell response to the FMDV O-SKR live-virus challenge. Indeed, respiratory syncytial virus (RSV) infection in humans also induced a detectable RSV-specific plasma cell burst from day 8 to 16 post viral challenge [215]. Interestingly, there was an association between individuals that exhibited a prolonged RSV-specific plasma cell burst and the length of time that they shed virus [215]. Wrammert *et al.* also suggest that following infection with the 2009 pandemic H1N1 influenza virus, H1N1-specific plasma cells are generated continuously whilst the infection is ongoing [228]. This suggesting a role for antigen-persistence to maintain both the RSV and also H1N1-specific plasma cell bursts following infection [215, 228]. The non-vaccinated control group of animals had begun to recover from FMDV infection by day 8pc (data not shown), which may explain why there are no detectable FMDV O-SKR-specific plasma cells in the peripheral blood by D14pc. Despite the reduced size of the plasma cell burst in peripheral blood at day 7 post infection, the animals still showed an increase in both virus neutralising and liquid phase blocking antibody titres, against both FMDV O1-Manisa and O-SKR. This data again suggests that there is a compartment of antibody secreting cells that are not detected in the peripheral blood, which is likely to be at the site of infection, as shown by Pega *et al* [153].

The plasma cells detected in the peripheral blood of the cattle in this study, following both vaccination and live-virus challenge, are likely to be extra-follicular in origin, inducted by the TI-2 nature of the FMDV capsid structure. Whilst it has been previously described by McHeyzer-Williams, that short-lived extra-follicular plasma cells remain in-situ and secrete antibody into the circulation after antigenic challenge [74], studies in mice have shown that extra-follicular plasma cells are able to exit the secondary lymphoid organ following viral challenge [229]. Thus, it is probable that the majority of the antigen-specific plasma cells induced following live-virus challenge (and vaccination) with FMDV are extra-follicular in origin, and remain in the lymphoid tissues at the site of infection. The plasma cells detected in peripheral blood are likely to be extra-follicular plasma cells that have exited the lymphoid tissue into the circulation. Although, Juleff *et al.* have shown that FMDV infection is also able to induce a TD response to the GH-loop of the FMDV capsid [198], thus it is also possible that a proportion of the antibody-secreting cells detected in the peripheral blood, following both vaccination and live-virus challenge, are the result of a TD response and originate from a GC reaction.

There was a positive correlation between the peak of the antigen-specific plasma cell responses following both vaccination and live-virus challenge and the antigen-specific

liquid-phase block antibody titres. There was no correlation between the virus neutralising antibody titre and the plasma cell response. This is in keeping with previously published data on cattle that showed a positive correlation between the antibody titre and the size of the plasma cell burst post booster vaccination with a TD antigen [124]. A correlation between the size of the antigen-specific plasma cell burst and the antibody titre has also been shown in humans, following immunisation with a polysaccharide vaccines [171, 230]. Vaccination and live-virus challenge stimulates the induction of antigen-specific plasma cells, and, as the number of these cells increase, it reasonable to assume that there would be a correlation between them and the antibody levels generated. The lack of correlation between the plasma cell response and the virus neutralising antibody titre is not surprising, as the ELIspot assay measures antibody secreting cells that produce antibodies that are able to bind antigen, rather than neutralise it. The lack of a correlation could also indicate that the number of antigen-specific B cells detected in the periphery does not reflect the total pool of antibody secreting plasma cells. Indeed, poor correlations between protective HA-inhibition antibody titres and the plasma cell response detected in peripheral blood during influenza vaccination are due to generation of local responses to antigen in the local lymphoid tissue, which is not adequately assessed by blood sampling [231].

Antibodies that were specific for the FMDV non-structural proteins were not detected in any of the animals until day 7 post infection. The timing of the emergence of these antibodies was consistent with a naïve B cell response. The FMDV non-structural protein 3ABC of the FMDV virion is not present in FMDV vaccine preparations, thus it is only encountered upon live-virus challenge. This data is consistent with a lack of detectable FMDV 3ABC specific antibodies prior to FMDV O-SKR live-virus challenge.

It has long been noted that acute cytopathic viral infections, such as vesicular stomatitis virus [232] and influenza virus [233], result in the rapid induction of antibody in a T-independent manner. T-independent type 2 antigens have regularly spaced repeating epitopes that are able to stimulate B cells in the absence of $CD4^+$ T cell help [166]. The FMDV capsid also has structural features that are likely to make it stimulate B cells in a TI-2 manner. Indeed, adoptive transfer studies in mice have shown that protection from FMDV infection is induced in a T-independent manner. It has been hypothesised that the accelerated induction of antibody in a T-independent manner provides a rapid means of stopping systemic spread of the virus [212]. Indeed, Pega *et al.* have recently demonstrated that the rapid induction of FMDV-specific IgM titre, post FMDV challenge, correlated with the reduction of FMDV viral RNA in the blood [153]. Juleff *et al.* have shown that cattle can produce class-switched antibody rapidly in response to FMDV challenge, despite being depleted of $CD4^+$ T cells, thus demonstrating the largely T-independent nature of FMDV [198]. Pega *et al.* have also recently demonstrated that

rapid induction of FMDV-specific plasma cells in local lymphoid tissue, following live-virus challenge, is consistent with a T-independent response. This study has revealed further evidence to support the hypothesis that FMDV is a largely TI-2 antigen, as there were no detectable FMDV-specific memory B cells in any of the cattle in this study, following either vaccination or live-virus challenge. As discussed in Chapter 2, immunisation of cattle with the TI-2 antigen TNP-Ficoll resulted in an undetectable number of antigen-specific memory B cells [218]. The lack of detectable FMDV-specific memory B cells in cattle is also consistent with other TI-2 antigens. Kelly *et al.* have shown, in humans, that following immunisation with the TI-2 antigen, meningococcal serogroup C polysaccharide, very low/undetectable numbers of memory B cells were detectable [171]. Although it should be noted that the presence of IgG memory B cells was only performed in the peripheral blood of the cattle. It has been noted previously, in humans, that the marginal zone of the spleen represented the major niche for memory B cells following immunisation with vaccinia virus [234]. The authors of this work also hypothesise that other secondary lymphoid organs could also be an additional reservoir for memory B cells [234]. Thus, it is possible that the lack of detectable memory B cells in cattle following vaccination and live-virus challenge is due to the lack of IgG^+ memory B cells in the peripheral circulation rather than a lack of generation. It may also be the case that the number of circulating memory B cells in these cattle is below the detection level of the ELIspot assay. A further possibility is that IgM^+ memory B cells are generated in response to FMDV vaccination and live-virus challenge, which would not be detected in an IgG-specific ELIspot assay. It has been previously demonstrated that IgM^+ memory B cells can be generated, in the spleen, that are specific for pneumococcal polysacchardies (TI-2 antigen) [235]. Thus it is entirely possible that FMDV is able to invoke an IgM^+ memory B cell response in the spleen that would not be detected by the ELIspot assay used in this study.

A PBMC proliferative response was also demonstrated, against both FMDV O1-Manisa and O-SKR, in all of the vaccinated animals following immunisation. The proliferative response was consistent with data previously published by Carr et al. [199]. Whilst data suggests that FMDV is a largely T-independent antigen, $CD4^+$ T cell depletion in cattle resulted in a significant reduction in the GH-loop specific antibody response [198]. The reduction in GH-loop specific antibodies following $CD4^+$ T cell depletion is attributed to the requirement of $CD4^+$ T cells to mount a class-switched antibody response, thus suggesting that the GH-loop is a TD antigen [198]. The GH-loop is a highly motile disorganised structure [213], which lends itself towards stimulating a $CD4^+$ T cell response. Carr *et al.* have also shown that in order to achieve an optimum B cell response, to inactivated FMDV vaccines, $CD4^+$ T cells must also be stimulated [199].

To conclude, this is the first study to assess the kinetics and magnitude of the systemic IgG plasma and memory B cell response following vaccination and live-virus challenge in cattle. The data from the study confirms that the current inactivated FMDV vaccine and indeed live-virus challenge is unable to induce a memory B cell response, adding to the considerable body of evidence that FMDV is largely a TI-2 antigen. Thus, to further improve the FMDV vaccine to increase the duration of immunity, the antigen must achieve a TD-like B cell response, which would induce long-lived plasma and memory B cells.

Chapter 4

Efferent lymphatic cannulation: a novel model to explore antigen-specific bovine B cell response to FMDV

4.1 Chapter objectives

Define the FMDV-specific B cell response after vaccination with novel FMDV vaccine antigens in peripheral blood and efferent lymph.

4.2 Introduction

The secondary lymphoid tissue is the site where naïve B cells interact with their cognate antigen and are stimulated to differentiate into antibody secreting plasma cells or quiescent memory B cells. The lymph node serves to filter lymph that drains the skin and mucosal surfaces and the lymphatic network serves to transport antigens into the lymph nodes that are located throughout the body. The lymphatic network of the cow is shown in Figure 4.1. Using cattle as an experimental model offers surgical access to the lymphatic system, allowing mononuclear cells to be collected as they exit a regional lymph node, without causing detrimental physiological effect to the animal [236].

Antigen is transported into the lymph nodes via a number of mechanisms depending upon the nature of the antigen. Antigen can be taken up by tissue-resident APCs

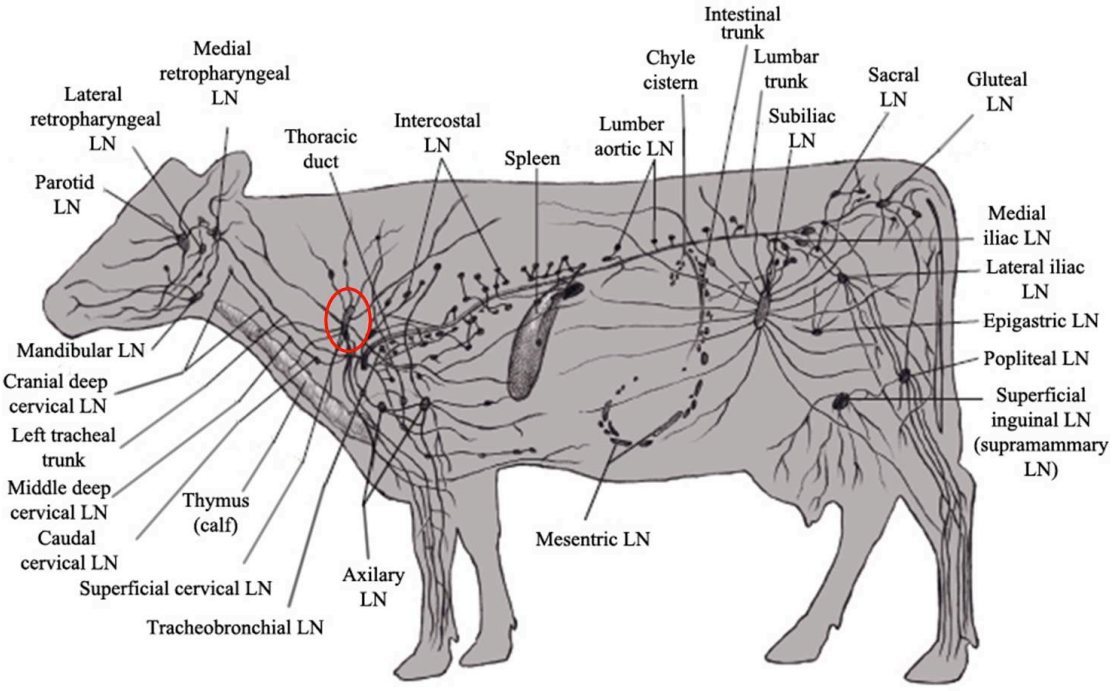


FIGURE 4.1: Schematic showing the bovine lymphatic system. The superficial cervical lymph node is indicated by the red circle. Adapted from [237]

prior to migrating to a regional lymph node. Low molecular weight (LMW, <70kDa) or immune complexed antigen drains from the tissue in the interstitial fluid then into the network of afferent lymphatic vessels. Lymphocytes enter the lymph node via the lymph and the high endothelial venules (HEVs, Figure 1.3). Naïve B cells, which express the chemokine receptor CXCR5, track along the conduit network to the B cell follicle following a CXCL13 chemokine gradient (Figure 1.3) [46]. Within the lymph node antigen-primed DCs preferentially settle around the HEV, presenting whole antigen on their surface for migrating naïve B cells to screen prior to travelling to the B cell follicle [47].

The tissue draining lymph enters the lymph node via the afferent lymphatic vessel into the subcapsular sinus (SCS, Figure 1.3). LMW antigen then diffuses, via the conduit network [51], directly into the margin of the B cell follicle, where it then rapidly enters the B cell follicle (Figure 1.3) [38, 39]. Lymph-borne particulate and large IC antigens are trapped in the subcapsular boundary [52]. The SCS macrophages capture the IC antigen, handing the IC complexes to passing B cells as they migrate into the B cell follicle [52, 53]. Once inside the follicle the B cell transfers the IC antigen to the surface of FDCs [39]. If B cells that collect the antigen from the SCS macrophage are antigen-specific they will engage their BCRs, allowing more antigen to be collected and trigger migration of the activated B cells toward the T cell region of the lymph node [52]. Once antigen is delivered to the B cell follicle, naïve B cells become activated by antigen. The

lymph then drains from the lymph node via the efferent lymphatic vessel. Resident and tissue-derived DCs also settle around the conduit network and probe the passing lymph for antigen as it flows through the lymph node [32, 42]. Whole antigen is also presented on the surface of DCs for B cells to encounter as they enter the lymph node via the HEV [39, 45]. If the cognate antigen is present on the DC, the B cell will stall, taking up antigen from the DC and remain outside of the B cell follicle, receiving $CD4^+$ T cell help from the surrounding T cells [45].

Upon BCR engagement, the BCR is then endocytosed along with the captured antigen, which is then processed to form MHCII-antigen complexes [61]. The MHCII-antigen complexes are then presented to $CD4^+$ T cells [61, 62]. Bidirectional signalling occurs between the B and the CD4 $^+$ T cell, providing TCR stimulation from the B cell and activation signals from the T cell, leading to activation of both cells [67]. The type of antigen determines the resulting B cell response. If the antigen is able to stimulate B cells without the requirement of $CD4^+$ T cell stimulation (TI-2 antigen) the resulting plasma cell response is likely to be extra-follicular in nature [161, 169]. If the B cell requires $CD4^+$ T cell help to become fully activated, then the resulting B cell response (i.e. germinal centre formation) will lead to the production of high affinity antibodies and the formation of long-lived plasma and memory B cells.

Lymphocytes exit the lymph node by migrating across the endothelial barrier of the efferent sinus, which leads to the efferent lymphatic vessel (Figure 1.3). Migration through the secondary lymphoid organ is regulated by the sphingosine 1-phosphate ($S1P_1$) receptors. Lymphocytes and endothelial cells express $S1P_1$ receptors. Binding of the S1P1 receptor by the ligand, S1P, leads to the egress of lymphocyte from the secondary lymphoid organ, overcoming the retention signals mediated by chemokines [40, 48]. There is a concentration gradient of S1P between the lymph node and the lymph and blood [238]. Highly motile lymphocytes are brought to the efferent sinuses through their random migration paths, and in the presence of S1P, exit the lymph node [39].

Protection from FMDV infection is mediated by antibody as determined by passive immunity studies [196]. However, studies in mice and cattle have revealed that the antibody response to FMDV is generated via a T-independent mechanism [197, 198]. This data is further corroborated by the lack of detectable FMDV-specific memory B cells following vaccination or live-virus challenge, suggesting that FMDV is a largely T-independent antigen (As discussed in Chapter 3). Other publications have also shown that TI-2 antigens are able to elicit an extra-follicular plasma cell response but with no memory B cell formation [122, 168, 169]. Thus, understanding the FMDV-specific B cell response in efferent lymph, as the antigen-specific cells exit the lymph node,

will further our knowledge of the kinetics of the FMDV-specific B cell responses post immunisation. Efferent lymphatic cannulation will also provide a method of collecting a higher proportion of antigen-specific B cells for use in immunoglobulin transcriptome analysis using deep sequencing.

The current FMDV vaccine is manufactured as a whole virus preparation that is produced in large-scale suspension or monolayer cultures of baby hamster kidney cells (BHK-21) [178]. The filtered FMDV antigens are then inactivated using the aziridine, binary ethyleneimine (BEI) and mixed with an adjuvant [178]. This method of vaccine production has a number of disadvantages, the most notable being the requirement of high level bio-secure containment during production [175]. Vaccine safety must also be proven after each batch is produced to ensure that vaccine is free from infectious virus [179]. Porta *et al.* have recently shown that non-infectious empty FMDV capsids can be efficiently produced in an insect cell line [210]. The empty capsids are structural mimics of authentic FMDV particle with no bio-security risk associated with their production [210]. They have also shown that the capsids are recognised by a range of anti-FMDV bovine sera [210].

The FMDV capsid is an inherently unstable structure which is sensitive to both heat and pH. Thermal stability differs between serotypes with A and Asia-1 being the most stable and SAT 1-3 the least. The O and C serotypes have intermediate thermal stability. There is an inverse correlation between the thermal stability of the FMDV virion and its immunogenicity, with 146S virus particles being more immunogenic, as compared to 75S and 12S, but the least thermostable [194, 195]. It is also of note that during the virus inactivation process that is required for vaccine production the thermal stability of all FMDV serotypes is likely to be reduced [194, 195]. Thus, good stability of the 146S structure is essential for promoting good vaccine efficacy and the poor thermal stability exhibited by the FMDV capsid may account for the lack of long-term immunity derived from FMDV vaccination [179]. This suggests that producing a mutated empty FMDV capsid that has improved thermal stability may increase the immunogenicity of the FMDV capsid, reduce the need for cold-chain storage during distribution and negate the bio-security risks associated with producing inactivated FMDV vaccines. Indeed, an empty FMDV capsid that has been mutated to increase its thermal properties has been produced by Claudine Porta (Pirbright Institute). This mutant FMDV O1-Manisa capsid (mutant-a) is stable at 56^{o}C for 2 hours (C. Porta, personal communication), which is a 30-fold improvement on the wild-type virus which is only stable at 49^{o}C for 4 minutes [195].

4.2.1 Efferent lymphatic cannulation

Afferent lymphatic cannulation has previously been described as a useful model to understand the biology of skin-draining dendritic cells [236]. The technique utilises the continuous flow of lymph from the tissues into a regional lymph node, in particular the prescapular lymph node (Figure 4.1). Removal of this node and the re-anastomosis of the afferent (in coming) with the efferent (out going) lymphatic vessels and subsequent cannulation of the recently joined lymphatic vessel allows direct access to the skin draining lymph and afferent lymph dendritic cells [236]. In large animals, lymph can be drained continuously for a prolonged period of time without detrimental physiological effect to the animal, thus proving it to be a useful tool in describing the biology of migrating immune cells [236]. Similar techniques have also been described, for different anatomical locations, in both sheep and rats [239, 240, 241]. However, the rat model combines both afferent and efferent lymph by cannulating the thoracic duct and thus does not truly describe either the afferent or efferent compartment [241].

The technique of efferent lymphatic cannulation applies the same principles of afferent lymphatic cannulation, i.e. gaining surgical access to the lymphatic vessels of a regional lymph node, but without the removal of the lymph node. Thus, by leaving the superficial cervical lymph node in-situ, any cells exiting the lymph node post cannulation will be collected and can further interrogated *ex vivo*. As described by Hope *et al.* lymph can be drained from an animal for up to 3 weeks without causing detrimental physiological impact to the animal [236]. Thus the technique lends itself to being an excellent model to study the antigen-specific B cell response post-vaccination in cattle.

To investigate the bovine antigen-specific plasma cell response to FMDV O-serotype antigens in efferent lymph, two experiments were performed. In both studies the efferent lymphatic vessel of the prescapular lymph node was surgically cannulated prior to the booster immunisation.

The first experiment characterised the kinetics of the plasma cell burst in efferent lymph, over a 7 day period, to inactivated FMDV O1-Manisa vaccine antigen and a control TD antigen (TNP-CGG). The kinetics of the B cell response in peripheral blood to the TD antigen, TNP-CGG, and inactivated FMDV O1-Manisa have previously been described in Chapters 2 and 3, respectively. Peripheral blood sampling was also performed in this study at the previously determined important time-points.

The second experiment utilised the data obtained from the first study to characterise the magnitude and kinetics of the FMDV O1-Manisa specific plasma and memory B cell response in both peripheral blood (post-primary and booster immunisation) and efferent

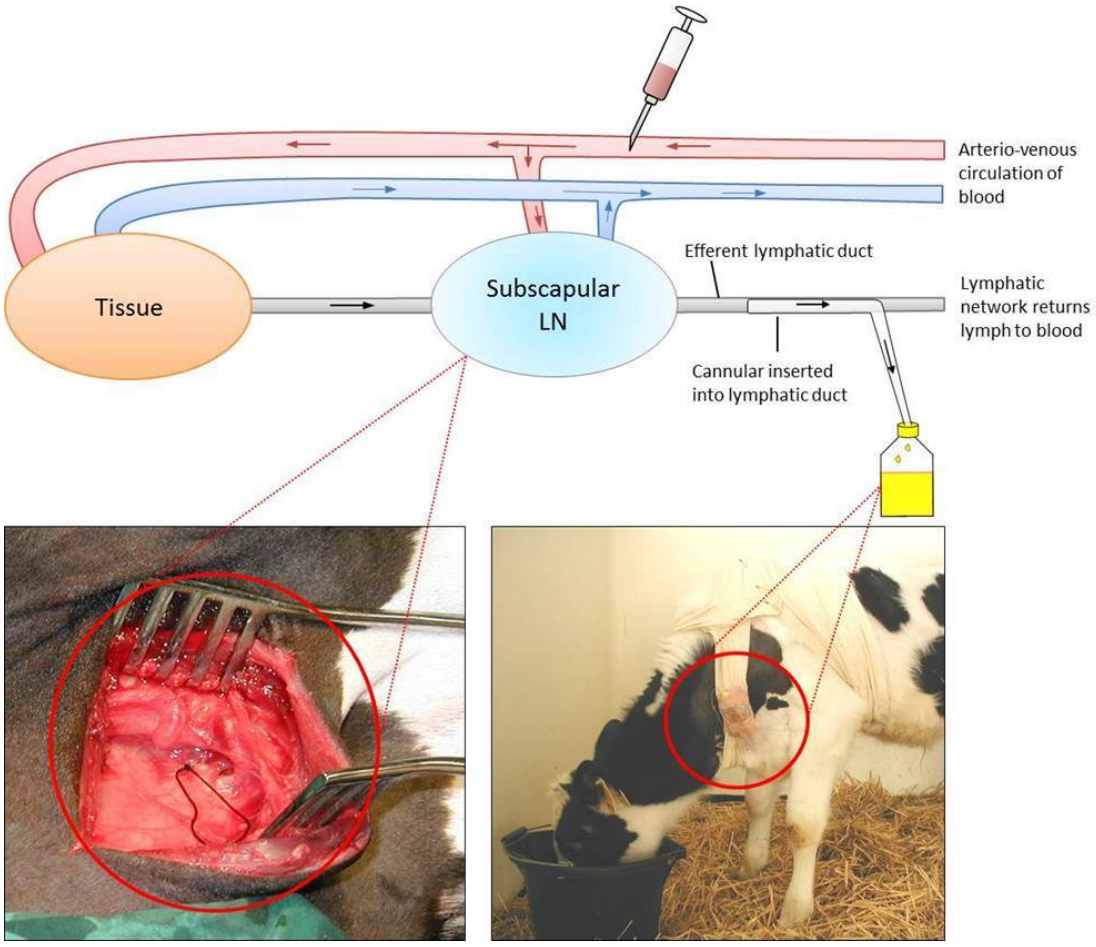


FIGURE 4.2: Schematic diagram showing the efferent lymphatic cannulation model. Vaccine is injected into the tissues (orange) that drain into the subscapular lymph node (light blue). The afferent lymphatic duct (grey) brings the vaccine antigen into the lymph node. Lymphocytes enter the lymph node via the HEV (red) or the afferent lymphatic duct (grey). Lymphocytes exit the lymph node via the efferent lymphatic duct (grey) where a cannula has been surgically inserted into the duct to collect the mononuclear cells as they exit the subscapular lymph node. Peripheral blood is collected by venipuncture. Photographic images are taken from [236]

lymph (post-booster immunisation only) following prime and booster immunisation with FMDV O1-Manisa empty capsid antigens.

4.3 Materials and methods

4.3.1 Calves and experimental protocol for TNP-CGG and FMDV O1-Manisa immunisations

Two, 8 month old, conventionally reared, Holstein-Friesian, male calves (FMDC8 and FMDC9, *Bos taurus*, Pirbright Institute) were immunised intramuscularly, with an emulsion of 3 mg of the hapten TNP-CGG (as described in 2.3.1) and 10μg FMDV O1-Manisa vaccine antigen (Merial Animal Health, Lyon, France) in IFA (as described in 2.3.1).

The efferent lymphatic cannulation procedure was then performed at day 39 post-primary immunisation (as detailed in 4.3.3). A booster immunisation (as detailed above) was then administered, intramuscularly, above the cannulated subscapular lymph node on day 40 post primary immunisation, with the previously described vaccine antigens.

Efferent lymph was collected continuously throughout the study period, and the efferent lymph from each 24-hour collection period were pooled to produce a daily time point sample. Peripheral blood samples were taken from each animal at days 0, 7, 40, 43, 44, 47 and 55 post-primary immunisation (pi), both serum and PBMCs were isolated from these samples. All experiments were approved by the Pirbright Institutes ethical review process and were in accordance with national guidelines on animal use.

The plasma cell response in the blood and lymph to all of the vaccine antigens (TNP, CGG and FMDV O1-Manisa) was monitored using an antigen-specific IgG ELIspot (as described in 2.3.4 and 3.3.2). The kinetics of the plasma cell response to TNP-CGG and FMDV O1-Manisa in the peripheral blood have been previously defined (Chapters 2 and 4). However, it was unknown if this kinetic would be similar in efferent lymph, thus ELIspots using efferent lymphatic mononuclear cells (ELMCs) were performed daily up to day 7 post booster immunisation (day 47 pi). Antigen-specific ELIspots were also performed using PBMCs on day 0, 7, 40 (D0pb), 43 (D3pb), 44 (D4pb), 47 (D7pb) and 55 (D14pb) post immunisation. Antigen-specific IgG titres were also calculated using the TNP- and FMDV O1-Manisa-specific ELISAs (methodology detailed in sections 2.3.5 and 4.3.6).

4.3.2 Calves and experimental protocol for FMDV O1-Manisa capsid antigen immunisations

Four, conventionally reared, Holstein-Friesian male calves were selected for this study (FMDC16 - 19, *Bos Taurus*, Pirbright Institute). Two calves (FMDC16 and FMDC18) were immunised with a FMDV O1-Manisa empty capsid material that was produced

using a vaccinia expression vector in a mammalian cell line (C. Porta, Pirbright Institute). The other two calves (FMDC17 and 19) were immunised with a stabilised FMDV O1-Manisa (mutant-a), that was again produced using a vaccinia expression system (C. Porta, Pirbright Institute). Each calf was immunised with 10μg FMDV capsid material in Montinide ISA 201 VG adjuvant (Seppic, Paris, France). The immunisations were administered intramuscularly, with half a dose above the subscapular lymph nodes on each side of the animal.

The efferent lymphatic cannulation procedure was then performed at day 20 post-primary immunisation (as detailed in 4.3.3). A booster immunisation (as detailed above) was then administered above the cannulated subscapular lymph node on day 21 post primary immunisation, with the previously described vaccine antigens.

Efferent lymph was collected continuously throughout the study period, and the efferent lymph from each 24-hour collection period was pooled to produce a daily time point sample. Matched peripheral blood samples were taken from each animal at days 0, 7, 14, 21 (D0pb), 24 (D3pb), 25 (D4pb), 28 (D7pb) and 35 (D14pb) post-primary immunisation. All experiments were approved by the Pirbright Institutes ethical review process and were in accordance with national guidelines on animal use.

The PBMCs and ELMCs were isolated using the methodology outlined in sections 2.3.2 and 4.3.4.1, respectively. Following isolation and enumeration the PBMCs and ELMCs were used in the FMDV-O1-Manisa specific IgG ELIspot to quantify the antigen-specific plasma and memory B cells present in the peripheral blood and efferent lymph post prime and booster immunisations (using the culture conditions described in section 2.3.3). Serum was also isolated at the same time points as the peripheral blood samples were taken and a FMDV O1-Manisa IgG ELISA was performed using these samples as the methodology described in section 4.3.6.

4.3.3 Efferent lymphatic cannulation technique

The surgical technique employed to cannulate the efferent lymphatic vessel is adapted from Hope *et al.* (2006) with the exception of removing the superficial cervical lymph node prior to surgical cannulation [236]. The surgery was performed by Dr Bryan Charleston and the post-operative care was provided by Helen Prentice and the Pirbright Institute's animal technicians.

Briefly, the animal was starved for 24 hours prior to surgery. A cannula was prepared from lengths of portex tubing (Smiths Medical International Ltd, Hythe, UK), following the procedure described in steps 8 - 12 in Hope *et al.* [236]. On the day of surgery

the animal was anaesthetised and the left pre-scapular region was prepared for surgery. The exact surgical site was identified by palpation of the superficial cervical lymph node, and an incision was made below this location (Figure 4.1). The efferent lymphatic vessel should be located adjacent to the superficial cervical artery and vein. An incision was made at the identified location and surgical retractors were used to reveal the underlying tissue. The efferent lymphatic vessel was identified by checking for lymph flow. Once a suitable site was located on the vessel, i.e. there were no branches or valves above the cannula entry point, the cannula was surgically inserted into the vessel and secured in position by ligature. Antibiotic was then applied liberally to the wound and the catheter was externalised on the animal via a separate skin incision. Once efferent lymph was shown to be flowing through the catheter the surgical incision was then closed. The calf was housed in a clean stable after recovery with access to both food and water. The cannula was inserted into a sterile tissue culture flask (T75, Sigma-Aldrich) which was attached to the animal via an elastoplast harness (see image in 4.2). The animal was given regular heparin and antibiotic therapy, at regular interval throughout the study, to maintain efferent lymph flow. The efferent lymph collection bottles were changed twice daily for as long as the cannula continued to flow, up to 4 weeks post-surgery [236].

4.3.4 Bovine mononuclear cell isolation

Fifty millilitres of heparinised peripheral blood was sampled, by venipuncture, from each calf at D0, D7, D21, D24, D25, D28 and D35. Bovine PBMCs were isolated from the heparinised peripheral blood using the methodology previously described in section 2.3.2.

4.3.4.1 Mononuclear cell isolation from efferent lymph

Mononuclear cells were isolated from efferent lymph using a modified version of the PBMC isolation protocol. Briefly, the twice daily collected efferent lymph samples were pooled to generate a single daily efferent lymph sample and the total volume of lymph collected from the animal was recorded. The efferent lymph was then centrifuged at 1500 x g for 5 minutes to pellet the efferent lymphatic mononuclear cells (ELMC). The supernatant was removed from the sample and the cell pellet was re-suspended in 50mL of dPBS (Invitrogen). The mononuclear cells were then isolated from the re-suspended efferent lymphatic cells using density centrifugation, as previously described in section 2.3.2.

A proportion (2 x 10^7 ELMCs) of the isolated ELMCs from FMDC8 and 9 were stored in 1mL of foetal calf serum containing 10% dimethyl sulfoxide (DMSO) and stored at

$^{-}70^{o}$C until required. A proportion (4 x 10^6 ELMCs) of the daily lymph collections from FMDC16 to 19 were stored in 1mL of TRIZol and stored at $^{-}70^{o}$C until required, further discussed in 5.

4.3.5 FMDV O1-Manisa and TNP-CGG-specific ELIspot assays

The FMDV O1-Manisa-specific ELIspots were performed on freshly isolated PBMCs and ELMCs from both cohorts of animals (FMDC8-9 and 16 -19) using the same methodology as described in 3.3.2. TNP- and CGG-specific IgG ELIspots were also performed, using the methodology previously described in 2.3.4 on ELMCs and PBMCs isolated from FMDC8 and 9 only.

4.3.6 FMDV O1-Manisa-specific IgG ELISA

96-well plastic plates (BD biosciences, Oxford, UK) were coated for 1 hour at room temperature with 100μl/well of $^{1}/_{5000}$ dilution of rabbit anti-FMDV O1-UKG polyclonal antibody (Pirbright Institute) in carbonate buffer. Following incubation, at room temperature, the plates were washed 5 times in PBS containing 1% Tween20 (Sigma-Aldrich). The plates were then blocked for 1 hour using 100μl/well of PBS containing 1% Tween20 and 4% dried milk (blocking buffer), followed by a washing step, as described above. The plates were then coated with 100μl/well of 1μg/mL inactivated FMDV O1-Manisa or O-SKR vaccine antigen (Merial Animal Health) in PBS containing 1% Tween20 and 4% dried milk. The plates were again washed, as described previously. Serum samples were serially diluted 1:3 in blocking buffer starting at $^{1}/_{50}$ dilution, and 100μl/well of each diluted serum was added before incubating the plate for 1 hour at room temperature. For determination of the plate background optical density (OD) values, some wells were incubated with blocking buffer alone. Following incubation, the plates were washed and incubated for 1 hour at room temperature after addition of 100μl/well of $^{1}/_{100,000}$ dilution of sheep anti-bovine IgG conjugated to horseradish peroxidase (AbD Serotec). Following this, the plates were incubated for 10 minutes with 3,3',5,5'-tetra-methyl benzidine (TMB, Sigma-Aldrich) substrate at room temperature. The reaction was stopped by the addition of 50μl of 1.2M H_2SO_4. The OD values at 450nm and 690nm were determined, at dual wavelength, for each well using a SpectraMAX 250 plate reader (Molecular devices, Sunnyvale, CA). The antigen-specific antibody titre was calculated as follows: the $\log_{10}$ values of sample dilutions were plotted against the $\log_{10}$ values of sample OD and a regression analysis was performed on the linear part of the curve allowing the endpoint titre to be calculated using an OD of twice the background. Results were expressed as the mean of duplicate determinations. The

mean IgG titres and the standard deviation were calculated, using standard statistical methods, for each immunisation and control group at each time point tested.

4.3.7 Fluorescent antibody staining of cells for analysis of surface antigens by flow cytometry

Absolute cell counts of the mononuclear cell subsets in efferent lymph post booster (TNP-CGG + FMDV O1-Manisa vaccine antigen) vaccination were calculated on the daily lymph samples collected from FMDC8 and 9 (daily samples from D0pb to D7pb). The bovine mononuclear cell subsets were identified using the following mouse monoclonal antibodies: CC8 to identify $CD4^+$ cells [242], CC63 to identify $CD8^+$ cells [242], CC15 to identify $WC1^+$ cells [243], CC51 to identify $CD21^+$ cells [244] and IL-A46 to identify $CD11^+$ cells[245]. The panel of monoclonals was used to identify $CD4^+$, $CD8^+$, and $\gamma\delta$ T cells, B cells and monocytes, respectively.

The stored ELMCs (in FCS + 10% DMSO) were gently defrosted using a 37^oC water bath and then was washed using warmed dPBS (37^oC) twice prior to staining for flow cytometric analysis. Once defrosted, ELMCs were enumerated and then resuspended at 10^7 cells/mL in FACS buffer (PBS + 1% bovine serum albumin (BSA, Sigma-Aldrich) + 0.1% Sodium Azide (Sigma-Aldrich) containing 10% normal goat serum (Sigma-Aldrich). The cells were incubated at 4^oC for 30 minutes. The primary antibodies were used at a working concentration of $^1/_{10}$, thus 10μl of the ascitic fluids was added to the appropriate wells of a 96-well plate. After the 30 minute incubation period, 100μl (10^6 cells/well) of the cell suspension was added to each well of the plate. The primary antibody/cell mixture was then incubated at 4^oC for 30 minutes. After the incubation period had elapsed the primary antibody was washed from the cell suspension, twice. The plate was centrifuged at 2000 r.p.m for 2 minutes, the supernatant was removed and the cell pellet was re-suspended by pulsing on a plate shaker at maximum speed for 5 seconds. FACS buffer (200μl) was then added to each well and the plate centrifuged again. The supernatant was once again removed and the pellet was re-suspended, as previously described. A $^1/_{200}$ dilution of the isotype matched secondary antibodies, conjugated to fluorescein isothiocyanate (FITC, Southern Biotechnology Associates, Birmingham, AL), was performed using FACS buffer. One hundred μl of the diluted secondary antibodies was added to the appropriate wells of the 96-well plate. The mononuclear cells were then incubated at 4^oC for 30 minutes. The cells were then washed twice, as previously described. After washing, the stained mononuclear cells were transferred into numbered FACS tubes (BD Biosciences, Oxford, UK) and fixated in 500μl PBS + 1% formaldehyde (Sigma-Aldrich). The fixed and stained ELMCs were acquired using a

FACScan flowcytometer (BD Biosciences). Viable cells were gated based upon the forward (FSC) and side scatter (SSC) plot and 50,000 cells were collected within that gate. Subsequent analysis was performed using FCS express software (De Novo Software, Los Angeles, CA).

4.4 Results

To determine the kinetics and magnitude of the antigen-specific plasma cell response in efferent lymph, two studies were performed. The first, consisting of two animals (FMDC8 and 9), involved a prime and booster immunisation with inactivated FMDV O1-Manisa vaccine antigen and TNP-CGG as a control antigen. As the kinetics of the antigen-specific plasma cell reponse in efferent lymph were unknown, vaccine antigen-specific (FMDV O1-Manisa, TNP- and CGG-) ELIspots were performed daily for up to 7 days after booster immunisation. Peripheral blood samples were taken from both animals at day 0 and day 7 post primary immunisation (pi) and at days 0, 3, 4, 7 and 14 post-booster (pb) immunisation. These time points were chosen as they have previously been defined as being the peaks of the antigen-specific plasma cell bursts for both TNP-CGG and FMDV-O1-Manisa, as discussed in Chapters 2 and 3, respectively.

After determining the kinetics of the antigen-specific plasma cell response in efferent lymph, the knowledge was then applied to a further four animals (FMDC16 to 19) which were given a primary and booster immunisation of either a wild-type (FMDC16 and 18) or mutant-a (FMDC17 and 19) FMDV O1-Manisa capsid antigens. Peripheral blood sampling was performed at the previously described time points and efferent lymph was collected and stored as daily samples. The FMDV O1-Manisa-specific ELIspot was performed at the predicted peaks of the plasma cell burst using both peripheral blood and efferent lymph mononuclear cells.

All six animals underwent successful efferent lymphatic cannulation surgery and demonstrated good lymph flow immediately after recovery. The average daily volume of efferent lymph collected from each animal ranged from 72.5 to 1062.5mL (Table 4.1). All of the animals, with the exception of FMDC17, showed good efferent lymph flow for at least 5 days post-booster immunisation (Table 4.1). Both FMDC8 and 9 had their cannulas removed after 7 days, as this was the end of the scheduled cannulation period. FMDC16, 18 and 19 removed their cannulas overnight on days 4, 5 and 6 post-booster immunisation, respectively (Table 4.1). FMDC17's cannula had a number of blockages from D0pb onwards which, despite regular back flushing, resulted in a diminished flow of lymph. The cannula was removed from this animal at D4pb (Table 4.1).

TABLE 4.1: Volume of efferent lymph obtain from each animal

Days post-booster immunisation	Efferent lymph volumes post efferent lymphatic cannulation (mL)					
	FMDC8	FMDC9	FMDC16	FMDC17	FMDC18	FMDC19
0	1200	1200	50*	100	450	300
1	1200	1000	375	NF	480	470
2	1000	1100	400	17.5**	500	500
3	1100	1100	500	100	275	490
4	900	1000	500		420	550
5	900	1100	350		480	500
6	800	1000	550			500
7	600	1000	550			
Mean	962.5	1062.5	409.4	72.5	434.2	453
S.D.	206.6	74.4	164.7	47.6	82.9	105.7

NF: No efferent lymph flow, cannula blocked, *: cannula partially blocked, **: cannula still partially blocked.

The volume of lymph drained from each animal post booster immunisation, which was administered the day after the efferent lymphatic cannulation technique was performed.

The number of mononuclear cells per mL of efferent lymph was not static within the daily efferent lymph collections over the time course of all the efferent lymphatic cannulation studies. FMDC8 and 9 had on average 0.276 x 10^6 efferent lymph mononuclear cells (ELMCs)/mL (range: 0.12 to 0.432 x10^6 ELMCs/mL) of efferent lymph at D0pb, which began to increase in number from D2pb, peaking at 1.155 x 10^6 ELMC/mL (range: 1.01 to 1.30 x 10^6ELMC/mL) at D3pb, and decreasing again by D5pb to 0.248 x 10^6 ELMC/mL (Figure 4.3).

A similar kinetic in the total number of ELMCs/mL of efferent lymph was also observed in the second group of efferent lymphatic cannulation animals (FMDC16 - 19, Figure 4.4). All of the animals showed a peak in the total number of ELMCs/mL of lymph at D4pb (mean: 6.99 x 10^6 ELMC/mL, range: 8.9 to 5.28 x 10^6 ELMC/mL), which then declined by D5pb to 2.04 x 10^6 ELMC/mL (range: 0.74 to 3.11 x 10^6 ELMC/mL, Figure 4.4). Prior to the increase in ELMC number from D3pb onwards, there was a decline in the number of ELMC/mL at D1pb, 2.587 x 10^6 ELMC/mL (range: 1.89 to 3.78 x 10^6 ELMC/mL), as compared to 4.44 x 10^6 ELMC/mL at D0pb (range: 2.56 to 6.64 x 10^6 ELMC/mL) and 3.88 x 10^6 ELMC/mL (range: 1.59 to 7.70 x 10^6 ELMC/mL) (Figure 4.4).

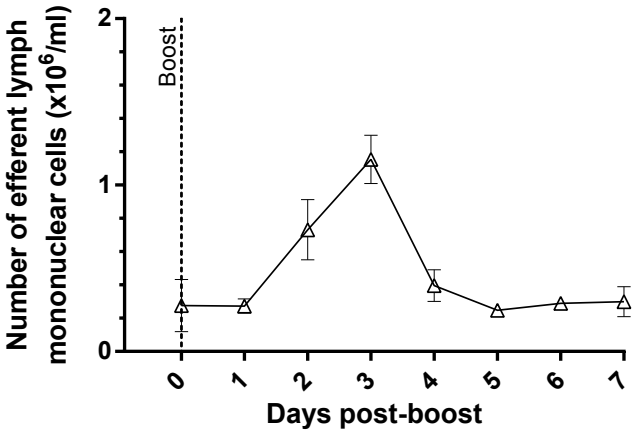


FIGURE 4.3: Kinetic of the mononuclear cell counts (x10^6/mL) in efferent lymph following efferent lymphatic cannulation after a prime and booster immunisation regime with TNP-CGG and FMDV O1-Manisa vaccine antigen. Data shown as mean of animal group ± range ($n = 2$).

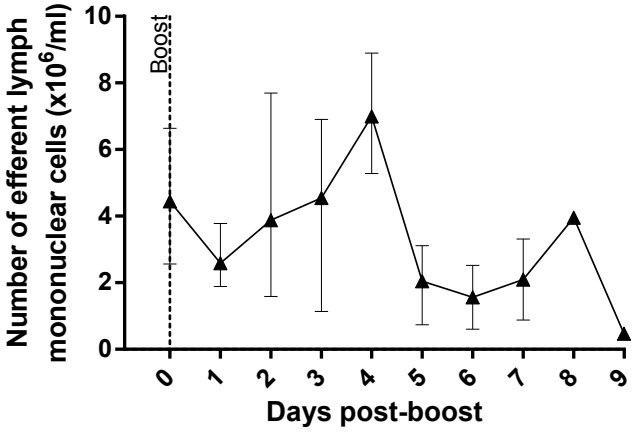


FIGURE 4.4: Kinetic of the mononuclear cell counts (x 10^6/mL) in efferent lymph following efferent lymphatic cannulation after a prime and booster immunisation regime with FMDV O1-Manisa capsid antigens vaccine antigen. Data shown as mean of animal group ± range ($n = 4$).

4.4.1 Kinetics of mononuclear cell subsets in efferent lymph post booster immunisation

To establish the kinetics of the individual mononuclear cell subsets, a panel of monoclonal murine antibodies was used to identify $CD4^+$ (CC8) , $CD8^+$ (CC63), and $\gamma\delta$ (CC15) T cells, B cells (CC51) and monocytes (IL-A46) in the daily efferent lymph samples (FMDC8 and 9 only) using flow cytometry (Figure 4.5).

The absolute number of $CD21^+$ B cells, $CD4^+$ T cells and $WC1^+$ $\gamma\delta$ T cells were similar at D0pb (0.11 x 10^6/mL ± 0.09 range, 0.05 x 10^6/mL ± 0.003 range and 0.09 x 10^6/mL ± 0.06 range, respectively, Figure 4.5). At D1pb, both the $CD4^+$ T cells and $CD21^+$ B cell counts decreased to 0.04 x 10^6/mL ± 0.01 range and 0.05 x 10^6/mL ± 0.04 range, respectively (Figure 4.5). However the $WC1^+$ $\gamma\delta$ T cells increased in their absolute cell count at D1pb (0.16 x 10^6/mL ± 0.04 range, Figure 4.5). After the peak in $\gamma\delta$ T cell numbers at D2pb (0.33 x 10^6/mL ± 0.17 range), the cell count of this T cell subset gradually declined and then plateaued at D4pb (0.61 x 10^6/mL ± 0.03 range, Figure 4.5). The $CD4^+$ T cells began to increase in absolute cell count from D2pb (0.20 x 10^6/mL ± 0.05 range), peaking at D3pb (0.429 x 10^6/mL ± 0.16 range) before plateauing from D4pb onwards (0.09 x 10^6/mL ± 0.02 range, Figure 4.5). The $CD21^+$ B cells also increased in absolute cell count from D2pb onwards, peaking at D3pb (0.24 x 10^6/mL ± 0.12 range) but then declining in cell count by D5pb (0.11 x 10^6/mL ± 0.02 range, Figure 4.5).

The $CD11^+$ monocyte population cell count remained constant throughout the time-course at a daily average of 0.01 x 10^6/mL (range: 0.003 to 0.03 x 10^6/mL, data not shown). The $CD8^+$ T cell population was also fairly consistent with a daily average cell count of 0.04 x 10^6/mL (range: 0.01 to 0.11 x 10^6/mL, data not shown). However, there was an increase in the absolute $CD8^+$ T cell count at D3pb (0.11 x 10^6/mL ± 0.03 range, Data not shown).

4.4.2 Antigen-specific plasma cell kinetics following primary and booster immunisation with TNP-CGG and inactivated FMDV O1-Manisa in peripheral blood and efferent lymph

To determine the kinetics of antigen-specific plasma cell burst in efferent lymph, two animals (FMDC8 and 9) were given a primary and booster immunisation with TNP-CGG and inactivated FMDV O1-Manisa (O1M) vaccine antigen (Merial Animal Health). Antigen-specific ELIspots were performed on the efferent lymph samples daily to determine the kinetics of the plasma cell burst, post-boost, in efferent lymph.

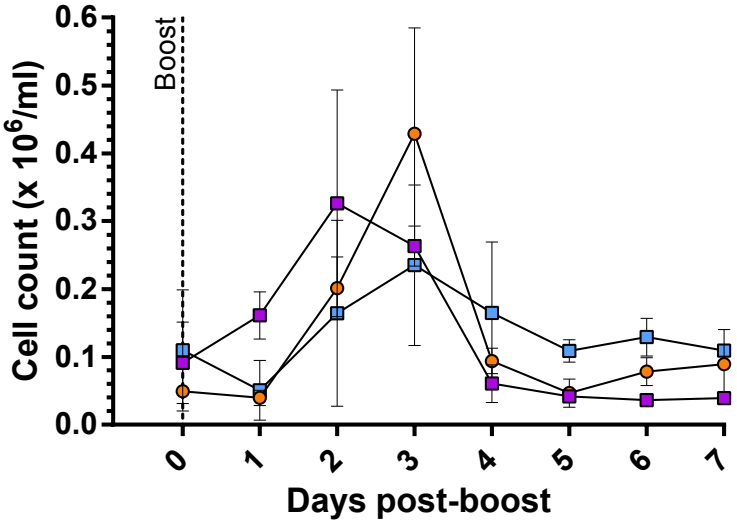


FIGURE 4.5: Kinetic of the absolute cell counts of $CD21^+$ B cells (blue squares), $CD4^+$ T cells (orange circles) and WC1 $^+$ $\gamma\delta$ T cells (purple squares) in efferent lymph following prime and booster immunisation with TNP-CGG and FMDV O1-Manisa vaccine antigen. Data shown as mean of animal group ± range ($n = 2$).

Following prime and booster immunisation, a peak of antigen-specific plasma cells was detected in peripheral blood at D7 post-primary immunisation (pi, TNP: 9±3, CGG: 45±1, O1M: 6±3 -specific ASCs per 10^6 PBMCs, Figure 4.6). After the primary plasma cell burst the antigen-specific plasma cell numbers were undetectable by D40pi (D0pb, Figure 4.6). Following booster immunisation, at D40pi (D0pb) there was a second peak of antigen-specific plasma cells at D4pb (D44pi, TNP: 159±144 range, CGG: 1054±765, O1M: 110±22 -specific ASCs per 10^6 PBMCs). At D7pb (D47pi) there was a reduced number of detectable antigen-specific plasma cells in the peripheral blood (TNP: 3.5 ±3.5, CGG: 18.5 ±0.5, O1M: 7.5 ±0.5 -specific ASCs per 10^6 PBMCs, Figure 4.6). By D14pb (D55pi) both the TNP and FMDV O1-Manisa specific plasma cells were undetectable in peripheral blood, with only a small number of CGG-specific plasma cells detectable (CGG: 15 ± 10 -specific ASCs per 10^6 PBMCs, Figure 4.6).

Both animals underwent efferent lymphatic cannulation surgery prior to the booster immunisation being administered. Efferent lymph was collected continuously for 7 days after booster immunisation and the antigen-specific ELIspots were performed daily. On the day of boost, D0pb (D40pi), there were detectable plasma cells in the efferent lymph, specific for all three of the vaccine antigens (TNP: 31 ± 10 range, CGG: 361 ± 224 range , O1M: 9 ± 1 range -specific ASCs per 10^6 ELMCs, Figure 4.6). At D1pb (D41) there was a decrease in the number of detectable TNP and CGG-specific plasma cells in efferent lymph (TNP: 0, CGG: 88 ± 58 range, Figure 4.6). The number of antigen-specific

plasma cells began to increase for all vaccine antigens from D3pb (D43pi), peaking at D4pb (D44pi, TNP: 319 ± 140, CGG: 6519 ± 2516, O1M: 471 ± 49 -specific ASCs per 10^6 ELMCs, Figure 4.6). At the peak of the secondary plasma cell burst (D4pb, D44pi) there was at least a two-fold increase in the number of antigen-specific plasma cells present in efferent lymph, as compared to peripheral blood (TNP: 159±144 TNP-specific ASCs per 10^6 PBMC vs. 319±140 TNP-specific ASCs per 10^6 ELMC). At D7pb the cannulas were removed from both animals but there were still detectable antigen-specific plasma cells in the efferent lymph (TNP: 170±140, CGG: 954±673, O1M:163±62 -specific ASCs per 10^6 ELMCs, Figure 4.6). There was a significantly higher ($P = 0.0313$, t-test) number of antigen-specific plasma cells in efferent lymph as compared to peripheral blood at D7pb (D47pi).

4.4.3 Antibody titre kinetics following primary and booster immunisation with TNP-CGG and inactivated FMDV O1-Manisa in peripheral blood

Following primary and booster immunisation with TNP-CGG and inactivated FMDV O1-Manisa (O1M) vaccine antigen (Merial Animal Health), the antigen-specific IgG titres were determined by ELISA (Figure 4.7). The TNP-specific IgG titres in serum taken from peripheral blood began to increase in both FMDC8 and 9 from D7pi (TNP: 218 ±36 -specific IgG titre), which further increased at D13pi (TNP: 8843 ±6316 -specific IgG titre, Figure 4.7A). Post booster immunisation there was a further increase in the TNP-specific IgG titres from D7pb (D47pi, TNP: 30553 ±17679 -specific IgG titre, Figure 4.7A). The FMDV O1-Manisa specific IgG titres also showed a similar kinetic during the prime and booster vaccination strategy, although the increase in FMDV O1-Manisa specific IgG titres did not begin to increase until D13pi (O1M: 715 ±440 -specific IgG titre, Figure 4.7B). There was also an increase in FMDV O1-Manisa IgG titres following booster immunisation, particularly from D7pb onwards (D47pi, O1M: 3648.5 ±365.5 -specific IgG titre, Figure 4.7B).

4.4.4 Antigen-specific plasma cell kinetics following primary and booster immunisation with FMDV O1-Manisa capsids in peripheral blood and efferent lymph

The data from the pilot study has shown that the timing of the antigen-specific plasma cell burst in efferent lymph is similar to that of peripheral blood. Using this knowledge, a further four animals were used for efferent lymphatic cannulation studies. The animals were given a prime and booster immunisation (D21pi) of either wild-type FMDV

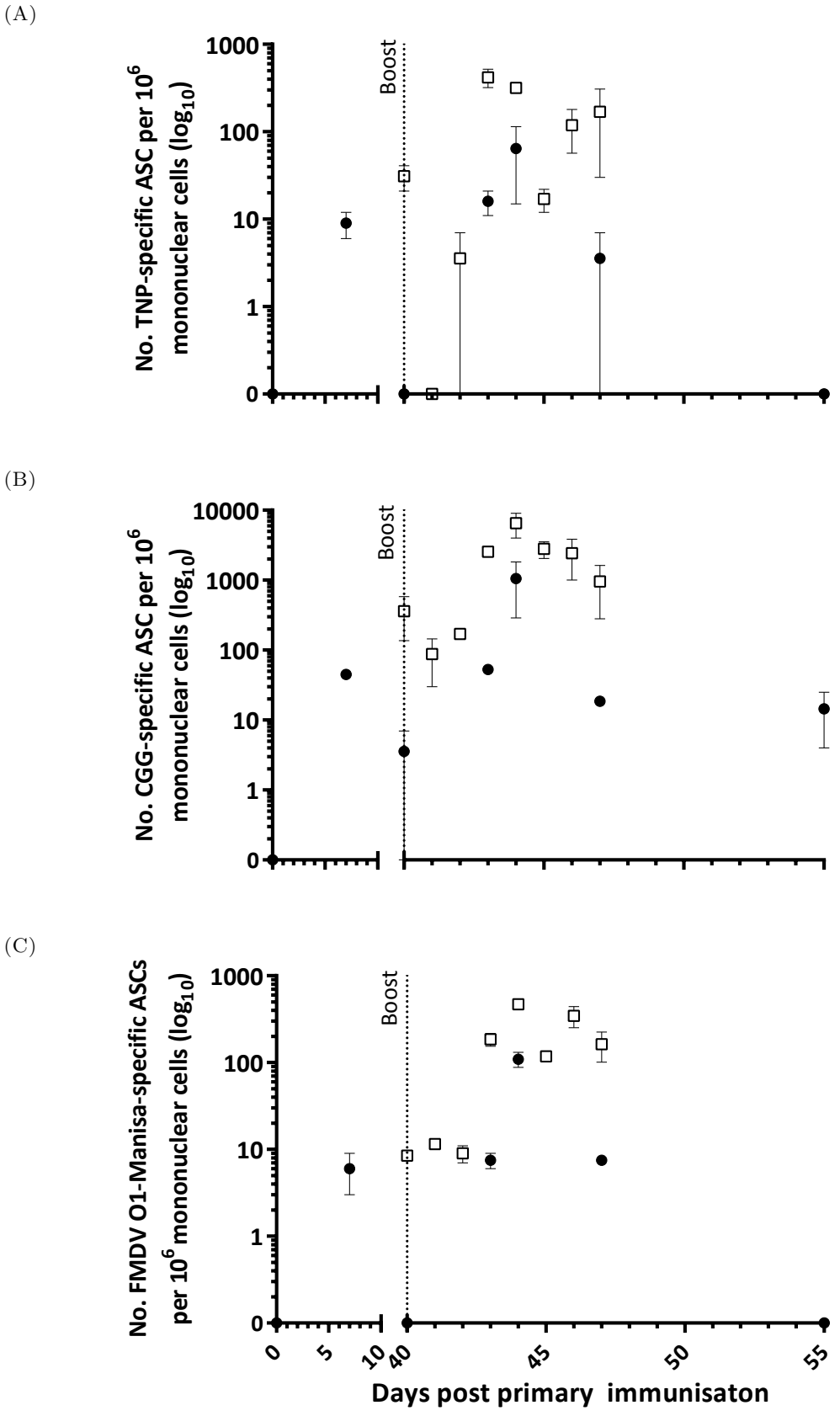
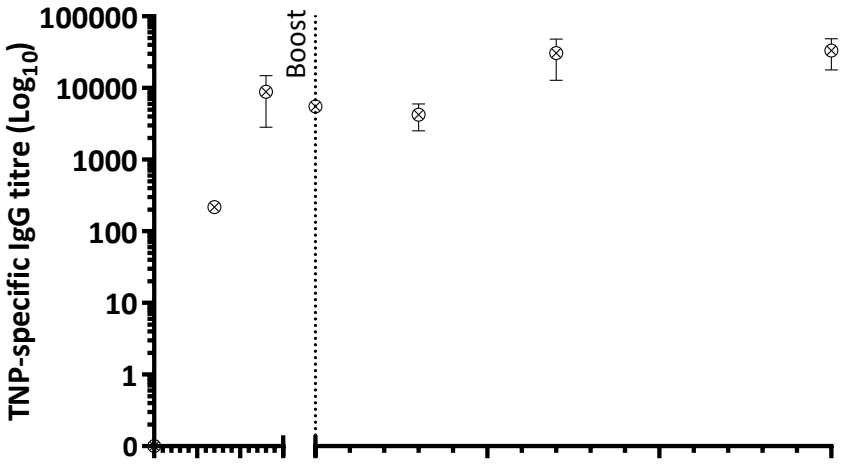


FIGURE 4.6: Kinetic of the (A) TNP- , (B) CGG- and (C) FMDV O1-Manisa specific plasma cell response in peripheral blood (closed circles) and efferent lymph (open squares). Booster immunisation was administered on day 40 (indicated by vertical dotted line). Efferent lymphatic cannulation procedure was performed on day 39 post primary immunisation. Results are expressed as the grouped mean of duplicate determinations from each animal ± the group range ($n = 2$).

(A)



(B)

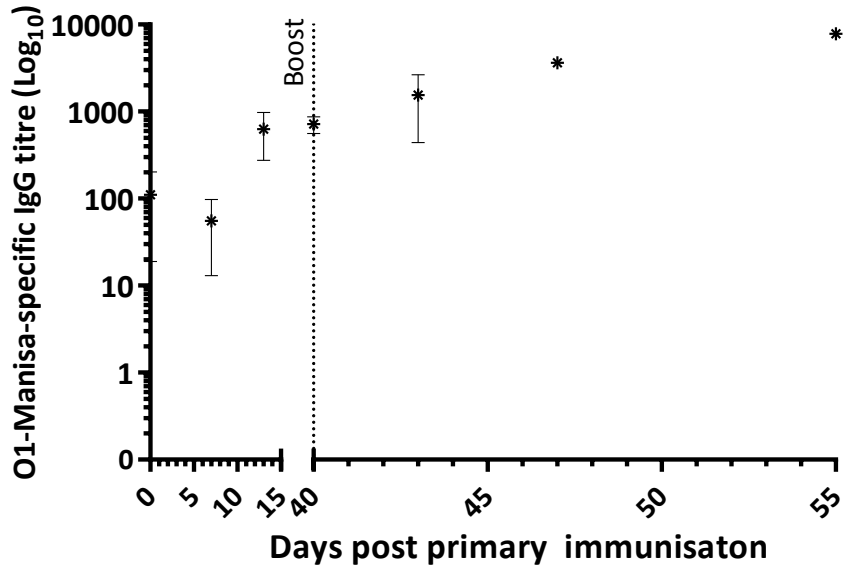


FIGURE 4.7: Kinetic of the (A) TNP- (crossed circles) and (B) FMDV O1-Manisa (black stars) -specific IgG titres in peripheral blood. Booster immunisation was administered on day 40 (indicated by vertical dotted line). Efferent lymphatic cannulation procedure was performed on day 39 post primary immunisation. Results are expressed as the grouped mean of duplicate determinations from each animal ± the group range ($n = 2$).

O1-Manisa capsid (FMDC16 and 18) or a stabilised mutant-a FMDV O1-Manisa capsid (FMDC17 and 19). FMDV O1-Manisa specific ELIspots were performed on both PBMC and ELMC (post-boost only) samples at D0pi, D7pi, D14pi, D21pi (D0pb), D24pi (D3pb), D25pi (D4pb), D28pi (D7pb) and D25pi (D14pb).

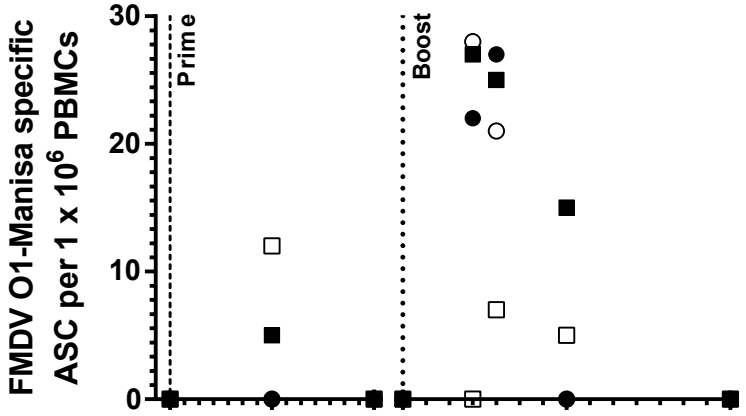
Following primary immunisation there was a detectable FMDV O1-Manisa-specific plasma cell burst at D7pi in the two animals that received the stabilised mutant-a FMDV O1-Manisa capsid (FMDC17 and FMDC19: 5 and 12 FMDV O1-Manisa specific ASCs per 10^6 PBMCs, Figure 4.8A). The animals that received the wild-type FMDV O1-Manisa (FMDC16 and 18) had no detectable antigen-specific plasma cells post primary immunisation (Figure 4.8A). Post booster immunisation a burst of FMDV O1-Manisa-specific plasma cells was observed at D3-4pb (D24-25pi) in all four animals (FMDC16: 27 (D4pb), FMDC17: 27 (D3pb), FMDC18: 28 (D3pb), FMDC19: 7 (D4pb) -specific ASCs per 10^6 PBMCs, Figure 4.8A). By D7pb (D28pi) the number of antigen-specific plasma cells had decreased and were only detectable in the animals that received the stabilised mutant-a FMDV O1-Manisa capsid antigen (FMDC17: 15, FMDC19: 5 -specific ASCs per 10^6 PBMCs, Figure 4.8A). There were no detectable antigen-specific plasma cells by D14pb (D35pi) in the peripheral blood (Figure 4.8A).

Post booster immunisation there were also detectable antigen-specific plasma cells in efferent lymph with a similar kinetic to that shown in peripheral blood (Figure 4.8B). All of the animals removed their cannulas before D7pb, thus ELIspots were only performed on D0, D3 and D4 post-booster-immunisation. There were no detectable antigen-specific plasma cells on the day of booster immunisation in the efferent lymph (Figure 4.8B). However a burst of antigen-specific plasma cells was demonstrated at days 3-4pb in all four animals in peripheral blood (FMDC16: 6 (D4pb), FMDC17: 7 (D3pb), FMDC18: 29 (4pb), FMDC19: 11 (D4pb) -specific ASCs per 10^6 PBMCs, Figure 4.8B). The timing of the antigen-specific plasma cell burst in efferent lymph was in keeping with that shown in peripheral blood.

4.4.5 Antigen-specific memory B cell kinetics following primary and booster immunisation with FMDV O1-Manisa capsids in peripheral blood

The kinetics of FMDV O1-Manisa-specific memory B cell response was also assessed, in peripheral blood, following a prime and booster vaccination with either a wild-type (FMDC16 and 18) or stabilised mutant-a (FMDC17 and 19) FMDV O1-Manisa capsid antigens. There were no detectable antigen-specific memory B cells in any of the animals from D0pi to D21pi (D0pb, Figure 4.9). There was a burst of antigen-specific memory B

(A)



(B)

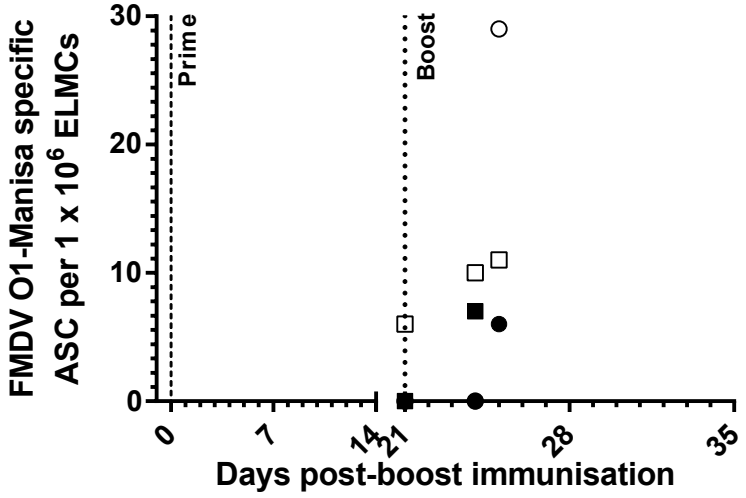


FIGURE 4.8: Kinetic of the FMDV O1-Manisa specific plasma cell response in (A) in peripheral blood and (B) efferent lymph from FMDC16 (closed circles, w/t O1-Manisa capsid), FMDC17 (closed squares, m/t O1-Manisa capsid), FMDC18 (open circles, w/t O1-Manisa capsid) and FMDC19 (open squares, m/t O1-Manisa capsid). Primary immunisation was given at day 0 (D0) and the booster immunisation was administered on day 21 (D21), indicated by vertical dotted lines. Efferent lymphatic cannulation procedure was performed on day 20 post primary immunisation. Results are expressed as the mean of duplicate determinations from each animal.

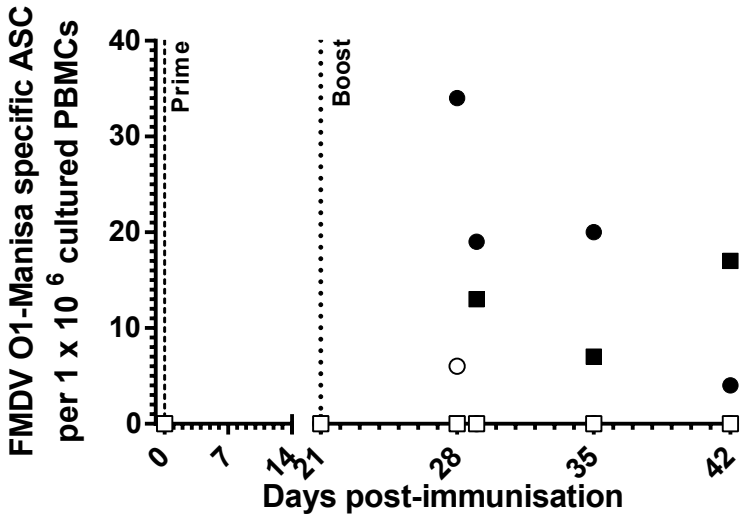


FIGURE 4.9: Kinetic of the FMDV O1-Manisa specific memory B cell response in peripheral blood from FMDC16 (closed circles, w/t O1-Manisa capsid), FMDC17 (closed squares, m/t O1-Manisa capsid), FMDC18 (open circles, w/t O1-Manisa capsid) and FMDC19 (open squares, m/t O1-Manisa capsid). Primary immunisation was given at day 0 (D0) and the booster immunisation was administered on day 21 (D21), indicated by vertical dotted lines. Results are expressed as the mean of duplicate determinations from each animal.

cells in 3 of the 4 animals at days 7 to 8pb (D28 - 29pi, FMDC16: 34 (D7pb), FMDC17: 13 (D8pb), FMDC18: 6 (D7pb) -specific ASCs per 10^6 cultured PBMCs, Figure 4.9). Antigen-specific memory B cells were still detectable in half of the animals by D14pb (D35pi, FMDC16: 4, FMDC17: 17 -specific ASCs per 10^6 cultured PBMCs, Figure 4.9).

4.4.6 Antibody titre kinetics following following primary and booster immunisation with FMDV O1-Manisa capsid antigens

Following primary and booster immunisation with either a wild-type (FMDC16 and 18) or stabilised mutant-a (FMDC17 and 19) FMDV O1-Manisa capsid antigen the antigen-specific IgG titres were determined by ELISA (Figure 4.10). The FMDV O1-Manisa-specific IgG titres in serum taken from peripheral blood began to increase in all of the animals from D7pi (FMDC16: 27, FMDC17: 104, FMDC18: 108, FMDC19: 475 FMDV O1-Manisa-specific IgG titres), and had further increased by D21pi (D0pb, FMDC16: 114, FMDC17: 953, FMDC18: 267, FMDC19: 3353 FMDV O1-Manisa-specific IgG titres, Figure 4.10). Post booster immunisation there was a further increase in the O1-Manisa-specific IgG titres from D3pb (D24pi, FMDC16: 205, FMDC17: 815, FMDC18: 341, FMDC19: 8153 FMDV O1-Manisa-specific IgG titres, Figure 4.10). The FMDV O1-Manisa-specific IgG titres remained elevated until the end of the study (D14pb (D35pi)

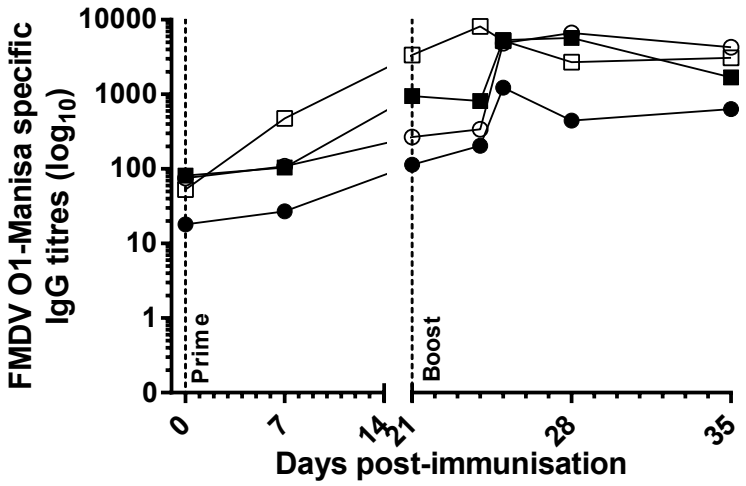


FIGURE 4.10: Kinetic of the FMDV O1-Manisa specific IgG titres from FMDC16 (closed circles, w/t O1-Manisa capsid), FMDC17 (closed squares, m/t O1-Manisa capsid), FMDC18 (open circles, w/t O1-Manisa capsid) and FMDC19 (open squares, m/t O1-Manisa capsid) following a primary and booster immunisation with FMDV O1-Manisa capsid antigens. Primary immunisation was given at day 0 (D0) and the booster immunisation was administered on day 21 (D21), indicated by vertical dotted lines. Results are expressed as the mean of duplicate determinations from each animal.

FMDC16: 634, FMDC17: 1690, FMDC18: 4297, FMDC19: 3079 FMDV O1-Manisa-specific IgG titres, Figure 4.10). Linear regression models have shown that there was no positive correlation between the magnitude of the FMDV O1-Manisa-specific plasma cell response and the end-point IgG titre.

4.5 Discussion

This is the first study to describe the magnitude and kinetics of the antigen-specific plasma cell response in both efferent lymph and peripheral blood, following immunisation with either an inactivated FMDV O1-Manisa vaccine antigen or FMDV O1-Manisa empty capsid antigens. Briefly, the FMDV O1-Manisa-specific plasma cell response in peripheral blood was characterised by a burst of antigen-specific plasma cells at day 7 post primary immunisation, which was also associated with an increase in the titre of FMDV O1-Manisa specific IgG antibodies. Following booster immunisation there was another burst of FMDV O1-Manisa-specific plasma cells in both efferent lymph and peripheral blood, from days 3 to 4pb, which was coupled with a further increase in FMDV O1-Manisa IgG antibody titres. The timing of the FMDV O1-Manisa-specific plasma cell bursts detected were in keeping with those shown in the previously discussed FMDV O1-Manisa vaccination study (Chapter 3). Moreover, the timing of the plasma

cell burst following primary immunisation is in keeping with previously published data, in peripheral blood, from both humans [171, 214, 215] and cattle [124, 218], with a number of different antigens. There are currently no publications detailing the kinetics of the antigen-specific B cell response in efferent lymph.

In all of the animals, with the exception of FMDC8, that underwent efferent lymphatic cannulation the total number of mononuclear cells in efferent lymph decreased during the first few days following booster immunisation, before beginning to increase in number from day 2 - 3 post booster immunisation. During the early stages of an immune response, lymphoid organs undergo shut down, leading to a reduction in the egress of lymphocytes from the lymph node [246]. An increase in TNF leads to an increase in local S1P production, disrupting the S1P gradient between the lymph and the lymph node [49]. This leads to retention of the lymphocytes in the lymph node [49]. Lymph node shut down has also been described in sheep that have undergone efferent lymphatic cannulation [247]. McConnell *et al.* demonstrated a reduction in total lymphocyte number in efferent lymph in the hours following antigenic challenge, which continued for up to 24 hours post vaccination, although the length of lymph node shut down was dependent upon the immunising antigen [247].

When the mononuclear cell subsets were investigated the number of $CD21^+$ B cells and $CD4^+$ T cells decreased immediately after booster immunisation. It has been documented that during the first few days post antigenic challenge, antigen-specific lymphocytes down regulate their S1P receptor expression, leading to an accumulation of antigen-specific lymphocytes in the lymph node, increasing their ability to interact with the antigen [50]. Indeed McConnell *et al.* also demonstrated a 15% decrease in the percentage of B cells (indicated by surface Ig expression) in efferent lymph in the first 24 hours after vaccination [247]. The number of $CD21^+$ B cells began to increase in the efferent lymph 3 to 4 days post booster immunisation, this coincided with the peak of the antigen-specific plasma cell burst post-boost. It has been shown, in mice, that following booster immunisation, splenic B cells regain S1P receptor expression from day 3pb, allowing the antigen-specific IgG plasma cells to migrate from the secondary lymphoid organ to the bone marrow [248]. The $CD4^+$ T cell numbers also showed an increase from day 2 to 3 post booster immunisation. It has previously been documented that once activated, $CD4^+$ T cells exit the lymph node via re-expression of the S1P receptor, permitting the antigen-specific $CD4^+$ T cell to exit the lymph node [50].

However, whilst the number of B and $CD4^+$ T cells decreased immediately after booster vaccination, the number of $\gamma\delta$ T cells rapidly increased in efferent lymph. $\gamma\delta$ T cells are the most highly abundant lymphocyte subset in cattle and are an innate-like lymphocyte that are able to respond to both pathogen-associated molecular patterns (PAMPs) and

antigen presented by an APC via the engagement with the $\gamma\delta$ T cell receptor [249]. These cells have a pre-activated phenotype that enables them to respond rapidly to antigenic challenge [250]. They are also able to influence antigen-presentation by APCs and recruit monocytes to the site of antigenic challenge [251]. The rapid egress of $\gamma\delta$ T cells from the lymph node immediately after booster immunisation suggests that these cells are early responders to antigenic challenge and are not under the same regulatory mechanisms of lymph node egress as bovine $CD4^+$ T cells and B cells.

When developing the efferent lymphatic cannulation model to detect antigen-specific plasma cells in efferent lymph, a TD control antigen (TNP-CGG) was used alongside the inactivated FMDV O1-Manisa vaccine antigen. The control antigen (TNP-CGG) was used to ensure detection of antigen-specific long-lived plasma cells in efferent lymph. Following booster vaccination (inactivated FMDV O1-Manisa plus TNP-CGG), antigen-specific plasma cells were detectable in efferent lymph, but not in peripheral blood, on the day of boost. Thus antigen-specific plasma cells are still exiting the regional lymph node for a prolonged period post primary immunisation. Indeed it has been documented, in mice, that germinal centres remain established within the secondary lymphoid organs for up to 21 days post immunisation with a TD antigen [252]. The data from this study suggests that there are still established germinal centres present in the bovine regional lymph node on the day of booster immunisation that are producing antigen-specific plasma cells.

Whilst the kinetics of the antigen-specific plasma cell response in both peripheral blood and efferent lymph was similar, regardless of the immunising antigen, the magnitude of the response was different. The magnitude of the TNP-, CGG- and FMDV O1-Manisa-specific plasma cell response following booster vaccination with inactivated FMDV O1-Manisa plus TNP-CGG was much greater than the response in peripheral blood. The magnitude of FMDV O1-Manisa specific plasma cell response was also greater in both efferent lymph and peripheral blood following immunisation with inactivated FMDV O1-Manisa plus TNP-CGG as compared to immunisation with empty FMDV O1-Manisa capsid antigens. Carr *et al.* have recently shown that stimulating the $CD4^+$ T cell response during FMDV vaccination is important for generating an optimum protective antibody titre in cattle [199]. It has also been shown that conjugation of a TD antigen (mutant diphtheria toxoid CRM_{197}) to a TI-2 antigen can increase the magnitude of the plasma cell response to a TI-2 antigen (capsular polysaccharide of serogroup C *Neisseria meningitidis*)[171]. Thus it is possible that the addition of the TD control antigen (TNP-CGG) has boosted the FMDV O1-Manisa-specific response, possibly via bystander stimulation of the FMDV O1-Manisa B cell response by the CD4+ T cell response against the TD antigen, TNP-CGG.

Studies in both cattle and mice have shown that FMDV is a largely T-independent antigen [197, 198]. Literature suggests that TI-2 antigens are capable of generating a very good extra-follicular plasma cell response [169]. It has been shown that B cells that are stimulated by antigen that has a high density of B cell epitopes preferentially induce an extra-follicular plasma cell response [227]. Thus, it could be hypothesised that the TI-2 antigens induce a strong extra-follicular plasma cell response due to the high density of repeating B cell epitopes [227]. Studies in mice have shown that extra-follicular plasma cells are able to exit the lymph node and circulate the periphery [229]. Thus, taking this data into account the antibody secreting cells detected following FMDV immunisation are likely to be extra-follicular plasma cells that are not long-lived.

Following primary and booster immunisation with both the wild-type and the stabilised mutant-a FMDV O1-Manisa capsid antigens there was a burst of detectable FMDV O1-Manisa-specific plasma cells following primary immunisation in peripheral blood and in both blood and efferent lymph following booster immunisation. The magnitude of the response to both FMDV capsid antigens was similar in both peripheral blood and efferent lymph, post booster immunisation. Also, the magnitude of the FMDV O1-Manisa-specific plasma cell response following primary immunisation with the FMDV O1-Manisa capsid antigens was similar to that achieved following primary immunisation using the conventional inactivated FMDV O1-Manisa antigen, as previously discussed in Chapter 3. This suggests that FMDV O1-Manisa capsid antigens may be used as a suitable replacement for conventional inactivated FMDV O1-Manisa vaccines, although further studies would be required to confirm if the empty capsid antigens are able to provide protection from live-virus challenge.

Doel *et al.* suggested that increasing the thermal stability of the FMDV capsid would lead to an increase in the immunogenicity of the stabilised capsid [179, 194, 195]. The data from this small group of animals does not show an increase in the magnitude of the antigen-specific B cell response, in fact the response was comparable between the wild-type and the stabilised mutant-a FMDV O1-Manisa empty capsids. However, the mutant-a FMDV O1-Manisa empty capsid is stable at 56^{o}C for 2 hours (C. Porta, personal communication), which is a 30-fold improvement on the wild-type virus which is only stable at 49^{o}C for 4 minutes [195]. Whilst the data presented here does not suggest that stabilisation has increased capsid immunogenicity, it has improved the ease with which this vaccine can be distributed by reducing the cold-chain requirement.

In three of the four animals that received the FMDV O1-Manisa empty capsid antigens, FMDV O1-Manisa-specific memory B cells were detectable in peripheral blood from days 7 to 8 following booster immunisation, albeit at a reduced number as compared to a TD antigen. It has long been documented that TI-2 antigens are able to induce

memory B cell development in the absence of germinal centre formation [253, 254]. The TI-2 memory B cell population has fewer isotype switched cells, with V-regions that are less mutated and are not long-lived [39, 113]. Berkowska *et al.* have shown that $CD27^{+}IgM^{+}IgD^{+}$ resemble marginal zone B cells and are formed in response to TI-2 antigens [151]. Litinskiy et al. have demonstrated that class switching can be induced in the absence of GC formation by APRIL and BAFF, thus providing GC-independent memory B cells with a mechanism of becoming class-switched [144]. Indeed, $CD27^{-}IgA^{+}$ class-switched memory B cells have been described in both humans and mice, that are induced independently of $CD4^{+}$ T cell help and are found in the marginal zone of the spleen and in the GALT [151, 255, 256]. Kelly *et al.* have also shown that following immunisation with a TI-2 antigen (serogroup C Menigococcal capsular polysaccharide) a very low number of antigen-specific memory B cells were generated [171]. Since the majority of TI-2 induced memory B cells are IgM, it may mean that they are not detected in the IgG ELIspot assay used to detect FMDV-specific memory B cells in this study.

To conclude, this data shows that the efferent lymphatic cannulation technique can be used to study the bovine antigen-specific plasma cell response in efferent lymph and can provide a useful tool for studying the dynamics of the bovine B cell response in further detail. Due to a lack of bovine-specific reagents that will allow the sorting of plasma and memory B cells the efferent lymphatic cannulation technique can utilised to collect antigen-specific B cells from cattle following immunisation.

Chapter 5

Using next generation sequencing to explore the bovine B cell response to FMDV vaccination in peripheral blood and efferent lymph.

5.1 Chapter objectives

1. Investigate the bovine immunoglobulin repertoire following primary and booster vaccination.
2. Identify potentially FMDV-specific immunoglobulin transcripts.

5.2 Introduction

Antibodies produced by plasma cells play a key role in protecting an individual against pathogenic challenge. Both antibody secreting plasma cells and memory B cells are induced in response to antigenic stimulation, providing an individual with a mechanism of protection against future antigenic challenges. In order to achieve this an individual must develop a broad array of different antibody specificities. For example, humans are able to generate a repertoire of approximately 1 x 10^7 antibodies with unique specificities. Homologs of immunoglobulin and recombination activating genes (RAG) have been found in all known jawed vertebrates, although the germline arrangement of the

immunoglobulin gene segments and recombination mechanisms differ between different species [257]. The diversity seen within the immunoglobulin repertoire is achieved via four mechanisms, and different vertebrates have developed a number of variations upon these mechanisms to generate diversity.

The first mechanism of generating diversity is via gene segment recombination. The variable region (V region) of both the heavy and light chain are formed by recombination of the variable (V), diversity (D, heavy chain only) and joining (J) gene segments (Figure 5.1). Humans have a huge number of V, D and J heavy chain gene segments, 44 V, 27D and 6J, and also a large number of V and J light chain gene segments, 77 V and 20J [258]. Thus recombining different V(D) and J gene segments, termed recombinational diversity, leads to a broad array of heavy and light chain V regions. By contrast, cattle have relatively few V D and J gene heavy chain gene segments, 10 V, 3D and 2J, and 33 V and 4J functional light chain gene segments [259, 260]. Thus, cattle have a comparatively limited pool of gene segments from which to generate a broad array of heavy and light chain V regions.

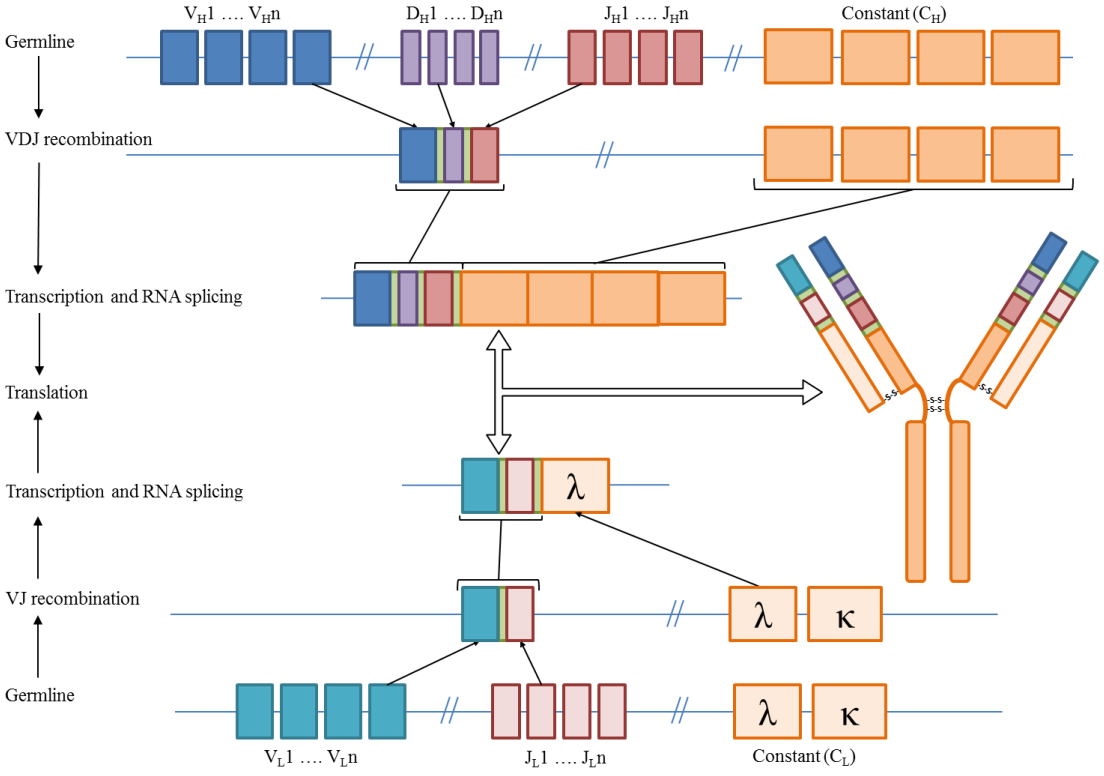


FIGURE 5.1: Schematic diagram of immunoglobulin recombination events. Green segments represent regions of junctional diversity. Adapted from [261].

The second mechanism of increasing the degree of diversity within the V region repertoire is via the process of recombining the V(D)J gene segments. Junctional diversity is generated between the gene segments during the process of recombination (Figure 5.1).

Exonucleases trim the ends of the gene segments whilst terminal deoxynucleotidyl transferase (TdT) adds random nucleotides between the recombined gene segments. However, the extra nucleotides only accounts for the addition of a few amino acids at each junction [262].

The third mechanism of generating repertoire diversity is combinatorial diversity, i.e. the combined variability of both the heavy chain and light chain V regions (Figure 5.1) [263]. Although, not all jawed vertebrates have immunoglobulins that have both a heavy and light chain, both camelids and sharks express bi-valent heavy chain only antibodies that differ in their structures [264, 265]. All three of the previously described processes occur during progenitor B cell development in the bone marrow.

The final mechanism of further increasing the primary immunoglobulin repertoire is via post-recombinational modifications, namely somatic hypermutation (SHM) and gene conversion. Gene conversion, is the principle mechanism of increasing immunoglobulin diversity in both chickens and rabbits. In chickens, the primary immunoglobulin repertoire is highly restricted by the presence of only one functional V_H and V_L gene. During B cell development, within the Bursa of Fabricius, gene conversion replaces regions within the rearranged heavy and light chains with sequences derived from V_H and V_L pseudogenes [266, 267]. There is very little evidence of gene conversion as a mechanism for diversifying the primary immunoglobulin repertoire in cattle [268] and most other vertebrates. Thus gene conversion appears to have evolved in a few species as a mechanism of increasing the immunoglobulin repertoire diversity. Somatic hypermutation adds point mutations to targeted areas within the V region, namely the V(D)J junction. The process is facilitated by the enzyme activation-induced cytidine deaminase (AID), which deaminates cystosine residues to uracils within a WRCY motif, resulting in either the mismatched base being removed, repaired or incorporated into the sequence during replication [269]. In humans and mice, SHM occurs in response to antigen within the germinal centre. However, in cattle and sheep the expansion of the primary immunoglobulin repertoire occurs in the ileal Peyer's patch (IPP) [270, 271]. In cattle and sheep, the development of the B cell receptor repertoire begins during foetal development, first in the bone marrow to the pre-B cell stage and then in the IPP [11], where there is a high level of AID expression. Thus, SHM of bovine heavy and light chain V regions occurs in the absence of antigen within the foetal IPP [270]. Demonstrating that cattle have developed a mechanism of diversifying the primary immunoglobulin repertoire, via SHM (in the absence of antigenic stimulation), despite having very limited V(D)J gene segments repertoire.

The immunoglobulin V region is variable. However the variability is largely constrained to the complementarity determining regions (CDR). There are 3 CDRs within each of

the heavy and light chain V regions, which form looping immunoglobulin folds that protrude from the main body of the V region. The variable CDRs are interspersed with less-variable framework regions (FRs) that provide the structural stability of the molecule. The CDR1 and 2 are encoded by V gene segment and tend to be less variable than the CDR3, which spans the VDJ (VJ in light chain) junction, and is the most variable of the CDRs. The heavy and the light chain CDRs form the antigen-binding domain of the immunoglobulin molecule, which in humans is a flat or undulating surface that interacts with the antigen [272].

Until recently, accurately assessing the breadth of an individual's immunoglobulin repertoire at the nucleotide level has been difficult. Owing to the broad array of immunoglobulin diversity generated within an individual, only a very small fraction of these sequences has previously been investigated [273]. However, next generation sequencing (NGS) allows the sequencing of thousands of immunoglobulin reads in a high-throughput manner. Thus NGS is able to achieve a much greater sequencing depth than could previously be achieved by cloning and Sanger sequencing. Therefore, NGS lends itself well to sequencing the broad array of V region immunoglobulin transcripts found within the bovine immunoglobulin repertoire, and allows comparisons to be made between the naïve and post-vaccination immunoglobulin repertoires. NGS has recently been used in mice to identify antigen-specific immunoglobulin sequences [274] and in zebrafish to assess the global immunoglobulin repertoire [275]. NGS has also been utilised in humans to assess the differences between the immunoglobulin repertoire of naïve (IgM^+, $CD19^+$, $CD27^-$) and IgM and IgG memory B cell subsets (IgM^+, $CD19^+$, $CD27^+$ and IgG^+, $CD19^+$, $CD27^-$), respectively [276].

However, there are currently no studies that have assessed the bovine heavy and light chain immunoglobulin repertoire during the course of an immune response. By investigating the IgG bovine immunoglobulin repertoire at the peak of the antigen-specific plasma cell responses, following primary and booster FMDV vaccination, will allow identification of FMDV-specific immunoglobulin sequences.

5.3 Materials and methods

5.3.1 Calves and immunisation protocol

Four conventionally reared Holstein-Friesian male calves were recruited for this study (FMDC16 - 19, *Bos Taurus*, Pirbright Institute). Two calves (FMDC16 and FMDC18) were immunised with a FMDV O1-Manisa empty capsid material produced in a mammalian cell line using a vaccinia expression vector (produced by Claudine Porta, Pirbright

Institute). The other two calves were immunised with a stabilised FMDV O1-Manisa (mutant-a), which was again produced in a vaccinia expression system (Claudine Porta, Pirbright Institute). Each calf was given 10μg FMDV capsid material in Montinide ISA 201 VG adjuvant (Seppic, Paris, France), immunised intramuscularly, with half a dose administered above the subscapular lymph node on either side of the animal. The stabilised FMDV O1-Manisa mutant-a capsid antigen is stable at 56^{o}C for 2 hours (C. Porta, personal communication), which is a 30-fold improvement on the wild-type virus which is only stable at 49^{o}C for 4 minutes [195].

The efferent lymphatic cannulation procedure was then performed at day 20 post-primary immunisation (as detailed in 4.3.3). A booster immunisation (as detailed above) was then administered above the cannulated subscapular lymph node on day 21 post primary immunisation.

Efferent lymph was drained continuously throughout the study period, and the efferent lymph from each 24-hour collection period was pooled to produce a daily time point sample. Peripheral blood samples were taken from each animal at days 0, 7, 14, 21, 24, 25, 28 and 35 post-primary immunisation (Figure 5.2).

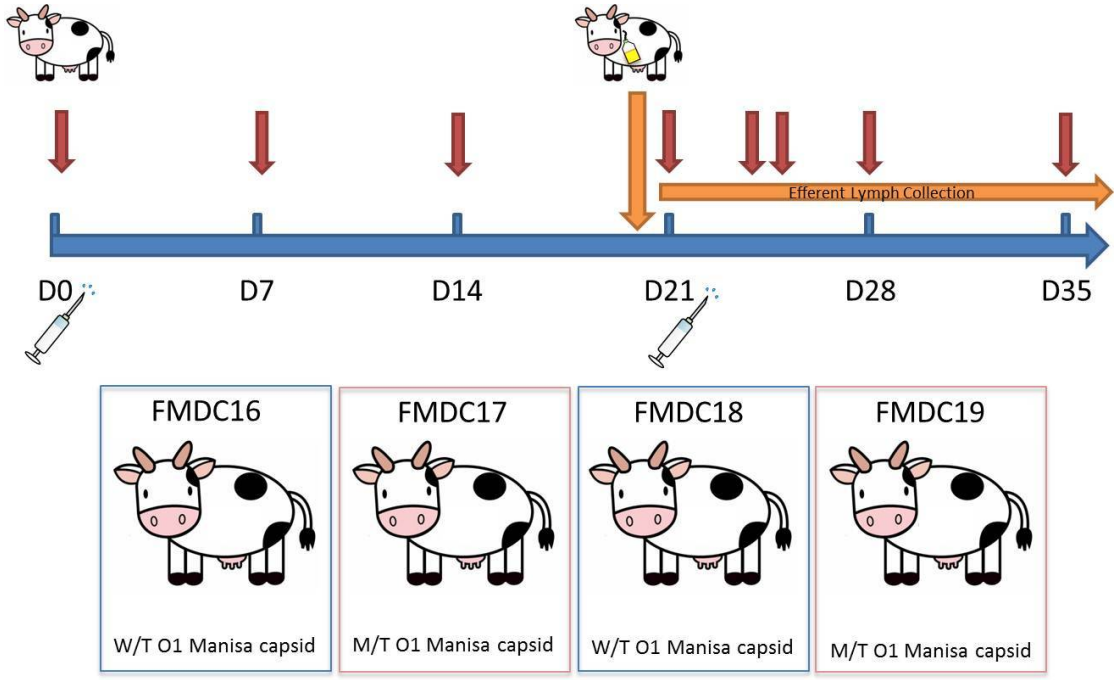


FIGURE 5.2: Schematic representation of experimental protocol used for the FMDV capsid vaccination and efferent lymphatic cannulation procedure. The red arrows indicates the time points at which venous blood was taken and the yellow horizontal arrow the period of time lymph was drained from the animal.Vaccination is indicated by the syringe symbols and efferent lymph. The vaccine antigen given to each animal is indicated in the boxes below the schematic (W/T: wild-type, M/T: mutant).

5.3.2 Selection of samples for sequencing

As detailed in Chapter 4, the kinetics of the O1-Manisa plasma cell response were determined in both peripheral blood and efferent lymph following immunisation with FMDV O1-Manisa capsids. The samples selected for next generation sequencing were day 0 (D0, all animals), the peak of the plasma cell burst post-primary immunisation (D7, all animals) and the peak of the plasma cell burst post-booster immunisation (D24 - FMDC17 and 18, D25 - FMDC16 and 19).

5.3.3 Bovine PBMC isolation

Mononuclear cells were isolated from peripheral blood and efferent lymph using the methodology previously described in 2.3.2 and 4.3.4.1, respectively. Following isolation and enumeration, 4 x 10^7 mononuclear cells were pelleted by centrifugation in RNase-free tubes (5 mins at 1200g) and the supernatant removed. The pellet was then homogenised by gentle pipetting in 1000μl TRIzol® LS reagent (Invitrogen). The homogenate was left at room temperature for 5 minutes to allow complete dissociation of the nucleoprotein complexes before being stored at $^{-}70^{o}$C until required.

5.3.4 Total RNA extraction from bovine mononuclear cells

Total ribonucleic acid (RNA) was extracted from the stored, homogenised bovine mononuclear cells using TRIzol® LS (Invitrogen) according to the manufacturers protocol.

Briefly, the homogenised bovine mononuclear cell pellet was allowed to thaw at room temperature. Once defrosted, 270μl of chloroform was added to the homogenised bovine mononuclear cells in TRIzol® LS reagent and mixed thoroughly for 15 seconds. The samples were then incubated at room temperature for 15 minutes, followed by centrifugation at 4^{o}C for 15 minutes at 12,000 x g. The aqueous phase, which contains the RNA, was then transferred into an RNase-free tube, using a sterile fine tip plastic pasteur pipette. The RNA was then precipitated from the aqueous phase by adding 667μl of isopropanol and mixed gently. The tubes were then incubated at room temperature for 10 mins followed by centrifugation at 12,000 x g at 4^{o}C for 10 minutes. After centrifugation, the supernatant was removed and the remaining RNA pellet was resuspended by adding 1333μl 75% ethanol. The RNA pellet was then centrifuged at 7500 x g at 4^{o}C for 5 minutes. After washing, the supernatant was removed from the RNA pellet and allowed to air dry, until no liquid was visible on the pellet. The dried RNA pellet was then resuspended in RNase free molecular grade H_2O.

The bovine mononuclear cell RNA was quantified by UV spectrophotometry, taking the optical density values at 260 and 280 wavelengths using a Nanodrop 2000 spectrophotometer (Thermo Scientific, Wilmington, DE, USA).

TABLE 5.1: Details of samples and MID tags used for bovine IgG and Igλ 454-sequencing

	Center for Genomic research (Liverpool University)		Biochemistry department (Cambridge University)	
Locus	IgG	IgG	Igλ	IgG
	Pool 1(1/2 plate)	Pool 2 (1/2 plate)	Pool 1 (1/2 plate)	Pool 2 (1/2 plate)
MID1	FMDC16_D7_PBMC	FMDC18_D24_PBMC	FMDC16_D25_PBMC	FMDC17_D24_PBMC*
MID2			FMDC16_D25_ELMC	FMDC17_D24_ELMC**
MID3	FMDC16_D25_PBMC	FMDC18_D24_ELMC	FMDC17_D24_PBMC	FMDC16_D0_PBMC
MID4	FMDC16_D25_ELMC	FMDC19_D7_PBMC	FMDC17_D24_ELMC	FMDC17_D0_PBMC
MID5	FMDC17_D7_PBMC	FMDC19_D7_PBMC	FMDC18_D24_PBMC	FMDC18_D0_PBMC
MID6	FMDC17_D24_PBMC	FMDC19_D7_PBMC	FMDC18_D24_ELMC	FMDC19_D0_PBMC
MID7	FMDC17_D24_ELMC	FMDC19_D25_PBMC	FMDC19_D25_PBMC	FMDC18_D21_PBMC
MID8	FMDC18_D7_PBMC	FMDC19_D25_ELMC	FMDC19_D25_ELMC	FMDC18_D21_ELMC

* control sample sequenced at both facilities. ** sample had a poor 5′-RACE ready cDNAyield during the first round of sequencing so was repeated from stored RNA.

Details of the molecular identifier (MID) tagged primer used with each sample. The naming convention for the samples is 'Animal identification _ sample time point post primary immunisation _ sample type' e.g. a PBMC sample taken at day 7 post primary immunisation from FMDC16 would be identified as FMDC16_D7_PBMC.

5.3.5 Bovine immunoglobulin heavy and light chain constant region primer design

The complete germline sequence of the bovine immunoglobulin loci, in particular the heavy chain locus, is yet to be completely defined. The current draft of the bovine genome (3.1) has been derived from bovine PBMCs and thus does not represent the true germline sequence of the V_H and V_L gene segments; SHM introduces nucleotide substitutes to the germ line sequence of B cells, which would be present in the genomic bovine PBMC DNA used to define the current draft of the bovine genome [268, 277, 278]. Previous studies that have explored the bovine immunoglobulin heavy chain sequences had used a highly conserved region of the V_H leader sequence [279], however, there was no evidence of a similar conserved leader sequence for the V_L gene segments.

At the time of starting this study, the number and sequence of the bovine V_H and V_L gene segments was unknown and there were no published conserved sequences at the 5′

end of the heavy and light chain V regions. Therefore, to amplify the complete Ig heavy and light chain V regions a 5′ rapid amplification of cDNA ends (5′-RACE) strategy was implemented. This approach allowed amplification of the 5′ end of the IgG, Igκ and Igλ V-region transcript without the need for a set of 5′ V gene specific primers. A 3′ gene specific primer (GSP) targeted at the 3′ end of the V region is also required in the 5′-RACE strategy.

Primers to the 5′ end of the IgG (heavy chain constant region 1, CH1), Igκ and Igλ (light chain constant region 1, CL1) were designed using sequences obtained from NCBI Genbank searches [280]. The sequences from the loci of interest were then aligned and suitable primer sites were identified at the 5′ end of the constant region 1 domain. Two 3′ IgG1, IgG2 and IgG2 constant region 1 (CH1) specific primers (BtaIgG*GSP1 and GSP2) were designed by aligning bovine sequences of the IgG CH1 domain (Figure 5.3, GSP1: 5′-GGGTAGACTTTCGGGGCTGTGGTGG-3′, GSP2: 5′-CACCGGCTCGGGCATGTAGCTGG-3′). The two IgG 3′ primers were designed to amplify all IgG isotypes but GSP2 allows discrimination between IgG1, IgG2 and IgG3, due to the presence of a T/A/C polymorphism at nucleotide 40 (Figure 5.3). Igλ and κ 3′ primers were designed for both loci using the same approach (Figures 5.4, 5′-CGAGGGTGSGGACTTGGGCTGAC-3′ and Figure 5.5, 5′-GAAGACGGATGGCTC-AGCATCAGACC-3′, respectively).

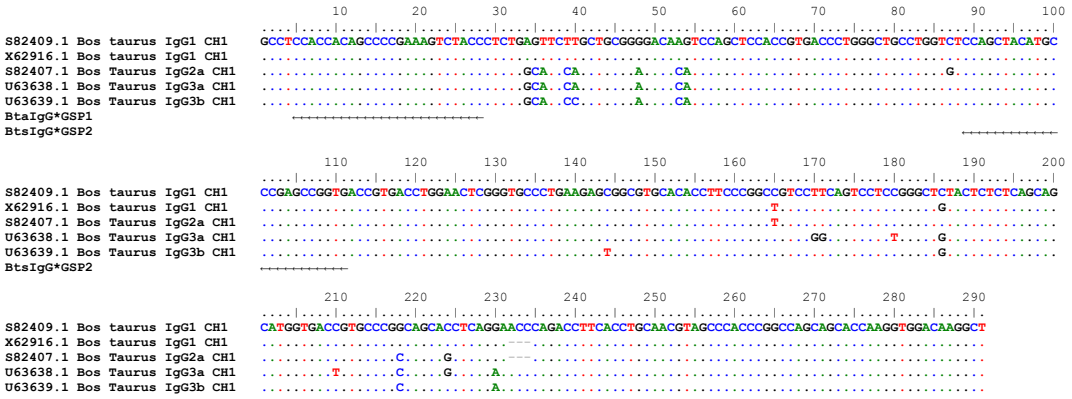


FIGURE 5.3: Nucleotide sequence alignment of *Bos taurus* IgG1, 2a, 3a and 3b (Genbank accession numbers: S82409, X62916, S82407, U63638 and U63693, respectively) heavy chain constant region domain 1 (CH1) and primer BtaIgG*GSP1 and BtaIgG*GSP2 binding site.

5.3.6 Bovine immunoglobulin heavy and light chain primer validation

Primer validation and polymerase chain reaction (PCR) optimisation was performed prior to the 5′-RACE amplification of the bovine heavy and light chain V regions.

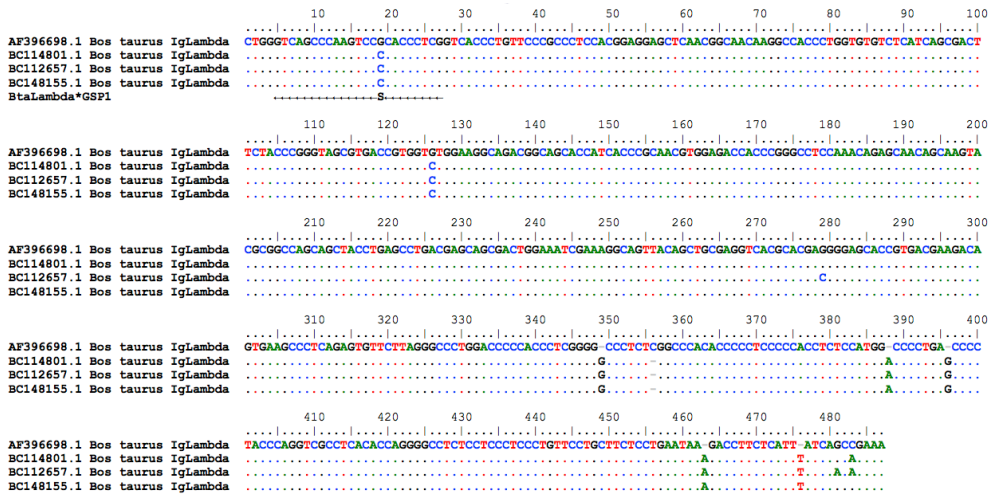


FIGURE 5.4: Nucleotide sequence alignment of *Bos taurus* Igλ (Genbank accession numbers:AF396698, BC114801, BC112657 and BC148155) light chain constant region domain 1 (CH1) and primer BtaLam*GSP1 binding site.

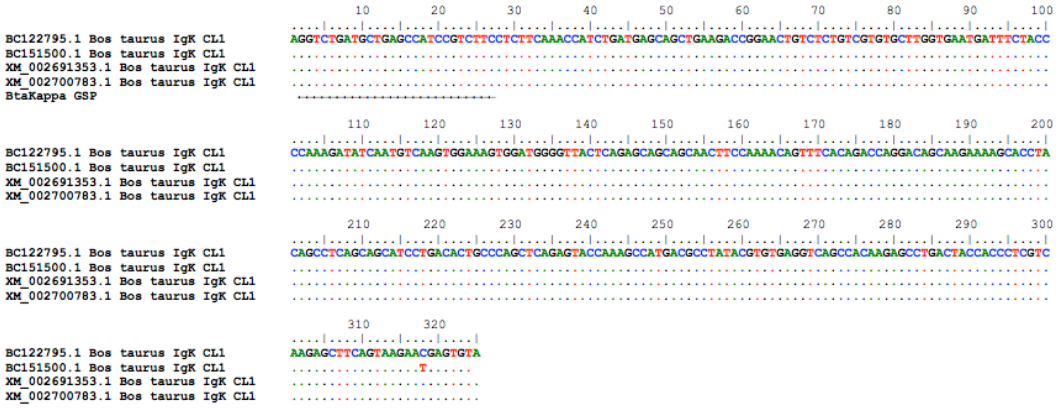


FIGURE 5.5: Nucleotide sequence alignment of *Bos taurus* Igκ (Genbank accession numbers: BC122795, BC151500, XM002691353, XM002700783) light chain constant region domain 1 (CL1) and primer BtaKappa*GSP1 binding site.

The gene specific primers described in section 5.3.7 were validated using cDNA prepared from bovine PBMCs from a previous laboratory experiment. The validation process tested the bovine IgG (BtaIgG*GSP1 and GSP2), Igκ (BtaIgKappa GSP) and Igλ (BtaIgLambda GSP) gene specific primers with different PCR cycling parameters (Table 5.2 and Figure 5.6A) and different high fidelity DNA polymerase enzymes (Figure 5.6B). All of the PCRs were set up using the parameters described in Table 5.2 with the exception of reactions 5 - 8 in 5.6B which used BIO-X-ACT Short DNA Polymerase (Bioline Ltd, London, UK) at the same volumes of Advantage 2 polymerase mix described in section 5.4.

TABLE 5.2: PCR cycling parameters for amplification of bovine immunoglobulin transcripts

Programme 1			Programme 2		
Temperature (^{o}C)	Time (seconds)	Cycles	Temperature (^{o}C)	Time (seconds)	Cycles
94	30		94	30	
72	120	5	68	30	25
94	30		72	120	
70	30				
72	120	5			
94	30				
68	30	25			
72	120				

PCR cycling parameters tested using Bovine IgG, Igλ and Igκ gene specific primers using the 5′-RACE PCR reaction set up described in Table 5.4.

As shown in Figure 5.6A positive PCR products were only visible for all of the GSP primers tested when PCR 'Programme 1' (Table 5.2) thermal cycling parameter was used (lanes 5 - 8). The use of PCR 'Programme 2' (lanes 1 - 4) resulted in complete loss of PCR amplification. Therefore the thermal cycling parameters used in all further 5′-RACE PCR amplifications were 'Programme 1'. In order to reduce the risk of PCR error, the number of second round PCR cycles was reduced from 25 to 16 cycles, the reduction in cycles still yielded enough DNA for 454 sequencing.

Two different high-fidelity DNA polymerase enzymes were also tested, to ensure maximum yield of the 5′-RACE PCR reactions (Figure 5.6B). The Advantage 2 DNA polymerase (lanes 1 -4) produced clearly visible and defined PCR products when visualised on a 2% agarose gel. The BIO-X-ACT Short DNA Polymerase (lanes 5 - 8) also yielded visible PCR products and also high molecular weight smears on the gel, indicating sub optimum PCR amplification. Therefore it was concluded that Advantage 2 DNA polymerase should be used for optimum 5′-RACE PCR amplification.

All of the gene-specific primers tested IgG (BtaIgG*GSP1 and GSP2), Igκ (BtaIgKappa GSP) and Igλ (BtaIgLambda GSP) yielded PCR products that were within the expected size range of approximately 500bp (Figure 5.6). However, BtaIgG*GSP2 yielded a slightly larger PCR product (approximately 550bp) and, as the size of the PCR products were approaching the upper size limit of 454-sequencing platform (500bp), it was concluded that BtaIgG*GSP1 would be used to amplify the bovine IgG transcripts.

(A)

(B)

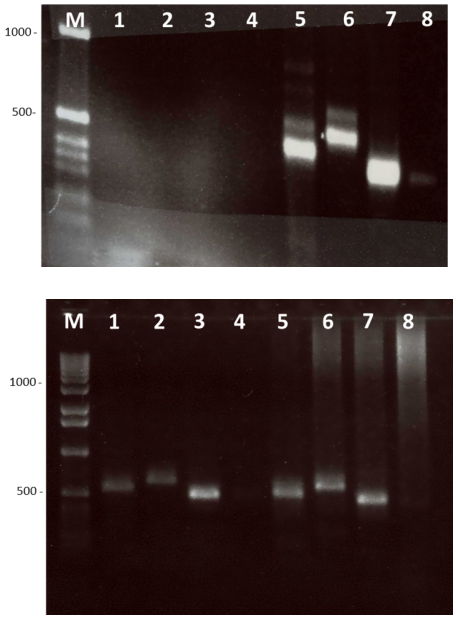


FIGURE 5.6: Gene-specific primer evaluation using bovine PBMC cDNA. On both 1 % agarose gel images BtaIgG*GSP1 is shown in lanes 1 and 5, BtaIgG*GSP2 in lanes 2 and 6, BtaIgLambda GSP1 in lanes 3 and 7 and BtaIgKappa GSP in lanes 4 and 8. The expected product size for all loci tested was ≈ 500bp. (A) PCR cycling parameter testing: lanes 1 - 4 using PCR programme 2 and lanes 5 - 8 using PCR programme 1 (see Table 5.2 for thermal cycling parameters used), M = 1kb DNA ladder (Invitrogen). (B) evaluation of different high fidelity Taq polymerase enzymes, lanes 1 - 4 Advantage 2 DNA polymerase, lanes 5 - 8 Accuzyme DNA polymerase (Bioline Ltd, London, UK), M = 100bp DNA ladder (New England Biolabs Inc, Ipswich, MA). Both PCR set ups were performed by Karen Billington.

The bovine Igκ amplification was very low (but present) in all of the PCR validation steps (Figure 5.6A lane 8 and B lanes 4 and 8), with the exception using PCR 'programme 2' (Table 5.2) which resulted in complete failure of all PCR reactions. It was therefore concluded that the bovine Igκ loci was expressed at very low levels in cattle and therefore it would not be pursued for 454-sequencing as it was unlikely to yield enough DNA, during amplification, for the downstream applications.

5.3.7 Bovine immunoglobulin heavy and light chain 5′-RACE strategy

Primer validation and PCR optimisation were performed prior to the 5′-RACE amplification.

Based upon the primer validation results, Igλ and IgG (GSP1) V region were used for 5′-RACE amplification (see section 5.4.2.1). The Igκ 5′-RACE amplification was not pursued.

Having confirmed which GSP sequences were suitable for 5′-RACE amplification, fusion primers were then designed to amplify the bovine IgG and Igλ 5′-RACE ready cDNA. The fusion primer design includes the previously described GSP sequences, a 454-specific sequence that is required to anneal the amplicon to the DNA capture bead and also a molecular identifier sequence (MID) to enable Ig transcript amplicon library multiplexing during 454-sequencing (see table 5.3).

Following RNA extraction and quantification, the bovine mononuclear cell total RNA was used for IgG and Igλ V region amplicon library synthesis using the SMARTer 5′-RACE kit (Clontech Laboratories Inc, Mountain View, CA), in accordance with the manufacturer's instructions.

Briefly, the first strand cDNA synthesis was performed by adding 1μl 5′-CDS primer A to 1μg of RNA, diluted to a final volume of 3.75μl with molecular grade H_2O. The reaction was then gently mixed and briefly spun in a microfuge to collect contents at the bottom of the tube. The spun down tube was then incubated in a thermal cycler for 72 ^{o}C for 3 minutes followed by 42^{o}C for 2 minutes and then cooled to 4^{o}C (Figure 5.7, step 1.). The tubes are then spun down again. One μl of the SMARTer IIa oligo was then added to each reaction, and mixed gently using a pipette tip. A master mix was then added, which contained 4μl of a prepared buffer mix (containing 2μl 5x first-strand buffer, 1μl 20mM DTT and 1μl 10mM dNTP) and 0.25μl RNase inhibitor (40u/l). After gentle mixing 1μl of the SMARTScribe, reverse-transcriptase was added to each reaction and the tubes were mixed by very gentle pipetting. The tubes were then spun down again. They were then incubated in a thermal cycler for 90 min at 42^{o}C then 10 min at 70^{o}C (Figure 5.7, steps 2 and 3). The 5′-RACE ready cDNA was the diluted with 20μl tricine-EDTA buffer and stored at $^-$20^{o}C until required for the 5′-RACE PCR.

Table 5.3: Bovine IgG and Igλ constant region MID tagged primer sequences

Primer name	Primer sequence (5′ - 3′)
BtaIgG* GSP1 MID1	*CTATGCGCCTTGCCAGCCCGC***TCAG**ACGAGTGCGTGGGTAGA CTTTCGGGGCTGTGGTGG
BtaIgG* GSP1 MID2	*CTATGCGCCTTGCCAGCCCGC***TCAG**ACGCTCGACAGGGTAGA CTTTCGGGGCTGTGGTGG
BtaIgG* GSP1 MID3	*CTATGCGCCTTGCCAGCCCGC***TCAG**AGACGCACTCGGGTAGA CTTTCGGGGCTGTGGTGG
BtaIgG* GSP1 MID4	*CTATGCGCCTTGCCAGCCCGC***TCAG**AGCACTGTAGGGGTAGA CTTTCGGGGCTGTGGTGG
BtaIgG* GSP1 MID5	*CTATGCGCCTTGCCAGCCCGC***TCAG**ATCAGACACGGGGTAGA CTTTCGGGGCTGTGGTGG
BtaIgG* GSP1 MID6	*CTATGCGCCTTGCCAGCCCGC***TCAG**ATATCGCGAGGGGTAGA CTTTCGGGGCTGTGGTGG
BtaIgG* GSP1 MID7	*CTATGCGCCTTGCCAGCCCGC***TCAG**CGTGTCTCTAGGGTAGA CTTTCGGGGCTGTGGTGG
BtaIgG* GSP1 MID8	*CTATGCGCCTTGCCAGCCCGC***TCAG**CTCGCGTGTCGGGTAGA CTTTCGGGGCTGTGGTGG
BtaLambda GSP1 MID1	*CTATGCGCCTTGCCAGCCCGC***TCAG**ACGAGTGCGTCGAGGG TGSGGACTTGGGCTGAC
BtaLambda GSP1 MID2	*CTATGCGCCTTGCCAGCCCGC***TCAG**ACGCTCGACACGAGGG TGSGGACTTGGGCTGAC
BtaLambda GSP1 MID3	*CTATGCGCCTTGCCAGCCCGC***TCAG**ACGCTCGACACGAGGG TGSGGACTTGGGCTGAC
BtaLambda GSP1 MID4	*CTATGCGCCTTGCCAGCCCGC***TCAG**AGCACTGTAGCGAGGG TGSGGACTTGGGCTGAC
BtaLambda GSP1 MID5	*CTATGCGCCTTGCCAGCCCGC***TCAG**ATCAGACACGCGAGGG TGSGGACTTGGGCTGAC
BtaLambda GSP1 MID6	*CTATGCGCCTTGCCAGCCCGC***TCAG**ATATCGCGAGCGAGGG TGSGGACTTGGGCTGAC
BtaLambda GSP1 MID7	*CTATGCGCCTTGCCAGCCCGC***TCAG**CGTGTCTCTACGAGGG TGSGGACTTGGGCTGAC
BtaLambda GSP1 MID8	*CTATGCGCCTTGCCAGCCCGC***TCAG**CTCGCGTGTCCGAGGG TGSGGACTTGGGCTGAC

Bovine IgG and Igλ fusion primer sequences for amplicon library amplification by PCR. The primer structure from 5′ to 3′ is as follows: 25 mer 454 sequencing annealing primer B required to anneal the amplicon to the DNA capture bead (*italics*), the annealing primer sequence must always end in the 4 mer key sequence, required for 454-sequence calibration (**bold**), 10 mer multiplex identifier sequence (MID) which allows bar coding of multiple amplicon libraries (underlined), the final 3′ part of the primer is the gene-specific segment allowing amplification of the bovine IgG or Igλ V region.

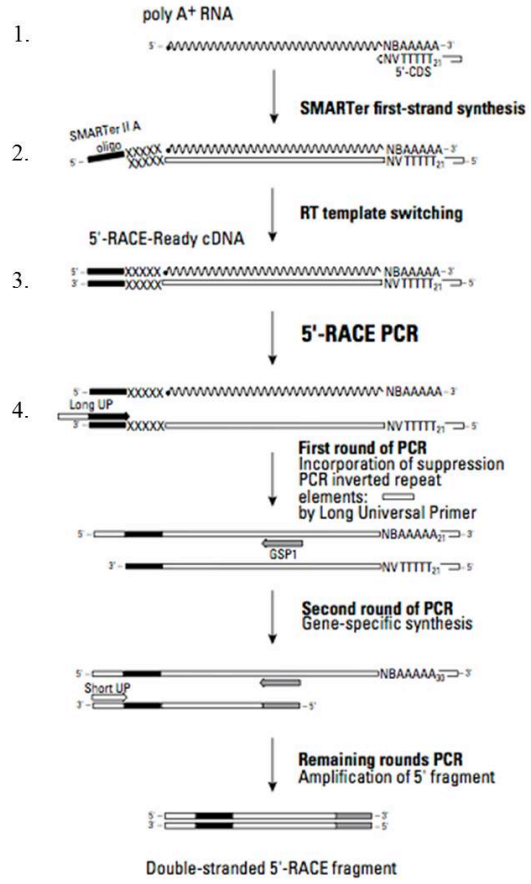


FIGURE 5.7: Schematic diagram show the experimental steps involved in producing a bovine immunoglobulin 5′-RACE library. UP: Universal primer. Adapted from [281]

The bovine Ig transcript amplicons were amplified using the high-fidelity DNA polymerase, Advantage® 2 (Clontech), to minimise PCR error. The PCR reaction set up is shown in Table 5.4 and the 5′-RACE ready cDNA samples and fusion primers used in the reaction are detailed in Table 5.1. The 5′-RACE PCR reactions were set up on ice in RNase-free 0.2mL PCR tubes.

The following thermal cycling parameters were used: initial denaturation at 94^{o}C for 60 secs, followed by 5 cycles of 94^{o}C for 30 sec and 72^{o}C for 120 sec, followed by 5 cycles of 94^{o}C for 30 sec, 72^{o}C for 30 sec and 72^{o}C for 120 sec, followed 16 cycles of 94^{o}C for 30 sec, 68^{o}C for 30 sec and 72^{o}C for 120 sec (Figure 5.7, step 4).

Table 5.4: 5′-RACE PCR reaction set up

PCR reaction component	5′-RACE PCR	UPM only (-ve control)	GSP1 only (-ve control)
10x Advantage 2 buffer	5	5	5
dNTP (10mM)	1	1	1
UPM (x10)	5	5	-
GSP1*	1	-	1
PCR grade H2O	34.5	35.5	39.5
5′-RACE ready cDNA*	2.5	2.5	2.5
50x Advantage 2 polymerase mix	1	1	1
Total reaction volume	50	50	50

* See Table 5.1 for details of which 5′-RACE ready cDNA samples were used with which MID tagged GSP.

Details of the individual components used in the 5′-RACE PCR reactions to amplify the V regions of bovine IgG and Igλ. All volumes given in μl.

5.3.8 PCR product visualisation and quantification

Following 5′-RACE PCR the IgG and Igλ amplicon libraries were then visualised on 2% agarose gel, containing 0.5 μg/mL Ethidium Bromide buffered with 1 x Tris/Borate/EDTA buffer. The PCR bands were excised from the gel and the PCR product was extracted from the agarose gel using the QiaQuick gel extraction kit, according to the manufacturer's protocol (Qiagen GmbH, Hilden, Germany).

PCR products were quantified using the Quant-iT^{TM} PicoGreen® dsDNA reagent (Invitrogen), according to the manufacturer's protocol. Briefly, a five point serial dilution of the DNA standard was made from 1ng/mL to 1μg/mL using the 1x TE(Tris/EDTA) buffer provided. The samples of interest are diluted 1:50 with the 1 x TE buffer. Both the standard and the test samples were then added to the 96-well flat bottomed black polypropylene plate (Sigma-Aldrich) in triplicate (100μl per well). The Quant-iT Picogreen reagent was then diluted 1:200 with 1 x TE buffer and 100μl was added to each reaction well. The plate was then incubated in the dark for 5 minutes at room temperature. The sample fluorescence was then measured using a Tecan Infinite M200 fluorometer (Tecan, Mannedorf, Switzerland), with an excitation wavelength of 480nm and an emission wavelength of 520nm. All sample values were normalised against the blank standard and the sample DNA concentrations calculated from the 5-point standard curve.

After quantification, the 454-sequencing samples were diluted to 10ng/μl and shipped to the 454-sequencing facilities.

5.3.9 454-sequencing

454-sequencing was performed at the Centre for Genomic Research (CGR, Liverpool University, Liverpool, UK) and the Biochemistry Department at the University of Cambridge (Cambridge University, Cambridge, UK). Details of which samples were sequenced by each centre are given in Table 5.1. Both sequencing centres followed the standard manufacturer's protocols for amplicon library multiplexing, emulsion PCR (emPCR) amplification and 454-sequencing from the 3′ end of the amplicon (unidirectional).

The bovine Ig amplicon libraries were multiplexed at equimolar concentrations prior to emPCR amplification, details of the pooling strategy are given in Table 5.1. The emPCR was performed using a GS FLX Titatium emPCR kit (Lib-A, Roche Diagnostics GmBH, Mannheim, Germany) using DNA capture B beads. The process of emPCR allows clonal amplification of a single stranded amplicon, whilst it is ligated to a DNA capture bead. Performing this step in a water-oil emulsion ensures that only one bead is present within each microreactor (Figure 5.8, step 2). After the emPCR, the DNA coated beads are purified and then added to the picotitre plate, one bead per well. Enzyme coated beads are also added to the plate, filling the space around the DNA coated bead (Figure 5.8, step 3). The picotitre plate is then inserted into the GS FLX+ sequencer (Roche). Nucleotides are then flowed sequentially over the microtitre plate and a light signal is emitted when a complimentary nucleotide is incorporated into the template strand (Figure 5.8, step 3). The amount of light emitted is proportional to the number of nucleotides incorporated into the template strand. Each time a nucleotide is flowed over the flow cell any light signals emitted from a well are captured by a CCD camera.

The captured images are then processed and a sequence, based upon the captured light emission patterns, is built for each well. Each read was binned according to the MID tag (Table 5.3, 10mer sequence next to the key sequence) and an .sff file was produced by the instruments software. The .sff files were used for all subsequent analysis.

5.3.10 Immunoglobulin sequence analysis

The packaged .sff.gz files were obtained from the sequencing centres and unpackaged to reveal the .sff file. Each of the .sff files was labelled with its MID tag and the pool

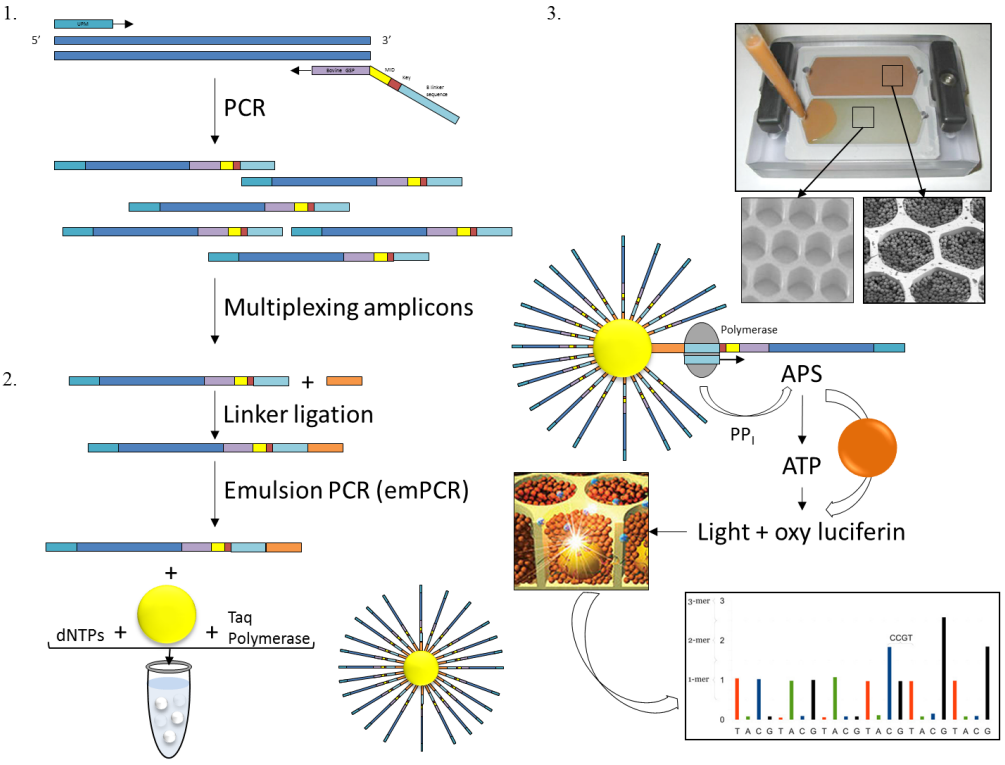


FIGURE 5.8: Schematic diagram show the experimental steps involved in the unidirectional 454 sequencing process. 1. 5′-RACE amplicon library is produced as described in section 5.3.7. 2. Emulsion PCR (emPCR) step: a B-adaptor linker is ligated onto the single-stranded amplicon and the amplicon is then ligated to an excess of DNA B capture beads, ensuring only one DNA fragment per bead. A water-oil emulsion is then made, with dNTPs and Taq polymerase. Thus clonal amplification of the bead-immobilised amplicon is achieved within each microreactor (bubble). 3. The microreactors are then broken and the DNA coated beads are concentrated. The enriched DNA coated beads are then added to the microtitre plate, one bead per well. Sulfurylase and luciferase coated beads are also added to each well, to fill the space around the DNA coated bead. The picrotitre plates are then added to the flow cell. Nucleotides are flowed sequentially (Thymine (T), Cytosine (C), Adenosine (A) and Guanine (G), TCAG) across the picrotitre plate. If a nucleotide is complimentary to the template strand a light signal is generated, and captured by the CCD camera. The amount of light generated by the addition of a complimentary nucleotide is proportional to the number of nucleotides incorporated. The key sequence (TCAG) at the beginning of the sequence is used to calibrate the signal.

location code (Table 5.1). The sff. files were then extracted using sff_extract on the Bio Linux 7 platform, using the following command:

```
sff_extract -s >new_file_name<_in.454.fasta
-q >new_file_name<_in.454.fasta.qual -x >new_file_name<_traceinfo_
in.454.xml MIDX_Pool_location_code.sff
```

This command produced the following files: new_file_name .fasta, .fasta.qual and a trace.info.454.xml file for each of the .sff files. Following extraction the sample .fasta 454-sequence file was then assembled using the MIRA assembler [282]. MIRA was chosen as it is a *de novo* assembler that will handle 454-sequence data. Assembling the sample reads resulted in groups of highly similar IgG or Igλ reads. This allowed a consensus sequence from each group of reads to be generated, which was referred to as the Ig consensus transcript sequence. This approach reduced the size, of a very large and complex dataset, thereby aiding the analysis.

The following command was used to assemble the 454 sequence data:

```
mira --project=>file_name< --job=denovo,est,accurate,454,
454_SETTINGS -CL:msvs=no >&log_assembly.txt
```

After assembly, the resulting .caf file was converted to a Gap4 compatible file, which allowed visualisation of the grouped reads. The following command was used for the conversion:

```
caf2gap -project >file_name<_out -version 0 <
>file_name<_out.caf > caf2gap.out 2> caf2gap.err
```

The resulting Gap4 compatible file was then visualised using the Gap 4 programme [283]. The number of individual reads generated by the 454 sequencing and the subsequent number of groupings made by MIRA are shown in Table 5.5.

The MIRA assembly generated Ig read grouping were then ranked, in descending order, based upon the number of reads within each group. The ordered Ig consensus transcript sequences were then exported from Gap4 in .fasta format. The Ig consensus transcript sequences were adjusted, to reflect their sequence rank, using a python script (Chapter B.1).

The ranked contigs were then aligned using the multiple alignment programme, MAFFT, using the default settings [284]. After alignment the results were exported in .fasta format and saved using the sample name as the file name. The aligned .fasta format file was then adjusted to remove of any Staden-associated nomenclature from the identification string using another python code (Chapter B.2).

5.3.11 Ig sequence abundance calculation

For each sample that was sequenced, the MIRA assembly generated Ig read groups, placing highly identical sequence reads within the same group. These groups were then ranked, in descending order, based upon the number of reads within each grouping. To calculate the relative abundance of each Ig consensus transcript (group), a percentage calculation was made based upon the number of Ig reads within each grouping and the total number of reads within the sample. The relative abundance percentage was then calculated using Excel 2010. The area under the curve (AUC) was calculated using Graphpad prism for the top 200 contigs for each sample.

Further investigation into the top 50 consensus transcripts revealed that each IgG transcript grouping contains > 2 sub-populations of non-100% identical reads. These sub-populations account for >10 sequences within each transcript group. This is despite the MIRA assembler being used at the highest stringency settings. These sequence polymorphisms are single nucleotide polymorphisms, which are unlikely to be PCR or pyrosequencing error, given the polymorphism frequency, the pyrogram quality and the lack of association with homo polymer repeats. Therefore, it is likely the polymorphisms represent biologically relevant point mutations within an otherwise almost identical transcript.

5.3.12 Identifying highly similar Ig transcripts at multiple time points

In order to identify if there are any highly similar Ig transcripts present in both the D7 and D24/5 samples from the same animal, a MIRA assembly was performed using concatenated .caf files. This allowed MIRA to assemble any highly similar reads together from both D7 and D24/5 within the same read grouping. The resulting .caf file was then subjected to a data extraction process using Pentaho (see Chapter B.3 for details of the pipeline used). A relational database was then constructed from the extracted data using Microsoft SQL server (see Chapter B.4 for the SQL procedure used). Any reads that had been grouped together by MIRA were identified in the database and their relative abundances calculated from the original single time point MIRA assembly .caf files. This allows visualisation of the change in relative abundances between D7 and D24/5.

5.3.13 Complementarity determining region identification

The CDR regions were identified using the programme Paratome [285, 286]. Paratome is a high-throughput web-based programme that is able to rapidly and accurately identify

amino acids that are involved in antigen interactions within a V region amino acid sequence [278, 285].

To identify the position, length and composition of the CDR1, 2 and 3 regions in the bovine IgG and Igλ V regions, the aligned nucleotide sequences were translated and the V region sequences were trimmed to reflect only the V region using the sequence alignment editor, Bioedit (Ibis Biosciences, Carlsbad, CA). The amino acid sequences were then exported in a .fasta format and uploaded to the Paratome web-server. The resulting CDR identification text file was then manipulated using Pentaho (see B.4) and the resulting CDR1, 2 and 3 lengths and amino acid compositions were determined using Microsoft Excel 2010.

5.3.14 Immunoglobulin structure modelling

The predicted structure models of the Igλ and IgG transcripts were preformed using SWISS-MODEL using the default parameter settings and bovine immunoglobulin heavy and light chain template structures recently published by Wang *et al.* (IgG: PDB:4K3DH or 4K3EH, Igλ PDB:4K3DL) [262]. The Z score was also calculated for each model, describing the likelihood that a given model is of comparable quality to the template structure, which has previously been confirmed by x-ray crystallography A Z-score of 0 would indicate complete structural identity with the template structure, whilst negative scores indicate low confidence in the structure. The QMEAN Z-score is an indicator of the quality of the model, a score of <1 is the highest confidence interval [287]. The models generated for both IgG and Igλ had high confidence scores for the whole structure, with the exception of the CDR3 regions, which gave low confidence scores. The resulting .pbd files were visualised using PyMol software. The Paratome predicted CDR regions were highlighted on each of the predicted models [262, 288, 289, 290].

5.4 Results

Following prime and booster immunisation with O1-Manisa FMDV capsid material the timing and magnitude of the O1-Manisa-specific plasma cell burst was determined using an ELIspot assay in both peripheral blood (post primary immunisation) and peripheral blood and efferent lymph (post booster immunisation, see Chapter 4). Using the afore mentioned ELIspot assay, the peak of the post primary (D7) and booster immunisation (D24/5) was determined in both peripheral blood and efferent lymph for each animal (see Chapter 4) and next generation sequencing was employed on these samples to further

interrogate the heavy and light chain immunoglobulin transcript repertoire at these time points.

In total, 16 samples had their IgG heavy chain Igλ V region repertoire sequenced, a peripheral blood (PBMC) sample from day 0 (D0), 7 (D7, peak of plasma cell burst post primary immunisation) and 24/5 (D24/5, peak of plasma cell burst post booster immunisation) and a matched efferent lymph (ELMC) sample taken at the peak of the plasma cell burst post booster immunisation (D24/5) from each animal (4 samples per animal). The IgG heavy chain V region sequencing returned on average 31218 reads per sample (range: 68011 − 9729) which after assembly resulted in, on average, 4787 consensus IgG transcripts generated per sample (range: 9729 − 1879, Table 5.5).

A total of 8 Igλ light chain V regions were sequenced, and were matched to peripheral blood and efferent lymph samples taken at the peak of the plasma cell burst post booster immunisation (D24/5) from each animal (2 samples per animal). The 454 sequencing generated on average 6502 reads per sample (range: 8978 − 4288) which resulted in an average of 538 consensus Igλ transcripts per sample (range: 814 − 240) after assembly (Table 5.5).

Table 5.5: Total number of IgG and Igλ reads and consensus transcripts

				Number of Reads	Number of consensus transcripts (Average length (nt))
IgG	FMDC16	PBMC	D0	41170	6945 (439)
			D7	14224	3395 (495)
			D25	17213	3730 (494)
		ELMC	D25	15121	1879 (489)
	FMDC17	PBMC	D0	40425	6721 (446)
			D7	9729	2385 (493)
			D24	49468	3718 (491)
		ELMC	D24	13480	3229 (479)
	FMDC18	PBMC	D0	44535	8198 (452)
			D7	18106	4182 (494)
			D25	18649	4288 (494)
		ELMC	D25	68011	6658 (498)
	FMDC19	PBMC	D0	57538	9188 (482)
			D7	26954	4558 (494)
			D25	11283	2897 (494)
		ELMC	D25	53582	4625 (499)
Igλ	FMDC16	PBMC	D25	7624	702 (404)
		ELMC		6504	424 (464)
	FMDC17	PBMC	D24	5686	240 (444)
		ELMC		8978	814 (378)
	FMDC18	PBMC	D24	6063	637 (373)
		ELMC		4288	429 (377)
	FMDC19	PBMC	D25	8372	726 (378)
		ELMC		4497	339 (425)

Total number of IgG and Igλ transcripts generated by 454-sequencing and the number of consensus transcripts generated by the MIRA assembly procedure.

5.4.1 Bovine IgG heavy chain

5.4.1.1 The abundance pattern of IgG V region transcripts increases post-vaccination

To assess if there was a change in the frequency distribution of IgG transcripts following prime and booster immunisations with FMDV O1-Manisa capsids, the distribution of the top 200 most abundant IgG transcripts was investigated (Figure 5.9). The top 200 transcripts was used as the cut off for investigation as antigen-specific transcripts are likely to be within this data group. For each time point, prior to immunisation (D0) and at the peak of the plasma cell burst post primary- (D7) and booster immunisation (D24/5) the area under the curve was calculated for each IgG transcript distribution (Figure 5.9 and Table 5.6). A large difference between the distribution of the transcript abundances (area under the curve, AUC) at a given time point would indicate a change in the IgG transcript distribution (i.e. an increased AUC value would suggest an increase in the dominance of an individual IgG transcript at that particular time point).

TABLE 5.6: Distribution of IgG transcripts at D0, D7 and D24/5 post primary immunisation in peripheral blood and efferent lymph

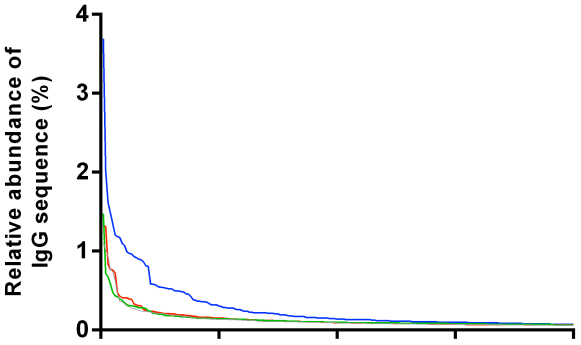
	FMDC16				FMDC17				FMDC18				FMDC19			
	PBMC			ELMC	PBMC			ELMC	PBMC			ELMC	PBMC			ELMC
	D0	D7	D25	D25	D0	D7	D24	D24	D0	D7	D24	D24	D0	D7	D25	D25
AUC	26.86	27.01	29.1	56.66	28.26	29.57	45.44	27.8	24.68	25.95	24.39	27.96	19.71	39.72	27.37	40.09
Max.	1.105	1.476	1.325	3.690	1.165	0.894	3.526	1.439	0.918	1.696	1.705	1.198	0.683	1.580	1.409	1.829
Min.	0.061	0.063	0.064	0.073	0.059	0.082	0.097	0.067	0.0561	0.061	0.064	0.066	0.050	0.067	0.071	0.084

Calculated area under the curve (AUC) values, the maximum and minimum relative abundance for the distribution of the top 200 most abundant IgG consensus transcripts at D0, D7 and D24/5 from FMDC16 to 19 shown in Figure 5.9.

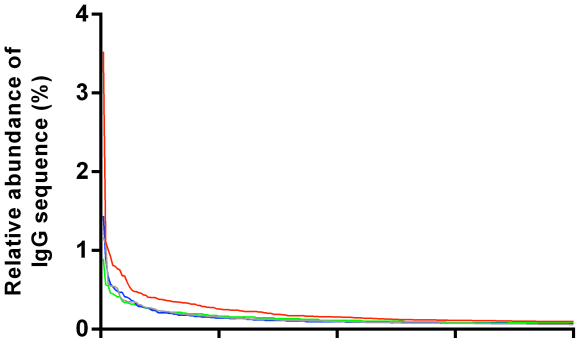
FMDC16 showed an increase in the area under the curve from D0 (26.86) to both D7 post-primary immunisation (27.01) which further increased at D25 in both peripheral blood and efferent lymph (PBMC: 29.1 and ELMC: 56.66, Figures 5.9A and 5.10A and Table 5.6). There was a statistically significant increase in the AUC D0 and the efferent lymph sample at D25($P < 0.001$, Tukey's multiple comparison, Figure 5.10A). Indeed, there was an increase in the relative abundance of the most dominant transcript during the time course, increasing from 1.105% at D0 to 3.69% at D25 in the efferent lymph (Table 5.6). Although, the dominant transcript sequences were not the same at any time point.

There was also change in the distribution of top 200 IgG transcripts in animal FMDC17, from 28.26 at D0 to 45.44 at D24 post-primary immunisation in the peripheral blood ($P < 0.001$, Tukey's multiple comparison, Figures 5.9B and 5.10B and Table 5.6). However, in contrast to FMDC16, FMDC17 showed a decreased AUC value at D24 in efferent

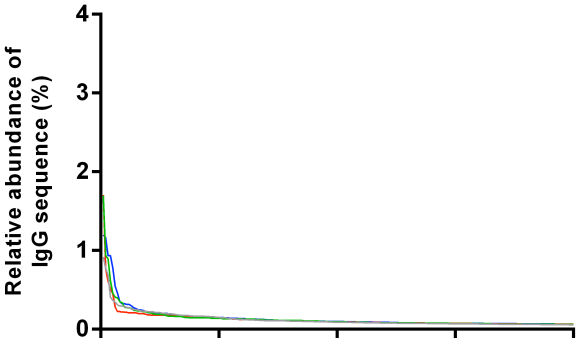
(A)



(B)



(C)



(D)

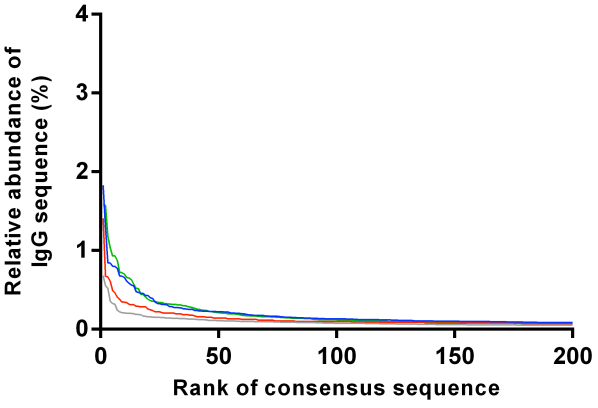
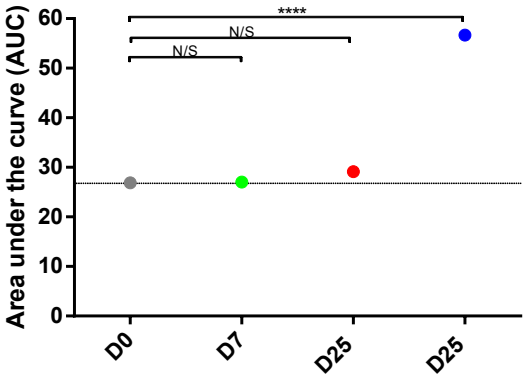
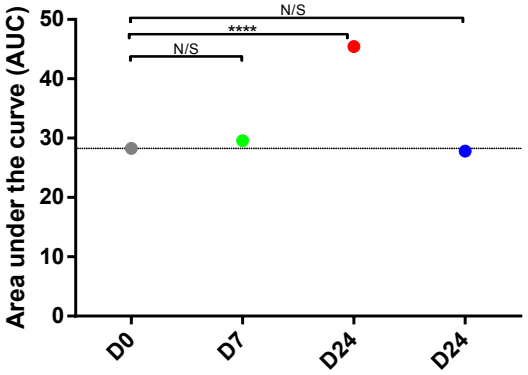


FIGURE 5.9: Relative abundance of the top 200 bovine IgG transcripts from (A) FMDC16, (B) FMDC17, (C) FMDC18 and (D) FMDC19 at D0(grey line), D7 (green line) and D24/5 post primary immunisation from peripheral blood (Red, PBMC) and efferent lymph (Blue, ELMC).

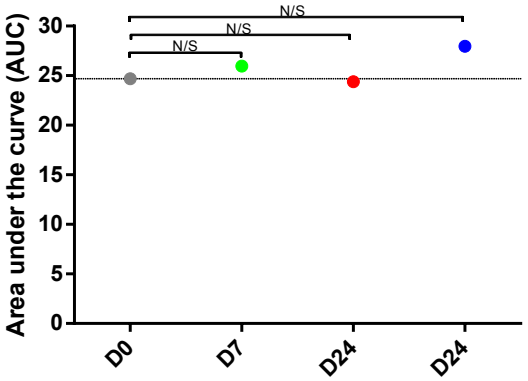
(A)



(B)



(C)



(D)

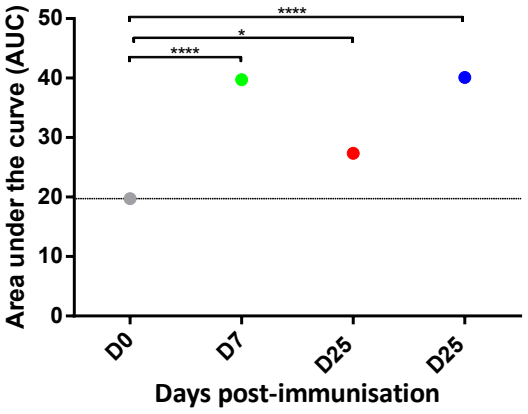


FIGURE 5.10: Area under the curve values of the top 200 bovine IgG transcripts from (A) FMDC16, (B) FMDC17, (C) FMDC18 and (D) FMDC19 at D0 (grey), D7 (green) and D24/5 post primary immunisation from peripheral blood (Red, PBMC) and efferent lymph (Blue, ELMC). Horizontal dotted line indicates the AUC value at D0 for each animal. N/S = Non significant. * = $P < 0.05$, **** = $P > 0.001$.

lymph (27.8) as compared to all other time points in that animal (Table 5.6). However, there was increase in relative abundance of the most dominant transcript from 1.165 % at D0 to 3.526% at D25 in the peripheral blood (Table 5.6). Although the sequences of the dominant transcripts were not the same, this data indicates that immunisation had an effect upon the distribution of the IgG transcripts at the peak of the post booster plasma cell burst in this animal.

FMDC18 also demonstrated a change in the distribution of the relative abundance of IgG transcripts following primary immunisation, 24.68 (D0) as compared to 25.95 (D7, Figure 5.9CC and 5.10C and Table 5.6). There was also increase in the AUC from D7 (25.95) as compared to the D24 efferent lymph sample (27.96, Figures 5.9C and 5.10C and Table 5.6). However, the D24 peripheral blood sample had a decreased AUC value (24.39) compared with both the efferent lymph sample from the same time point (27.96) and the D7 sample (25.95, Figures 5.9C and 5.10C and Table 5.6). Although there was no statistical significance in the difference in AUC values at the different time points sampled, there was an increase in the relative abundance of the most dominant IgG transcript. In the peripheral blood sample there was an increase in the relative abundance of the most dominant IgG transcripts from D0 (0.918%) to D7 (1.696%) and to D24 (1.705%). The efferent lymph sample at D24 does show a decrease in the relative abundance of the most dominant transcript, as compared to the time matched peripheral blood sample (1.198% vs. 1.705%) but is still higher than the D0 sample (Table 5.6), indicating that the primary vaccination has led to an increase in the most dominant IgG transcripts in this animal.

The final animal, FMDC19, also demonstrated a change in the distribution of IgG transcripts following primary immunisation (Figures 5.9D and 5.10D and Table 5.6). There was an increase in the AUC value from D0 to D7, 19.71 versus 39.72, respectively ($P < 0.001$, Tukey's multiple comparison). There was also a change in the transcript distribution from D7 to D25 in efferent lymph (ELMC), 39.72 as compared to 40.09. However, at D25 in peripheral blood there was a decreased AUC value (27.37) as compared to both its time matched efferent lymph and the D7 samples (40.09 and 39.72, respectively) (Table 5.6). As with the other animals, FMDC19 also showed an increase in the relative abundance of the most dominant IgG transcript following primary immunisation, from D0 (0.683%) to D7 (1.508%) and D25 (ELMC: 1.829%, PBMC: 1.409%).

These results show that vaccination with purified FMDV O1-Manisa capsid material has lead to a statistically significant increase in the distribution the IgG transcripts from D0 to the peak of the primary and booster antigen-specific plasma cell burst (D7 and D24/5, respectively) in both peripheral blood and efferent lymph (Figure 5.10).

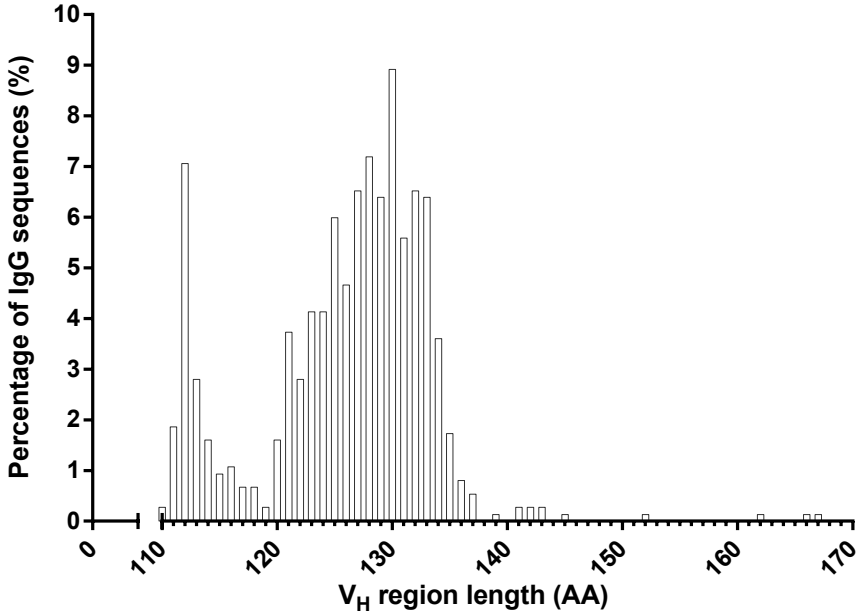


FIGURE 5.11: Total amino acid length of the top 50 most dominant IgG heavy chain V regions from D0, D7 and D24/5 post-primary immunisation in peripheral blood and efferent lymph ($n = 751$).

5.4.1.2 Bovine immunoglobulin heavy V regions show variation in length

The variable (V) region of the immunoglobulin molecule is formed via recombination of the V, (D) and J gene segments; during the recombination events nucleotides are added and/or excised from the gene segment junctions. This process generates junctional diversity within the V region and alterations in the total length of the V region. To investigate the degree of V region length diversity exhibited in cattle the top 50 most dominant IgG heavy chain consensus transcripts from each sample point were translated and trimmed to reflect only the V region and the total V region length (aa) was calculated (Figure 5.11).

The IgG V region had a large degree of length variability, ranging from 110aa to 167aa (Figure 5.11). The distribution of IgG V regions is bimodal, with two predominant peaks, one peak 112aa (7.06 % of all IgG transcripts investigated) and the other at 130aa (8.92% of all IgG transcripts investigated, Figure 5.11).

To investigate where the variation in V region length occurs in the IgG heavy chain trancripts, the V region sequences were analysed using Paratome software to predict the sequences of the complementarity determining regions (CDRs).

Three CDR regions were identified within the IgG V region. The range of CDR lengths is shown in Table 5.7. The predicted CDR1 and 2 region lengths of the IgG heavy chain

were 7 - 11 and 11 - 17, respectively (Table 5.7). However the range of predicted CDR3 length (4 to 61aa) was very different as compared to the CDR1 and 2 regions (Table 5.7).

TABLE 5.7: Bovine IgG V region predicted CDR lengths

V region	Complementarity determining regions		
	CDR1	CDR2	CDR3
IgG	5 – 13 (9)	11 – 18 (13)	4 – 61 (21)

Range of predicted CDR lengths of the IgG V regions. The median length for each CDR is given in brackets. (IgG transcripts $n = 752$.)

5.4.1.3 Variation of the amino acid residues occurs within the predicted CDR regions of the bovine heavy and light chain V-regions

Bovine IgG heavy chain V region transcripts have a very large degree of length variation, particularly within the CDR3 region. To further investigate the extent of variation within the V region, the degree of amino acid deviation was investigated across the full length of the IgG heavy chain V region and mapped against the predicted CDR regions (Figure 5.12). The degree of amino acid deviation was calculated for each amino acid position using the following methodology. The most abundant amino acid and the total number of possible amino acids were determined at each residue position within the V region. The most abundant amino acid value was then subtracted from the total number of possible amino acids to give the number of amino acids that deviated from the most abundant at each residue position. The percentage degree of deviation was then calculated from the number of deviant amino acid residues versus the total number of residues at each position.

The regions of high amino acid variability predominantly fall within the predicted CDR1, 2 and 3 regions (shaded in blue) of the IgG heavy chain V region (Figure 5.12). The CDR3 region of IgG showed an increased degree of amino acid variation, as compared to the CDR1 and 2 (Figure 5.12). The lack of variation shown between residues 140 to 160 within the CDR3 was due to the variation in the CDR3 length, as shown in Table 5.7. This data suggests that the IgG CDR3 region is variable in both length and amino acid residues composition and is likely to play a predominant role in the specificity of individual bovine immunoglobulin molecules.

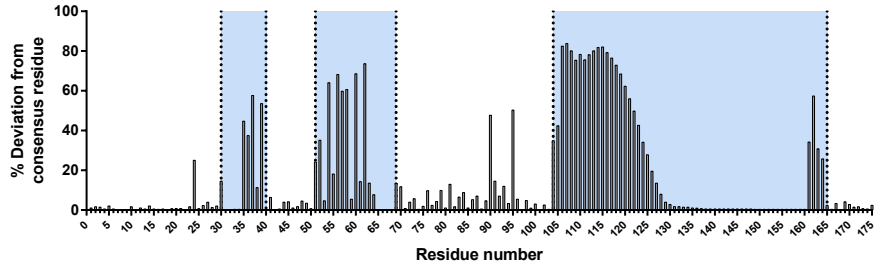


FIGURE 5.12: Amino acid variation of the bovine IgG heavy chain V region taken from the top 50 most abundant transcripts taken from D0, D7 and D24/5 post primary immunisation in both peripheral blood and efferent lymph. Percentage amino acid deviation was calculated from each amino acid residue position following sequence alignment. The Paratome predicted CDR1, 2 and 3 regions are shaded in blue. (n = 752).

5.4.1.4 Variation in bovine IgG heavy chain CDR3 length is not affected by repeated immunisations

The cattle CDR3 region of the IgG V region is highly variable in both length and amino acid composition. The highly variable heavy chain CDR3 length is unique to cattle immunoglobulins [291]. To establish whether immunisation had an effect upon the distribution of IgG CDR3 lengths were calculated at D0 (grey) and at the peak of the antigen-specific plasma cell bursts post primary (D7, green) and booster immunisation (D24/5, peripheral blood: red, efferent lymph: blue, Figure 5.13).

As previously described, the total IgG V region had a bimodal distribution of lengths, that had a predominant mean of 112aa and 130aa. The distribution of the CDR3 region lengths was investigated in the top 150 most abundant IgG heavy chain V region transcripts, as at the peak of the antigen-specific response (D7 and D24/5) these transcripts may be antigen-specific. The distribution of CDR3 lengths demonstrated a bimodal distribution, with one distribution spanning 4 to 12 aa and the other 14 to 32aa (Figure 5.13). The distribution of the CDR3 lengths did not alter, remaining bimodal and polyclonal, at the D0 to D7 and D24/5 time points, with no clear change in the peak of the distributions. A low frequency of super long CDR3 regions (>41aa in length) was identified in all of the animals (Table 5.8). The super long CDR3 regions were not consistently found in all time points in all animals, with transient detection at D0 (FMDC16, 17 and 18), D7 and D24/5 (FMDC18 and 19, Table 5.8).

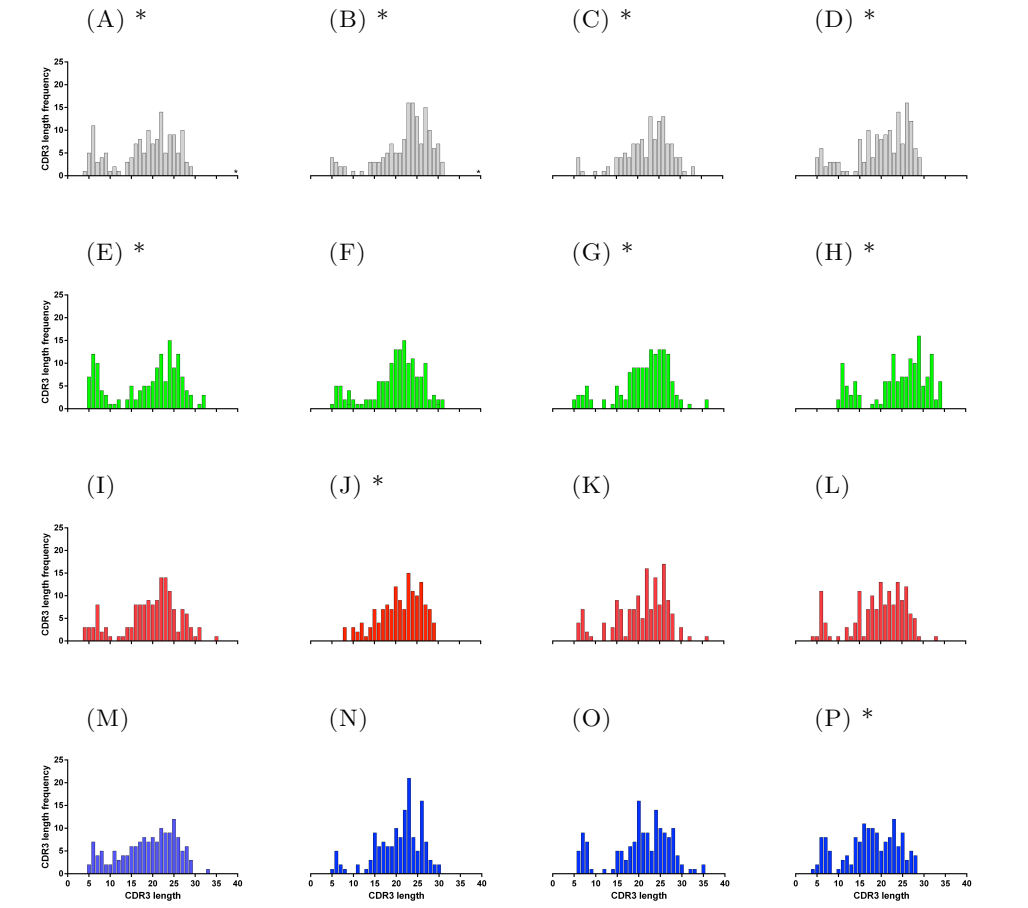


FIGURE 5.13: Distribution of CDR3 lengths, as predicted by Paratome, at D0 (grey bars), D7 (green bars) and D24/5 in peripheral blood (red bars) and efferent lymph (blue bars) post primary immunisation from FMDC16 (A, E, I, M), FMDC17 (B, F, J, N), FMDC18 (C, G, K, O) and FMDC19 (D, H, L , P). Top 150 most abundant IgG V region consensus transcripts taken from each animal (n = 2400 IgG transcripts). $*$ = CDR3 lengths of >40 amino acids (super long CDR3s) identified and described in Table 5.8.

TABLE 5.8: Number and length of super long CDR3 regions found in bovine IgG heavy chain transcripts

CDR3 length (AA)	FMDC16				FMDC17				FMDC18				FMDC19			
	D0	D7	D25		D0	D7	D24		D0	D7	D24		D0	D7	D24	
	PB	PB	PB	EL	PB	PB	PB	EL	PB	PB	PB	EL	PB	PB	PB	EL
41-45							1							1		
46-50							1		2					1		2
51-55									5	1				2		
56-60							1		5							
>61	8				1				14				1			

Number of super long CDR3 lengths in the top 150 most abundant IgG consensus sequences at each sampling point from each animal. Complementarity determining region 3 defined using Paratome software [285, 286] (n = 2400). PB = PBMC, EL = ELMC.

5.4.1.5 Bovine IgG individual transcript abundances alter following booster immunisation.

Within the bovine IgG heavy chain V region repertoire there is a broad range of CDR3 lengths (4 - 71aa), the distribution of which does not differ during the course of an immune response. However, immunisation does lead to a change in the relative abundance of the most dominant transcript from the day of immunisation (D0) to the peak of antigen-specific plasma cell response following the primary and secondary immunisations (D7 and D24/5, respectively).

The increase in the relative abundance of dominant transcripts at D7 and D24/5 may indicate that these transcripts are antigen-specific. It has been previously shown in mice that highly dominant immunoglobulin transcripts post booster immunisation are likely to be antigen-specific [274]. In order to identify bovine IgG transcripts that may be antigen-specific a MIRA assembly was performed, for each animal, with the D7 and D24/5 combined data. Any IgG reads from both D7 and D24/5 that were clustered together increased the likelihood of that transcript being antigen-specific. A relational database was then used to identify any reads that were assembled together and the relative change in abundance was calculated for each transcript using the abundance frequencies calculated from the single time point assemblies.

Figure 5.14 shows the dynamics of the relative abundance of associated IgG reads at D24/5 and D7 in both peripheral blood (red) and efferent lymph (blue). It is notable that all of the animals have a number of matched IgG read partners between D24/5 and D7 in both peripheral blood and efferent lymph. The presence of multiple partners may indicates the process of SHM; with D7 IgG reads undergoing SHM to increase the affinity of the BCR for its cognate antigen and clonal selection to increase their relative abundance at D24/5. There is also a large increase in the relative abundance of the matched IgG reads from D7 to D24/5, indicating that these sequences may be antigen-specific.

Using this approach the highly dominant transcripts identified at the D24/5 time point, in both peripheral blood and efferent lymph, have multiple partnered reads at D7 (Figure 5.14). The finding of multiple partners at D7 is likely to represent the narrowing of 'relevant' IgG transcripts to one specificity (sequence) at the peak of the secondary plasma cell response.

There is a general increase in the relative abundance of the matched reads from D7 to D24/5, with the exception of FMDC18 which shows a highly dominant transcript partnered at D7 (PBMC, 1.696%) and D24 (ELMC, 1.198%, Figure 5.14). The increase in the relative abundance of sequences from D7 to D24/5 could represent the clonal

selection of antigen-specific sequences leading to an increase in the relative abundance of that transcript.

It is also of note that highly dominant transcripts present at D7 generally decrease in their relative abundance at D24/5 (Figure 5.14). These could represent less relevant IgG sequences, that are out-competed by transcripts that have a higher affinity for their cognate antigen during the plasma cell burst post booster immunisation (D24/5).

Overall, this data shows that the dynamics of the IgG transcript abundance during an antigen-specific plasma cell burst is complex and the pattern of partnered D7 and D24/5 transcripts is very striking. IgG V region sequences that are highly dominant at the peak of the secondary plasma cell burst (D24/5) and that have matched partner sequences at the peak of the primary plasma cell burst (D7) are likely to be antigen-specific.

5.4.2 Bovine Ig light chain

5.4.2.1 Cattle exhibit low levels of immunoglobulin light-chain κ expression

Amplification of the bovine Igκ V region resulted in a PCR product that was visible, but clearly at a lower level of amplification than the IgG and Igλ PCR products (Figures 5.6A lane 8 and B lanes 4 and 8). This is in keeping with previously published data [292, 293]. It was therefore concluded that the bovine Igκ loci was expressed at very low levels in cattle.

5.4.2.2 Bovine immunoglobulin light chain V region shows little variation in length

Bovine IgG heavy chain V regions show a very large degree of variability in the length of the V region, with a bimodal distribution of lengths (see section 5.4.1.2). To investigate if this phenomena also occurs in bovine light chain V regions, the top 50 most dominant Igλ consensus transcripts were selected from each sample point, translated and trimmed to reflect only the V region and the total V region length was calculated (Figure 5.15). The top 50 most abundant transcripts were selected for further analysis as beyond this point the relative abundance of each consensus transcript plateaus. Thus, antigen-specific transcripts are likely to be found in the top 50 most abundant Igλ transcripts.

The Igλ V regions varied in length by only 14aa, ranging from 100 to 114aa, with a median length of 109aa (Figure 5.15). There is a Gausian distribution of V region lengths with 61.59% of all of the Igλ transcripts investigated being 109aa in length (Figure 5.15).

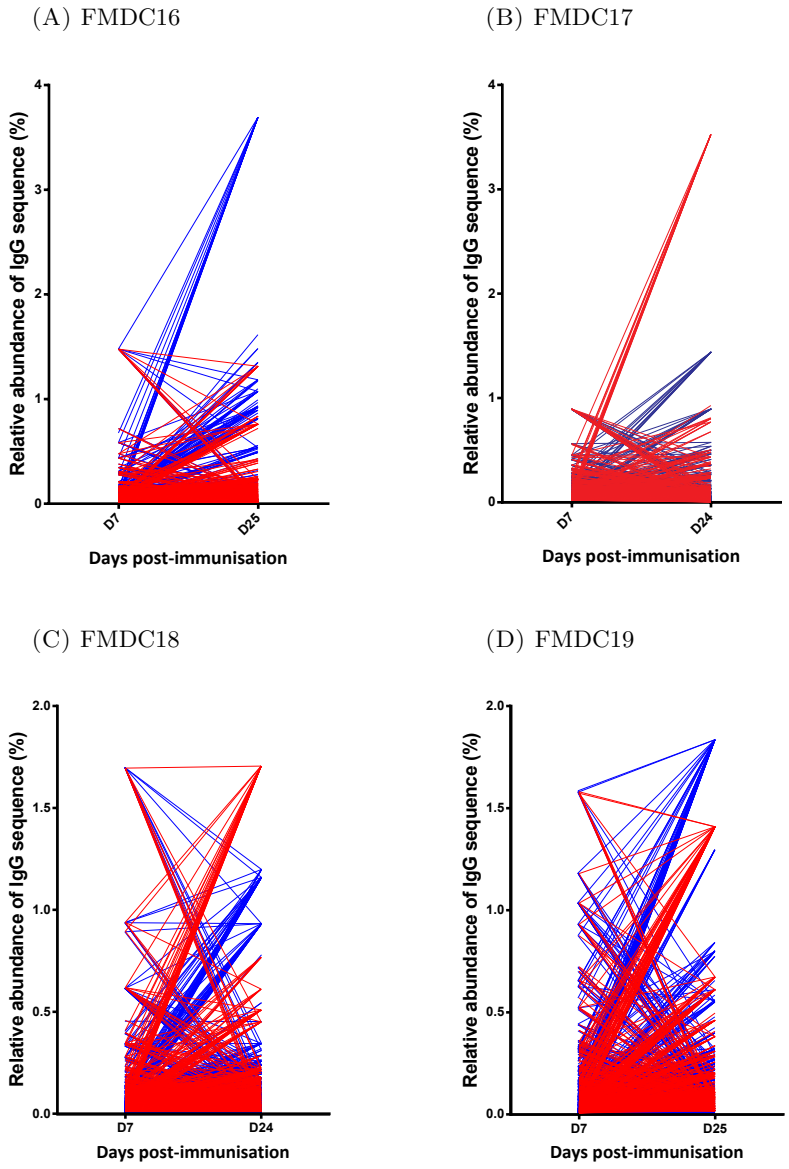


FIGURE 5.14: Dynamics of bovine IgG heavy-chain transcripts at the peak of plasma cell burst post-primary (D7) and post-booster immunisation (D24/5, PBMC: Red, ELMC: Blue) post-immunisation in (A) FMDC16, (B) FMDC17, (C) FMDC18 and (D) FMDC19. A MIRA assembly (D7 and D24/5 PBMC or ELMC) was constructed to determine which IgG heavy chain transcripts were highly similar between the two time points. The relative abundances of the transcripts was determined from the individual time point MIRA assemblies, and partnered IgG transcripts were identified using a relational database.

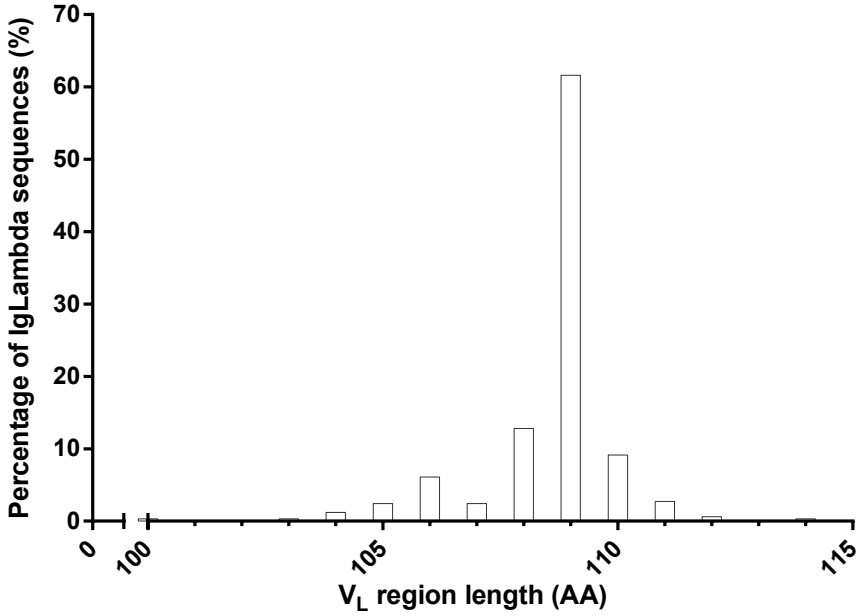


FIGURE 5.15: Total amino acid length of the top 50 most dominant Igλ V regions transcripts at D24/5 post primary immunisation in peripheral blood and efferent lymph (n= 327)

To investigate where the variation in the Igλ V region length occurs in the Igλ transcripts, the V region sequences were analysed using Paratome software to predict the sequences of the complementarity determining regions (CDRs) within the Igλ V regions.

TABLE 5.9: Bovine Igλ predicted CDR lengths

V region	Complementarity determining regions		
	CDR1	CDR2	CDR3
Igλ	7 – 11 (10)	11 – 17 (12)	4 – 14 (10)

Range of predicted CDR lengths of the Igλ V regions. The median length for each CDR is given in brackets. (Igλ transcripts n = 328.)

Three CDR regions were identified within the Igλ V regions. The range of CDR lengths is shown in Table 5.9. The predicted CDR1 and 2 region lengths of both the Igλ and IgG had a similar range of amino acid length (Table 5.9). However the range of predicted CDR3 length was very different between the Igλ (4 to 14 aa) compared to the IgG predicted length (4 to 61aa) (Table 5.9), suggesting that the CDR3 region length is very different between the bovine Igλ and IgG transcripts.

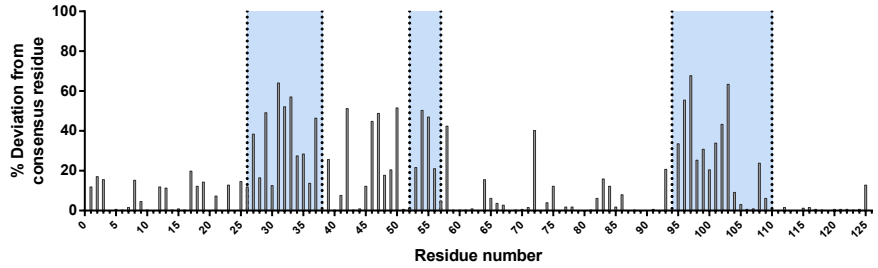


FIGURE 5.16: Amino acid variation of the bovine Igλ V regions calculated from the top 50 most abundant transcripts taken from all animals at D24/5 post primary immunisation from peripheral blood and efferent lymph. Percentage amino acid deviation calculated from the most abundant amino acid residue at each position following sequence alignment. The Paratome predicted CDR1, 2 and 3 regions are shaded in blue. (n = 328 transcripts).

5.4.2.3 Bovine immunoglobulin light chain V regions show amino acid variation within predicted CDRs

Bovine Igλ transcripts exhibited a range of V region lengths, particularly within the predicted CDR regions. To explore the degree of variation within the V region further, the degree of amino acid variation was investigated across the full length of the Igλ V region and the degree of amino acid variation was mapped against the predicted CDR regions (Figure 5.16). The degree of amino acid deviation was calculated for each amino acid position using the methodology described in 5.4.1.3.

The regions of high amino acid variability predominantly fell within the predicted CDR1, 2 and 3 regions (shaded in blue) on the Igλ V regions (Figures 5.16). As compared to the IgG heavy chain (Figure 5.12) V region, the Igλ V region showed more amino acid variability within the framework regions (FR), in particular Igλ FR2 shows quite a large degree of variability (Figure 5.16).

5.4.2.4 The relative abundance of Igλ transcripts is similar between peripheral blood and efferent lymph

To investigate if there was a relationship between the frequency distribution of bovine Igλ transcripts, the relative transcript abundance of the top 200 consensus transcripts were compared between peripheral blood (PBMC) and efferent lymph (ELMC) for each animal at the peak of antigen-specific plasma cell burst post booster immunisation (D24/5) and the AUC was calculated for each curve.

At D25 post primary immunisation the top 200 most abundant Igλ transcripts of FMDC16 showed a disparate distribution between peripheral blood (PBMC, AUC:

74.93) as compared to efferent lymph (ELMC, AUC: 81.71, Figure 5.17A). FMDC17 demonstrated the opposite trend, with the peripheral blood sample at D24 having a higher AUC value (84.72) as compared to the time-matched efferent lymph sample (71.65, Figure 5.17B). FMDC18 demonstrated the same trend as FMDC16, with the distribution of Igλ consensus transcripts having a slightly higher AUC in efferent lymph as compared to peripheral blood, 84.55 versus 79.00 (Figure 5.17C). Finally FMDC19 also had slightly higher AUC in efferent lymph compared to peripheral blood, 87.93 and 79.47, respectively (Figure 5.17D).

In general, the distribution of the bovine Igλ consensus transcripts is similar between both peripheral blood and efferent lymph at D24/5 post-primary immunisation, but in FMDC16, 18 and 19 efferent lymph shows a slightly increased AUC value as compared to peripheral blood ($P < 0.05$, Mann-Whitney test, Figure 5.17).

5.4.2.5 Predominance of one light-chain V-region at peak of plasma cell response

The distribution of the Igλ transcripts is similar between peripheral blood and efferent lymph in all of the animals at the peak of the secondary plasma cell response. The top 10 Igλ transcripts account for between 39.89 (FMDC19, PBMC) and 68.19 (FMDC17, PBMC) of all of the Igλ transcripts within that animal (Table 5.10). In contrast, the top 10 most abundant IgG heavy chain V region transcripts at D24/5 only accounted for between 5.21% (FMDC18, PBMC) and 15.87% (FMDC16, ELMC).

The top 3 most abundant Igλ transcripts accounted for between 16.75% (FMDC19,PBMC) and 44.10% (FMDC17, PBMC) of all of the Igλ transcripts (Table 5.10). By comparison, the top 10 IgG transcripts at the same time point only accounted for between 7.32% (FMDC16, ELMC) and 2.74% (FMDC19, PBMC) of all the IgG heavy chain V region transcripts.

Moreover, there was a large predominance of the most abundant Igλ transcript (Table 5.10, rank 1) in all of the samples investigated (ranging from 28.09% to 6.77%) with the exception of the efferent lymph (ELMC) sample taken from FMDC18 (Table 5.10). This sample (FMDC18, ELMC) showed three Igλ transcripts that are highly similar in abundance (6.76, 6.62 and 6.11%, Table 5.10 ranks 1 - 3). The clear predominance of one Igλ transcript at the peak of the secondary plasma cell burst (D24/5) would indicate that this transcript is likely to be antigen-specific or structurally important for the antigen-specific IgG heavy chain.

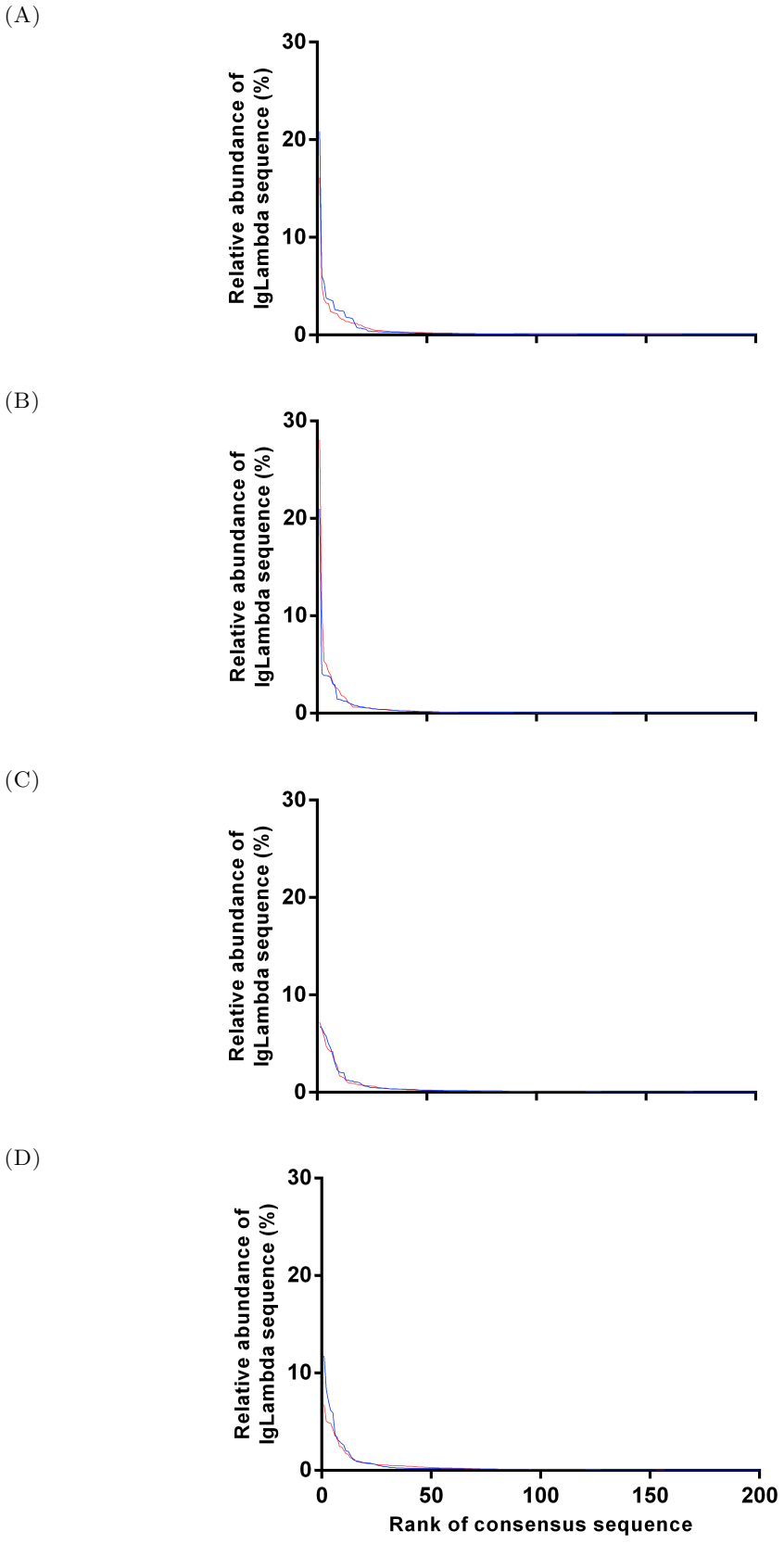


FIGURE 5.17: Percentage relative abundance of the top 200 bovine Igλ transcripts at D24/5 post primary immunisation from (A) FMDC16, (B) FMDC17, (C) FMDC18 and (D) FMDC19 from peripheral blood (Red, PBMC) and efferent lymph (Blue, ELMC).

TABLE 5.10: Relative abundance of the top 10 Igλ transcripts at peak of antigen-specific plasma cell burst following booster immunisation (D24/5).

Rank	FMDC16		FMDC17		FMDC18		FMDC19	
	PBMC	ELMC	PBMC	ELMC	PBMC	ELMC	PBMC	ELMC
1	16.11	20.85	28.09	20.98	7.21	6.76	6.77	11.76
2	5.04	6.07	10.68	4.1	6.50	6.62	5.06	8.34
3	3.66	5.43	5.33	3.89	5.77	6.11	4.92	7.12
4	3.27	3.78	5.07	3.89	4.77	5.76	4.87	6.18
5	3.24	3.69	4.31	3.84	4.39	5.01	4.29	5.96
6	2.41	3.60	3.94	3.7	4.22	4.55	3.54	3.76
7	2.32	3.52	3.18	3.02	4.21	3.82	3.46	3.22
8	2.23	2.58	2.71	2.94	3.12	2.99	2.46	3.02
9	2.18	2.58	2.59	1.45	2.79	2.33	2.44	2.80
10	1.80	2.49	2.29	1.43	1.72	2.08	2.08	2.62
Total (%)	42.26	54.59	68.19	49.24	44.7	46.03	39.89	54.78

Relative abundance (%) of the top 10 most abundant bovine Igλ transcripts at the peak of the FMDV O1-Manisa specific plasma cell burst, (D24/5 post-primary immunisation) in both peripheral blood (PBMC) and efferent lymph (ELMC).

5.4.3 Predicted structures of bovine immunoglobulin heavy and light chain V regions

5.4.3.1 Highly dominant Igλ transcripts are similar between animals

There is a clear predominance of at least one Igλ transcript at the peak of the antigen-specific plasma cell burst post booster vaccination. An alignment of the amino acid sequences of the 3 most abundant Igλ transcripts has shown a high degree of similarity between a number of the transcripts (Figures 5.18 and 5.19). By aligning the nucleotide sequences of the top 3 most abundant Igλ transcripts and then translating them into the amino acid sequence it was apparent that there were a number of Igλ sequences that were identical between peripheral blood (PBMC) and efferent lymph (ELMC) within the same animal. Figure 5.19 shows the sequence identity matrix generated for all of the Igλ transcripts interrogated showing the proportion of identical residues. Identical sequences are shown in the matrix as 1 (e.g. FMDC18's second most abundant Igλ transcripts in both peripheral blood (PBMC) and efferent lymph (ELMC) are identical, at the amino acid level). The sequence identity matrix also showed some identical Igλ transcripts that are shared between out-bred animals; FMDC18's second most abundant Igλ transcripts in both blood and efferent lymph were identical to FMDC17's third most abundant

transcript in efferent lymph (Figure 5.19). There were also a number of transcripts that had a sequence identity of >0.99, meaning they differ from one another by only one amino acid residue (Figure 5.19). This showed the presence of highly similar transcripts in both peripheral blood and efferent lymph at a single time-point in one animal and that there were also highly similar Igλ transcripts shared between out bred animals.

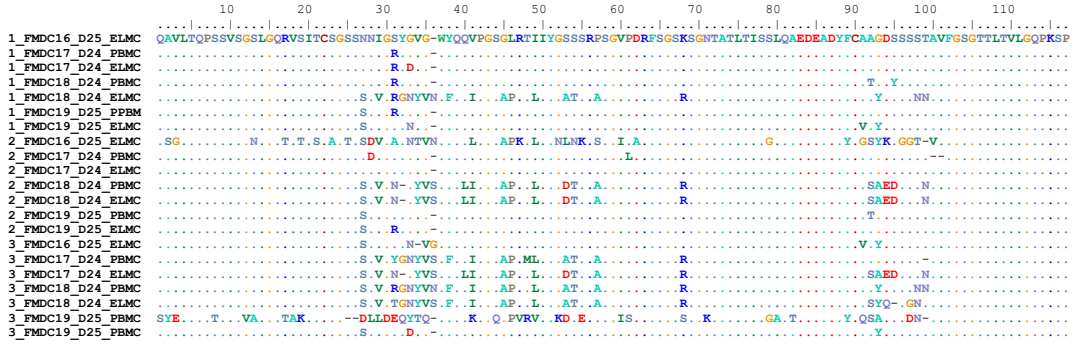


FIGURE 5.18: Sequence alignment of the amino acid sequences for the top 3 most abundant Igλ transcripts from FMDC16, FMDC17, FMDC18 and FMDC19 in both peripheral blood and efferent lymph, with the exception of FMDC16 which is efferent lymph only due to a lack of full length transcripts in the top 3 most abundant transcripts. The sequence identity scores between sequences are shown in Figure 5.19. The sequence identity matrix, generated using BioEdit software, compares the top 3 most abundant Igλ transcripts with one another and calculates the proportion of identical residues within the aligned Igλ transcripts.

			1							2							3							
			FMDC16		FMDC17		FMDC18		FMDC19		FMDC16		FMDC17		FMDC18		FMDC19		FMDC16		FMDC17		FMDC18		FMDC19	
			ELMC		PBMC	ELMC	PBMC	ELMC	PBMC	ELMC	ELMC		PBMC	ELMC	PBMC	ELMC	PBMC	ELMC	ELMC		PBMC	ELMC	PBMC	ELMC	PBMC	ELMC
1	FMDC16	ELMC			0.991	0.982	0.974	0.829	0.982	0.965	0.666		0.965	1	0.82	0.82	0.982	0.982	0.94		0.837	0.82	0.829	0.803	0.629	0.974
	FMDC17	PBMC	0.991			0.991	0.982	0.837	0.991	0.956	0.666		0.956	0.991	0.82	0.82	0.974	0.991	0.931		0.837	0.82	0.837	0.803	0.629	0.965
		ELMC	0.982	0.991			0.974	0.837	0.982	0.956	0.666		0.948	0.982	0.811	0.811	0.965	0.982	0.931		0.837	0.811	0.837	0.803	0.629	0.974
	FMDC18	PBMC	0.974	0.982	0.974			0.82	0.974	0.939	0.658		0.939	0.974	0.82	0.82	0.974	0.974	0.914		0.82	0.82	0.82	0.803	0.62	0.948
		ELMC	0.829	0.837	0.837	0.82			0.846	0.846	0.717		0.794	0.829	0.897	0.897	0.829	0.846	0.854		0.948	0.897	1	0.94	0.606	0.846
	FMDC19	PBMC	0.982	0.991	0.982	0.974	0.846			0.965	0.675		0.948	0.982	0.829	0.829	0.982	1	0.94		0.846	0.829	0.846	0.811	0.629	0.974
		ELMC	0.965	0.956	0.956	0.939	0.846	0.965			0.692		0.931	0.965	0.811	0.811	0.965	0.965	0.974		0.837	0.811	0.846	0.82	0.629	0.982
2	FMDC16	ELMC	0.666	0.666	0.666	0.658	0.717	0.675	0.692				0.658	0.666	0.692	0.692	0.675	0.675	0.7		0.698	0.692	0.717	0.717	0.612	0.683
	FMDC17	PBMC	0.965	0.956	0.948	0.939	0.794	0.948	0.931		0.658			0.965	0.786	0.786	0.948	0.948	0.905		0.803	0.786	0.794	0.769	0.612	0.939
		ELMC	1	0.991	0.982	0.974	0.829	0.982	0.965		0.666		0.965		0.82	0.82	0.982	0.982	0.94		0.837	0.82	0.829	0.803	0.629	0.974
	FMDC18	PBMC	0.82	0.82	0.811	0.82	0.897	0.829	0.811		0.692		0.786	0.82		1	0.829	0.829	0.82		0.897	1	0.897	0.897	0.606	0.82
		ELMC	0.82	0.82	0.811	0.82	0.897	0.829	0.811		0.692		0.786	0.82	1		0.829	0.829	0.82		0.897	1	0.897	0.897	0.606	0.82
	FMDC19	PBMC	0.982	0.974	0.965	0.974	0.829	0.982	0.965		0.675		0.948	0.982	0.829	0.829		0.982	0.94		0.837	0.829	0.829	0.811	0.629	0.974
		ELMC	0.982	0.991	0.982	0.974	0.846	1	0.965		0.675		0.948	0.982	0.829	0.829	0.982		0.94		0.846	0.829	0.846	0.811	0.629	0.974
3	FMDC16	ELMC	0.94	0.931	0.931	0.914	0.854	0.94	0.974		0.7		0.905	0.94	0.82	0.82	0.94	0.94			0.846	0.82	0.854	0.829	0.623	0.957
	FMDC17	PBMC	0.837	0.837	0.837	0.82	0.948	0.846	0.837		0.698		0.803	0.837	0.897	0.897	0.837	0.846	0.846			0.897	0.948	0.923	0.603	0.837
		ELMC	0.82	0.82	0.811	0.82	0.897	0.829	0.811		0.692		0.786	0.82	1	1	0.829	0.829	0.82		0.897		0.897	0.897	0.606	0.82
	FMDC18	PBMC	0.829	0.837	0.837	0.82	1	0.846	0.846		0.717		0.794	0.829	0.897	0.897	0.829	0.846	0.854		0.948	0.897		0.94	0.606	0.846
		ELMC	0.803	0.803	0.803	0.803	0.94	0.811	0.82		0.717		0.769	0.803	0.897	0.897	0.811	0.811	0.829		0.923	0.897	0.94		0.598	0.82
	FMDC19	PBMC	0.629	0.629	0.629	0.62	0.606	0.629	0.629		0.612		0.612	0.629	0.606	0.606	0.629	0.629	0.623		0.603	0.606	0.606	0.598		0.629
		ELMC	0.974	0.965	0.974	0.948	0.846	0.974	0.982		0.683		0.939	0.974	0.82	0.82	0.974	0.974	0.957		0.837	0.82	0.846	0.82	0.629	

Key: 1, 0.9, 0.8, 0.7, 0.6, 0.5

FIGURE 5.19: Sequence identity matrix showing the number of amino acid differences between each of the top 3 most abundant bovine Igλ transcripts taken from FMDC16, 17, 18 and 19 in both peripheral blood (PBMC) and efferent lymph (ELMC) at D24/5 post primary immunisation.

In order to look at the relationship between these highly similar Igλ sequences, a phylogenetic tree was constructed using the neighbour-joining method, plotting the number of residue differences between the Igλ sequences (Figure 5.20). The phylogenetic tree showed that there are 2 main branches of Igλ sequence clusters and two outlying transcripts (2_FMDC16_D25_ELMC and 3_FMDC19_D24_PBMC, Figure 5.20). Within the

2 main clusters there are then several sub branches that do not differ greatly in their distances (Figure 5.20).

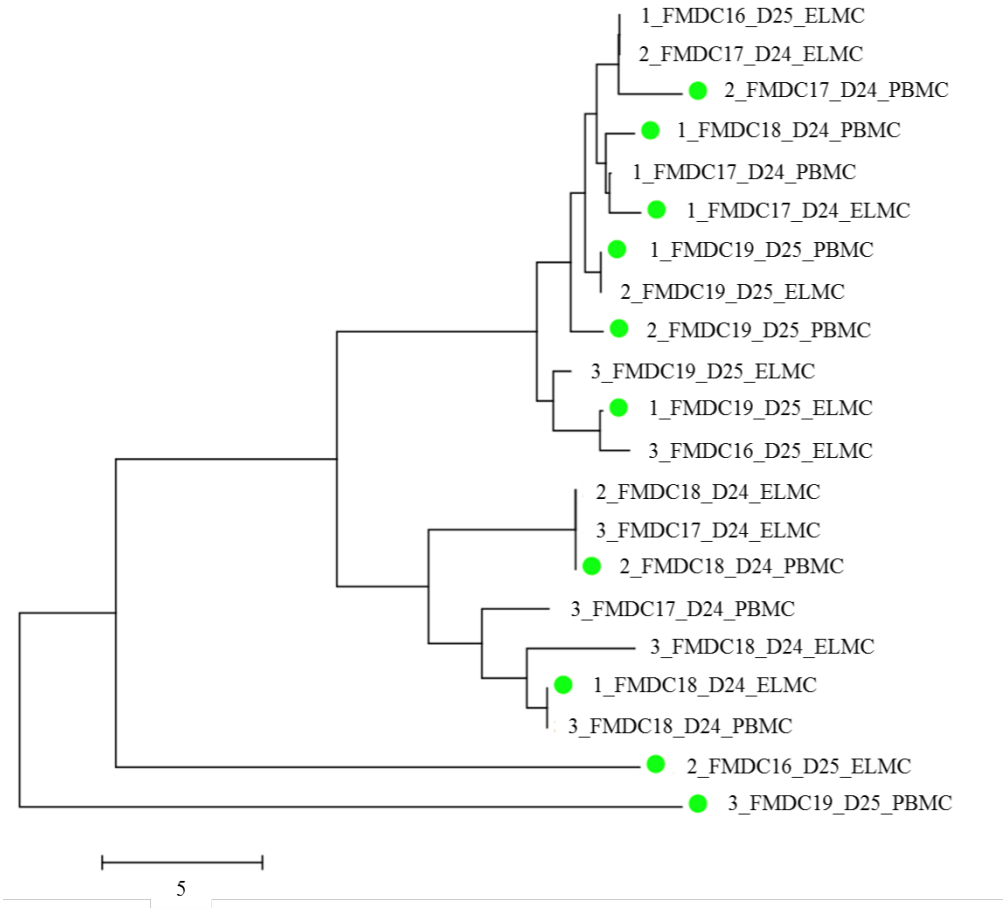


FIGURE 5.20: Phylogenetic tree reconstructed using neighbour-joining method showing the number of amino acid differences between each of the top 3 most abundant bovine Igλ transcripts taken from FMDC16, 17, 18 and 19 in both peripheral blood (PBMC) and efferent lymph (ELMC) at D24/5 post primary immunisation. The highlighted sequences (green circles) were selected as representative examples from each group of Igλ transcripts and used for modelling (See section 5.4.3.2).

5.4.3.2 The predicted Igλ structure is very similar between animals

The highly dominant Igλ transcripts are shared between the out-bred animals at the same time-point. To investigate whether the transcripts differed in their predicted structures, a representative sequence from each of the Igλ transcript clusters was selected from the previously described phylogenetic tree (Figure 5.20, green dots, Figure 5.21). These sequences were then modelled using SWISS-MODEL against the template of a previously described bovine light chain antibody (BLV1H12, PDB:4K3D) [262, 288, 289, 290]. The models generated by SWISS-MODEL had an acceptable confidence score (Z-score),

with only slight loss of confidence in the variable CDR regions of the model (Table 5.11). An overlay of the modelling results showed that the predicted structures of the Igλ transcripts are highly similar, with the framework regions being identical between all of the modelled transcripts (Figure 5.21). The previously described (section 5.4.1.3) predicted CDR regions are highlighted in a different colour for each of the modelled sequences (see Table 5.11). This identified that there are slight structural variations in the CDR1, 2 and 3 regions, which is in keeping with the amino acid sequence data previously described. Overall this data suggests that there is very little variation in the amino acid sequences or predicted structure of the most abundant Igλ light chain sequences in cattle at the peak of the antigen-specific plasma cell response.

TABLE 5.11: Bovine Igλ sequences selected for modelling

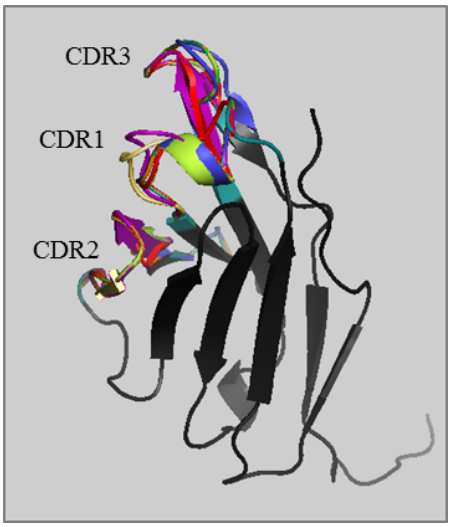
	Relative abundance (%)	QMean Z-score	CDR3 model colour
1_FMDC17_D24_ELMC	20.98	0.28	Royal blue
1_FMDC18_D24_ELMC	6.76	0.85	Lemon
1_FMDC18_D24_PBMC	7.21	0.08	Brown
1_FMDC19_D24_ELMC	11.76	0.33	Green
2_FMDC16_D25_ELMC	6.07	-0.59	Lime green
2_FMDC17_D24_PBMC	10.68	-0.62	Purple
2_FMDC18_D24_PBMC	6.62	1.01	Orange
2_FMDC19_D24_ELMC	8.34	0.29	Teal
3_FMDC19_D24_PBMC	4.92	-0.15	Red

Bovine Igλ transcript sequences selected for modelling based upon phylogenetic clustering (see Figure 5.20). The QMEAN Z-score is an indicator of the quality of the model, a score of <1 is the highest confidence interval [287]. PBMC = peripheral blood mononuclear cells, ELMC = efferent lymph mononuclear cells. CDR3 model colour shown in Figure 5.21.

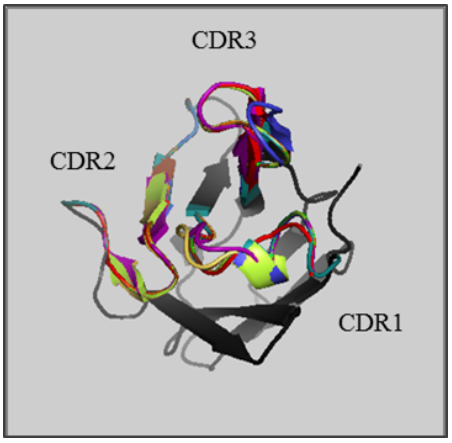
5.4.3.3 The predicted structure of bovine IgG heavy chain V-region suggests that the elongated CDR3 region is involved in antigen-binding

The IgG CDR3 region has the highest amino acid diversity and length variability of all the CDR regions. Analysis of amino acid frequencies within the expressed CDR3 regions showed a predominance of tyrosine (Y) and glycine (G) residues, that accounted for 29.04% of the CDR3 amino acid residues (Y = 13.08%, G = 15.96%, Figure 5.22A). There was a positive correlation between the number of glycine residues present with a CDR3 region and its length (R^2 = 0.8229, Figure 5.22B. There was, however, no correlation between the length of the CDR3 and the tyrosine residue content (R^2 = 0.2323, Data not shown).

(A)



(B)



(C)

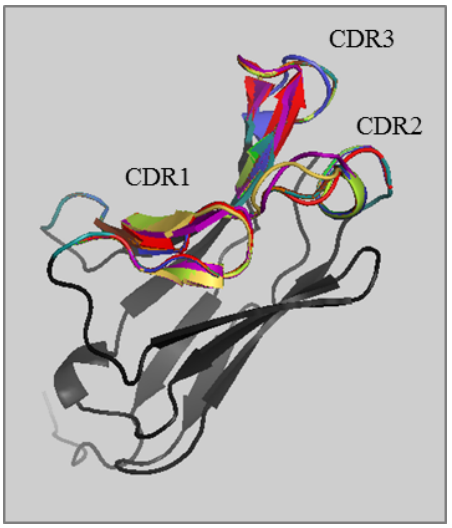


FIGURE 5.21: An overlay of 9 predicted models of the bovine Igλ V region pictured (A) to the left, (B) from the top, and (C) to the right. Details of the chosen Igλ sequences modelled are shown in Figure 5.20 and the Z-scores for the models and the transcript relative abundances are given in Table 5.11. All models were based on the bovine light-chain antibody BLV1H12 (PDB:4K3D, Z-score 0.99) [262, 288, 289, 290].

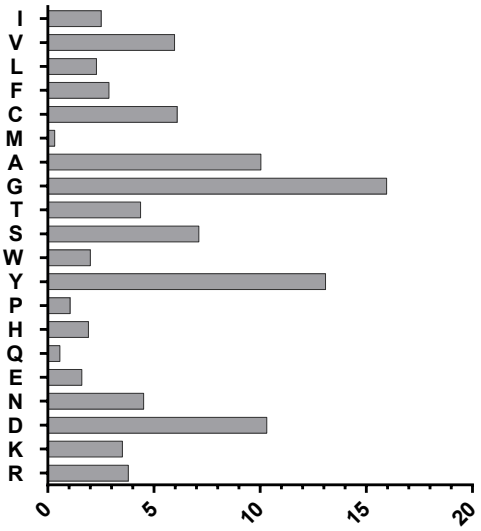
Previous studies in humans have shown that there is a correlation between the heavy chain CDR3 length and the number of cysteine residues, with the increased number of cysteine residues present in the lengthened CDR3 providing structural support, via intra-chain disulphide bonds [294]. In cattle, cysteine residues (C) accounted for 6.10% of all the amino acids within the expressed CDR3 regions (Figure 5.22A), in contrast to the IgG CDR1 and 2 regions, where cysteine residue frequency was 0.06 and 2.71%, respectively (Data not shown). There was also a positive correlation between the number of cysteine residues present within a CDR3 region and its length ($R^2 = 0.892$, Figure 5.22B). There was also a conserved cysteine residue at the 5′ end of the CDR3 region in all IgG heavy chain transcripts. Within all of the super long CDR3 regions interrogated there was always an even number of cysteine residues present within the predicted CDR3 region (Data not shown).

Clearly, the amino acid composition of the IgG CDR3 region, in particular the number of cysteine residues, is an important feature of the IgG V region. The variable length of the CDR3 is also a key feature of the bovine IgG V region structure. SWISS-MODEL was used to predict the structure of three IgG V regions with a range of CDR3 lengths (24, 61 and 71aa, Figure 5.23) [289].

The crystal structure of two bovine antibodies that have super long CDR3s (61 and 56aa length) have recently been resolved, using x-ray crystallography, by Wang *et al* (PDB: 4K3D and 4K3E, respectively) [262]. Using both of these resolved structures as templates for the modelling of IgG transcripts from this study, the modelling results showed that SWISS-MODEL would only produce a predicted model for the experimental IgG transcripts with one but not both of the templates structures. This was due to the sequence homology of the CDR3 region between the experimental transcripts and the chosen template. If the CDR3 region in the experimental transcript was altered to be more homologous to the template CDR3, then the structure was successfully modelled (Data not shown). This phenomenon was due to the high levels of diversity seen in the CDR3 region, which reduced the overall confidence (Z-score) of the model, thus making SWISS-MODEL fail. However, in all of the predicted IgG V region models there was a high level of confidence for the rest of the model structure, excluding the CDR3 region.

All of the models show an elongated CDR3 loop that protrudes from the main body of the structure, with a stalk and head-like structure (Figure 5.23), which is similar to the template structures. The head-like structure becomes more complex as the CDR3 region lengthens (Figure 5.23). In the models depicting the super long CDR3 loops (61 and 71aa, Figures 5.23B and C, respectively) the cysteine residues located within the CDR3 region are highlighted in red. It is clear that these, disulphide bond forming, residues

(A)



(B)

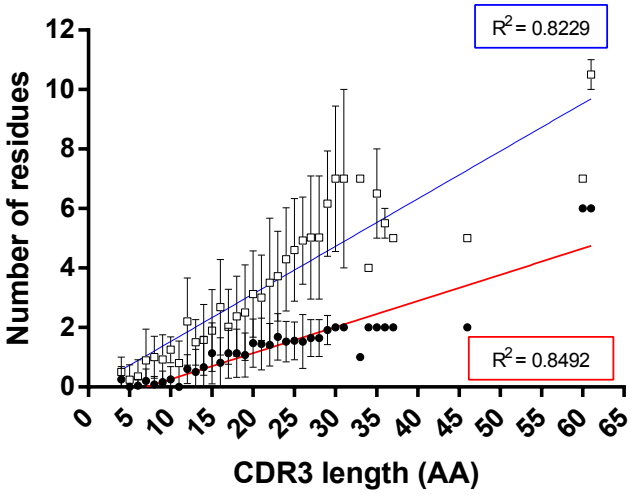


FIGURE 5.22: (A) Amino acid frequency within the IgG V region CDR3. (B) Correlation between the number of cysteine (C, black circles, red trend line) and glycine (open squares, blue trend line) residues and the length of the CDR3 region (aa). Linear regression model was used to calculate the R^2 value. Top 50 most abundant transcripts taken from D0, D7 and D24/5 post primary immunisation in both peripheral blood and efferent lymph ($n = 752$).

play a key role in the head structure of the CDR3 loop. In all of the models the CDR1 and 2 loops are much smaller than the CDR3 loop and have a very similar structure.

The pronounced structure of the CDR3 region suggests that this region is the area that is likely to interact with antigen, and that the CDR1 and 2 regions are more likely to provide structural support to the elongated CDR3 structure. This is also supported by the lack of light chain variation in structure, as shown in section 5.4.3.2. Modelling the pairing of a dominant IgG V region transcript at the peak of the post booster vaccination antigen-specific plasma cell burst (FMDC18, efferent lymph, D24, IgG transcript abundance 1.198%, CDR3 length 25aa) with the most dominant Igλ V region transcript from the same sample (transcript abundance 6.76%) (Figure 5.24). The confidence of both the predicted IgG and Igλ V region models was acceptable (-1.13 and 0.88, respectively), but as with the other IgG heavy chain V regions modelled, the highly variable CDR3 region reduced the overall Z score of the model.

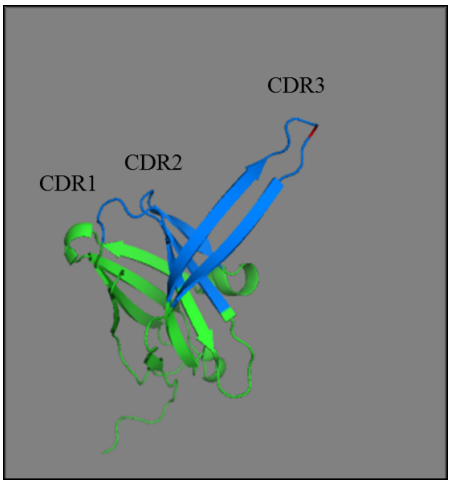
When the models of the heavy and light chain V regions are combined it is clear that the CDR3 region of the IgG heavy chain V region protrudes from the structure, with the other heavy chain CDR regions along with the light chain CDR regions offering structural support to the IgG CDR3 stem-like structure (Figure 5.24).

5.5 Discussion

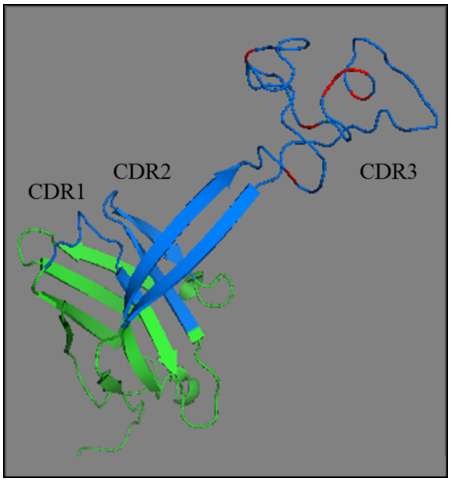
This is the first study to assess the immunoglobulin transcript repertoire at the peak of the antigen-specific plasma cell burst post-primary and -booster immunisation in cattle. Using the O1-Manisa FMDV-specific ELIspot, the timing of the antigen-specific plasma cell burst post-primary (D7) and booster immunisation (D24/5) was determined in both peripheral blood and efferent lymph (see Chapter 4). Having determined the timing and magnitude of the antigen-specific plasma cell bursts, next generation sequencing was then employed to further interrogate the immunoglobulin transcript repertoire at the peaks of the plasma cell response. The use of deep sequencing allows a depth of sequence coverage that cannot be achieved by Sanger sequencing, thus making it a powerful platform for assessing the broad array of immunoglobulin transcripts present during an antigen-specific response [295].

During the evaluation of the gene-specific primers used in this study it was shown that there was a very low level of Igκ expression, suggesting that cattle exhibit a predominantly Igλ restricted light-chain usage (Figure 5.6). This finding is in keeping with other previously published reports, which show that 95% of bovine light chains are Igλ

(A)



(B)



(C)

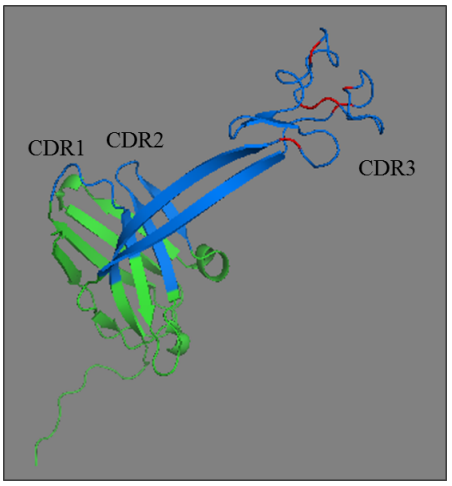
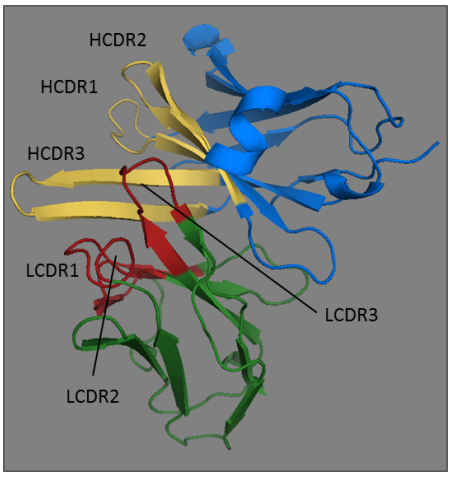
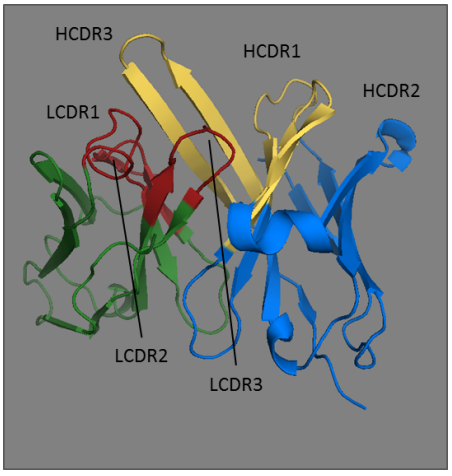


FIGURE 5.23: Predicted structure of bovine IgG regions. The predicted CDR regions are shown in blue and framework regions in green. CDR3 region cysteine residues are highlighted in red. (A) Example of a IgG V regions with a 24aa length CDR3 region, taken from FMDC16 at D25 in efferent lymph (relative transcript abundance 0.534%). The model Z score was −1.35 and was predicted using the bovine antibody template BLV1H12 (PDB: 4K3D H-chain, Z-score: −0.94). (B) Example of a IgG V region with a 61aa length CDR3 region taken from FMDC16 at D0 (relative transcript abundance 0.335%).The model Z score was −1.62 and was predicted using the bovine antibody template BLV5B8 (PDB: 4K3E H-chain, Z-score: −0.44). (C) An example of an IgG V region with a 71aa length CDR3 region (relative transcript abundance 0.115%).The model Z-score was −1.35 and was predicted using the bovine antibody template BLV1H12 (PDB: 4K3D H-chain, Z-score: −0.94) [262, 288, 289, 290].

(A)



(B)



(C)

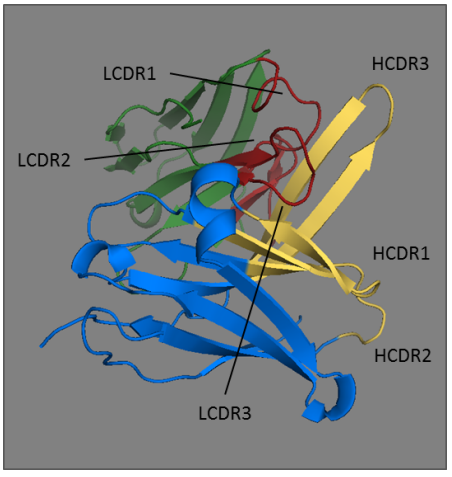


FIGURE 5.24: Predicted structure of the combined bovine IgG and Igλ V region, predicted CDR regions are shown in yellow (IgG) and red (Igλ) and framework regions in blue (IgG) and green (Igλ). Structure viewed from the (A) left, (B) front and (C) right. Both the IgG and Igλ V regions were modelled using the most abundant transcript sequences from FMDC18 at D24 from efferent lymph. The IgG model had a Z score of −1.13 and was predicted using the bovine antibody template BLV1H12 (PDB: 4K3D H-chain, Z-score: −0.94). The Igλ model had a Z score of 0.88 and was predicted using the bovine antibody template BLV1H12 (PDB: 4K3D L-chain, Z-score 0.99) [262, 288, 289, 290].

restricted [292, 293]. The bovine Vκ and Jκ gene segments are found in a 250kb genomic segment on Chromosome 11 [259]. The genomic structure of this loci is relatively uncomplicated as compared to humans and mice [259]. Twenty two Vκ (8 functional), 3 Jκ and 1 constant region κ gene segments were identified during the recent annotation of the 3.1 *Bos Taurus* genome [259]. The relatively small number of functional Vκ and Jκ gene segments identified suggests that there is preferential usage of Igλ light chains in cattle [259, 293]. Indeed, Ekman *et al.* has shown the presence of a sequence that is highly homologous to the murine κ deleting element (KDE) located 28.5kb downstream of the bovine Igκ locus [259]. The KDE serves to control the expression of non-functional Igκ VJ rearrangements, eliminating the kappa locus before the Igλ locus can undergo rearrangement, thus providing a mechanism of allelic exclusion [9]. Ekman *et al.* has shown that the orientation of the bovine Igκ locus permits recombination exclusively by deletion, thereby promoting Igλ light-chain restriction in cattle.

At the peak of the antigen specific plasma cell burst there was an increase in the relative abundance of the most dominant IgG transcripts in both peripheral blood and efferent lymph, as compared to the pre-immunisation transcript repertoire. Similar studies in mice using bone marrow derived mononuclear cells have shown that highly abundant heavy chain V region transcripts, that are present at day 6 post-booster immunisation, are antigen-specific [274]. These mice were immunised with a range of different antigens, all induced differing degrees of serological response; the relative abundance of the highly-abundant, antigen-specific transcripts ranged from $\approx 1\%$ to 10% [274]. Despite the broad range of transcript relative abundances shown, when the transcripts were expressed 78% of them were specific for the immunising antigen [274]. The relative abundance of the dominant IgG transcripts at the peak of the plasma cell response in this study are in keeping with the work of Reddy *et al.* [274] and suggests that these highly abundant transcripts may be FMDV O1-Manisa specific .

A comparison of the IgG repertoires at the peak of plasma cell bursts following primary (D7) and booster D24/5) IgG transcript repertoires was made to confirm antigen-specificity of the highly abundant IgG transcripts. If an IgG transcript were antigen-specific it is likely to be present within the primary plasma cell burst repertoire (D7), but perhaps at a relatively low abundance. Antigen-specific IgG transcripts that were present in the plasma cell burst Ig repertoire post primary vaccination should be boosted to become a with a higher relative abundance in the post booster plasma cell burst Ig repertoire. Indeed, the comparison of these two time points has shown that highly abundant IgG transcripts at the peak of the secondary plasma cell burst had matched transcripts that were of a lower abundance at the peak of the primary plasma cell burst. However, what was unexpected was the presence of more than one IgG transcripts at the peak of the antigen-specific plasma cell response following primary immunisation;

these were matched with a highly abundant IgG transcript at the peak of the plasma cell burst following booster immunisation. The process of somatic hypermutation serves to improve the antibody affinity by 1 to 3 orders of magnitude [296]. This finding may represent the process of affinity maturation, whereby antigen-specific primary plasma cell transcripts undergo somatic hypermutation resulting in an improved affinity for the cognate antigen. These higher affinity transcripts then undergo clonal selection, thereby increasing the transcript relative abundance during the post booster plasma cell burst. There were also some transcripts that decreased in relative abundance from the primary plasma cell burst to the secondary burst, these transcripts may be of a lower affinity for the antigen and so are out-competed by other transcripts that have a higher affinity for the antigen.

As shown by Reddy *et al.* highly abundant transcripts present within the immunoglobulin repertoire following primary and booster immunisation are likely to be antigen-specific [274], therefore the presence of these transcripts during both phases of the plasma cell response (primary and secondary plasma cell bursts) adds weight to the argument that these IgG transcripts are antigen-specific. Although, the specificity of these transcripts is yet to be determined.

In humans and mice, the structure of the variable region is maintained by the highly conserved framework regions, whilst the variable CDR regions of both the heavy and light chains form an undulating antigen-recognition site [262]. In cattle the regions with the highest amino acid variability within both the heavy and light chain V regions were also found in the three predicted complementarity determining regions (CDRs), in keeping with other published data for mammalian antibodies [297]. The length of the bovine CDR1 and 2 regions of both the heavy and light chain were similar to other previously published data [259, 278].

However, the bovine IgG CDR3 region was unusual in its length diversity, as compared to human and mouse [294]. The over-representation, of both tyrosine and glycine residues in the bovine IgG CDR3, as compared to the heavy chain CDR1 and 2, is in keeping with other bovine immunoglobulin heavy chain data [278]. The tyrosine and glycine residues accounted for 29.04% of the bovine IgG CDR3 amino acids, which is in keeping with data from human immunoglobulin heavy chain CDR3s [294]. Both tyrosine and glycine residues play an important role in the ability of the antibody to bind antigen. Tyrosine residues stabilise antigen-antibody interactions whilst glycine residues provide conformational flexibility to the antibody structure [297]. Thus the positive correlation between the number of glycine residues and CDR3 length in bovine IgG antibodies (R^2 = 0.8492) is likely to increase the CDR3 regions conformational flexibility. This finding is unique to cattle, as studies of both human and mice immunoglobulin heavy chain

CDR3 regions have shown that glycine prevalence decreased with an increase in CDR3 length [294].

Cysteine residues are also of structural importance as they form disulphide bonds which provide structural stability. Cattle exhibit a much greater frequency of cysteine residues within the IgG CDR3 region as compared to humans and mice (6.10% compared to 1.21% and 0.35%, respectively) [278, 294]. Indeed, there was a positive correlation between the number of cysteine residues within the bovine IgG CDR3 region and the regions length. There is a conserved cysteine residue at the 5′ end of the CDR3 and within the super long CDR3 regions there was always an even number of cysteine residues, suggesting disulphide bond formation [298]. Thus cysteine residues clearly play an increasingly important role in the structural stability of the IgG CDR3 region as the region's length increases.

Another unusual feature of the bovine IgG CDR3 region is the very broad range of length variability, ranging from 4 to 61aa. Humans typically have a heavy chain CDR3 length of 8 to 16 amino acids [262]. The bovine IgG CDR3 region's broad range of lengths had a bimodal distribution, that did not alter during the course of an antigen specific response. Suggesting that the diverse range and distribution of CDR3 lengths is an inherent feature of the bovine IgG repertoire.

The structure of three bovine IgG V regions, of varying lengths, was predicted using the recently resolved crystal structure of a bovine antibody as a template [262]. The resulting models suggested that the CDR3 loop of the IgG V regions forms a highly unusual head and stem-like structure that protrudes away from the main body of the immunoglobulin V region. The IgG heavy chain V regions modelled did not suggest any deviation from the recently published structure from Wang *et al.* [262]. The CDR1 and 2 regions of the IgG V region were highly similar in structure in all 3 models. The CDR1 and 2 regions of the IgG V region are germline encoded regions of sequence variability within the V_H gene segment (see Chapter C.1). There are 36 bovine V_H gene segments, of which only 10 are functional [260]. The functional bovine V_H segments are all from the same family and have a sequence identity of >80%. There are only 8 unique CDR1 and 2 pairs in the germline encoded bovine V_H gene segments, therefore, aside from the introduction of point mutations, there is very little variability within the CDR1 and 2 regions. Whereas, the IgG CDR3 region is highly diverse and is unique in structure. Studies in transgenic mice that express a single V_H gene have shown that the highly diverse CDR3 region of the heavy chain confers the antigen-binding ability of the antibody, whilst the CDR1 and 2 regions are more 'generic' antigen-binding regions [299].

The CDR3 region falls at the junction V_H, D_H and J_H gene segments. Given that the V_H gene segment diversity is very low and that the use of only 1 J_H was observed in this

study (Data not shown) and others [279, 300], the variation in CDR3 length must be generated by the bovine D_H gene segments, the extra nucleotide addition during gene recombination and further diversification by somatic hypermutation [268]. There are 3 bovine D_H gene segments, all of which are functional [301]. The germline sequences of the bovine D_H gene segments differ significantly in length from 13aa (D_H1), 18aa (D_H3) and 48aa (D_H2) [301]. Indeed, Wang *et al.* have recently resolved the crystal structure of a bovine antibody that has a super long CDR3 region (61aa). These unusual antibodies utilise the long D_H2 gene segment and a unique V_H gene segment (V_HBUL) that is located in the immunoglobulin loci on chromosome 21 [262]. The head and stalk-like structure demonstrated by Wang *et al.* features spatially separated cysteine residues in the head structure that are able to form microfolds, via disulphide bonds, to give the antigen-binding specificity of the antibody [262]. Interestingly, Wang *et al.* have demonstrated that the D_H2 gene segment contains the RGYW motif, that is recognised by AID and 81% of the D_H2 residues can be mutated to a cysteine residue by SHM [262]. The two super long CDR3 regions modelled from this study also have the key characteristics described by Wang *et al.*, and had a sequence identity of >72% with the recently resolved bovine immunoglobulin structure [262]. Thus cattle appear to have evolved a unique mechanism of diversifying the limited germline encoded gene segments by forming an elongated CDR3 structure that relies upon AID mediated mutation to form unique patterns of cysteine residues [262]. However, in cattle, these super long CDR3 antibodies were only transiently present in the top 50 most abundant IgG transcripts during the course of the immune response and their abundance is not boosted during the plasma cell burst post immunisation. It could be hypothesised that cattle have evolved these super long CDR3 regions to increase the diversity of their antibody repertoire by allowing more flexibility in the antibody binding domain, thus enabling binding of more conserved deeply embedded epitopes on pathogens, and thus lending themselves towards a more cross-reactive or naturally occurring antibody phenotype. The data from this study would suggest that bovine antibodies with a super long CDR3 region (>40aa in length) are not likely to be FMDV-specific, as their abundance appears not to be boosted following immunisation with FMDV O1-Manisa. Studies in influenza and Human immunodeficiency virus (HIV) have shown that broadly neutralising cross-reactive antibodies have an elongated and highly mutated CDR3 regions [302, 303].

Studies of human antibodies have clearly demonstrated that the elongated CDR3 region of the immunoglobulin heavy chain confers all of the antibody binding capability of the antibody [303]. Ekiert *et al.* have shown that a broadly neutralising antibody directed against the HA antigen on influenza A binds its cognate antigen solely via the elongated CDR3 loop (24aa) of the heavy chain [303]. Cattle exhibit a bimodal distribution of heavy chain CDR3 lengths, with the larger of the distribution had a median of 24aa

in lengths. This, and the bovine heavy chain modelling data, suggests that the CDR3 region is also likely to confer the binding capabilities of the bovine immunoglobulin molecule. This is further confirmed by the predicted model of the complete bovine immunoglobulin heavy and light chain V region, showing the CDR3 region of the heavy chain protruding from the main body of the molecule, with the other heavy chain and light chain CDR regions offering structural support to the CDR3 loop.

There is a predominance of at least one Igλ transcript at the peak of the post-boost antigen-specific plasma cell burst. These transcripts were highly similar, between the animals, in their amino acid sequences and predicted structures. Despite there being a greater number of functional germline encoded Igλ V_L than V_H gene segments, 33 vs. 10, respectively, there was a large predominance of a single Igλ transcript at the peak of the antigen-specific plasma cell response. Coupled with the high degree of Igλ sequence similarity seen between the out-bred animals suggests that there is a large degree of Igλ transcript restriction within the bovine immunoglobulin repertoire. There has been no comparisons made between the highly dominant heavy-chain V region sequences between the animals.

In humans and mice both the heavy and light chain CDR1, 2 and 3 form the antigen binding site [262]. However, cattle heavy chains exhibit elongated CDR3 regions coupled with the small degree of variation shown in the highly dominant light chain transcripts suggesting that the light chain has very little involvement in the antigen-binding capabilities of all bovine immunoglobulins. Bovine antibodies that carry the super long CDR3 heavy chain are restricted to only one Igλ light chain, which acts as a structural support for the head and stalk structure of the heavy chain CDR3 [262, 304]. Although data from this study would suggest that these super long CDR3 antibodies are unlikely to be FMDV O1-Manisa specific, it does suggest that all bovine antibodies are highly restricted in their Igλ light chain usage, thus suggesting a structural rather than antigen binding role for all bovine immunoglobulin light chains. As shown in the bovine immunoglobulin modelling data in this study, Igλ V region offers a structural rather than antigen-specific role within the bovine immunoglobulin molecule in response to FMDV immunisation. Production of synthetic human antibodies using phage-display libraries have also shown that the light-chain V region has a less important in antigen-binding as compared to the heavy-chain V region [305].

This is the first study to assess the heavy and light-chain immunoglobulin repertoire during the course of an immune response in both efferent lymph and peripheral blood. Using an antigen-specific ELIspot assay, to determine the timing and magnitude of the plasma cell burst, and next generation sequencing to interrogate the immunoglobulin repertoire at these specific time points has identified IgG and Igλ transcripts that are likely to

be FMDV-specific. Cattle have developed a unique structural characteristic that allows them to have an effective and broad array of antibodies, without the requirement of a large repertoire of germline encoded gene segments. Structural studies have shown that the elongated heavy chain CDR3 region is likely to provide the antigen specificity of the molecule, whilst Igλ light chains provide a structural support. It is therefore likely that bovine antibodies recognise and interact with their cognate antigens differently, as compared to how human and mice antibodies. The structural differences in demonstrated by bovine antibodies is also likely to have had an impact upon pathogen evolution. The disparity between cattle and mouse antibody structure and may also explain why successful FMDV vaccination protocols that have achieved protective results in mice have not translated cattle [306]. Thus understanding how these unusual structures interact with their cognate antigen (e.g. FMDV) and defining the epitopes that are bound by these antibodies will inform better vaccine design within the host species.

Chapter 6

Conclusions and further work

6.1 Conclusions

Foot and mouth disease virus is a highly contagious pathogen that has a large socio-economic impact upon countries in which the virus is endemic. Studies in cattle and mice have shown that protection from the virus is antibody-mediated. However, the inactivated FMDV vaccines are unable to achieve long durations of immunity in cattle; regular repeated immunisations are required to maintain protective antibody titres.

6.1.1 The kinetics of the B cell response to antigen in cattle is similar to that in mice and humans

The classical description of the B cell response is that following immunisation with antigen leads to the induction of antigen-specific antibodies that are isotype-switched and of a high affinity. Formation of germinal centres results in the induction of long-lived plasma cells, which secrete antibody into the periphery, and memory B cells. Immunising cattle with a TD antigen results in the induction of a plasma and memory B cell response that has a similar timing and magnitude to data reported in humans [171, 214, 215]. The T-dependent B cell response in cattle was characterised by a burst of antigen-specific plasma cells occurring 7 days after the primary vaccination, which was coupled with an increase in antigen-specific IgG titres. In keeping with the central dogma of immunological priming, the plasma cell burst post booster vaccination was larger and more rapid. Antigen-specific memory B cells induced following prime and booster vaccinations remained detectable in the circulation of the cattle for over 6 months. Although, the numbers of antigen-specific IgG^+ memory B cells declined from their peak number 8 days post booster immunisation. This finding is in keeping with

other previously published studies in mice [307, 308] and suggests that IgG^+ memory B cells have a finite life-span, unlike descriptions of IgM^+ memory B cells [308]. It has been proposed that IgM^+ memory B cells serve as an 'archive' of previous B cell responses that can be called upon once the IgG^+ memory B cell pool has been depleted [308].

Sustaining a long duration of immunity against antigen is dependent upon the survival/-maintenance of antigen-specific long-lived plasma cells and memory B cells. However, there is evidence that long-lived plasma cells are not life-long and have a finite life-span. Thus, mechanisms exist to maintain protective antibody titres for long periods of time with a diminishing pool of long-lived plasma cells. There are, however, conflicting lines of evidence as to how the memory B cell and long-lived plasma cell pools are maintained. Bernasconi *et al.* have shown that stimulating a B cell response, by antigenic challenge, results in a burst of antigen-specific plasma cells post immunisation and also a burst of plasma cells that are specific for antigens that an individual has been previously immunised with, called 'recall' responses [134]. The bystander stimulation of 'recall' antigen-specific memory B cells to differentiate into plasma cells provides a mechanism of replenishing the long-lived plasma cell pool without the need for a persistent source of antigen. Indeed, data presented in this thesis has also demonstrated that immunisation of cattle with a third-party antigen (TD-antigen) also results in a small burst of 'TD recall' antigen-specific plasma and memory B cells. The small burst of recall antigen-specific plasma cells was not coupled with an increase in the antigen-specific IgG titres. These findings are consistent with those of Bernasconi *et al.* and present a mechanism of maintaining a pool of immunoglobulin titres without the need for a re-immunisation with a cognate antigen. However, other research groups have shown that the maintenance of the memory B cell pool is exclusively cognate antigen-dependent [309]. The exact mechanism of how the long-lived plasma and memory B cell pools are maintained is yet to be elucidated, but despite the conflicting evidence presented to-date, it is likely that maintenance of the memory B cell pool may be cognate antigen-dependent, whilst the long-lived plasma cell pool could be maintained by bystander stimulation from third-party antigens. Indeed, Ahuja *et al.* have demonstrated in mice, that maintenance of the long-lived plasma cell pool is independent of the memory B cell pool [310]. One possible explanation for the bystander stimulation of the memory B cell pool, following immunisation with a third party antigen, could be the prolonged stimulation of T_{FH} cells by antigen. Recher *et al.* have shown that prolonged, strong activation of T_{FH} cells resulted in bystander activation of non-cognate B cells [311]. Thus, under the right conditions (i.e. TD antigen with a potent adjuvant), the circulating IgG^+ memory B cells that are specific to a 'recall' antigen could be activated by bystander signals from T_{FH} cells, resulting in the rapid induction of antibody secreting plasmablasts. Memory

B cells have a lower activation threshold [312] and can be activated by polyclonal stimuli, thus could be activated by a non-cognate antigen via bystander stimulation [134]. IgG^+ memory B cells have been shown to enter into survival niches that are proximal to vestigial GCs [123], thus allowing interaction between the IgG^+ memory B cells, FDCs and T_{FH} cells. It has recently been shown that FDCs are able to sequester antigen in non-degradative compartments that are periodically re-displayed in the FDC surface to cognate B cells [55], thus providing a mechanism of presenting antigen to cognate memory B cells and providing bystander stimulation to non-cognate memory B cells.

Studies in mice have shown that upon activation, IgG^+ memory B cells are able to rapidly differentiate into antibody secreting cells [307]. This has been confirmed by data presented in this thesis and by others [124], which show a rapid induction of IgG secreting plasma cells following booster immunisation, presumably due to the activation of IgG^+ memory B cells that were induced following primary immunisation. However, studies in mice have shown that re-stimulated IgG^+ memory B cells do not re-enter the GC and remain as extra-follicular plasmablasts [307]. Since the GC is the site of long-lived plasma cell determination it is therefore unlikely that re-stimulated IgG^+ memory B cells will become long-lived plasma cells [112]. 'Bystander' stimulation of the memory B cells is an attractive mechanism to replenish the long-lived plasma and memory B cell pool in the absence of any re-immunising antigen. However, evidence would suggest that the resulting increase in both plasma and memory B cells that are specific for 'recall' antigens, following third-party immunisation, is the result of bystander stimulation of memory B cells but does not result in replenishment of the long-lived plasma or memory B cell pool.

6.1.2 Foot-and-mouth disease virus does not induce memory B cells

Vaccination with inactivated FMDV is unable to induce long-duration of immunity. Juleff *et al.* have shown that cattle can produce class-switched antibody rapidly in response to FMDV challenge, despite being depleted of $CD4^+$ T cells, thus demonstrating the largely T-independent nature of FMDV [198]. Pega *et al.* have also recently demonstrated that rapid induction of FMDV-specific plasma cells in local lymphoid tissue, following live-virus challenge, is also consistent with a T-independent response. TI-2 antigens have regularly-spaced, repeating epitopes that are able to stimulate B cells in the absence of $CD4^+$ T cell help [166]. The FMDV capsid is composed of 4 structural proteins that are arranged in a protomer which combine to form the capsid. Thus, the structure of FMDV is likely to have multiple repeating epitopes, thereby stimulating B cells in a TI-2 manner. Adoptive transfer studies of splenic B cells from pre-immune mice

into irradiated recipient mice, show that protection from FMDV infection is induced in a T-independent manner [197].

There are 5 antigenic sties on the FMDV capsid, including the GH-loop, which is regarded as being highly immunogenic [313]. The GH-loop is used, by FMDV, as the integrin cell attachment site [213]. The GH-loop is located within the VP1 protein (135 - 156) and is a fully exposed, highly disordered, and mobile structure [213]. These structural features are likely to lend itself towards being a T-D epitope. Indeed, CD4+ T cell depletion, in cattle, resulted in the reduction of class-switched (IgG) G-H loop (VP1 135-156) specific antibodies, which indicates that the antibody response to this epitope is dependent upon the presence of $CD4^+$ T cells to develop the antibody response [198]. During FMDV live-virus challenge, $CD4^+$ T cell depletion also resulted in the loss of class-switched antibody responses to non-structural proteins, which again indicates the T-dependency of the NSP-specific antibody response [198]. Thus despite the T-D nature of the GH-loop, $CD4^+$ T cell depleted cattle were able to mount a protective neutralising antibody response, presumably in a TI-2 manner, to the other 4 antigenic sites of the FMDV capsid [198]. Indeed, immunisation of cattle with synthetic peptides that represented the GH-loop have been shown to induce a neutralising antibody response and limited protection against viral challenge [205]. However, more recent studies using chimeric viruses which has VP1 GH-loop substitutions, have shown that the G-H loop is not required to induce a strong neutralising antibody response or a protective immune response following vaccination with inactivated virus [314]. A recent study to attempt to broaden the GH-loop peptide vaccine by incorporating promiscuous T_H epitopes that were derived from highly antigenic proteins of pathogens into the variable amino acid positions of the GH-loop [206]. Whilst this approach was successful in swine, inducing a high level of protection against FMDV live-virus challenge [206]. The peptide vaccine induced low VNT titres post-vaccination and failed to protect against live-virus challenge [206].

A number of MHC class II and MHC class I restricted T cell epitopes, which are presented to $CD4^+$ and $CD8^+$, T cell respectively, have been identified on the FMDV capsid. Indeed, both $CD4^+$ and $CD8^+$ T cell FMDV specific responses have been observed previously in cattle [315, 316]. However, the role of cellular immunity in the control of FMDV is still unclear, although there is some speculation that it is involved in the clearance of FMDV from persistently infected animals [317]. Glass et al. showed that cattle with different MHC class II haplotypes were able to demonstrate a T cell proliferative response to a region of the GH-loop (VP1 140 - 158) [315]. A further $CD4^+$ T cell epitope has been determined in the VP4 protein of the FMDV capsid (VP4 20-34), which can be presented by at least four different MHC class II haplotypes [318]. Two further MHC class II restricted epitopes have been identified in VP1 (66 -

80) and VP4 (22 - 36), although this was limited to cattle with a similar MHC class II genetic background [319]. Analysis of gamma interferon (IFN-γ)-producing $CD8^+$ T cells responding to stimulation with FMDV-derived peptides revealed one putative CD8+ T cell epitope present within VP4 (795 - 803) of FMDV serotype O UKG/2001 [320]. The putative epitope is highly conserved between all 7 FMDV serotypes [320]. Indeed, $CD8^+$ T cells from FMDV serotype O-vaccinated that were defined as having the A31 haplotype recognized APCs loaded with the putative epitope (VP4 795 - 803) from all 7 FMDV serotypes [320]. This data suggests that $CD8^+$ T cells that recognise this defined epitope would be cross-reactive to the equivalent peptide derived from all FMDV serotypes, although this CD^+T cell epitope would be restricted to cattle with the genetic background of the A31 haplotype [320]. Despite fairly extensive study there is only limited data on both CD4+ and $CD8^+$ T cell responses in cattle, which suggests that FMDV is a largely TI-2 antigen, with a limited number T cell epitopes that are able to invoke a T-D response in cattle.

Data presented in this thesis has shown that vaccination and live-virus challenge with FMDV resulted in the induction of FMDV-specific plasma cells but in the absence of memory B cell induction. These findings are in keeping with the largely TI-2 nature of the FMDV capsid. Empty FMDV capsid antigens are structurally indistinguishable from FMDV virions [210]; primary immunisation of these empty FMDV capsid was also only able to induce a FMDV-specific plasma cell response without memory B cell induction. This suggests that the structure of the FMDV capsid is what drives the T-independent B cell response to FMDV. Whilst memory B cell induction was seen in half of the cattle that were boosted with FMDV empty capsid, the magnitude of the memory B cell response was very low as compared to a TD antigen response. These memory B cells are likely to have been induced in the absence of productive GC formation [254]. It has been demonstrated that memory B cells that are generated independently of the germinal centre are not long-lived [113]. However, it is of note that the FMDV-specific plasma and memory B cell response following prime and booster immunisation with conventional inactivated FMDV antigen has not been investigated to date. Thus FMDV-specific memory B cells may be generated following prime and booster vaccination with conventional inactivated FMDV antigen.

It has been hypothesised that the accelerated induction of antibody (i.e. an extra-follicular response), in a T-independent manner, provides a rapid means of stopping systemic spread of viruses [212]. Acute viral infection can result in depots of antigen which persist in draining lymph nodes long after complete clearance of the virus has been achieved [321, 322]. It is also of note, that acute viral infections can result in the persistence of GCs [323]. Germinal centre formation is promoted by T_{FH} [75]. It has been shown that viral persistence will preferentially direct $CD4^+$ T cells towards

the T_{FH} compartment, presumably due to the T cell priming signals received from the DCs [324]. Indeed, maintenance of the T_{FH} cell phenotype is dependent upon antigen and GC B cell interaction [325]. Thus, persistence of viral antigens is likely to drive long-term antibody responses via promotion of the GC environment and generation of long-lived plasma and memory B cells.

Juleff *et al.* have shown that FMDV can be found in the light-zone of the germinal centre for up to 38 days post-infection [136]. Furthermore, FMDV has also been identified in the GCs of African Buffalo more than 1 year after live-virus challenge (N. Juleff, personal communication). Also, it has been shown in studies of both cattle and mice that FMDV is a largely TI-2 antigen [197, 198]. Achtman *et al.* has shown in TI-2 antigens are able to induce persistent GC formation in CCR7 knock-out mice [326]. These finding are consistent with those of Juleff *et al.* in FMDV infected cattle and buffalo [198]. Achtman *et al.* also demonstrated that despite the induction of persistent GC formation, which contained both T_{FH} and FDCs, there was no formation of memory B cells [326]. Data presented in this thesis are consistent with this finding, showing a lack of detectable FMDV-specific memory B cells in cattle following immunisation or live-virus challenge. Indeed, immunisation of cattle with the TI-2 antigen, TNP-Ficoll, also resulted in an undetectable number of antigen-specific memory B cells [218].

Cattle that have recovered from FMDV live-virus challenge remain protected from further re-challenge, with the same FMDV strain, for many years [327]. This suggests that FMDV challenge results in the development of a long-lasting antibody response that is able to protect the animal from re-challenge. However, data from the FMDV challenge study presented in this thesis showed that the FMDV-specific plasma cell burst in the non-vaccinated animals was of a lower magnitude post live-virus challenge than the response seen in animals following primary vaccination. However, the non-vaccinated control animals did develop virus-neutralising antibody titres that were of a similar magnitude to the vaccinated animals. This suggests that during FMDV infection the majority of plasma cells are not found in the circulation. Indeed, Pega *et al.* have shown that FMDV infection results in the rapid induction of plasma cells at the site of viral replication [153]. Thus it is hypothesised that the sustained antibody response seen in cattle that have recovered from FMDV challenge is the result of continuous stimulation of naïve B cells into isotype-switched extra-follicular plasma cells, at the site of antigen persistence (viral replication), rather than the induction of functional GCs and the long-lived plasma and memory B cells that result from them. This is likely to be due to the nature of the FMDV antigen and its ability to induce a rapid T-independent B cell response. Indeed, Salt *et al.* demonstrated that local IgA production in the pharyngeal mucosa was dependent upon the presence of replicating FMDV [328]. It has also been shown in RSV infected humans that prolonged RSV-specific plasma cell burst post

infection is due to continued virus shedding, suggesting a role for antigen-persistence being required to maintain a protective plasma cell response [215]. This suggests that the maintenance of FMDV-specific immunoglobulin titres is the result of continuous stimulation of naïve B cells into isotype-switched extra-follicular B cells.

However, not all vaccines against viruses induce poor levels of long-term immunity. The vaccines against both the Yellow fever virus (YF-17D, live-attenuated) and the Smallpox virus (live-virus) are able to induce extremely long-lasting immunity. Smallpox vaccine is able to stimulate antigen-specific antibodies and memory B cells that are detectable in individuals for more than 50 years post-vaccination [123]. The Yellow fever vaccine, YF-17D, is also able to induce long-lasting neutralising antibodies for up to 60 years post vaccination [329]. The maintenance of the neutralising antibody titres is also durable; Yellow fever virus-specific neutralising antibodies are still detectable, even after extensive immunosuppression following solid organ transplantation [330]. Vaccination with YF-17D results in a systemic acute viral infection which is cleared within 7 days [331]. This results in the triggering of multiple pathogen-associated molecular pattern receptors, including TLRs 2, 7, 8, 3 and 9 and cytosolic receptors RIG-I and MDA 5 [332]. The activation of multiple PAMPS leads to the activation of both myeloid and plasmacytoid DCs, which in turn result in activation of a wide range of stimulatory pathways and the activation of both naïve $CD4^+$ T cells and the resulting stimulation of B cells [332]. T_{FH} cell differentiation begins during antigen priming presented by DCs, which leads to the upregulation of Bcl-6 and CXCR5 [76]. Thus, this data shows the importance of DC priming and the positive impact this can have upon the downstream immune response to antigen. By stimulating TLR signalling pathways YF-17D has generated a very long-duration of immunity in individuals that have not had any further exposure to Yellow Fever virus [332]. Thus demonstrating the importance of innate signalling to produce a long-lived B cell response to antigen.

6.1.3 Bovine immunoglobulins are structurally different to human and mouse

Cattle have very few germline encoded V, D and J gene segments, as compared to humans and mice. Thus the recombinational potential of the bovine immunoglobulin repertoire is limited. However, despite the limitations of recombinational diversity, cattle are still able to generate effective B cell responses against a broad array of antigens. Data presented in this thesis and by others has shown that the structure of the heavy chain V region of the bovine immunoglobulin is different to that of mice and humans [262, 278]. Studies in transgenic mice have shown that the CDR3 region of the heavy chain V region confers most of the antigen-interaction capabilities of the whole

antibody antigen-binding domain (V_H + V_L)[299]. However, structural studies [262] and predicted structures presented in this thesis have shown that the elongated heavy chain CDR3 region of the bovine immunoglobulin is likely to provide the only point of antigen-interaction for the bovine immunoglobulin, whilst the Igλ light chain provides structural support to the elongated heavy chain CDR3 [262]. This structural difference in the bovine immunoglobulin antigen-binding domain indicates that the bovine antibody will recognise different epitopes on the antigen as compared to mouse antibodies. Thus, previously identified epitopes on the FMDV capsid that have been defined using mouse antibodies are unlikely to be recognised by bovine-antibodies and vice versa. By combining the antigen-specific ELIspot assay, to pin-point the peak of B cell response following vaccination, with deep sequencing techniques, highly abundant bovine IgG and Igλ transcripts have been identified, which are likely to be FMDV-specific immunoglobulin transcripts. Although, without expressing these transcripts it is not possible to confirm their specificities. However, studies in mice, have demonstrated that highly abundant immunoglobulin heavy chain transcripts that are identified in the post booster immunisation immunoglobulin transcript repertoire are highly likely to be antigen-specific [274]. Thus it is likely that the highly abundant IgG and Igλ transcripts that were identified in this study are FMDV-specific. The dynamic changes shown in highly similar IgG transcript abundances over the course of the immune response is likely to represent selection of BCR specificities following the primary and booster vaccinations. One possible use for future repertoire studies is to enable predication of protection. This could be achieved by comparing the naïve immunoglobulin repertoire with the repertoires post primary and booster immunisation it may be possible to define FMDV protective B cell responses in cattle.

To conclude, the kinetics of both the bovine plasma and memory B cell response to antigen is similar to that demonstrated in both humans and mice. However, the bovine antibody V region structure is not the same and is likely to interact with its cognate antigen differently. Thus, improving our knowledge of how the bovine BCR interacts with FMDV will aid and improve future vaccine design.

6.2 Further work

6.2.1 Improved FMDV vaccines

Foot-and-mouth disease virus is a highly contagious disease that is very difficult to control. The virus is able to spread rapidly, making the disease of high economic importance in both the developed and developing worlds. The current FMDV vaccines is unable to

induce long-term immunity, and repeated immunisation is required to maintain protective antibody titres. The short duration of immunity achieved by the current FMDV vaccines has been attributed to the largely TI nature of the antigen [197, 198]. The lack of detectable FMDV-specific memory B cells, following either vaccination or live-virus challenge adds further evidence to support the hypothesis that FMDV is a largely TI-2 antigen. This finding is also consistent with other TI-2 antigens, in both humans and cattle [171, 218].

Data in this thesis has shown that the addition of a TD antigen into the conventional FMDV vaccine is able to boost the numbers of FMDV-specific plasma cells. Whilst the number of memory B cells were not determined under this vaccination regime, it could be hypothesised that the addition of a TD component to the vaccine could lead to an increase in FMDV-specific memory B cell numbers. It has previously been shown in humans that conjugation of the Diphtheria toxin protein CRM197 (TD antigen) to serogroup C meningococcal polysaccharide (TI-2 antigen) induces antigen-specific memory B cells, when the TI-2 antigen alone did not induce B cell memory [171]. Thus conjugation of a TD antigen (e.g. TTC), which has been shown in cattle to induce a good memory B cell response, to the FMDV capsid could be utilised in FMDV vaccine strategies to drive a TD-like response against FMDV, thereby promoting the development of long-term immunological memory against FMDV.

The B cell response to both empty wild-type and thermo-stable FMDV capsids has been shown to be similar to that of the conventional inactivated FMDV vaccine antigen. However, the thermostable FMDV capsids represent significant advantages in production and distribution by reducing the need for cold-chain storage and negating the stringent requirements of biosecurity during production. The addition of a thermostabilising mutation to the wild-type empty capsid demonstrates that the FMDV capsid can be engineered to have an altered phenotype. Seago *et al.* have also recently shown that the infectious FMDV virus can be engineered, through reverse genetics, to contain a hemagglutinin (HA) or FLAG-tag which can be utilised to improve the virus purification processes [333]. Thus, the genetic modifications that have been used to tag the infectious virus could also be applied to the thermostable FMDV empty capsid, which could allow a TD antigen to be conjugated to the FMDV capsid.

Providing the correct innate signalling to DCs has been shown to improve the neutralising antibody response [332]. Kasturi *et al.* have recently developed biodegradable synthetic nano particles that contained dual TLR triggers (MPL - TLR4 and R837 - TLR7) and the hemagglutinin antigen (H5) from the avian influenza virus H5N1 [334]. Immunisation of mice with the nano particles with dual TLR ligands resulted in the induction of increased antigen-specific neutralising antibody titres, persistent GCs formation and

detectable plasma cell response in the lymph nodes for >1.5 years post-immunisation [334]. This technique could also be applied to FMDV, by using bovine TLR ligands, along with FMDV capsids could increase the duration of the FMDV-specific plasma cell response.

6.2.2 Resolving the crystal structure of bovine antibodies

The structure of the super long CDR3 (>50aa) bovine antibodies has been resolved recently by Wang *et al.*[262]. The crystal structure of the shorter length CDR3 bovine antibodies is yet to be solved. These shorter length CDR3 antibodies represent the 'normal' heavy chain repertoire in cattle and resolving their structure will help to understand the epitopes that are bound by these antibodies. By using the ELIspot assay to determine the peak of the antigen-specific response following immunisation, bovine heavy chain immunoglobulin sequences have been identified that are likely to be FMDV-specific. Expression of these sequences would confirm their specificity. For the expression of the bovine immunoglobulin with a super long CDR3, Wang *et al.* expressed a bovine derived CH1 and V region with a human IgG1 Fc region using the human embryonic kidney cell line (HEK293T); they also co-transfected the HEK293T cell line with a single bovine light-chain [262]. Data shown in this thesis also suggests that the bovine heavy and light chain pairing is unlikely to affect the antigen binding capability of the expressed antibody. As the highly abundant bovine Igλ sequences are highly similar within the animals and also between out bred animals and are therefore likely to be promiscuous in their pairing with the heavy-chain.

There are currently four defined antigenic sites on the FMDV capsid, that have been defined using murine monoclonal antibodies [335]. Given that bovine antibody heavy chains possess an elongated CDR3 region, the structure of the antigen binding domain of bovine antibodies is quite different to murine antibodies [262]. Therefore, epitopes recognised by cattle antibodies are likely to be different to the previously defined epitopes. By solving the structure of FMDV-specific bovine antibodies and identifying where these antibodies bind to their cognate antigen, will enable the identification of bovine-specific epitopes on the FMDV capsid. Understanding the epitopes that are recognised by cattle antibodies will help inform future vaccine design.

6.2.3 Broadly neutralising cross reactive antibodies in cattle

Cattle that have recovered from FMDV infection are, in general, protected against homologous but not heterologous re-challenge [179]. However, evidence suggests that the clinical symptoms shown by cattle during heterologous FMDV re-challenge may lessen in

animals that have been previously challenged [179]. Indeed, Cottral and Gailiunas were able to demonstrate that 3 rounds of challenge with multiple FMDV serotypes resulted in animals that were resistant to further FMDV challenges [336]. These animals had clearly developed cross-reactive neutralising antibodies that were able to protect them against further serotype challenges. There has been some recent work in the HIV-1 and Influenza research fields which suggests that individuals can develop these antibodies naturally after extensive affinity maturation [228, 337].

Understanding how the bovine antibodies interact with their cognate antigen can begin to inform vaccine design and allow preferential activation of specific aspects of the B cell response. As demonstrated by Paus *et al.*, increasing the affinity of the B cell epitopes on an TD antigen can drive the B cell response towards a TI-2 response [227]. Equally, altering the spatial density of the B cell epitopes on the same TD antigen can also promote a TI-2 response [227]. Clearly, the TI-2 response that FMDV induces is not conducive to the development of a long duration of immunity. Thus, by understanding the bovine B cell epitopes on the FMDV capsid, the capsid could be engineered to alter the B cell epitopes and promote a TD response in addition to the TI-2 that is currently induced.

The data presented in this thesis was used to underpin part of a Wellcome Trust strategic award that was successfully funded in May 2013. The grant is due to start in November 2013. The overarching aim of the project is to identify broadly neutralising FMDV-specific antibodies in cattle and in collaboration, with the Structural Biology group at The University of Oxford, identify the epitopes that are recognised by the antibodies. This will be achieved by administering sequential vaccinations with different serotypes of FMDV. The FMDV-specific ELIspot will then be used to pin-point the peak of the antigen-specific plasma cell response following each vaccination. Following the final sequential vaccination, the animals will undergo efferent lymphatic cannulation. The antigen-specific B cell response to all vaccine antigens will be monitored in efferent lymph and peripheral blood. The subscapular lymph node and also spleen will be sampled when the animal is euthanased. Deep sequencing will then be employed to interrogate both the heavy and light chain bovine immunoglobulin repertoire at the peak of the antigen-specific B cell response, following each vaccination. Deep sequencing will also be performed on the subscapular lymph node and spleen samples taken at the end of the study. Bioinformatic techniques will then be employed to identify immunoglobulin transcripts that are highly similar between the sampling points within the animal and comparisons between the animals. Using the bovine immunoglobulin expression technique discussed in section 6.2.2, any immunoglobulin transcripts of interest (i.e. occurrence at multiple time points) will be expressed and then the epitopes to which they bind will be mapped on the FMDV capsid.

The data presented in this thesis will underpin the development of novel FMDV vaccines. Increasing the duration of immunity achieved from FMDV vaccination will also result in improved control strategies against FMDV.

Appendix A

List of Publications

Published manuscripts:

- Grant CF, Lefevre EA, Carr B V, Prentice H, Gubbins S, Pollard AJ, Charreyre C, Charleston B: **Assessment of T-dependent and T-independent immune responses in cattle using a B cell ELISPOT assay**. *Vet Res* 2012,**43**:68. Highly accessed. **Impact Factor: 4.06**. **HIGHLY ACCESSED**

- Schley D, Tanaka RJ, Leungchavaphongse K, Shahrezaei V, Ward J, Grant C, Charleston B, Rhodes CJ: **Modelling the Influence of Foot-and-Mouth Disease Vaccine Antigen Stability and Dose on the Bovine Immune Response**. *PLoS One* 2012, **7**:e30435. **Impact factor: 4.09**.

Manuscripts in progress:

- 'Cattle exhibit limited variability in the Igλ repertoire.'

- 'Assessing the systemic adaptive immune response following vaccination and live-virus challenge with foot-and-mouth disease virus (FMDV).'

Appendix B

Bioinformatic scripts and procedures

The following scripts and procedures have been written by Owen Ball with input from me as to how the data should be visualised as the end result.

B.1 Python script to rank the bovine Ig trancript FASTA files

```
import os

#Set Variables
location = "/Users/owenball/Desktop/FMDC18/"

#Get List of Files in Directory
listing = os.listdir(location)

#Loop over Each File
for filename in listing:

    #Read ImportFile and Create OutputFile
    file = open(location + filename, "r")
    outputfile = open(location + filename + "_Ranked", "w")

    #Create List from File Rows
    rows = list(file)

    #Create Counter
    count = 0

    #Loop over Each row in File
    for row in rows:
```

```
        #Check to see if row is Header Row
        if row.find(">") != -1:

            #Increment Count for Each Header Row
            count += 1

            #String Transformations
            row = row.replace(" \n", "\n")
            row = row.replace(" ", "_")

            #Only add new Lines After the First Sequence
            row = row.replace(">", ">" + str(count) + "_")

        #Make no Changes to Sequence Rows
        else:
            row = row

        #Output Ranked File
        outputfile.writelines(row)
```

B.2 Python script to strip Gap4 related nomenclature from the sequence name

```
import os
import re

#Set Variables
location = "/home/clare/454_sequencing_bovine_IgG_FMDV/Python_script_
 to_rename_contig_files/"

#Get List of Files in Directory
listing = os.listdir(location)

#Loop over Each File
for filename in listing:

    #Read ImportFile and Create OutputFile
    file = open(location + filename, "r")
    outputfile = open(location + filename.rstrip(".fasta") + "_Renamed.fasta", "w")

    #Create List from File Rows
    rows = list(file)

    #Create Counter
    count = 0

    #Loop over Each row in File
    for row in rows:

        #Check to see if row is Header Row
        if row.find(">") != -1:
```

```
        #Increment Count for Each Header Row
        count += 1

        #String Transformations
        row = re.sub("\_OUT.+", "", row)

    #Make no Changes to Sequence Rows
    else:
        row = row

    #Output Ranked File
    outputfile.writelines(row)
```

B.3 Pentaho pipeline to extract IgG reads from MIRA assembly .caf files

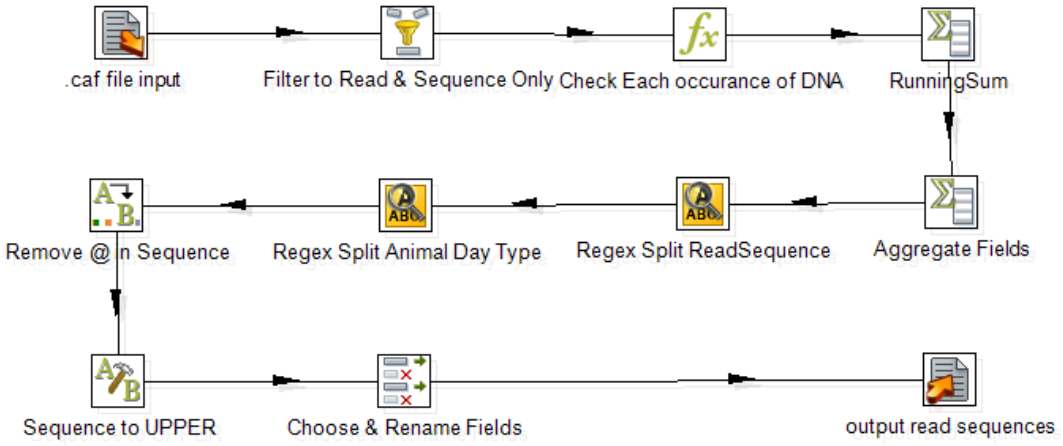


FIGURE B.1: Pentaho pipeline used to extract the read name and read sequence from the .caf generated by the MIRA assembly programme.

B.4 SQL server procedures

```
BEGIN
-- Uncomment & Declare Variables here for Testing
DECLARE @Animal VARCHAR(10)
DECLARE @Day INT
DECLARE @Type VARCHAR(4)
DECLARE @ComparisonDay INT

-- Set Variable Values
```

```
SELECT @Animal = 'FMDC16'
SELECT @Day = 4
SELECT @Type = 'PBMC'
SELECT @ComparisonDay = 7

-- Part 1 Analysis Code Starts Here:
-- Step 7: Join to return sequence data from reads
SELECT samples.*
                ,RA.read_sequence
FROM
(
-- Step 6: calculate contig_abundance for D7 and join to data
SELECT D4.*
,D7.contig_abundance as contig_abundance_@ComparisonDay
FROM
(
-- Step 5: Join to source tables for animal to return associated read_names,
 day and sample type
        SELECT finallkp.allsample_contig_name
                ,finallkp.allsample_read_name
                ,finallkp.contig_count as contig_count_@Day
                ,finallkp.contig_abundance as contig_abundance_@Day
                ,samples.read_name
                ,samples.read_day
                ,samples.type
        FROM (
-- Step 4: Join again to AllSamples table to return the allsample read names
        SELECT ALLSC.allsample_contig_name
                ,ALLSC.contig_count
                ,ALLSC.contig_abundance
                ,ALLS2.read_name AS allsample_read_name
        FROM (
-- Step 3: Join read data to AllSamples table to return 1 record for each
 allsample_contig_name along with contig count and abundance
        SELECT ALLS.contig_name AS allsample_contig_name
                ,MAX(reads.contig_count) AS contig_count
                ,MAX(reads.contig_abundance) AS contig_abundance
        FROM (
-- Step 2: Join count data to source table to get read names for each contig
        SELECT counts.contig_name
                ,counts.contig_count
                ,counts.contig_abundance
                ,A.read_name
        FROM (
-- Step 1: Calculate count and abundance for each contig in D4 ELMC
        SELECT contig_name
                ,count(contig_name) AS contig_count
                ,cast(count(contig_name) AS FLOAT) / cast((
        SELECT count(*) AS total_rows
        FROM sample.Animals
        WHERE animal = @Animal
        AND read_day = @Day
        AND [type] = @Type
                ) AS FLOAT) AS contig_abundance
        FROM sample.Animals
```

```
        WHERE animal = @Animal
        AND read_day = @Day
        AND [type] = @Type
        GROUP BY contig_name) counts
        INNER JOIN sample.Animals A ON counts.contig_name = A.contig_name
                ) reads
        INNER JOIN sample.AllSamples ALLS ON reads.read_name =
        ALLS.read_name
        GROUP BY ALLS.contig_name
                ) ALLSC
        INNER JOIN sample.AllSamples ALLS2 ON ALLSC.allsample_contig_name =
         ALLS2.contig_name
                ) finallkp
        INNER JOIN (
        SELECT *
        FROM sample.Animals
        WHERE animal = @Animal
                ) samples ON finallkp.allsample_read_name = samples.read_name
                ) D4
LEFT JOIN -- Changed from INNER to LEFT to return all read days
        (-- Day 7 Abundance by Read
        SELECT counts.contig_name
                ,counts.contig_count
                ,counts.contig_abundance
                ,A.read_name
        FROM (
        SELECT contig_name
                ,count(contig_name) AS contig_count
                ,cast(count(contig_name) AS FLOAT) / cast((
        SELECT count(*) AS total_rows
        FROM sample.Animals
        WHERE animal = @Animal
        AND read_day = @ComparisonDay
                ) AS FLOAT) AS contig_abundance
        FROM sample.Animals
        WHERE animal = @Animal
        AND read_day = @ComparisonDay
        GROUP BY contig_name) counts
        INNER JOIN sample.Animals A ON counts.contig_name = A.contig_name) D7

        ON D4.read_name = D7.read_name) samples

-- Using INNER JOIN here to return only matching data. Revert to LEFT to see
 everything
INNER JOIN sequence.Animals RA
ON samples.read_name = RA.read_name

-- Ordering by most abundant
ORDER BY samples.contig_count_@Day DESC, samples.allsample_contig_name

-- Part 2 Analysis Code Starts Here:
-- Step 7: Select Distinct
SELECT DISTINCT  @Animal animal_name
                                ,samples.contig_abundance_@Day
                                ,samples.contig_abundance_@ComparisonDay
```

```
FROM
(
-- Step 6: calculate contig_abundance for D7 and join to data
        SELECT D4.*
        ,D7.contig_abundance as contig_abundance_@ComparisonDay
        FROM
        (
-- Step 5: Join to source tables for animal to return associated read_names,
 day and sample type
        SELECT finallkp.allsample_contig_name
                ,finallkp.allsample_read_name
                ,finallkp.contig_count as contig_count_@Day
                ,finallkp.contig_abundance as contig_abundance_@Day
                ,samples.read_name
                ,samples.read_day
                ,samples.type
        FROM (
-- Step 4: Join again to AllSamples table to return the allsample read names
        SELECT ALLSC.allsample_contig_name
                ,ALLSC.contig_count
                ,ALLSC.contig_abundance
                ,ALLS2.read_name AS allsample_read_name
        FROM (
-- Step 3: Join read data to AllSamples table to return 1 record for each
 allsample_contig_name along with contig count and abundance
        SELECT ALLS.contig_name AS allsample_contig_name
                ,MAX(reads.contig_count) AS contig_count
                ,MAX(reads.contig_abundance) AS contig_abundance
        FROM (
-- Step 2: Join count data to source table to get read names for each contig
        SELECT counts.contig_name
                ,counts.contig_count
                ,counts.contig_abundance
                ,A.read_name
        FROM (
-- Step 1: Calculate count and abundance for each contig in D4 ELMC
        SELECT contig_name
                ,count(contig_name) AS contig_count
                ,cast(count(contig_name) AS FLOAT) / cast((
        SELECT count(*) AS total_rows
        FROM sample.Animals
        WHERE animal = @Animal
        AND read_day = @Day
        AND [type] = @Type
                ) AS FLOAT) AS contig_abundance
        FROM sample.Animals
        WHERE animal = @Animal
        AND read_day = @Day
        AND [type] = @Type
        GROUP BY contig_name) counts
        INNER JOIN sample.Animals A ON counts.contig_name = A.contig_name
                                    ) reads
        INNER JOIN sample.AllSamples ALLS ON reads.read_name = ALLS.read_name
        GROUP BY ALLS.contig_name
                                ) ALLSC
```

```
        INNER JOIN sample.AllSamples ALLS2 ON ALLSC.allsample_contig_name =
         ALLS2.contig_name
                        ) finallkp
        INNER JOIN (
        SELECT *
        FROM sample.Animals
        WHERE animal = @Animal
                ) samples ON finallkp.allsample_read_name = samples.read_name
                ) D4
        INNER JOIN (-- Day 7 Abundance by Read
        SELECT counts.contig_name
                ,counts.contig_count
                ,counts.contig_abundance
                ,A.read_name
        FROM (
        SELECT contig_name
                ,count(contig_name) AS contig_count
                ,cast(count(contig_name) AS FLOAT) / cast((
        SELECT count(*) AS total_rows
        FROM sample.Animals
        WHERE animal = @Animal
        AND read_day = @ComparisonDay
                        ) AS FLOAT) AS contig_abundance
        FROM sample.Animals
        WHERE animal = @Animal
        AND read_day = @ComparisonDay
        GROUP BY contig_name) counts
        INNER JOIN sample.Animals A ON counts.contig_name = A.contig_name) D7

        ON D4.read_name = D7.read_name) samples

-- Ordering by most abundant
ORDER BY samples.contig_abundance_@Day
 DESC,samples.contig_abundance_@ComparisonDay DESC

END
```

B.5 Pentho pipeline to extract Paratome identified CDRs from .txt files

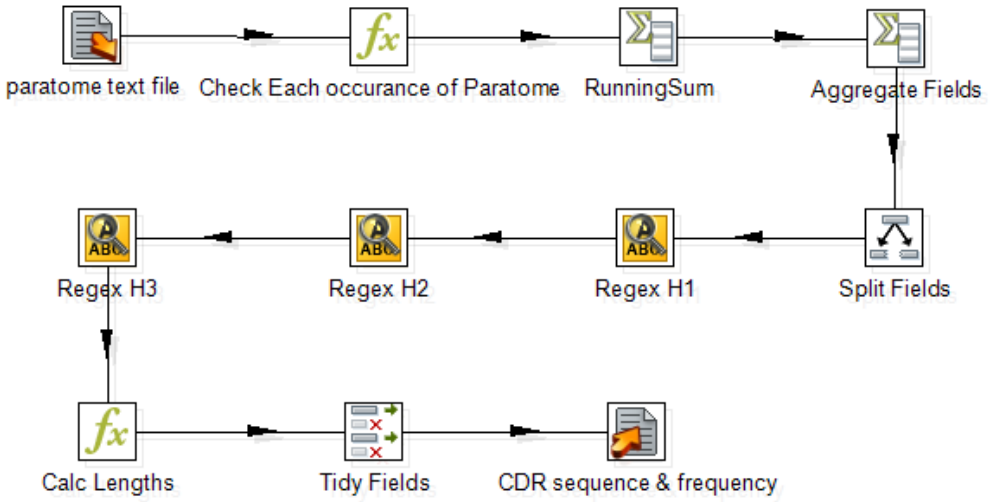


FIGURE B.2: Pentaho pipeline used to extract the predicted CDR1, 2 and 3 region sequences identified by the Paratome software.

Appendix C

Bovine immunoglobulin variable gene segment sequences

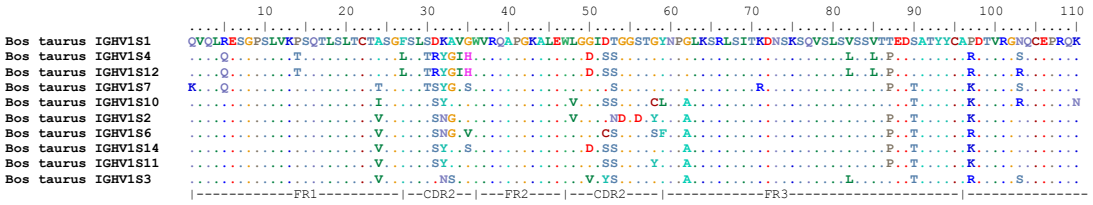


FIGURE C.1: Amino acid sequence alignment of the 10 functional bovine IGHV1 gene segments. There are 36 IGHV genes in the bovine genome, of which 10 are functional. The functional IGHV1 genes are highly similar with >80% sequence identity. Adapted from [260]

Bibliography

[1] D. Charron. Autologous white blood cell transfusion: toward a younger immunity. *Hum. Immunol.*, 68(10):805–812, 2007.

[2] K. Rajewsky. Clonal selection and learning in the antibody system. *Nature*, 381 (6585):751–758, 1996.

[3] S. Tonegawa. Somatic generation of antibody diversity. *Nature*, 302(5909):575–581, 1983.

[4] F.W. Alt and D. Baltimore. Joining of immunoglobulin heavy chain gene segments: implications from a chromosome with evidence of three D-JH fusions. *Proc. Natl. Acad. Sci. U. S. A.*, 79(13):4118–4122, 1982.

[5] J.P. Manis, Y. Gu, R. Lansford, E. Sonoda, R. Ferrini, L. Davidson, K. Rajewsky, and F.W. Alt. Ku70 is required for late B cell development and immunoglobulin heavy chain class switching. *J. Exp. Med.*, 187(12):2081–9, 1998.

[6] A. Agrawal, Q.M. Eastman, and D.G. Schatz. Transposition mediated by RAG1 and RAG2 and its implications for the evolution of the immune system. *Nature*, 394(6695):744–51, 1998.

[7] W.G. Kerr, M.D. Cooper, L. Feng, P.D. Burrows, and L.M. Hendershot. Mu heavy chains can associate with a pseudo-light chain complex (psi L) in human pre-B cell lines. *Int. Immunol.*, 1(4):355–61, 1989.

[8] M. Ogawa, E. ten Boekel, and F. Melchers. Identification of CD19(-)B220(+)c-Kit(+)Flt3/Flk-2(+)cells as early B lymphoid precursors before pre-B-I cells in juvenile mouse bone marrow. *Int. Immunol.*, 12(3):313–24, 2000.

[9] W.B. Graninger, P.L. Goldman, C.C. Morton, S.J. O'Brien, and S.J. Korsmeyer. The kappa-deleting element. Germline and rearranged, duplicated and dispersed forms. *J. Exp. Med.*, 167(2):488–501, 1988.

[10] P. Matthias and A.G. Rolink. Transcriptional networks in developing and mature B cells. *Nat. Rev. Immunol.*, 5(6):497–508, 2005.

[11] A. Ekman, T. Pessa-Morikawa, J. Liljavirta, M. Niku, and A. Iivanainen. B-cell development in bovine fetuses proceeds via a pre-B like cell in bone marrow and lymph nodes. *Dev. Comp. Immunol.*, 34(8):896–903, 2010.

[12] M.A. Hall and J.S. Lanchbury. Healthy human T-cell receptor beta-chain repertoire. Quantitative analysis and evidence for J beta-related effects on CDR3 structure and diversity. *Hum. Immunol.*, 43(3):207–218, 1995.

[13] C.J. Wu, A. Chillemi, E.P. Alyea, E. Orsini, D. Neuberg, R.J. Soiffer, and J. Ritz. Reconstitution of T-cell receptor repertoire diversity following T-cell depleted allogeneic bone marrow transplantation is related to hematopoietic chimerism. *Blood*, 95(1):352–359, 2000.

[14] M. Reth, J. Hombach, J. Wienands, K.S. Campbell, N. Chien, L.B. Justement, and J.C. Cambier. The B-cell antigen receptor complex. *Immunol. Today*, 12(6): 196–201, 1991.

[15] J.M. Dal Porto, S.B. Gauld, K.T. Merrell, D. Mills, A.E. Pugh-Bernard, and J. Cambier. B cell antigen receptor signaling 101. *Mol. Immunol.*, 41(6-7):599–613, 2004.

[16] R.A. Manz, A.E. Hauser, F. Hiepe, and A. Radbruch. Maintenance of serum antibody levels. *Annu. Rev. Immunol.*, 23:367–86, 2005.

[17] C.A. Janeway, P. Travers, and M. Walport. B-cell activation by armed helper T cells. In *Immunobiology: The Immune System in Health and Disease*, chapter 9, pages Section: 9–4. Garland Science, New York, 5th ed. edition, 2001. URL `http://www.ncbi.nlm.nih.gov/books/NBK27142//#A1192`.

[18] J.V. Ravetch and S. Bolland. IgG Fc receptors. *Annu. Rev. Immunol.*, 19:275–90, 2001.

[19] F. Nimmerjahn and J.V. Ravetch. Fc-receptors as regulators of immunity. *Adv. Immunol.*, 96:179–204, 2007.

[20] H.W. Schroeder Jr. and L. Cavacini. Structure and function of immunoglobulins. *J. Allergy Clin. Immunol.*, 125(2):S41–S52, 2010.

[21] D.M. Czajkowsky and Z. Shao. The human IgM pentamer is a mushroom-shaped molecule with a flexural bias. *Proc. Natl. Acad. Sci. U. S. A.*, 106(35):14960–5, 2009.

[22] M.F. Bachmann, T.M. Kundig, C.P. Kalberer, H. Hengartner, and R.M. Zinkernagel. How many specific B cells are needed to protect against a virus? *J. Immunol.*, 152(9):4235–4241, 1994.

[23] C. Snapper and W. Paul. Interferon-gamma and B cell stimulatory factor-1 reciprocally regulate Ig isotype production. *Science*, 236(4804):944–947, 1987.

[24] C.M. Snapper, T.M. McIntyre, R. Mandler, L.M. Pecanha, F.D. Finkelman, A. Lees, and J.J. Mond. Induction of IgG3 secretion by interferon gamma: a model for T cell-independent class switching in response to T cell-independent type 2 antigens. *J. Exp. Med.*, 175(5):1367–71, 1992.

[25] L. Hangartner, R.M. Zinkernagel, and H. Hengartner. Antiviral antibody responses: the two extremes of a wide spectrum. *Nat Rev Immunol*, 6(3):231–243, 2006.

[26] R. Geisberger, M. Lamers, and G. Achatz. The riddle of the dual expression of IgM and IgD. *Immunology*, 118(4):429–37, 2006.

[27] J.E. Butler. Antigen receptors, their immunomodulation and the immunoglobulin genes of cattle and swine. *Livest. Prod. Sci.*, 42(2-3):105–121, 1995.

[28] B. Earley, M. McGee, R.J. Fallon, N.J. Drennan, M. Murray, and J.A. Farrell. Serum immunoglobulin concentrations in suckled calves and dairy-herd calves. *Ir. J. Agric. Food Res.*, 39(3):401 – 7, 2000.

[29] H.P. Roost, M.F. Bachmann, A. Haag, U. Kalinke, V. Pliska, H. Hengartner, and R.M. Zinkernagel. Early high-affinity neutralizing anti-viral IgG responses without further overall improvements of affinity. *Proc. Natl. Acad. Sci. U. S. A.*, 92(5): 1257–1261, 1995.

[30] M.C. Outlaw and N.J. Dimmock. IgG neutralization of type A influenza viruses and the inhibition of the endosomal fusion stage of the infectious pathway in BHK cells. *Virology*, 195(2):413–421, 1993.

[31] P. Roben, J.P. Moore, M. Thali, J. Sodroski, C.F. Barbas, and D.R. Burton. Recognition properties of a panel of human recombinant Fab fragments to the CD4 binding site of gp120 that show differing abilities to neutralize human immunodeficiency virus type 1. *J. Virol.*, 68(8):4821–4828, 1994.

[32] M. Bajénoff, J.G. Egen, H. Qi, A.Y.C. Huang, F. Castellino, and R.N. Germain. Highways, byways and breadcrumbs: directing lymphocyte traffic in the lymph node. *Trends Immunol.*, 28(8):346–352, 2007.

[33] C. Park, S. Yoon, R.J. Armitage, and Y.S. Choi. Follicular dendritic cells produce IL-15 that enhances germinal center B cell proliferation in membrane-bound form. *J. Immunol.*, 173(11):6676–83, 2004.

[34] A.K. Szakal, M.H. Kosco, and J.G. Tew. Microanatomy of lymphoid tissue during humoral immune responses: structure function relationships. *Annu. Rev. Immunol.*, 7:91–109, 1989.

[35] C.T. Schnizlein, M.H. Kosco, A.K. Szakal, and J.G. Tew. Follicular dendritic cells in suspension: identification, enrichment, and initial characterization indicating immune complex trapping and lack of adherence and phagocytic activity. *J. Immunol.*, 134(3):1360–8, 1985.

[36] J.G. Tew, T.E. Mandel, and A.W. Burgess. Retention of intact HSA for prolonged periods in the popliteal lymph nodes of specifically immunized mice. *Cell. Immunol.*, 45(1):207–212, 1979.

[37] D. Qin, J. Wu, K.A. Vora, J.V. Ravetch, A.K. Szakal, T. Manser, and J.G. Tew. Fc gamma receptor IIB on follicular dendritic cells regulates the B cell recall response. *J. Immunol.*, 164(12):6268–6275, 2000.

[38] U.H. von Andrian and T.R. Mempel. Homing and cellular traffic in lymph nodes. *Nature Rev. Immunol.*, 3:867–878, 2003.

[39] M.D. Cahalan and I. Parker. Choreography of cell motility and interaction dynamics imaged by two-photon microscopy in lymphoid organs. *Annu. Rev. Immunol.*, 26:585–626, 2008.

[40] J.G. Cyster. Chemokines, sphingosine-1-phosphate, and cell migration in secondary lymphoid organs. *Annu. Rev. Immunol.*, 23:127–59, 2005.

[41] J.L. Gowans. Lymphocytes. *Harvey Lect.*, 64:87–119, 1968.

[42] M. Sixt, N. Kanazawa, M. Selg, T. Samson, G. Roos, D.P. Reinhardt, R. Pabst, M.B. Lutz, and L. Sorokin. The Conduit System Transports Soluble Antigens from the Afferent Lymph to Resident Dendritic Cells in the T Cell Area of the Lymph Node. *Immunity*, 22(1):19–29, 2005.

[43] M.J. Miller, S.H. Wei, I. Parker, and M.D. Cahalan. Two-photon imaging of lymphocyte motility and antigen response in intact lymph node. *Science*, 296 (5574):1869–1873, 2002.

[44] M. Miyasaka and T. Tanaka. Lymphocyte trafficking across high endothelial venules: dogmas and enigmas. *Nat. Rev. Immunol.*, 4(5):360–370, 2004.

[45] H. Qi, J.G. Egen, A.Y. Huang, and R.N. Germain. Extrafollicular activation of lymph node B cells by antigen-bearing dendritic cells. *Science*, 312(5780):1672–1676, 2006.

[46] J.G. Cyster. B cell follicles and antigen encounters of the third kind. *Nat. Immunol.*, 11(11):989–96, 2010.

[47] M. Bajenoff, S. Granjeaud, and S. Guerder. The strategy of T cell antigen-presenting cell encounter in antigen-draining lymph nodes revealed by imaging of initial T cell activation. *J. Exp. Med.*, 198:715–724, 2003.

[48] S. Mandala, R. Hajdu, J. Bergstrom, E. Quackenbush, J. Xie, J. Milligan, R. Thornton, G. Shei, D. Card, C. Keohane, M. Rosenbach, J. Hale, C.L. Lynch, K. Rupprecht, W. Parsons, and H. Rosen. Alteration of lymphocyte trafficking by sphingosine-1-phosphate receptor agonists. *Science*, 296(5566):346–9, 2002.

[49] S. Spiegel and S. Milstien. Sphingosine-1-phosphate: an enigmatic signalling lipid. *Nat. Rev. Mol. Cell Biol.*, 4(5):397–407, 2003.

[50] M. Matloubian, C.G. Lo, G. Cinamon, M.J. Lesneski, Y. Xu, V. Brinkmann, M.L. Allende, R.L. Proia, and J.G. Cyster. Lymphocyte egress from thymus and peripheral lymphoid organs is dependent on S1P receptor 1. *Nature*, 427(6972): 355–60, 2004.

[51] S.F. Gonzalez, L.A. Pitcher, T. Mempel, F. Schuerpf, and M.C. Carroll. B cell acquisition of antigen in vivo. *Curr. Opin. Immunol.*, 21(3):251–257, 2009.

[52] T.G. Phan, I. Grigorova, T. Okada, and J.G. Cyster. Subcapsular encounter and complement-dependent transport of immune complexes by lymph node B cells. *Nat. Immunol.*, 8(9):992–1000, 2007.

[53] F.D. Batista and N.E. Harwood. The who, how and where of antigen presentation to B cells. *Nat. Rev. Immunol.*, 9(1):15–27, 2009.

[54] E.R. Unanue, J.C. Cerottini, and M. Bedford. Persistence of antigen on the surface of macrophages. *Nature*, 222(5199):1193–1195, 1969.

[55] B.A. Heesters, P. Chatterjee, S.F. Kim, Y.A.and Gonzalez, T Kuligowski, M.P.and Kirchhausen, and M.C. Carroll. Endocytosis and Recycling of Immune Complexes by Follicular Dendritic Cells Enhances B Cell Antigen Binding and Activation. *Immunity*, 38(6):1164–75, 2013.

[56] J. Sáez de Guinoa, L. Barrio, M. Mellado, and Y.R. Carrasco. CXCL13/CXCR5 signaling enhances BCR-triggered B-cell activation by shaping cell dynamics. *Blood*, 118(6):1560–9, 2011.

[57] N.E. Harwood and F.D. Batista. Early events in B cell activation. *Annu. Rev. Immunol.*, 28:185–210, 2010.

[58] D. Depoil, M. Weber, B. Treanor, S.J. Fleire, Y.R. Carrasco, N.E. Harwood, and F.D. Batista. Early events of B cell activation by antigen. *Sci. Signaling*, 2(63): pt1, 2009.

[59] Y.R. Carrasco, S.J. Fleire, T. Cameron, M.L. Dustin, and F.D. Batista. LFA-1/ICAM-1 Interaction Lowers the Threshold of B Cell Activation by Facilitating B Cell Adhesion and Synapse Formation. *Immunity*, 20(5):589–599, 2004.

[60] M.I. Yuseff, A. Reversat, D. Lankar, J. Diaz, I. Fanget, P. Pierobon, V. Randrian, N. Larochette, F. Vascotto, C. Desdouets, B. Jauffred, Y. Bellaiche, S. Gasman, F. Darchen, C. Desnos, and A.M. Lennon-Duménil. Polarized secretion of lysosomes at the B cell synapse couples antigen extraction to processing and presentation. *Immunity*, 35(3):361–74, 2011.

[61] M.I. Yuseff, P. Pierobon, A. Reversat, and A.M. Lennon-Duménil. How B cells capture, process and present antigens: a crucial role for cell polarity. *Nat. Rev. Immunol.*, 13(7):475–486, 2013.

[62] X. Chen and P.E. Jensen. The expression of HLA-DO (H2-O) in B lymphocytes. *Immunol. Res.*, 29(1-3):19–28, 2004.

[63] F.D. Batista and M.S. Neuberger. Affinity dependence of the B cell response to antigen: a threshold, a ceiling, and the importance of off-rate. *Immunity*, 8(6): 751–9, 1998.

[64] T.O. Nashar and J.R. Drake. The pathway of antigen uptake and processing dictates MHC class II-mediated B cell survival and activation. *J. Immunol.*, 174 (3):1306–16, 2005.

[65] N.A. Mitchison. T-cell-B-cell cooperation. *Nat. Rev. Immunol.*, 4(4):308–12, 2004.

[66] K. Reif, E.H. Ekland, L. Ohl, H. Nakano, M. Lipp, R. Förster, and J.G. Cyster. Balanced responsiveness to chemoattractants from adjacent zones determines B-cell position. *Nature*, 416(6876):94–9, 2002.

[67] S. Duchez, M. Rodrigues, F. Bertrand, and S. Valitutti. Reciprocal polarization of T and B cells at the immunological synapse. *J. Immunol.*, 187(9):4571–80, 2011.

[68] T. Okada, M.J. Miller, I. Parker, M.F. Krummel, M. Neighbors, S.B. Hartley, A. O'Garra, M.D. Cahalan, and J.G. Cyster. Antigen-engaged B cells undergo chemotaxis toward the T zone and form motile conjugates with helper T cells. *PLoS Biol.*, 3(6):e150, 2005.

[69] W.J. Poo, L. Conrad, and C.A. Janeway. Receptor-directed focusing of lymphokine release by helper T cells. *Nature*, 332(6162):378–80, 1988.

[70] C.C. Goodnow, C.G. Vinuesa, K.L. Randall, F. Mackay, and R. Brink. Control systems and decision making for antibody production. *Nat. Immunol.*, 11(8):681–688, 2010.

[71] I.C. MacLennan, K.M. Toellner, A.F. Cunningham, K. Serre, D.M. Sze, E. Zuniga, M.C. Cook, and C.G. Vinuesa. Extrafollicular antibody responses. *Immunol. Rev.*, 194:8–18, 2003.

[72] A.F. Cunningham, F. Gaspal, K. Serre, E. Mohr, I.R. Henderson, A. Scott-Tucker, S.M. Kenny, M. Khan, K.M. Toellner, P.J.L. Lane, and I.C.M. MacLennan. Salmonella induces a switched antibody response without germinal centers that impedes the extracellular spread of infection. *J. Immunol.*, 178(10):6200–7, 2007.

[73] I.C. MacLennan. Germinal centers. *Annu. Rev. Immunol.*, 12:117–39, 1994.

[74] M.G. McHeyzer-Williams. B cells as effectors. *Curr. Opin. Immunol.*, 15(3):354–361, 2003.

[75] S. Crotty. The 1-1-1 fallacy. *Immunol. Rev.*, 247(1):133–42, 2012.

[76] M.A. Kroenke, D. Eto, M. Locci, M. Cho, T. Davidson, E.K. Haddad, and S. Crotty. Bcl6 and Maf cooperate to instruct human follicular helper CD4 T cell differentiation. *J. Immunol.*, 188(8):3734–44, 2012.

[77] Y.S. Choi, R. Kageyama, D. Eto, T.C. Escobar, R.J. Johnston, L. Monticelli, C. Lao, and S. Crotty. ICOS receptor instructs T follicular helper cell versus effector cell differentiation via induction of the transcriptional repressor Bcl6. *Immunity*, 34(6):932–46, 2011.

[78] J. Jacob, R. Kassir, and G. Kelsoe. In situ studies of the primary immune response to (4-hydroxy-3-nitrophenyl)acetyl. I. The architecture and dynamics of responding cell populations. *J. Exp. Med.*, 173(5):1165–1175, 1991.

[79] G.M. Griffiths, C. Berek, M. Kaartinen, and C. Milstein. Somatic mutation and the maturation of immune response to 2-phenyl oxazolone. *Nature*, 312(5991): 271–275, 1984.

[80] C.G. Vinuesa and J.G. Cyster. How T cells earn the follicular rite of passage. *Immunity*, 35(5):671–80, 2011.

[81] A. Brauninger, W. Yang, H.H. Wacker, K. Rajewsky, R. Kuppers, and M.L. Hansmann. B-cell development in progressively transformed germinal centers: similarities and differences compared with classical germinal centers and lymphocyte-predominant Hodgkin disease. *Blood*, 97(3):714–719, 2001.

[82] S.D. Wagner and M.S. Neuberger. Somatic hypermutation of immunoglobulin genes. *Annu. Rev. Immunol.*, 14:441–57, 1996.

[83] T. Dörner, S.J. Foster, N.L. Farner, and P.E. Lipsky. Somatic hypermutation of human immunoglobulin heavy chain genes: targeting of RGYW motifs on both DNA strands. *Eur. J. Immunol.*, 28(10):3384–96, 1998.

[84] C. Rada, M.R. Ehrenstein, M.S. Neuberger, and C. Milstein. Hot Spot Focusing of Somatic Hypermutation in MSH2-Deficient Mice Suggests Two Stages of Mutational Targeting. *Immunity*, 9(1):135–141, 1998.

[85] K. van Nierop and C. de Groot. Human follicular dendritic cells: function, origin and development. *Semin. Immunol.*, 14(4):251–257, 2002.

[86] A.E. Hauser, T. Junt, T.R. Mempel, M.W. Sneddon, S.H. Kleinstein, S.E. Henrickson, U.H. von Andrian, M.J. Shlomchik, and A.M. Haberman. Definition of germinal-center B cell migration in vivo reveals predominant intrazonal circulation patterns. *Immunity*, 26(5):655–67, 2007.

[87] Y. Zhang, M. Meyer-Hermann, L.A. George, M.T. Figge, M. Khan, M. Goodall, S.P. Young, A. Reynolds, F. Falciani, A. Waisman, C.A. Notley, M.R. Ehrenstein, M. Kosco-Vilbois, and K.M. Toellner. Germinal center B cells govern their own fate via antibody feedback. *J. Exp. Med.*, 210(3):457–464, 2013.

[88] J.Y. Bonnefoy, S. Henchoz, D. Hardie, M.J. Holder, and J. Gordon. A subset of anti-CD21 antibodies promote the rescue of germinal center B cells from apoptosis. *Eur. J. Immunol.*, 23(4):969–972, 1993.

[89] J. Choe and Y.S. Choi. IL-10 interrupts memory B cell expansion in the germinal center by inducing differentiation into plasma cells. *Eur. J. Immunol.*, 28(2):508–515, 1998.

[90] S.A. Camacho, M.H. Kosco-Vilbois, and C. Berek. The dynamic structure of the germinal center. *Immunol. Today*, 19(11):511–514, 1998.

[91] I. Yusuf, R. Kageyama, L. Monticelli, R.J. Johnston, D. Ditoro, K. Hansen, B. Barnett, and S. Crotty. Germinal center T follicular helper cell IL-4 production is dependent on signaling lymphocytic activation molecule receptor (CD150). *J. Immunol.*, 185(1):190–202, 2010.

[92] G.D. Victora, T.A. Schwickert, D.R. Fooksman, A.O. Kamphorst, M. Meyer-Hermann, M.L. Dustin, and M.C. Nussenzweig. Germinal center dynamics revealed by multiphoton microscopy with a photoactivatable fluorescent reporter. *Cell*, 143(4):592–605, 2010.

[93] D. Zotos, J.M. Coquet, Y. Zhang, A. Light, K. D'Costa, A. Kallies, L.M. Corcoran, D.I. Godfrey, K. Toellner, M.J. Smyth, S.L. Nutt, and D. Tarlinton. IL-21 regulates germinal center B cell differentiation and proliferation through a B cell-intrinsic mechanism. *J. Exp. Med.*, 207(2):365–78, 2010.

[94] K.L. Good-Jacobson and M.J. Shlomchik. Plasticity and heterogeneity in the generation of memory B cells and long-lived plasma cells: the influence of germinal center interactions and dynamics. *J. Immunol.*, 185(6):3117–25, 2010.

[95] C. Arpin, J. Dechanet, C. Van Kooten, P. Merville, G. Grouard, F. Briere, J. Banchereau, and Y.J. Liu. Generation of memory B cells and plasma cells in vitro. *Science*, 268(5211):720–722, 1995.

[96] M. Muramatsu, K. Kinoshita, S. Fagarasan, S. Yamada, Y. Shinkai, and T. Honjo. Class Switch Recombination and Hypermutation Require Activation-Induced Cytidine Deaminase (AID), a Potential RNA Editing Enzyme. *Cell*, 102(5):553–563, 2000.

[97] Z. Xu, H. Zan, E.J. Pone, T. Mai, and P. Casali. Immunoglobulin class-switch DNA recombination: induction, targeting and beyond. *Nat. Rev. Immunol.*, 12 (7):517–31, 2012.

[98] T.R. Mosmann, H. Cherwinski, M.W. Bond, M.A. Giedlin, and R.L. Coffman. Two types of murine helper T cell clone. I. Definition according to profiles of lymphokine activities and secreted proteins. *J. Immunol.*, 136(7):2348–57, 1986.

[99] E.J. Pearce, P. Caspar, J.M. Grzych, F.A. Lewis, and A. Sher. Downregulation of Th1 cytokine production accompanies induction of Th2 responses by a parasitic helminth, Schistosoma mansoni. *J. Exp. Med.*, 173(1):159–66, 1991.

[100] S.Q. Crome, A.Y. Wang, and M.K. Levings. Translational mini-review series on Th17 cells: function and regulation of human T helper 17 cells in health and disease. *Clin. Exp. Immunol.*, 159(2):109–19, 2010.

[101] M.S. Sundrud, S.M. Grill, D. Ni, K. Nagata, S.S. Alkan, A. Subramaniam, and D. Unutmaz. Genetic reprogramming of primary human T cells reveals functional plasticity in Th cell differentiation. *J. Immunol.*, 171(7):3542–9, 2003.

[102] Y. Maeda, H. Ohtsuka, M. Tomioka, and M. Oikawa. Effect of progesterone on Th1/Th2/Th17 and regulatory T cell-related genes in peripheral blood mononuclear cells during pregnancy in cows. *Vet. Res. Commun.*, 37(1):43–9, 2013.

[103] J. Zhang, F.W. Alt, and T. Honjo. Regulation of class switch recombination of the immunoglobulin heavy chain genes. In *Immunoglobulin Genes*, chapter 11, pages 235–265. Academic Press, London, 2nd ed. edition, 1995.

[104] F.D. Finkelman, J. Holmes, I.M. Katona, J.F. Urban, M.P. Beckmann, L.S. Park, K.A. Schooley, R.L. Coffman, T.R. Mosmann, and W.E. Paul. Lymphokine control of in vivo immunoglobulin isotype selection. *Annu. Rev. Immunol.*, 8:303–33, 1990.

[105] M. Muramatsu, H. Nagaoka, R. Shinkura, N.A. Begum, and T. Honjo. Discovery of activation-induced cytidine deaminase, the engraver of antibody memory. *Adv. Immunol.*, 94:1–36, 2007.

[106] U. Klein and R. Dalla-Favera. Germinal centres: role in B-cell physiology and malignancy. *Nat. Rev. Immunol.*, 8(1):22–33, 2008.

[107] S. Park, H. Zan, Z. Pal, J. Zhang, A. Al-Qahtani, E.J. Pone, Z. Xu, T. Mai, and P. Casali. HoxC4 binds to the promoter of the cytidine deaminase AID gene to induce AID expression, class-switch DNA recombination and somatic hypermutation. *Nat. Immunol.*, 10(5):540–50, 2009.

[108] E.J. Pone, J. Zhang, T. Mai, C.A. White, G. Li, J.K. Sakakura, P.J. Patel, A. Al-Qahtani, H. Zan, Z. Xu, and P. Casali. BCR-signalling synergizes with TLR-signalling for induction of AID and immunoglobulin class-switching through the non-canonical NF-κB pathway. *Nat. Commun.*, 3:767, 2012. ISSN 2041-1723.

[109] D.M. Tarlinton and K.G. Smith. Dissecting affinity maturation: a model explaining selection of antibody-forming cells and memory B cells in the germinal centre. *Immunol. Today*, 21(9):436–441, 2000.

[110] K.G. Smith, A. Light, G.J. Nossal, and D.M. Tarlinton. The extent of affinity maturation differs between the memory and antibody-forming cell compartments in the primary immune response. *EMBO J.*, 16(11):2996–3006, 1997.

[111] Y. Takahashi, H. Ohta, and T. Takemori. Fas is required for clonal selection in germinal centers and the subsequent establishment of the memory B cell repertoire. *Immunity*, 14(2):181–92, 2001.

[112] M.J. Shlomchik and F. Weisel. Germinal center selection and the development of memory B and plasma cells. *Immunol. Rev.*, 247(1):52–63, 2012.

[113] S.M. Anderson, L.G. Hannum, and M.J. Shlomchik. Memory B cell survival and function in the absence of secreted antibody and immune complexes on follicular dendritic cells. *J. Immunol.*, 176(8):4515–9, 2006.

[114] J.F. Fecteau, G. Côté, and S. Néron. A new memory CD27-IgG+ B cell population in peripheral blood expressing VH genes with low frequency of somatic mutation. *J. Immunol.*, 177(6):3728–36, 2006.

[115] D.C. Macallan, D.L. Wallace, Y. Zhang, H. Ghattas, B. Asquith, C. de Lara, A. Worth, G. Panayiotakopoulos, G.E. Griffin, D.F. Tough, and P.C.L. Beverley. B-cell kinetics in humans: rapid turnover of peripheral blood memory cells. *Blood*, 105(9):3633–40, 2005.

[116] E. Helmreich, M. Kern, and H.N. Eisen. The secretion of antibody by isolated lymph node cells. *J. Biol. Chem.*, 236:464–73, 1961.

[117] T. Hibi and H.M. Dosch. Limiting dilution analysis of the B cell compartment in human bone marrow. *Eur. J. Immunol.*, 16(2):139–45, 1986.

[118] J.J. Haaijman, H.R. Schuit, and W. Hijmans. Immunoglobulin-containing cells in different lymphoid organs of the CBA mouse during its life-span. *Immunology*, 32 (4):427–34, 1977.

[119] P. Vieira and K. Rajewsky. The half-lives of serum immunoglobulins in adult mice. *Eur. J. Immunol.*, 18(2):313–6, 1988.

[120] P.H. Brodeur and H.H. Wortis. Regulation of thymus-independent responses: unresponsiveness to a second challenge of TNP-Ficoll is mediated by hapten-specific antibodies. *J. Immunol.*, 125(4):1499–505, 1980.

[121] T.V. Obukhanych and M.C. Nussenzweig. T-independent type II immune responses generate memory B cells. *J. Exp. Med.*, 203(2):305–10, 2006.

[122] C.G. de Vinuesa, M.C. Cook, J. Ball, M. Drew, Y. Sunners, M. Cascalho, M. Wabl, G.G. Klaus, and I.C. MacLennan. Germinal centers without T cells. *J. Exp. Med.*, 191(3):485–94, 2000.

[123] S. Crotty, P. Felgner, H. Davies, J. Glidewell, L. Villarreal, and R. Ahmed. Cutting edge: long-term B cell memory in humans after smallpox vaccination. *J. Immunol.*, 171(10):4969–73, 2003.

[124] E.A. Lefevre, B.V. Carr, H. Prentice, and B. Charleston. A quantitative assessment of primary and secondary immune responses in cattle using a B cell ELISPOT assay. *Vet. Res.*, 40(1):3, 2009.

[125] Y. Aiba, K. Kometani, M. Hamadate, S. Moriyama, A. Sakaue-Sawano, M. Tomura, H. Luche, H.J. Fehling, R. Casellas, O. Kanagawa, A. Miyawaki, and T. Kurosaki. Preferential localization of IgG memory B cells adjacent to contracted germinal centers. *Proc. Natl. Acad. Sci. U. S. A.*, 107(27):12192–7, 2010.

[126] M.F. Bachmann, U.H. Rohrer, T.M. Kundig, K. Burki, H. Hengartner, and R.M. Zinkernagel. The influence of antigen organization on B cell responsiveness. *Science*, 262(5138):1448–1451, 1993.

[127] S.R. Brodeur, F. Angelini, L.B. Bacharier, A.M. Blom, E. Mizoguchi, H. Fujiwara, A. Plebani, L.D. Notarangelo, B. Dahlback, E. Tsitsikov, and R.S. Geha. C4b-binding protein (C4BP) activates B cells through the CD40 receptor. *Immunity*, 18(6):837–848, 2003.

[128] M.K. Slifka, M. Matloubian, and R. Ahmed. Bone marrow is a major site of long-term antibody production after acute viral infection. *J. Virol.*, 69(3):1895–1902, 1995.

[129] R.A. Manz, M. Löhning, G. Cassese, A. Thiel, and A. Radbruch. Survival of long-lived plasma cells is independent of antigen. *Int. Immunol.*, 10(11):1703–11, 1998.

[130] K. Tokoyoda, T. Egawa, T. Sugiyama, B.I. Choi, and T. Nagasawa. Cellular niches controlling B lymphocyte behavior within bone marrow during development. *Immunity*, 20(6):707–18, 2004.

[131] M.M. Kawano, K. Mihara, N. Huang, T. Tsujimoto, and A. Kuramoto. Differentiation of early plasma cells on bone marrow stromal cells requires interleukin-6 for escaping from apoptosis. *Blood*, 85(2):487–94, 1995.

[132] J.A. Brieva, E. Roldán, M.L. De la Sen, and C. Rodriguez. Human in vivo-induced spontaneous IgG-secreting cells from tonsil, blood and bone marrow exhibit different phenotype and functional level of maturation. *Immunology*, 72(4):580–3, 1991.

[133] R.A. Manz and A. Radbruch. Plasma cells for a lifetime? *Eur. J. Immunol.*, 32 (4):923–7, 2002.

[134] N.L. Bernasconi, E. Traggiai, and A. Lanzavecchia. Maintenance of serological memory by polyclonal activation of human memory B cells. *Science*, 298(5601): 2199–2202, 2002.

[135] T.E. Mandel, R.P. Phipps, A.P. Abbot, and J.G. Tew. Long-term antigen retention by dendritic cells in the popliteal lymph node of immunized mice. *Immunology*, 43(2):353–62, 1981.

[136] N. Juleff, M. Windsor, E. Reid, J. Seago, Z. Zhang, P. Monaghan, I.W. Morrison, and B. Charleston. Foot-and-mouth disease virus persists in the light zone of germinal centres. *PloS one*, 3(10):e3434, 2008.

[137] F. Mackay and P. Schneider. Cracking the BAFF code. *Nat. Rev. Immunol.*, 9(7): 491–502, 2009.

[138] K.A. Vora, L.C. Wang, S.P. Rao, Z.Y. Liu, G.R. Majeau, A.H. Cutler, P.S. Hochman, M.L. Scott, and S.L. Kalled. Cutting edge: germinal centers formed in the absence of B cell-activating factor belonging to the TNF family exhibit impaired maturation and function. *J. Immunol.*, 171(2):547–551, 2003.

[139] G.T. Mantchev, C.S. Cortesao, M. Rebrovich, M. Cascalho, and R.J. Bram. TACI is required for efficient plasma cell differentiation in response to T-independent type 2 antigens. *J. Immunol.*, 179(4):2282–2288, 2007.

[140] F. Mackay and P. Schneider. TACI, an enigmatic BAFF/APRIL receptor, with new unappreciated biochemical and biological properties. *Cytokine Growth Factor Rev.*, 19(3-4):263–276, 2008.

[141] M. Yang, H. Hase, D. Legarda-Addison, L. Varughese, B. Seed, and A.T. Ting. B Cell Maturation Antigen, the Receptor for a Proliferation-Inducing Ligand and B Cell-Activating Factor of the TNF Family, Induces Antigen Presentation in B Cells. *J. Immunol.*, 175(5):2814–2824, 2005.

[142] H. Hase, Y. Kanno, M. Kojima, K. Hasegawa, D. Sakurai, H. Kojima, N. Tsuchiya, K. Tokunaga, N. Masawa, M. Azuma, K. Okumura, and T. Kobata. BAFF/BLyS can potentiate B-cell selection with the B-cell coreceptor complex. *Blood*, 103(6): 2257–2265, 2004.

[143] F. Mackay, P. Schneider, P. Rennert, and J. Browning. BAFF AND APRIL: a tutorial on B cell survival. *Annu. Rev. Immunol.*, 21:231–264, 2003.

[144] M.B. Litinskiy, B. Nardelli, D.M. Hilbert, B. He, A. Schaffer, P. Casali, and A. Cerutti. DCs induce CD40-independent immunoglobulin class switching through BLyS and APRIL. *Nat. Immunol.*, 3(9):822–9, 2002.

[145] D. Allman and S. Pillai. Peripheral B cell subsets. *Curr. Opin. Immunol.*, 20(2): 149–157, 2008.

[146] C.A. Janeway and R. Medzhitov. Innate immune recognition. *Annu. Rev. Immunol.*, 20:197–216, 2002.

[147] F. Martin and J.F. Kearney. B1 cells: similarities and differences with other B cell subsets. *Curr. Opin. Immunol.*, 13(2):195–201, 2001.

[148] A. Cerutti, M. Cols, and I. Puga. Marginal zone B cells: virtues of innate-like antibody-producing lymphocytes. *Nat. Rev. Immunol.*, 13(2):118–32, 2013.

[149] J.C. Weill, S. Weller, and C.A. Reynaud. Human marginal zone B cells. *Annu. Rev. Immunol.*, 27:267–85, 2009.

[150] S. Weller, M.C. Braun, B.K. Tan, A. Rosenwald, C. Cordier, M.E. Conley, A. Plebani, D.S. Kumararatne, D. Bonnet, O. Tournilhac, G. Tchernia, B. Steiniger, L.M. Staudt, J.L. Casanova, C.A. Reynaud, and J.C. Weill. Human blood IgM "memory" B cells are circulating splenic marginal zone B cells harboring a prediversified immunoglobulin repertoire. *Blood*, 104(12):3647–54, 2004.

[151] M.A. Berkowska, G.J.A. Driessen, V. Bikos, C. Grosserichter-Wagener, K. Stamatopoulos, A. Cerutti, B. He, K. Biermann, J.F. Lange, M. van der Burg, J.J.M. van Dongen, and M.C. van Zelm. Human memory B cells originate from three distinct germinal center-dependent and -independent maturation pathways. *Blood*, 118(8):2150–8, 2011.

[152] L. Collins Kelley, E.A. Mahaffey, D.I. Bounous, D.F. Antczak, and R.L. Brooks. Detection of equine and bovine T- and B-lymphocytes in formalin-fixed paraffin-embedded tissues. *Vet. Immunol. Immunopathol.*, 57(3):187–200, 1997.

[153] J. Pega, D. Bucafusco, S. Di Giacomo, J.M. Schammas, D. Malacari, A.V. Capozzo, J. Arzt, C. Pérez-Beascoechea, E. Maradei, L.L. Rodríguez, M.V. Borca, and M. Pérez-Filgueira. Early adaptive immune responses in the respiratory tract of foot-and-mouth disease virus-infected cattle. *J. Virol.*, 87(5):2489–95, 2013.

[154] L. Genestier, M. Taillardet, P. Mondiere, H. Gheit, C. Bella, and T. Defrance. TLR agonists selectively promote terminal plasma cell differentiation of B cell subsets specialized in thymus-independent responses. *J. Immunol.*, 178(12):7779–86, 2007.

[155] K. Attanavanich and J.F. Kearney. Marginal zone, but not follicular B cells, are potent activators of naive CD4 T cells. *J. Immunol.*, 172(2):803–11, 2004.

[156] K.R. Alugupalli, J.M. Leong, R.T. Woodland, M. Muramatsu, T. Honjo, and R.M. Gerstein. B1b lymphocytes confer T cell-independent long-lasting immunity. *Immunity*, 21(3):379–90, 2004.

[157] K. Hayakawa, R.R. Hardy, and L.A. Herzenberg. Progenitors for Ly-1 B cells are distinct from progenitors for other B cells. *J. Exp. Med.*, 161(6):1554–68, 1985.

[158] C.G. Vinuesa and P.P. Chang. Innate B cell helpers reveal novel types of antibody responses. *Nat. Immunol.*, 14(2):119–126, 2013.

[159] D.A. Kaminski and J. Stavnezer. Enhanced IgA class switching in marginal zone and B1 B cells relative to follicular/B2 B cells. *J. Immunol.*, 177(9):6025–9, 2006.

[160] K.A. Fairfax, L.M. Corcoran, C. Pridans, N.D. Huntington, A. Kallies, S.L. Nutt, and D.M. Tarlinton. Different kinetics of blimp-1 induction in B cell subsets revealed by reporter gene. *J. Immunol.*, 178(7):4104–11, 2007.

[161] J.J. Mond, A. Lees, and C.M. Snapper. T cell-independent antigens type 2. *Annu. Rev. Immunol.*, 13:655–692, 1995.

[162] E.B. Jacobson, L.H. Caporale, and G.J. Thorbecke. Effect of thymus cell injections on germinal center formation in lymphoid tissues of nude (thymusless) mice. *Cell. Immunol.*, 13(3):416–430, 1974.

[163] R.K. Gershon and K. Kondo. Cell interactions in the induction of tolerance: the role of thymic lymphocytes. *Immunology*, 18(5):723–37, 1970.

[164] F.M.C. Gaspal, F.M. McConnell, M. Kim, D. Gray, M.H. Kosco-Vilbois, C.R. Raykundalia, M. Botto, and P.J.L. Lane. The generation of thymus-independent germinal centers depends on CD40 but not on CD154, the T cell-derived CD40-ligand. *Eur. J. Immunol.*, 36(7):1665–73, 2006.

[165] M.E.M. El Shikh, R.M. El Sayed, A.K. Szakal, and J.G. Tew. T-independent antibody responses to T-dependent antigens: a novel follicular dendritic cell-dependent activity. *J. Immunol.*, 182(6):3482–91, 2009.

[166] M. Feldmann and A. Easten. The relationship between antigenic structure and the requirement for thymus-derived cells in the immune response. *J Exp Med*, 134 (1):103–119, 1971.

[167] Q. Vos, A. Lees, Z.Q. Wu, C.M. Snapper, and J.J. Mond. B-cell activation by T-cell-independent type 2 antigens as an integral part of the humoral immune response to pathogenic microorganisms. *Immunol. Rev.*, 176:154–170, 2000.

[168] J.J. Mond, Q. Vos, A. Lees, and C.M. Snapper. T cell independent antigens. *Curr. Opin. Immunol.*, 7(3):349–354, 1995.

[169] E.E. Adderson. Antibody repertoires in infants and adults: effects of T-independent and T-dependent immunizations. *Springer Semin. Immunopathol.*, 23(4):387–403, 2001.

[170] J.L. Marshall, Y. Zhang, L. Pallan, M. Hsu, M. Khan, A.F. Cunningham, I.C.M. MacLennan, and K. Toellner. Early B blasts acquire a capacity for Ig class switch recombination that is lost as they become plasmablasts. *Eur. J. Immunol.*, 41(12): 3506–12, 2011.

[171] D.F. Kelly, M.D. Snape, E.A. Clutterbuck, S. Green, C. Snowden, L. Diggle, L.M. Yu, A. Borkowski, E.R. Moxon, and A.J. Pollard. CRM197-conjugated serogroup C meningococcal capsular polysaccharide, but not the native polysaccharide, induces persistent antigen-specific memory B cells. *Blood*, 108(8):2642–2647, 2006.

[172] A.J. Pollard, K.P. Perrett, and P.C. Beverley. Maintaining protection against invasive bacteria with protein-polysaccharide conjugate vaccines. *Nat. Rev. Immunol.*, 9(3):213–220, 2009.

[173] F.Y. Avci, X. Li, M. Tsuji, and D.L. Kasper. A mechanism for glycoconjugate vaccine activation of the adaptive immune system and its implications for vaccine design. *Nat. Med.*, 17(12):1602–9, 2011.

[174] K.E. Brehm, N. Kumar, H.H. Thulke, and B. Haas. High potency vaccines induce protection against heterologous challenge with foot-and-mouth disease virus. *Vaccine*, 26(13):1681–1687, 2008.

[175] G.J. Belsham, T. Jackson, D. Paton, and B. Charleston. *Foot-and-Mouth disease*. John Wiley & Sons, Chichester, 2009.

[176] J.S. Salt. The carrier state in foot and mouth disease–an immunological review. *Br. Vet. J.*, 149(3):207–23, 1993.

[177] B. Dransfield. Foot-and-mouth disease virus - influentialpoints critique, `http://influentialpoints.com/Gallery/Foot-and-mouth_disease_virus.htm`, 2012. Last visited on 19/05/2013.

[178] H.G. Bahnemann. Binary ethylenimine as an inactivant for foot-and-mouth disease virus and its application for vaccine production. *Arch. Virol.*, 47(1):47–56, 1975.

[179] T.R. Doel. Natural and vaccine-induced immunity to foot and mouth disease: the prospects for improved vaccines. *Revue Scientifique et Technique de l'OIE*, 15(3): 883–911, 1996.

[180] Vaccinum Aphtharum Epizooticarium Inactivatum Ad Ruminantes. Foot-and-mouth disease (ruminants) vaccine (inactivated). *European Pharmacopoeia (Veterinary)*, page Monograph 0063, 1993.

[181] M.J. Grubman, M.P. Moraes, F.D.S. Segundo, L. Pena, and T. de los Santos. Evading the host immune response: how foot-and-mouth disease virus has become an effective pathogen. *FEMS Immunol. Med. Microbiol.*, 53(1):8–17, 2008.

[182] B.W. Mahy. *Foot and mouth disease virus*, volume 288. Springer, New York, 2005.

[183] M.J. Grubman and B. Baxt. Foot-and-mouth disease. *Clin. Microbiol. Rev.*, 17 (2):465–493, 2004.

[184] E. Gasteiger, A. Gattiker, C. Hoogland, I. Ivanyi, R.D. Appel, and A. Bairoch. ExPASy: The proteomics server for in-depth protein knowledge and analysis. *Nucleic Acids Res.*, 31(13):3784–3788, 2003.

[185] N.J. Knowles and A.R. Samuel. Molecular epidemiology of foot-and-mouth disease virus. *Virus Res.*, 91(1):65–80, 2003.

[186] OIE and FAO. Annual OIE/FAO FMD Reference Laboratory Network Report. *Annual OIE/FAO network reports*, 2008.

[187] R.P. Kitching. A recent history of foot-and-mouth disease. *J. Comp. Pathol.*, 118 (2):89–108, 1998.

[188] D.J. Paton, K.J. Sumption, and B. Charleston. Options for control of foot-and-mouth disease: knowledge, capability and policy. *Philos. Trans. R. Soc. Lond. B. Biol. Sci.*, 364(1530):2657–2667, 2009.

[189] V. O'Donnell, J.M. Pacheco, D. Gregg, and B. Baxt. Analysis of foot-and-mouth disease virus integrin receptor expression in tissues from naive and infected cattle. *J. Comp. Pathol.*, 141(2-3):98–112, 2009.

[190] A. Berinstein, M. Roivainen, T. Hovi, P.W. Mason, and B. Baxt. Antibodies to the Vitronectin Receptor (Integrin Alpha(V)Beta(3)) Inhibit Binding and Infection of Foot-and-Mouth-Disease Virus to Cultured-Cells. *J. Virol.*, 69(4):2664–2666, 1995.

[191] S. Berryman, S. Clark, P. Monaghan, and T. Jackson. Early events in integrin alphavbeta6-mediated cell entry of foot-and-mouth disease virus. *J. Virol.*, 79(13): 8519–34, 2005.

[192] R. Kühn, N. Luz, and E. Beck. Functional analysis of the internal translation initiation site of foot-and-mouth disease virus. *J. Virol.*, 64(10):4625–31, 1990.

[193] M.A. Devaney, V.N. Vakharia, R.E. Lloyd, E. Ehrenfeld, and M.J. Grubman. Leader protein of foot-and-mouth disease virus is required for cleavage of the p220 component of the cap-binding protein complex. *J. Virol.*, 62(11):4407–4409, 1988.

[194] T.R. Doel and W.K.T. Chong. Comparative immunogenicity of 146S, 75S and 12S particles of foot-and-mouth disease virus. *Arch. Virol.*, 73(2):185–191, 1982.

[195] T.R. Doel and P.J. Baccarini. Thermal stability of foot-and-mouth disease virus. *Arch. Virol.*, 70(1):21–32, 1981.

[196] P. Auge de Mello, I. Gomes, and H.G. Bahnemann. The Vaccination of young cattle with an oil adjuvant foot-and-mouth disease vaccine. *Boletin del centro panamericano de fiebre aftosa*, 55:9, 1989.

[197] M.V. Borca, F.M. Fernández, A.M. Sadir, M. Braun, and A.A. Schudel. Immune response to foot-and-mouth disease virus in a murine experimental model: effective thymus-independent primary and secondary reaction. *Immunology*, 59(2):261–7, 1986.

[198] N. Juleff, M. Windsor, E.A. Lefevre, S. Gubbins, P. Hamblin, E. Reid, K. McLaughlin, P.C. Beverley, I.W. Morrison, and B. Charleston. Foot-and-mouth disease virus can induce a specific and rapid CD4+ T-cell-independent neutralizing and isotype class-switched antibody response in naive cattle. *J. Virol.*, 83(8): 3626–3636, 2009.

[199] B.V. Carr, E.A. Lefevre, M.A. Windsor, C. Inghese, S. Gubbins, H. Prentice, N.D. Juleff, and B. Charleston. CD4+ T-cell responses to foot-and-mouth disease virus in vaccinated cattle. *J. Gen. Virol.*, 94:97–107, 2013.

[200] G.A. Mayr, J. Chinsangaram, and M.J. Grubman. Development of replication-defective adenovirus serotype 5 containing the capsid and 3C protease coding regions of foot-and-mouth disease virus as a vaccine candidate. *Virology*, 263(2): 496–506, 1999.

[201] G.A. Mayr, V. O'Donnell, J. Chinsangaram, P.W. Mason, and M.J. Grubman. Immune responses and protection against foot-and-mouth disease virus (FMDV) challenge in swine vaccinated with adenovirus-FMDV constructs. *Vaccine*, 19(15-16):2152–62, 2001.

[202] M.P. Moraes, G.A. Mayr, P.W. Mason, and M.J. Grubman. Early protection against homologous challenge after a single dose of replication-defective human adenovirus type 5 expressing capsid proteins of foot-and-mouth disease virus (FMDV) strain A24. *Vaccine*, 20(11-12):1631–9, 2002.

[203] J.M. Pacheco, M.C.S. Brum, M.P. Moraes, W.T. Golde, and M.J. Grubman. Rapid protection of cattle from direct challenge with foot-and-mouth disease virus (FMDV) by a single inoculation with an adenovirus-vectored FMDV subunit vaccine. *Virology*, 337(2):205–9, 2005.

[204] S. Uddowla, J. Hollister, J.M. Pacheco, L.L. Rodriguez, and E. Rieder. A safe foot-and-mouth disease vaccine platform with two negative markers for differentiating infected from vaccinated animals. *Journal of virology*, 86(21):11675–85, 2012.

[205] O. Taboga, C. Tami, E. Carrillo, J.I. Núñez, A. Rodríguez, J.C. Saíz, E. Blanco, M.L. Valero, X. Roig, J.A. Camarero, D. Andreu, M.G. Mateu, E. Giralt, E. Domingo, F. Sobrino, and E.L. Palma. A large-scale evaluation of peptide vaccines against foot-and-mouth disease: lack of solid protection in cattle and isolation of escape mutants. *J. Virol.*, 71(4):2606–14, 1997.

[206] C.Y. Wang and A.M. Walfield. Site-specific peptide vaccines for immunotherapy and immunization against chronic diseases, cancer, infectious diseases, and for veterinary applications. *Vaccine*, 23(17-18):2049–56, 2005.

[207] L.L. Rodriguez, J. Barrera, E. Kramer, J. Lubroth, F. Brown, and W.T. Golde. A synthetic peptide containing the consensus sequence of the G-H loop region of foot-and-mouth disease virus type-O VP1 and a promiscuous T-helper epitope induces peptide-specific antibodies but fails to protect cattle against viral challenge. *Vaccine*, 21(25-26):3751–6, 2003.

[208] A. Beignon, F. Brown, P. Eftekhari, E. Kramer, J. Briand, S. Muller, and C.D. Partidos. A peptide vaccine administered transcutaneously together with cholera toxin elicits potent neutralising anti-FMDV antibody responses. *Vet. Immunol. Immunopathol.*, 104(3-4):273–80, 2005.

[209] C. Cubillos, B.G. de la Torre, A. Jakab, G. Clementi, E. Borrás, J. Bárcena, D. Andreu, F. Sobrino, and E. Blanco. Enhanced mucosal immunoglobulin A response and solid protection against foot-and-mouth disease virus challenge induced by a novel dendrimeric peptide. *J. Virol.*, 82(14):7223–30, 2008.

[210] C. Porta, X. Xu, S. Loureiro, S. Paramasivam, J. Ren, T. Al-Khalil, A. Burman, T. Jackson, G.J. Belsham, S. Curry, G.P. Lomonossoff, S. Parida, D. Paton, Y. Li, G. Wilsden, N. Ferris, R. Owens, A. Kotecha, E. Fry, D.I. Stuart, B. Charleston, and I.M. Jones. Efficient production of foot-and-mouth disease virus empty capsids in insect cells following down regulation of 3C protease activity. *J. Virol. Methods*, 187(2):406–12, 2013.

[211] C. Porta, A. Kotecha, A. Burman, T. Jackson, J. Ren, S. Loureiro, I.M. Jones, E.E. Fry, D.I. Stuart, and B. Charleston. Rational engineering of recombinant picornavirus capsids to produce safe, protective vaccine antigen. *PLoS Pathog.*, 9 (3):e1003255, 2013.

[212] M.F. Bachmann and R. M. Zinkernagel. Neutralizing antiviral B cell responses. *Annu. Rev. Immunol.*, 15:235–70, 1997.

[213] R. Acharya, E. Fry, D. Stuart, G. Fox, D. Rowlands, and F. Brown. The three-dimensional structure of foot-and-mouth disease virus at 2.9 A resolution. *Nature*, 337(6209):709–16, 1989.

[214] J.L. Halliley, S. Kyu, J.J. Kobie, E.E. Walsh, A.R. Falsey, T.D. Randall, J. Treanor, C. Feng, I. Sanz, and F.E. Lee. Peak frequencies of circulating human influenza-specific antibody secreting cells correlate with serum antibody response after immunization. *Vaccine*, 28(20):3582–3587, 2010.

[215] F.E. Lee, A.R. Falsey, J.L. Halliley, I. Sanz, and E.E. Walsh. Circulating antibody-secreting cells during acute respiratory syncytial virus infection in adults. *J. Infect. Dis.*, 202(11):1659–1666, 2010.

[216] K. Fink, N. Manjarrez-Orduño, A. Schildknecht, J. Weber, B.M. Senn, R.M. Zinkernagel, and H. Hengartner. B cell activation state-governed formation of germinal centers following viral infection. *J. Immunol.*, 179(9):5877–5885, 2007.

[217] K. Trautwein. Maul- und Klauenseuche. In W. Weichardt, editor, *Ergebnisse der Hygiene Bakteriologie Immunitätsforschung und experimentellen Therapie*, pages 561–696. Springer, Berlin, 1929.

[218] C.F.J. Grant, E.A. Lefevre, B.V Carr, H. Prentice, S. Gubbins, A.J. Pollard, C. Charreyre, and B. Charleston. Assessment of T-dependent and T-independent immune responses in cattle using a B cell ELISPOT assay. *Vet. Res.*, 43(1):68, 2012.

[219] R. Kitching, P. Barnett, D. Paton, and D. Mackay. *Foot and Mouth Disease*. O.I.E., Paris, 6th edition, 2008.

[220] L.J. Reed and H. Muench. A simple method of estimating fifty per cent endpoints. *Am. J. Epidemiol.*, 27(3):493–497, 1938.

[221] W.B. Martin and W.G. Chapman. The tissue culture colour test for assaying the virus and neutralizing antibody of foot and mouth disease and its application to the measurement of immunity in cattle. *Res. Vet. Sci.*, 2:53 – 61, 1961.

[222] C. Hamblin, I.T. Barnett, and R.S. Hedger. A new enzyme-linked immunosorbent assay (ELISA) for the detection of antibodies against foot-and-mouth disease virus. I. Development and method of ELISA. *J. Immunol. Methods*, 93(1):115–21, 1986.

[223] C. Hamblin, I.T. Barnett, and J.R. Crowther. A new enzyme-linked immunosorbent assay (ELISA) for the detection of antibodies against foot-and-mouth disease virus. II. Application. *J. Immunol. Methods*, 93(1):123–129, 1986.

[224] K.J. Sorensen, K.G. Madsen, E.S. Madsen, J.S. Salt, J. Nqindi, and D.K.. Mackay. Differentiation of infection from vaccination in foot-and-mouth disease by the detection of antibodies to the non-structural proteins 3D, 3AB and 3ABC in ELISA using antigens expressed in baculovirus. *Arch. Virol.*, 148:1461 – 1476, 1998.

[225] R. Agostino. In *Goodness-of-fit techniques*, volume 68, chapter 9 - Tests for the normal distribution, pages 367 – 413. M. Dekker, New York, 1986.

[226] J. Wrammert, K. Smith, J. Miller, W.A. Langley, K. Kokko, C. Larsen, N.Y. Zheng, I. Mays, L. Garman, C. Helms, J. James, G.M. Air, J.D. Capra, R. Ahmed, and P.C. Wilson. Rapid cloning of high-affinity human monoclonal antibodies against influenza virus. *Nature*, 453(7195):667–71, 2008.

[227] D. Paus, T.G. Phan, T.D. Chan, S. Gardam, A. Basten, and R. Brink. Antigen recognition strength regulates the choice between extrafollicular plasma cell and germinal center B cell differentiation. *J. Exp. Med.*, 203(4):1081–91, 2006.

[228] J. Wrammert, D. Koutsonanos, G. Li, S. Edupuganti, J. Sui, M. Morrissey, M. McCausland, I. Skountzou, M. Hornig, W.I. Lipkin, A. Mehta, B. Razavi, C. Del Rio, N. Zheng, J. Lee, M. Huang, Z. Ali, K. Kaur, S. Andrews, R.R. Amara, Y. Wang, S.R. Das, C.D. O'Donnell, J.W. Yewdell, K. Subbarao, W.A. Marasco, M.J. Mulligan, R. Compans, R. Ahmed, and P.C. Wilson. Broadly cross-reactive antibodies dominate the human B cell response against 2009 pandemic H1N1 influenza virus infection. *J. Exp. Med.*, 208(1):181–93, 2011.

[229] D. Finke, F. Baribaud, H. Diggelmann, and H. Acha-Orbea. Extrafollicular plasmablast B cells play a key role in carrying retroviral infection to peripheral organs. *J. Immunol.*, 166(10):6266–75, 2001.

[230] T. Nieminen, J. Eskola, and H. Käyhty. Pneumococcal conjugate vaccination in adults: circulating antibody secreting cell response and humoral antibody responses in saliva and in serum. *Vaccine*, 16(6):630–6, 1998.

[231] N. Baumgarth. How specific is too specific? B-cell responses to viral infections reveal the importance of breadth over depth. *Immunol. Rev.*, 255(1):82–94, 2013.

[232] T. Fehr, M.F. Bachmann, H. Bluethmann, H. Kikutani, H. Hengartner, and R.M. Zinkernagel. T-independent activation of B cells by vesicular stomatitis virus: no evidence for the need of a second signal. *Cell. Immunol.*, 168(2):184–92, 1996.

[233] B.O. Lee, J. Rangel-Moreno, J.E. Moyron-Quiroz, L. Hartson, M. Makris, F. Sprague, F.E. Lund, and T.D. Randall. CD4 T cell-independent antibody response promotes resolution of primary influenza infection and helps to prevent reinfection. *J. Immunol.*, 175(9):5827–38, 2005.

[234] M. Mamani-Matsuda, A. Cosma, S. Weller, A. Faili, C. Staib, L. Garçon, O. Hermine, O. Beyne-Rauzy, C. Fieschi, J. Pers, N. Arakelyan, B. Varet, A. Sauvanet, A. Berger, F. Paye, J. Andrieu, M. Michel, B. Godeau, P. Buffet, C. Reynaud, and J. Weill. The human spleen is a major reservoir for long-lived vaccinia virus-specific memory B cells. *Blood*, 111(9):4653–9, 2008.

[235] F. Capolunghi, S. Cascioli, E. Giorda, M.M. Rosado, A. Plebani, C. Auriti, G. Seganti, R. Zuntini, S. Ferrari, M. Cagliuso, I. Quinti, and R. Carsetti. CpG drives human transitional B cells to terminal differentiation and production of natural antibodies. *J. Immunol.*, 180(2):800–8, 2008.

[236] J.C. Hope, C.J. Howard, H. Prentice, and B. Charleston. Isolation and purification of afferent lymph dendritic cells that drain the skin of cattle. *Nat. Protoc.*, 1(2): 982–7, 2006.

[237] T. Kyaw. Lymphatic system and defense mechanism, `http://umkcarnivores3.files.wordpress.com/2012/03/l-6-lymphatic-system.pptx`, 2012. Last visited on 16/05/2013. Last visited on 16/05/2013.

[238] S. Pyne and N.J. Pyne. Sphingosine 1-phosphate signalling in mammalian cells. *Biochem. J.*, 349(2):385–402, 2000.

[239] M.R. Neeland, E.N.T. Meeusen, and M.J. de Veer. Afferent lymphatic cannulation as a model system to study innate immune responses to infection and vaccination. *Vet. Immunol. Immunopathol.*, 2013.

[240] H.H. Yen, J.L. Wee, K.J. Snibson, and J.P. Scheerlinck. Thoracic duct cannulation without thoracotomy in sheep: a method for accessing efferent lymph from the lung. *Vet. Immunol. Immunopathol.*, 129(1-2):76–81, 2009.

[241] C. Pugh. Characterization of nonlymphoid cells derived from rat peripheral lymph. *J. Exp. Med.*, 157(6):1758–1779, 1983.

[242] C.J. Howard, W.I. Morrison, A. Bensaid, W. Davis, L. Eskra, J. Gerdes, M. Hadam, D. Hurley, W. Leibold, J.J. Letesson, et al. Summary of workshop findings for leukocyte antigens of cattle. *Vet. Immunol. Immunopathol.*, 27(1): 21–27, 1991.

[243] H. Clevers, N.D. MacHugh, A. Bensaid, S. Dunlap, C.L. Baldwin, A. Kaushal, K. Iams, C.J. Howard, and W.I. Morrison. Identification of a bovine surface antigen uniquely expressed on CD4-CD8- T cell receptor gamma/delta+ T lymphocytes. *Eur. J. Immunol.*, 20(4):809–17, 1990.

[244] J. Naessens, J. Newson, N. McHugh, C.J. Howard, K. Parsons, and B. Jones. Characterization of a bovine leucocyte differentiation antigen of 145,000 mw restricted to b lymphocytes. *Immunology*, 69(4):525, 1990.

[245] G. Splitter and W.I. Morrison. Antigens expressed predominantly on monocytes and granulocytes: identification of bovine CD11b and CD11c. *Vet. Immunol. Immunopathol.*, 27(1):87–90, 1991.

[246] J.G. Hall and B. Morris. The immediate effect of antigens on the cell output of a lymph node. *Br. J. Exp. Pathol.*, 46(4):450–4, 1965.

[247] I. McConnell and J. Hopkins. Lymphocyte traffic through antigen-stimulated lymph nodes. I. Complement activation within lymph nodes initiates cell shutdown. *Immunology*, 42(2):217–23, 1981.

[248] K. Kabashima, N.M. Haynes, Y. Xu, S.L. Nutt, M.L. Allende, R.L. Proia, and J.G. Cyster. Plasma cell S1P1 expression determines secondary lymphoid organ retention versus bone marrow tropism. *J. Exp. Med.*, 203(12):2683–90, 2006.

[249] E. Guzman, S. Price, H. Poulsom, and J. Hope. Bovine $\gamma\delta$ T cells: Cells with multiple functions and important roles in immunity. *Vet. Immunol. Immunopathol.*, 148(1):161–167, 2012.

[250] M. Bonneville, R.L. O'Brien, and W.K. Born. Gammadelta T cell effector functions: a blend of innate programming and acquired plasticity. *Nat. Rev. Immunol.*, 10(7):467–78, 2010.

[251] M. Eberl, G.W. Roberts, S. Meuter, J.D. Williams, N. Topley, and B. Moser. A rapid crosstalk of human gammadelta T cells and monocytes drives the acute inflammation in bacterial infections. *PLoS pathogens*, 5(2):e1000308, 2009.

[252] N. Wittenbrink, A. Klein, A.A Weiser, J. Schuchhardt, and M. Or-Guil. Is there a typical germinal center? A large-scale immunohistological study on the cellular composition of germinal centers during the hapten-carrier-driven primary immune response in mice. *J. Immunol.*, 187(12):6185–96, 2011.

[253] T. Hosokawa. Studies on B-cell memory. II. T-cell independent antigen can induce B-cell memory. *Immunology*, 38(2):291–9, 1979.

[254] H. Toyama, S. Okada, M. Hatano, Y. Takahashi, N. Takeda, H. Ichii, T. Takemori, Y. Kuroda, and T. Tokuhisa. Memory B cells without somatic hypermutation are generated from Bcl6-deficient B cells. *Immunity*, 17(3):329–39, 2002.

[255] S. Fagarasan, K. Kinoshita, M. Muramatsu, K. Ikuta, and T. Honjo. In situ class switching and differentiation to IgA-producing cells in the gut lamina propria. *Nature*, 413(6856):639–43, 2001.

[256] P. Bergqvist, E. Gärdby, A. Stensson, M. Bemark, and N.Y. Lycke. Gut IgA class switch recombination in the absence of CD40 does not occur in the lamina propria and is independent of germinal centers. *J. Immunol.*, 177(11):7772–83, 2006.

[257] D.D. Eason, J.P. Cannon, R.N. Haire, J.P. Rast, D.A. Ostrov, and G.W. Litman. Mechanisms of antigen receptor evolution. *Semin. Immunol.*, 16(4):215–226, 2004.

[258] M. Lefranc, V. Giudicelli, C. Ginestoux, J. Jabado-Michaloud, G. Folch, F. Bellahcene, Y. Wu, E. Gemrot, X. Brochet, J. Lane, L. Regnier, F. Ehrenmann, G. Lefranc, and P. Duroux. IMGT, the international ImMunoGeneTics information system. *Nucleic Acids Res.*, 37(Database issue):D1006–12, 2009.

[259] A. Ekman, M. Niku, J. Liljavirta, and A. Iivanainen. Bos taurus genome sequence reveals the assortment of immunoglobulin and surrogate light chain genes in domestic cattle. *BMC immunol.*, 10(1):22, 2009.

[260] M. Niku, J. Liljavirta, K. Durkin, E. Schroderus, and A. Iivanainen. The bovine genomic DNA sequence data reveal three IGHV subgroups, only one of which is functionally expressed. *Dev. Comp. Immunol.*, 37(3-4):457–61, 2012.

[261] E. Hsu and L.A. Steiner. Primary structure of immunoglobulins through evolution. *Curr. Opin. Struct. Biol.*, 2(3):422–431, 1992.

[262] F. Wang, D.C. Ekiert, I. Ahmad, W. Yu, Y. Zhang, O. Bazirgan, A. Torkamani, T. Raudsepp, W. Mwangi, M.F. Criscitiello, I.A. Wilson, P.G. Schultz, and V.V. Smider. Reshaping Antibody Diversity. *Cell*, 153(6):1379–1393, 2013.

[263] T.T. Wu and E.A. Kabat. An analysis of the sequences of the variable regions of Bence Jones proteins and myeloma light chains and their implications for antibody complementarity. *J. Exp. Med.*, 132(2):211–50, 1970.

[264] K. Decanniere, A. Desmyter, M. Lauwereys, M.A. Ghahroudi, S. Muyldermans, and L. Wyns. A single-domain antibody fragment in complex with RNase A: non-canonical loop structures and nanomolar affinity using two CDR loops. *Structure*, 7(4):361–70, 1999.

[265] R.L. Stanfield, H. Dooley, M.F. Flajnik, and I.A. Wilson. Crystal structure of a shark single-domain antibody V region in complex with lysozyme. *Science*, 305 (5691):1770–3, 2004.

[266] C.B. Thompson and P.E. Neiman. Somatic diversification of the chicken immunoglobulin light chain gene is limited to the rearranged variable gene segment. *Cell*, 48(3):369–78, 1987.

[267] R.S. Becker and K.L. Knight. Somatic diversification of immunoglobulin heavy chain VDJ genes: evidence for somatic gene conversion in rabbits. *Cell*, 63(5): 987–97, 1990.

[268] S. Verma and R. Aitken. Somatic hypermutation leads to diversification of the heavy chain immunoglobulin repertoire in cattle. *Vet. Immunol. Immunopathol.*, 145(1-2):14–22, 2012.

[269] M.S. Neuberger and C. Rada. Somatic hypermutation: activation-induced deaminase for C/G followed by polymerase eta for A/T. *J. Exp. Med.*, 204(1):7–10, 2007.

[270] J. Liljavirta, A. Ekman, J.S. Knight, A. Pernthaner, A. Iivanainen, and M. Niku. Activation-induced cytidine deaminase (AID) is strongly expressed in the fetal bovine ileal Peyer's patch and spleen and is associated with expansion of the primary antibody repertoire in the absence of exogenous antigens. *Mucosal Immunol.*, 2013.

[271] C.A. Reynaud, C.R. Mackay, R.G. Müller, and J.C. Weill. Somatic generation of diversity in a mammalian primary lymphoid organ: the sheep ileal Peyer's patches. *Cell*, 64(5):995–1005, 1991.

[272] P.A. Ramsland, C.R. Brock, J. Moses, B.G. Robinson, A.B. Edmundson, and R.L. Raison. Structural aspects of human IgM antibodies expressed in chronic B lymphocytic leukemia. *Immunotechnology*, 4(3-4):217–29, 1999.

[273] C. Tian, G.K. Luskin, K.M. Dischert, J.N. Higginbotham, B.E. Shepherd, and J.E. Crowe. Evidence for preferential Ig gene usage and differential TdT and exonuclease activities in human naïve and memory B cells. *Mol. Immunol.*, 44(9): 2173–83, 2007.

[274] S.T. Reddy, X. Ge, A.E. Miklos, R.A. Hughes, S.H. Kang, K.H. Hoi, C. Chrysostomou, S.P. Hunicke-Smith, B.L. Iverson, P.W. Tucker, A.D. Ellington, and G. Georgiou. Monoclonal antibodies isolated without screening by analyzing the variable-gene repertoire of plasma cells. *Nat. Biotech.*, 28(9):965–9, 2010.

[275] J.A. Weinstein, N. Jiang, R.A. White, D.S. Fisher, and S.R. Quake. High-throughput sequencing of the zebrafish antibody repertoire. *Science*, 324(5928): 807–10, 2009.

[276] B.S. Briney, J.R. Willis, B.A. McKinney, and J.E. Crowe. High-throughput antibody sequencing reveals genetic evidence of global regulation of the naïve and memory repertoires that extends across individuals. *Genes Immun.*, 13(6):469–73, 2012.

[277] A. Gonzalez-Fernandez. Somatic Mutation of Immunoglobulin Chains: A Segment of the Major Intron Hypermutates as Much as the Complementarity-Determining Regions. *Proc. Natl. Acad. Sci. U. S. A.*, 91(26):12614–12618, 1994.

[278] P.A. Larsen and T.P.L. Smith. Application of circular consensus sequencing and network analysis to characterize the bovine IgG repertoire. *BMC immunol.*, 13 (1):52, 2012.

[279] M.C. Sinclair, J. Gilchrist, and R. Aitken. Bovine IgG repertoire is dominated by a single diversified VH gene family. *J. Immunol.*, 159(8):3883–9, 1997.

[280] D.A. Benson, M. Cavanaugh, K. Clark, I. Karsch-Mizrachi, D.J. Lipman, J. Ostell, and E.W. Sayers. GenBank. *Nucleic Acids Res.*, 41(Database issue):D36–42, 2013.

[281] Clontech Laboratories. *SMARTer RACE cDNA Amplification Kit User Manual*. Clontech Laboratories, Inc. A Takara Bio Company, Mountain View, CA, USA, 2012. URL `http://www.clontech.com/GB/Products/cDNA_Synthesis_and_Library_Construction/RACE_Rapid_Amplification_of_cDNA_Ends/5_Prime_RACE_and_3_Prime_RACE?sitex=10030:22372:US`.

[282] B. Chevreux, T. Wetter, and S. Suhai. Genome Sequence Assembly Using Trace Signals and Additional Sequence Information. *Computer Science and Biology: Proceedings of the German Conference on Bioinformatics (GCB)*, 99:45–56, 1999.

[283] R. Staden, K.F. Beal, and J.K. Bonfield. The Staden package, 1998. *Methods Mol. Biol. (N. Y., NY, U. S.)*, 132:115–30, 2000.

[284] K. Katoh and D.M. Standley. MAFFT multiple sequence alignment software version 7: improvements in performance and usability. *Mol. Biol. Evol.*, 30(4):772–80, 2013.

[285] V. Kunik, S. Ashkenazi, and Y. Ofran. Paratome: an online tool for systematic identification of antigen-binding regions in antibodies based on sequence or structure. *Nucleic Acids Res*, 40(Web Server issue):W521–4, 2012.

[286] V. Kunik, B. Peters, and Y. Ofran. Structural consensus among antibodies defines the antigen binding site. *PLoS Comput Biol*, 8(2):e1002388, 2012.

[287] P. Benkert, M. Biasini, and T. Schwede. Toward the estimation of the absolute quality of individual protein structure models. *Bioinformatics*, 27(3):343–50, 2011.

[288] K. Arnold, L. Bordoli, J. Kopp, and T. Schwede. The SWISS-MODEL workspace: a web-based environment for protein structure homology modelling. *Bioinformatics*, 22(2):195–201, 2006.

[289] T. Schwede. SWISS-MODEL: an automated protein homology-modeling server. *Nucleic Acids Res.*, 31(13):3381–3385, 2003.

[290] N. Guex and M.C. Peitsch. SWISS-MODEL and the Swiss-PdbViewer: an environment for comparative protein modeling. *Electrophoresis*, 18(15):2714–23, 1997.

[291] M. Koti, G. Kataeva, and A.K. Kaushik. Novel atypical nucleotide insertions specifically at VH-DH junction generate exceptionally long CDR3H in cattle antibodies. *Mol. Immunol.*, 47(11-12):2119–28, 2010.

[292] R. Aitken, A. Hosseini, and R. MacDuff. Structure and diversification of the bovine immunoglobulin repertoire. *Vet. Immunol. Immunopathol.*, 72(1-2):21–9, 1999.

[293] J.E. Butler. Immunoglobulin Gene Organization and the Mechanism of Repertoire Development. *Scand. J. Immunol.*, 45(5):455–462, 1997.

[294] M. Zemlin, M. Klinger, J. Link, C. Zemlin, K. Bauer, J.A. Engler, H.W. Schroeder, and P.M. Kirkham. Expressed murine and human CDR-H3 intervals of equal length exhibit distinct repertoires that differ in their amino acid composition and predicted range of structures. *J. Mol. Biol.*, 334(4):733–49, 2003.

[295] J. Glanville, W. Zhai, J. Berka, D. Telman, G. Huerta, G.R. Mehta, I. Ni, L. Mei, P.D. Sundar, G.M.R. Day, D. Cox, A. Rajpal, and J. Pons. Precise determination of the diversity of a combinatorial antibody library gives insight into the human immunoglobulin repertoire. *Proc. Natl. Acad. Sci. U. S. A.*, 106(48):20216–21, 2009.

[296] M. Oprea and T.B. Kepler. Genetic plasticity of V genes under somatic hypermutation: statistical analyses using a new resampling-based methodology. *Genome Res.*, 9(12):1294–304, 1999.

[297] L. Wu, K. Oficjalska, M. Lambert, B.J. Fennell, A. Darmanin-Sheehan, D. Ní Shúilleabháin, B. Autin, E. Cummins, L. Tchistiakova, L. Bloom, J. Paulsen, D. Gill, O. Cunningham, and W.J.J. Finlay. Fundamental characteristics of the immunoglobulin VH repertoire of chickens in comparison with those of humans, mice, and camelids. *J. Immunol.*, 188(1):322–33, 2012.

[298] S.S. Saini, B. Allore, R.M. Jacobs, and A. Kaushik. Exceptionally long CDR3H region with multiple cysteine residues in functional bovine IgM antibodies. *Eur. J. Immunol.*, 29(8):2420–6, 1999.

[299] J.L. Xu and M.M. Davis. Diversity in the CDR3 Region of VH Is Sufficient for Most Antibody Specificities. *Immunity*, 13(1):37–45, 2000.

[300] S.J. Berens, D.E. Wylie, and O.J. Lopez. Use of a single VH family and long CDR3s in the variable region of cattle Ig heavy chains. *Int. Immunol.*, 9(1):189–99, 1997.

[301] Y. Zhao, S.M. Jackson, and R. Aitken. The bovine antibody repertoire. *Dev. Comp. Immunol.*, 30(1-2):175–86, 2006.

[302] P.D. Kwong and I.A. Wilson. HIV-1 and influenza antibodies: seeing antigens in new ways. *Nat. Immunol.*, 10(6):573–8, 2009.

[303] D.C. Ekiert, A.K. Kashyap, J. Steel, A. Rubrum, G. Bhabha, R. Khayat, J.H. Lee, M.A. Dillon, R.E. O'Neil, A.M. Faynboym, M. Horowitz, L. Horowitz, A.B. Ward, P. Palese, R. Webby, R.A. Lerner, R.R. Bhatt, and I.A. Wilson. Cross-neutralization of influenza A viruses mediated by a single antibody loop. *Nature*, 489(7417):526–32, 2012.

[304] S.S. Saini, W. Farrugia, P.A. Ramsland, and A.K. Kaushik. Bovine IgM antibodies with exceptionally long complementarity-determining region 3 of the heavy chain share unique structural properties conferring restricted VH + Vlambda pairings. *Int. Immunol.*, 15(7):845–53, 2003.

[305] H.R. Hoogenboom and G. Winter. By-passing immunisation. Human antibodies from synthetic repertoires of germline VH gene segments rearranged in vitro. *J. Mol. Biol.*, 227(2):381–8, 1992.

[306] L.L. Rodriguez and C.G. Gay. Development of vaccines toward the global control and eradication of foot-and-mouth disease. *Expert Rev. Vaccines*, 10(3):377–87, 2011.

[307] I. Dogan, B. Bertocci, V. Vilmont, F. Delbos, J. Mégret, S. Storck, C.A. Reynaud, and J.C. Weill. Multiple layers of B cell memory with different effector functions. *Nat. Immunol.*, 10(12):1292–9, 2009.

[308] K.A. Pape, J.J. Taylor, R.W. Maul, P.J. Gearhart, and M.K. Jenkins. Different B cell populations mediate early and late memory during an endogenous immune response. *Science*, 331(6021):1203–7, 2011.

[309] M.J. Benson, R. Elgueta, W. Schpero, M. Molloy, W. Zhang, E. Usherwood, and R.J. Noelle. Distinction of the memory B cell response to cognate antigen versus bystander inflammatory signals. *J. Exp. Med.*, 206(9):2013–25, 2009.

[310] A. Ahuja, S.M. Anderson, A. Khalil, and M.J. Shlomchik. Maintenance of the plasma cell pool is independent of memory B cells. *Proc. Natl. Acad. Sci. U. S. A.*, 105(12):4802–7, 2008.

[311] M. Recher, K.S. Lang, L. Hunziker, S. Freigang, B. Eschli, N.L. Harris, A. Navarini, B.M. Senn, K. Fink, M. Lötscher, L. Hangartner, R. Zellweger, M. Hersberger, A. Theocharides, H. Hengartner, and R.M. Zinkernagel. Deliberate removal of T cell help improves virus-neutralizing antibody production. *Nat. Immunol.*, 5(9): 934–42, 2004.

[312] K.L. Good, D.T. Avery, and S.G. Tangye. Resting human memory B cells are intrinsically programmed for enhanced survival and responsiveness to diverse stimuli compared to naive B cells. *J. Immunol.*, 182(2):890–901, 2009.

[313] J.R. Crowther, C.A. Rowe, and R. Butcher. Characterization of monoclonal antibodies against a type SAT 2 foot-and-mouth disease virus. *Epidemiol. Infect.*, 111(2):391–406, 1993.

[314] V.L. Fowler, D.J. Paton, E. Rieder, and P.V. Barnett. Chimeric foot-and-mouth disease viruses: evaluation of their efficacy as potential marker vaccines in cattle. *Vaccine*, 26(16):1982–9, 2008.

[315] E.J. Glass, R.A. Oliver, T. Collen, T.R. Doel, R. Dimarchi, and R.L. Spooner. MHC class II restricted recognition of FMDV peptides by bovine T cells. *Immunology*, 74(4):594–9, 1991.

[316] A.J. Childerstone, L. Cedillo-Baron, M. Foster-Cuevas, and R.M. Parkhouse. Demonstration of bovine CD8+ T-cell responses to foot-and-mouth disease virus. *J. Gen. Virol.*, 80(3):663 – 669, 1999.

[317] M.C. Ilott, J.S. Salt, R.M. Gaskell, and R.P. Kitching. Dexamethasone inhibits virus production and the secretory IgA response in oesophageal-pharyngeal fluid in cattle persistently infected with foot-and-mouth disease virus. *Epidemiol. Infect.*, 118(2):181–7, 1997.

[318] M.J. Van Lierop, P.R. Nilsson, J.P. Wagenaar, J.M. Van Noort, J.D. Campbell, E.J. Glass, I. Joosten, and E.J. Hensen. The influence of MHC polymorphism on the selection of T-cell determinants of FMDV in cattle. *Immunology*, 84(1):79 – 85, 1995.

[319] W. Gerner, S.E. Hammer, K. Wiesmüller, and A. Saalmüller. Identification of major histocompatibility complex restriction and anchor residues of foot-and-mouth disease virus-derived bovine T-cell epitopes. *J. Virol.*, 83(9):4039 – 50, 2009.

[320] E. Guzman, G. Taylor, B. Charleston, and S.A. Ellis. Induction of a cross-reactive cd8+ t cell response following foot-and-mouth disease virus vaccination. *J. Virol.*, 84(23):12375–12384, 2010.

[321] T.S. Kim, M.M. Hufford, J. Sun, Y.X. Fu, and T.J. Braciale. Antigen persistence and the control of local T cell memory by migrant respiratory dendritic cells after acute virus infection. *J. Exp. Med.*, 207(6):1161–72, 2010.

[322] D.M. Jelley-Gibbs, D.M. Brown, J.P. Dibble, L. Haynes, S.M. Eaton, and S.L. Swain. Unexpected prolonged presentation of influenza antigens promotes CD4 T cell memory generation. *J. Exp. Med.*, 202(5):697–706, 2005.

[323] M.F. Bachmann. Induction of long-lived germinal centers associated with persisting antigen after viral infection. *J. Exp. Med.*, 183(5):2259–2269, 1996.

[324] L.M. Fahey, E.B. Wilson, H. Elsaesser, C.D. Fistonich, D.B. McGavern, and D.G. Brooks. Viral persistence redirects CD4 T cell differentiation toward T follicular helper cells. *J. Exp. Med.*, 208(5):987–99, 2011.

[325] D. Baumjohann, S. Preite, A. Reboldi, F. Ronchi, K.M. Ansel, A. Lanzavecchia, and F. Sallusto. Persistent Antigen and Germinal Center B Cells Sustain T Follicular Helper Cell Responses and Phenotype. *Immunity*, 38(3):596–605, 2013.

[326] A.H. Achtman, U.E. Höpken, C. Bernert, and M. Lipp. CCR7-deficient mice develop atypically persistent germinal centers in response to thymus-independent type 2 antigens. *J. Leukocyte Biol.*, 85(3):409–17, 2009.

[327] H.R. Cunliffe. Observations on the duration of immunity in cattle after experimental infection with foot-and-mouth disease virus. *Cornell Vet.*, 54:501–10, 1964.

[328] J.S. Salt, G. Mulcahy, and R.P. Kitching. Isotype-specific antibody responses to foot-and-mouth disease virus in sera and secretions of "carrier' and "non-carrier' cattle. *Epidemiol. Infect.*, 117(2):349–60, 1996.

[329] H. Coulange Bodilis, G. Benabdelmoumen, A. Gergely, C. Goujon, M. Pelicot, P. Poujol, and P.H. Consigny. [Long term persistence of yellow fever neutralising antibodies in elderly persons]. *Bull. Soc. Pathol. Exot. Ses Fil.*, 104(4):260–5, 2011.

[330] B. Wyplosz, C. Burdet, H. François, A. Durrbach, J.C. Duclos-Vallée, M.F. Mamzer-Bruneel, P. Poujol, O. Launay, D. Samuel, D. Vittecoq, and P.H. Consigny. Persistence of yellow Fever vaccine-induced antibodies after solid organ transplantation. *Am. J. Transplant.*, 13(9):2458–61, 2013.

[331] B. Pulendran, J. Miller, T.D. Querec, R. Akondy, N. Moseley, O. Laur, J. Glidewell, N. Monson, T. Zhu, H. Zhu, S. Staprans, D. Lee, M.A. Brinton, A.A. Perelygin, C. Vellozzi, P. Brachman, S. Lalor, D. Teuwen, R.B. Eidex, M. Cetron, F. Priddy, C. del Rio, J. Altman, and R. Ahmed. Case of yellow fever vaccine–associated viscerotropic disease with prolonged viremia, robust adaptive immune responses, and polymorphisms in CCR5 and RANTES genes. *J. Infect. Dis.*, 198 (4):500–7, 2008.

[332] B. Pulendran, J.Z. Oh, H.I. Nakaya, R. Ravindran, and D.A. Kazmin. Immunity to viruses: learning from successful human vaccines. *Immunol. Rev.*, 255(1):243–55, 2013.

[333] J. Seago, T. Jackson, C. Doel, E. Fry, D. Stuart, M.M. Harmsen, B. Charleston, and N. Juleff. Characterization of epitope-tagged foot-and-mouth disease virus. *J. Gen. Virol.*, 93(Pt 11):2371–81, 2012.

[334] S.P. Kasturi, I. Skountzou, R.A. Albrecht, D. Koutsonanos, T. Hua, H.I. Nakaya, R. Ravindran, S. Stewart, M. Alam, M. Kwissa, F. Villinger, N. Murthy, J. Steel, J. Jacob, R.J. Hogan, A. García-Sastre, R. Compans, and B. Pulendran. Programming the magnitude and persistence of antibody responses with innate immunity. *Nature*, 470(7335):543–7, 2011.

[335] J D Kitson, D McCahon, and G J Belsham. Sequence analysis of monoclonal antibody resistant mutants of type O foot and mouth disease virus: evidence for the involvement of the three surface exposed capsid proteins in four antigenic sites. *Virology*, 179(1):26–34, 1990.

[336] G.E. Cottral and P. Gailiunas. Experimental multiple infection of animals with foot-and-mouth disease viruses. *Proceedings of the Annual meeting of the U.S Animal Health Association*, 75:441–465, 1972.

[337] M.Y. Zhang, T. Yuan, J. Li, A. Rosa Borges, J.D. Watkins, J. Guenaga, Z. Yang, Y. Wang, R. Wilson, Y. Li, V.R. Polonis, S.H. Pincus, R.M. Ruprecht, and D.S. Dimitrov. Identification and characterization of a broadly cross-reactive HIV-1 human monoclonal antibody that binds to both gp120 and gp41. *PloS one*, 7(9): e44241, 2012.